

COAST BIOGEOCHEMISTRY IN THE ATLANTIC
OCEAN USING FLOW INJECTION
CHEMILUMINESCENCE

RACHEL URSULA SHELLEY

PLD 2011

This copy of the thesis has been supplied on condition that anyone who consults it is understood to recognise that its copyright rests with its author and that no quotation from the thesis and no information derived from it may be published without the author's prior consent.

**COBALT BIOGEOCHEMISTRY IN THE ATLANTIC
OCEAN USING FLOW INJECTION -
CHEMILUMINESCENCE**

by

RACHEL URSULA SHELLEY

A thesis submitted to the University of Plymouth
in partial fulfilment for the degree of

DOCTOR OF PHILOSOPHY

School of Geography, Earth and Environmental Sciences
Faculty of Science

May 2011

Dedicated to Petroc

Cobalt Biogeochemistry in the Atlantic Ocean using Flow Injection with Chemiluminescence Detection

Rachel Ursula Shelley

As ~ 50% of global photosynthesis occurs in marine environments, the factors regulating this process e.g. trace metal availability, have an impact on the global carbon cycle. The key cyanobacteria genera *Prochlorococcus* and *Synechococcus* have an absolute requirement for Co. Dissolved cobalt (dCo) concentrations in the open ocean are extremely low (5–120 pM). A sensitive flow injection technique using chemiluminescence detection (FI-CL) was developed (detection limit 4.5 pM dCo, RSD ≤ 4%). Seawater samples must be UV-irradiated prior to analysis, in order to liberate organically-bound Co.

A field study in the Sargasso Sea, demonstrated that aerosol Co was significantly more soluble than aerosol Fe over a range of aerosol dust deposition fluxes (1–1040 $\mu\text{g Fe m}^{-2} \text{d}^{-1}$) (8–100% for Co versus 0.44–45% for Fe). The dry deposition flux of aerosol Co was of the same order of magnitude as the advective upwelling flux (47–1540 $\text{pmol m}^{-2} \text{d}^{-1}$ and 1.7–1430 $\text{pmol m}^{-2} \text{d}^{-1}$ respectively). Wet deposition, dominated the total aerosol flux (~ 85%). The vertical distribution of dCo influenced *Prochlorococcus* abundance.

A regional study in the eastern North Atlantic gyre demonstrated that the highest rates of N_2 fixation occurred with the highest dFe concentrations (9.8 $\text{nM N L}^{-1} \text{h}^{-1}$, 0.6 nM respectively). No increase in primary production following additions of trace metals (Co, Cu, Fe, Zn) was observed. The addition of N resulted in an increase in primary production. However, there was no synergistic effect of trace metal plus N addition, suggesting that alleviation of N-limitation shifted the system to P-limitation.

On a meridional transect from ~ 50°N–50°S in the Atlantic Ocean, the highest concentrations of dCo (> 80 pM) coincided with low- O_2 (< 150 μM) upwelled water. The lowest dCo (< 20 pM) was observed in the eastern North Atlantic gyre. Lateral advection of continental Co and upwelling were identified as important sources of Co. The highly efficient recycling of Co in the euphotic zone is an important additional source.

Glossary

Analytical/Experimental

Co ²⁺ , Co(II)	Cobalt in the soluble 2+ oxidation state
Co ³⁺ , Co(III)	Cobalt in the insoluble 3+ oxidation state
Fe ²⁺ , Fe(II)	Iron in the soluble 2+ oxidation state (ferrous iron)
Fe ³⁺ , Fe(III)	Iron in the insoluble 3+ oxidation state (ferric iron)
CRM	Certified reference material
CTAB	Cetyl trimethylammonium bromide
dAl	Total dissolved aluminium (< 0.45 µm)
dCo	Total dissolved cobalt (< 0.2 or 0.45 µm)
dCu	Total dissolved copper (< 0.2 µm)
dFe	Total dissolved iron (< 0.2 or 0.45 µm)
dZn	Total dissolved zinc (< 0.2 µm)
HCl	Hydrochloric acid
LDPE	Low density polyethylene
NaOH	Sodium hydroxide
NASS	North Atlantic Surface Seawater (certified seawater NRCC, Canada)
nM	nmol L ⁻¹
pM	pmol L ⁻¹
PMT	Photon multiplier tube
TSR	Trautz-Schorigen Reaction
UHP water	Ultra-high purity water (18.2 MΩ cm ⁻¹)
UV	Ultraviolet
8-HQ	8-hydroxyquinoline
IDA (Toyopearl)	Iminodiacetic acid (Toyopearl AF-chelate 650M)
CSV	Cathodic stripping voltammetry
FI-CL	Flow injection with chemiluminescence detection
FI-FI	Flow injection with fluorometric detection
FI-spec	Flow injection with spectrophotometric detection
ICP-OES	Inductively coupled plasma-optical emission spectrometry

ICP-MS	Inductively coupled plasma-mass spectrometry
LC-CL	Liquid chromatography with chemiluminescence detection

Oceanographic

AMT	Atlantic Meridional Transect
BATS	Bermuda Atlantic Time-series Station
CO ₂	Carbon dioxide
CTD rosette	Conductivity, temperature and density probes mounted on a frame that holds the water column sampling bottles
DIC	Dissolved inorganic carbon
DOC	Dissolved organic carbon
FeAST	Fe Atmosphere Solubility and Transport (cruise)
GEOTRACES	An international study of marine biogeochemical cycles of trace elements and their isotopes
GEOTRACES GD	GEOTRACES deep (1000 m) seawater reference samples
GEOTRACES GS	GEOTRACES surface seawater reference samples
HNLC	High Nutrient, Low Chlorophyll
INSPIRE	Investigation of Near Surface Production of Iodocarbons: Rates and Exchanges (cruise)
ITCZ	Intertropical Convergence Zone
N ₂	Dinitrogen
NO ₂	Nitrous oxide
O ₂	Oxygen
PAR	Photosynthetically active radiation
SAFe	Sampling and Analysis of Fe
SAFe D	SAFe deep (1000 m) seawater reference samples
SAFe S	SAFe surface seawater reference samples
SOLAS	Surface Ocean Lower Atmosphere Study
SPM	Suspended particulate material

Biogeochemical Provinces

NADR	North Atlantic Drift Region
NAST	North Atlantic Sub-Tropical gyre
NATR	North Atlantic Tropical gyre Region
NATL-E	North Atlantic gyre (east)
WTRA	Western Tropical Atlantic
SATL	South Atlantic gyre
STC	Sub-Tropical Convergence
SSTC	Southern Sub-Tropical Convergence

Contents

Chapter 1 – Biogeochemical Cycling of Cobalt and Iron	1
1.1. Introduction	2
1.2. Biological functions of cobalt and iron	11
1.3. Biogeochemistry of cobalt and iron	13
1.3.1. The speciation of trace metals in seawater	13
1.3.2. Open ocean surface concentrations	17
1.3.3. Vertical distributions	22
1.3.4. Supply of trace metals to the surface ocean	27
1.3.5. Sources and sinks of trace metals to the ocean	28
1.3.5.1. Atmospheric deposition	29
1.3.5.2. Fluvial inputs	33
1.3.5.3. Sediments and upwelling, vertical mixing and lateral transport	34
1.3.5.4. Hydrothermal vent fluids	36
1.3.5.5. Regeneration of trace metals	37
1.3.5.6. Removal mechanisms	38
1.4. Co-limitation	39
1.5. Study area	41
1.6. Aims and Objectives	42
Chapter 2 – Analytical Methods	47
2.1. Introduction	48
2.2. Background	48
2.2.1. Flow Injection Analysis	48
2.2.2. Chemiluminescence	51
2.2.3. Dissolved Co and Fe	55
2.3. Aims and objectives	57
2.4. Determination of dCo in seawater using FI-CL	58
2.4.1. Introduction	58
2.4.2. Materials and procedures	59
2.4.2.1. Reagents	61
2.4.2.2. Procedures	62
2.4.3. Assessment	63
2.4.3.1. On-line chelating resins	63

2.4.3.2.	Reaction conditions	65
2.4.4.	Sample treatment for the determination of total dissolved cobalt.....	71
2.4.4.1.	UV-irradiation.....	71
2.4.4.2.	Addition of a reducing agent	73
2.4.5.	Analytical figures of merit.....	75
2.4.5.1.	Blanks and detection limits	76
2.4.5.2.	Accuracy and precision	77
2.4.6.	Discussion and recommendations	78
2.5.	Determination of dFe in seawater using FI-CL	81
2.5.1.	Introduction	81
2.5.2.	Materials and procedures	81
2.5.2.1.	Reagents	82
2.5.2.2.	Procedures	84
2.5.3.	Analytical figures of merit.....	85
2.5.3.1.	Blanks and detection limits	85
2.5.3.2.	Accuracy and precision	86
2.5.4.	Discussion	86
2.6.	Three pump FI-CL system for the determination of dCo and dFe	87
2.7.	Determination of dCu using ICP-MS with off-line preconcentration.....	89
2.7.1.	Introduction	89
2.7.2.	Materials and procedures	90
2.7.2.1.	Reagents	91
2.7.2.2.	Procedures	92
2.7.3.	Analytical figures of merit.....	94
2.7.3.1.	Blanks and detection limits	94
2.7.3.2.	Accuracy and precision	95
2.7.4.	Discussion and recommendations	95

Chapter 3 – Controls on Dissolved Cobalt in Surface Waters of the Sargasso Sea	98
3.1. Introduction	99
3.2. Methods	103
3.2.1. Study area	103
3.2.2. Seawater sample collection and treatment	104

3.2.3.	Air mass back trajectories	109
3.2.4.	Enumeration of phytoplankton groups	109
3.3.	Results and Discussion	110
3.3.1.	Hydrographic and biogeochemical observations	110
3.3.2.	Surface transects	113
3.3.3.	Fractional solubility of aerosol cobalt and iron	116
3.3.4.	Factors influencing the vertical distribution of cobalt.....	122
3.3.5.	Phytoplankton ecology.....	128
3.4.	Conclusions	131

Chapter 4 – The Impact of Trace Metal (Co, Cu, Fe) Additions on Productivity and Nitrogen Fixation in the Tropical Northeast Atlantic Ocean..... 133

4.1.	Introduction	134
4.1.1.	Aims and Objectives	136
4.2.	Methods	137
4.2.1.	Study region.....	137
4.2.2.	Sampling and ship-based bioassays	140
4.2.3.	Analytical techniques	147
4.3.	Results and Discussion.....	152
4.3.1.	Macronutrients	152
4.3.2.	Primary production.....	153
4.3.3.	Heterotrophic bacterial production	156
4.3.4.	Dissolved Co and Cu	158
4.3.5.	Dissolved Fe and N ₂ fixation.....	163
4.4.	Conclusions and recommendations	172

Chapter 5 – Dissolved Cobalt Distributions in Surface Waters During an Atlantic Meridional Transect (AMT-19)..... 174

5.1.	Introduction	175
5.2.	Materials and Methods.....	177
5.2.1.	Sampling.....	177
5.2.2.	Dissolved cobalt determination	180
5.2.3.	Ancillary measurements.....	181
5.3.	Results and Discussion.....	182

5.3.1. Hydrography	182
5.3.2. North-south distribution of macronutrients in the upper water column (< 200 m).....	185
5.3.3. North-south distributions of dCo in the upper water column(< 200 m.....	188
5.3.4. Chemical speciation of cobalt	204
5.3.5. Controls on dCo distribution in the Atlantic Ocean: a summary	206
5.3.5.1. Atmospheric inputs	206
5.3.5.2. Upwelling and advective transport.....	207
5.3.5.3. Biological processes affecting vertical dCo distributions	208
5.4. Conclusions	212
Chapter 6 – Conclusions and Future Work.....	214
6.1. Introduction	215
6.2. Development of analytical techniques for the determination of dissolved Co, Cu, Fe and Zn in seawater	216
6.3. Biogeochemical cycling of dCo in the Sargasso Sea	219
6.4. The impact of trace metals (Co, Cu and Fe) additions on productivity and nitrogen fixation rates in the tropical Northeast Atlantic Ocean.....	221
6.5. Dissolved Co in surface waters during an Atlantic Meridional Transect	223
Appendix	226
References.....	231

Figures

Figure 1. 1. The biological pump.....	3
Figure 1. 2. Distribution of primary production in the oceans	6
Figure 1. 3. Comparison of the average elemental quotas in five eukaryotic phytoplankton phyla	9
Figure 1. 4. (a) The nitrogen cycle showing the metal cofactors at each enzymatically catalysed step. (b) The principal metal requirements for carbon, nitrogen and phosphorus acquisition and assimilation by marine phytoplankton	11
Figure 1.5. Vertical profile of dCo from the northeast Atlantic Ocean	25
Figure 1. 6. Vertical profiles of dFe from high latitudes of the North Atlantic and the North Pacific.....	27
Figure 1. 7. Schematic diagram of the biogeochemical cycling of Fe in the ocean	29
Figure 1. 8. Dust fluxes to the worlds oceans based on a composite of three published modelling studies.....	30
Figure 1. 9. Saharan dust outbreak over the Canary Islands.....	31
Figure 2. 1. The Trautz-Schorigen Reaction	53
Figure 2. 2. The major steps in the oxidation of luminol	54
Figure 2. 3. FI-CL manifold configuration for the determination of dCo in seawater.	61
Figure 2. 4. Effect of two different chelating resins on sensitivity and elution profiles for a 50 pM standard in seawater	64
Figure 2. 5. Effect of the major seawater cations on the chemiluminescence signal	69
Figure 2. 6. FI-CL manifold configuration for the determination of dFe in seawater.	82
Figure 2. 7. Example of a calibration curve for dFe.....	85
Figure 2. 8. Three-pump flow injection manifold for the determination of dCo..	88
Figure 2. 9. Manifold configuration for the off-line preconcentration of dCu.....	91
Figure 2. 10. An example of a calibration curve of standard additions of dCu ..	94

Figure 3. 1. <i>FeAST-6</i> cruise track	105
Figure 3. 2. Vertical profiles of temperature, salinity and chlorophyll- <i>a</i>	111
Figure 3. 3. Comparison of vertical profiles of dCo in the vicinity of BATS	112
Figure 3. 4. Surface concentrations of dCo, dFe and dAl from 31-24° N	114
Figure 3. 5. Five day air mass back trajectory simulations.....	118
Figure 3. 6. Vertical profiles of dCo, dFe and dAl.....	123
Figure 3. 7. <i>Prochlorococcus</i> abundance versus dCo concentration	130
Figure 4. 1. The <i>INSPIRE</i> cruise stations	138
Figure 4. 2. Seven day composite satellite (MODIS) image of chlorophyll.....	139
Figure 4. 3. Experimental design for the 48 h incubation experiment	143
Figure 4. 4. The vacuum filtration system.	145
Figure 4. 5. Sub-sampling protocol for the 4.6 L incubation bottles at T ₄₈	146
Figure 4. 6. Primary production as determined by ¹⁴ C uptake rates	155
Figure 4. 7. Heterotrophic bacterial production rates	157
Figure 4. 8. Dissolved Co in bioassays conducted during <i>INSPIRE</i>	160
Figure 4. 9. Dissolved Cu in bioassays conducted during <i>INSPIRE</i>	163
Figure 4. 10. Dissolved Fe concentrations and N ₂ fixation rates at T ₀	165
Figure 4. 11. Saharan dust over the Cape Verde Islands.	166
Figure 4. 12. N ₂ fixation rates.....	168
Figure 4. 13. Relative contribution of individual diazotrophs to overall nifH gene expression	170
Figure 5. 1. <i>AMT-19</i> (a) cruise track (b) surface currents in the Atlantic Ocean	179
Figure 5. 2. North– south distributions of temperature and salinity	184

Figure 5. 3. Concentrations of macronutrients (nitrate, phosphate and silicate)	186
Figure 5. 4. The north-south distribution of dCo overlaid with potential density and, O ₂ overlaid with chl-a	189
Figure 5. 5. Examples of representative vertical profiles of dCo, temperature and salinity from different biogeochemical provinces: (a) NADR, (b) NATL-E, (c) WTRA, (d) SATL, (e) SATL/SSTC, (f) SSTC.	191
Figure 5. 6. Dissolved Co, salinity and temperature (left), and dCo, chl-a and O ₂ (right) in the ITCZ.	197
Figure 5. 7. Averaged concentrations of dCo (AMT-19) and TdCo (AMT-3) in surface waters (< 10 m)	205
Figure 5. 8. Dissolved Co versus <i>Prochlorococcus</i> abundance at (a) 16.5°N, NATL, (b) 11°N, WTRA, (c) 1° N, WTRA/ITCZ, (d) 28° S, SATL and (e) 33°S, SATL/SSTC.	210

Tables

Table 1. 1. Essential micro-nutrients and their function in important biogeochemical processes in the ocean	4
Table 1. 2. A selection of dissolved cobalt concentrations in the open ocean ..	18
Table 1. 3. A selection of dissolved iron concentrations in the open ocean	19
Table 1. 4. Sources and sinks of trace metals	28
Table 1. 5. Percentage solubility of selected trace metals from dust after a 120 min leach	32
Table 1. 6. Examples of potential nutrient co-limitation pairs in the marine environment	41
Table 2. 1. Comparison of 8-HQ and Toyopearl resin characteristics.....	65
Table 2. 2. Key analytical parameters.....	76
Table 2. 3. Reagent concentrations and analytical cycle timings used in this study	83
Table 2. 4. ICP-MS parameters for the determination of dissolved Cu in seawater samples following off-line extraction.....	93
Table 3. 1. Details of water-column trace metal sampling stations occupied during <i>FeAST-6</i>	103
Table 3. 2. (a) Aerosol Co and (b) Fe fluxes and fractional solubility during <i>FeAST-6</i>	116
Table 3. 3. (a) Aerosol Co and (b) Fe fluxes and fractional solubility during <i>FeATMISS-1</i>	120
Table 3. 4. Input of dCo from below the euphotic zone.....	128
Table 4. 1. Chlorophyll-a concentration and position of stations sampled during the <i>INSPIRE</i> cruise.....	139
Table 4. 2. Nitrate, ammonium, phosphate and silicate at T_0	153
Table 4. 3. Concentrations of dCo in the bioassay bottles	159
Table 4. 4. Concentrations of dCu in the bioassay bottles	162

Table 4. 5. Dissolved Fe and N ₂ fixation rates at T ₀	165
Table 5. 1. Description of the biogeochemical provinces sampled during <i>AMT-19</i>	178
Table 6. 1. Dominant controls on dCo distributions in the upper water column of the Atlantic Ocean.....	223
Table i. Concentrations of (a) dCo, (b) dFe and (c) dAl from the vertical cast stations (K1-K5) from <i>FeAST-6</i>	228
Table ii. Concentrations of dCo during <i>AMT-19</i>	229

ACKNOWLEDGEMENTS

Firstly, a big thank you to my supervisors Maeve Lohan, Paul Worsfold and Carol Robinson for your guidance and encouragement. In particular to Maeve, your boundless enthusiasm and faith in me has been an inspiration. Thank you also to the members of the BEACH group and/or fellow B509-ers past and present: Angie Milne, Marie Séguret, Simon Ussher and Neil Wyatt (fellow obsessives, aka. trace metal people), and to Jane Eagling, Estela Reinoso-Maset, Colin May, Luke Holmes, Leyla Shams, Apha, Gerald Maier, Patricia Cabedo-Sanz, Alba Navarro-Rodriguez, Bernhard Zachhuber, Fay Couceiro, Stephanie Handley-Sidhu, Malcolm Nimmo, Alan Tappin, Charly Braungardt, Gwen O'Sullivan, Richard Sandford, Mike Foulkes, John Rieuwerts, and to all the others I've missed - for laughs, drinks and just being there as part of an incredibly friendly and supportive research group. To Rob Clough, Andy Fisher, Andy Arnold, Andrew Tonkin and Claire Williams thank you for sharing your technical expertise. May your futures be bright.

My gratitude to the people I've been lucky enough to meet on research cruises, lab visits and conferences for your friendship and the opportunities you have given me: Bill Landing, Pete Morton, Andy Bowie, Ana Aguilar-Islas, Kristen Buck, Pete Sedwick and the 4th floor ACE-CRC group at the University of Tasmania.

To friends and family: to Mum, for *everything* – I could not have done this without you; to Minnow and Piran, for being there; to Dad, for your (mumbled) wisdom and all the discussions we can no longer have, and most of all to Petroc, for being the best son anyone could ever hope for and for never once complaining about having a part-time mother. To Leigh and Ahmed, I am indebted. To Nat, Nina, Ali and Sam, for a whole world of friendship. To all the other wonderful people I've met along the way that have touched my life (too many to mention), you are in my thoughts.

The funding for the work conducted here was provided by the Marine Institute at the University of Plymouth.

AUTHOR'S DECLARATION

At no time during the registration for the degree of Doctor of Philosophy has the author been registered for any other University award without prior agreement of the Graduate Committee.

This study was financed with the aid of a studentship from the Marine Institute at the University of Plymouth.

The work in this thesis was primarily the work of the author unless acknowledged otherwise. Relevant scientific seminars and conferences were regularly attended at which work was presented, research cruises were undertaken, external institutions were visited for experience and knowledge transfer and several papers prepared for publication (see Appendix).

Word count of main body of thesis

50 326 words

Signed..........

Date.....8/7/11.....

PUBLICATIONS:

Shelley, R.U., Sedwick, P.N., Bibby, T.S., Cabedo-Sanz, P., Church, T.M., Johnson, R.J., Macey, A.I., Marsay, C.M., Sholkovitz, E.R., Ussher, S.J., Worsfold, P.J. and Lohan, M.C. Controls on dissolved cobalt in surface waters of the Sargasso Sea. Submitted to *Global Biogeochemical Cycles*.

Turk, K.A., Rees, A.P., Zehr, J.P., Pereira, N., Swift, P., **Shelley, R.**, Lohan, M., Woodward, E.M.S., and Gilbert, J., 2011. Nitrogen fixation and nitrogenase (nifH) expression in tropical waters of the eastern North Atlantic. *ISME Journal*.
Doi: 10.1038/ismej.2010.205.

Shelley, R.U., Zachhuber, B., Sedwick, P.N., Worsfold, P.J. and Lohan, M.C. 2010. Determination of total dissolved cobalt in UV-irradiated seawater using flow injection with chemiluminescence detection. 2010. *Limnology and Oceanography:Methods*. **8**: 352 – 362.

PRESENTATIONS AND CONFERENCES ATTENDED:

Dec. 2010: *Biogeochemistry of Dissolved Cobalt (and Iron) in the Sargasso Sea*. 2nd Annual Biogeochemistry Research Centre Conference, University of Plymouth. (Oral presentation)

Sept. 2010: *Biogeochemistry of dissolved cobalt in the Sargasso Sea.* XIVth Biennial Conference, Challenger Society for Marine Science, National Oceanography Centre, Southampton. (Oral presentation)

July 2010: *Flow Injection – Chemiluminescence (FI-CL) for the Determination of Total Dissolved Cobalt.* Royal Society of Chemistry Analytical Research Forum, Loughborough University. (Oral presentation)

Feb. 2010: *Biogeochemistry of Dissolved Cobalt and Iron in the Sargasso Sea.* Ocean Sciences. Portland, Oregon, USA. (Oral presentation)

Dec. 2009: *Biogeochemistry of Dissolved Cobalt and Iron in the Sargasso Sea.* 1st Annual Biogeochemistry Research Centre Conference, University of Plymouth. (Oral presentation)

Sept. 2009: *Eddies on the Cycling of Dissolved Cobalt and Iron in the Sargasso Sea.* The Geological Society, Burlington House, London. *Impacts of dust deposition and Mesoscale* (Oral presentation)

Apr. 2009: *Total Dissolved Cobalt in the North Atlantic by Flow Injection with Chemiluminescence Detection.* Plymouth Marine Sciences Partnership Symposium, University of Plymouth. (Oral presentation)

Jan. 2009: *Determination of Total Dissolved Cobalt in Seawater by Flow Injection-Chemiluminescence (FI-CL).* Developing IMBER Science in the UK, University of Plymouth. (Poster)

Dec. 2008: *Flow Injection-Chemiluminescence (FI-CL) for the Determination of Total Dissolved Cobalt.* 5th Annual Biogeochemistry and Environmental Analytical Chemistry Conference, University of Plymouth. (Oral presentation)

Sept. 2008: *Flow Injection Chemiluminescence (FI-CL) for the determination of total dissolved Co.* XIIIth Biennial Conference, Challenger Society for Marine Science, University of Bangor. (Poster)

CO-AUTHORED PRESENTATIONS:

Sept. 2009: Worsfold, P.J., **Shelley, R.U.** and Zachhuber, B. *Flow Injection with Chemiluminescence for the Determination of Total Dissolved Cobalt in Open Ocean Waters.* Flow Analysis XI. Pollensa, Mallorca. (Oral presentation)

Nov. 2009: Dixon, J.L., Rees, A.P., **Shelley, R.U.** and Clark, D.R. *Microbial nutrient limitation in the Northeast Atlantic.* SOLAS meeting, Barcelona, Spain (Poster)

Nov. 2009: Malin, G. Hughes, C., Lee, G., Liss, P., Martino, M., Woeltjen, J., Nightingale, P., Airs, R., Allen, I., Archer, S., Beesley, A., Clarke, D.,

Cummings, D., Dixon, J., Goldson, L., Harris, C., Kimmance, S., Rees, A., Smyth, T., Stephens, J., Tarran, G., Tilstone, G., Woodward, M., Chance, R. and **Shelley, R.** *INSPIRE: Investigation of the Near-Surface Production of Iodocarbons: Rates and Exchanges*. SOLAS meeting, Barcelona, Spain.
(Poster)

Sept. 2008: Rees, A.P., Dixon, J.L., Clark, D.R., Woodward, E.M.S. and **Shelley, R.U.** *Nutrient limitation of microbial activity*. XIIIth Biennial Conference, Challenger Society for Marine Science, University of Bangor. (Oral presentation)

RESEARCH EXPERIENCE:

Nov. – Dec. 2007: UK-SOLAS research cruise *INSPIRE* (Investigation of Near-Surface Production of Iodocarbons: Rates and Exchanges). Collaborative study with researchers from Plymouth Marine Laboratory (PML) to assess the limitation of microbial processes by essential trace metals; Co, Cu, Fe, Zn.

Apr. 2008: Extended Ellett Line research cruise; a hydrographic time-series transect from the UK-Iceland.

Dec. 2008 – Apr. 2009: Steering committee member and session chair for the first Plymouth Marine Sciences Partnership Symposium (PMSP) held at the

University of Plymouth; a one day conference with contributions from all seven PMSP partners.

Apr. 2009: Oversaw visiting scientist, Johann Bown, LEMAR, Université de Brest, France, set up a FI-CL system for the determination of total dissolved cobalt (Shelley *et al.*, 2010).

Oct. – Nov. 2010: US GEOTRACES North Atlantic research cruise. Collection of aerosol and rainwater samples; in collaboration with Florida State University, USA.

Feb. – Apr. 2011: Visiting scientist at the University of Tasmania, Australia.
Study title: *Investigation of the dissolution of trace metals from Australian dusts.*
Funded as a STSM under COST Action ES0801: The ocean chemistry of bioactive trace elements and paleoclimate proxies.

Chapter 1

Biogeochemical Cycling of Cobalt and Iron

1.1. Introduction

It is currently estimated that between 40 and 50% of photosynthesis on Earth occurs in marine environments (Falkowski, 1994; Field *et al.*, 1998). Although phytoplankton account for just one percent of plant carbon on the planet, they account for approximately half of all carbon fixation (Falkowski *et al.*, 2000), thus, they have a fundamental role in the global carbon cycle and climate regulation (Chisholm *et al.*, 2001). Given that > 90% of marine primary production occurs in offshore, oceanic regions (Tortell *et al.*, 1999), it is hardly surprising that biogeochemical processes that occur in these regions can have global impacts.

In the surface layers of the ocean, photosynthetic organisms take up dissolved inorganic carbon (DIC) and macro and micro-nutrients to fix carbon into organic material. The production of organic matter and bio-minerals in surface waters, the sinking of these particles to depth, and the decomposition of the settling particles can be collectively described as the *biological pump* (Fig. 1.1). Fixed carbon, along with nitrogen, phosphorus and trace elements form the carbohydrates, lipids and proteins which comprise bulk organic matter. Upon formation, this organic matter may immediately be decomposed back to CO₂, phosphate, ammonia and other dissolved macro and micro-nutrients as a consequence of consumption by herbivorous zooplankton and/or bacterial degradation (de la Rocha, 2003). The rapid recycling of organic matter is a defining feature of marine systems, for instance, most of the planktonic biomass will be recycled within the upper few hundred meters of the water column,

accounting for approximately 90-95% of the total carbon fixed per year (Falkowski *et al.*, 2000). Although the biological pump is frequently described in relation to its impact on the cycling of carbon and the major nutrients (nitrate, phosphate and silicate), it has profound impacts on the biogeochemistry of many other micro-nutrients such as iron (Fe) and cobalt (Co). The biogeochemical cycling, concentrations and residence times of trace elements such as Fe and Co are significantly influenced by the biological pump through the process of incorporation into organic matter and biominerals (de la Rocha, 2003).

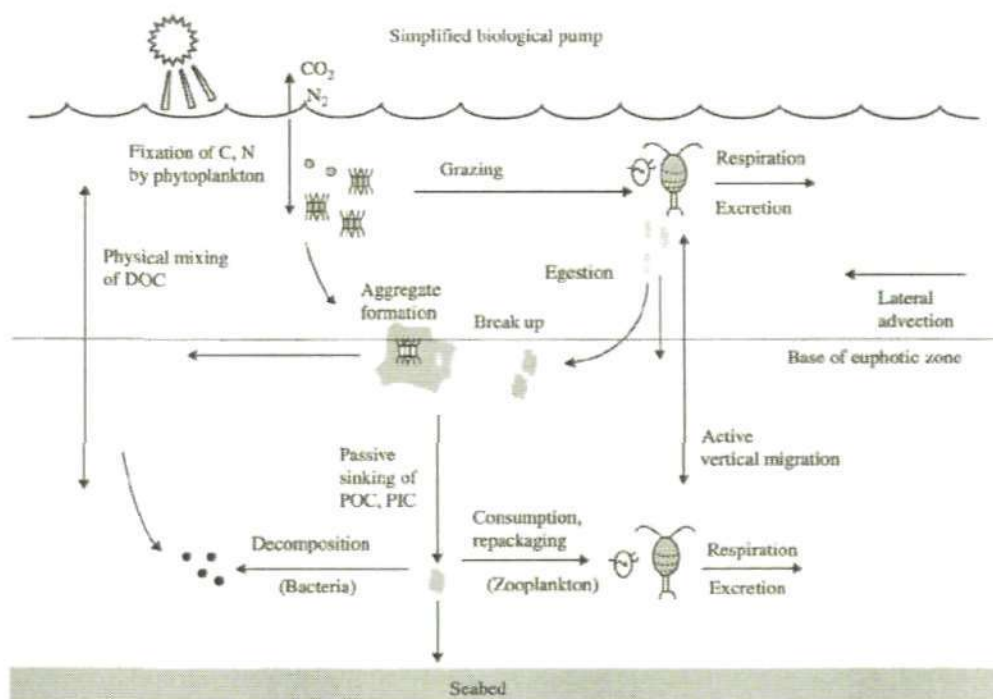


Figure 1. 1. The biological pump (reproduced from de la Rocha, 2003).

The macronutrients in seawater are nitrate, phosphate and silicate. Concentrations are usually reported in μM (although surface depletion in some oceanic regimes may reduce concentrations below nM levels). The term micronutrient refers to those elements in seawater that have been shown to be essential for phytoplankton growth, present in trace concentrations (typically pM-nM), e.g. Co. At present we have limited quantitative data regarding enzymatic intracellular processes and the corresponding trace metal requirements. Table 1.1 lists biochemical functions believed to correspond to major trace metal requirements in marine phytoplankton. Further research in the field of marine phytoplankton biochemistry is likely to add to the number of known cellular functions of trace metals (Morel and Price, 2003).

Table 1. 1. Essential micro-nutrients and their function in important biogeochemical processes in the ocean (based on Morel and Price, 2003).

Biogeochemical function	Trace metal
Carbon fixation	Fe, Mn
CO ₂ concentration (carbonic anhydrase)	Zn, Co, Cd
Silica uptake - large diatoms	Zn, Cd, Se
Calcifiers - coccolithophores	Co, Zn
N ₂ fixation	Fe, Mo, (V?)
Denitrification	Cu, Fe, Mo
Nitrification	Cu, Fe, Mo
Methane oxidation	Cu
Remineralisation pathways	Zn, Fe
Organic N utilisation	Fe, Cu, Ni
Organic P utilisation	Zn (Co?)
Formation of volatile species	Fe, Cu, V
Synthesis of photopigments	Fe and others
Vitamin B ₁₂	Co
Plastocyanin	Cu

Iron is the fourth most abundant element in the Earth's crust (de Baar and La Roche, 2003), yet in the open ocean it is present at very low concentrations (< 1 nM, Johnson *et al.*, 1997). It is an essential element for phytoplankton growth, however, large areas of the global ocean are now recognised as being Fe-limited (*e.g.* Coale *et al.*, 1996; Boyd *et al.*, 2000; 2007). It is well established that Fe limits net community production in the major high nutrient low chlorophyll (HNLC) regions of the oceans (Boyd *et al.*, 2007) (the three main HNLC regions are the Southern Ocean, the equatorial Pacific and the subarctic Pacific Ocean). These HNLC regions account for approximately 40% of the surface waters in the world oceans (Fig. 1.2). Furthermore, there is now evidence to suggest that Fe-limitation is not confined to remote off-shore waters, for example, the Peru upwelling regime and extensive parts of the Californian upwelling system are also Fe-limited (Bruland *et al.*, 2005 and references therein), as well as the chlorophyll-*a* maxima of oligotrophic regions (Morel *et al.*, 2008). In addition to limiting net community production, Fe regulates phytoplankton processes in a number of other oceanic locations, such as areas of the North Atlantic (Moore *et al.*, 2006; Nielsdottir *et al.*, 2009).

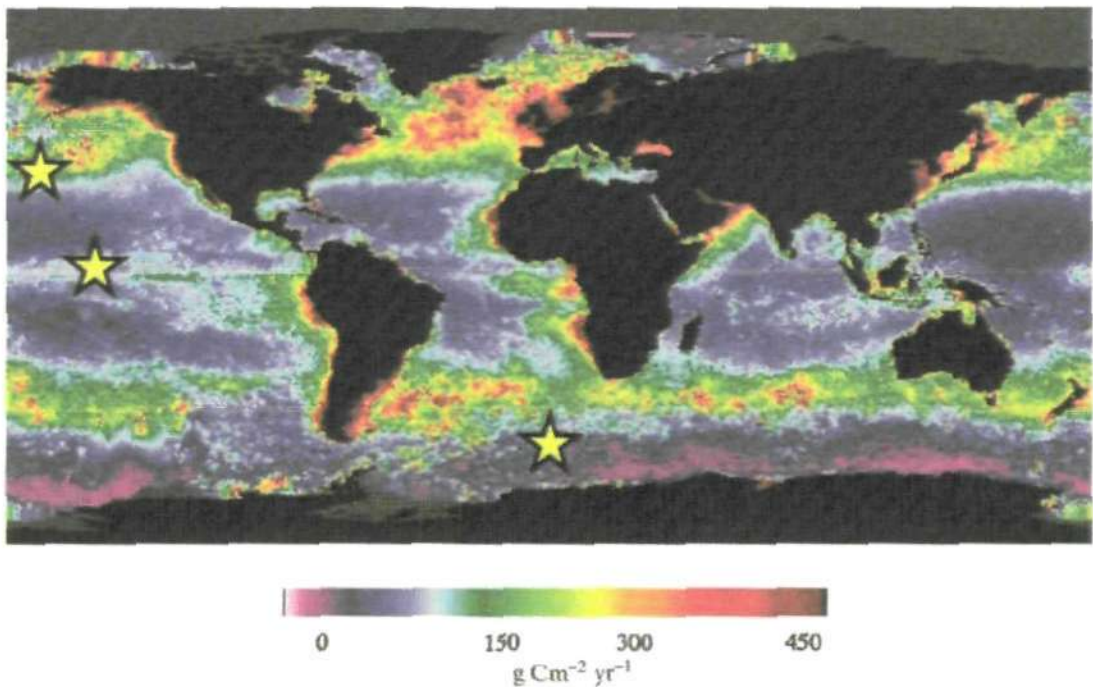


Figure 1. 2. Distribution of primary production in the oceans (de la Rocha, 2003), with the major HNLC regions marked. HNLC regions are replete with the major nutrients but exhibit lower than expected primary production (reproduced from de Baar and La Roche, 2003).

As early as the 1920s the paradox of Antarctic waters, replete with the major nutrients but having low primary production, was first observed (de Jong *et al.*, 1998). However, it was not until the pioneering work of John Martin in the late 1980s/early 1990s that the *iron hypothesis* was proposed (Martin, 1990). Martin noted the inverse correlation between atmospheric CO₂ concentrations and the dust content of the Vostok ice cores from Antarctica. He proposed that primary production in HNLC regions could be stimulated by means of increased Fe inputs owing to higher dust loading via long-range atmospheric transport, and that such stimulation could have significant impacts on the global climate as a consequence of intense drawdown of CO₂ and lead to a reduction of atmospheric temperatures. However, the validity of this theory has been called into question following the results of a number of meso-scale Fe fertilization

experiments and modelling exercises, which failed to provide any evidence of significant carbon export to deep waters (Chisholm *et al.*, 2001; Boyd *et al.*, 2000; 2004; 2007; de Baar *et al.*, 2005; Zeebe and Archer, 2005; Blain *et al.*, 2007; Buesseler *et al.*, 2008; Pollard *et al.*, 2009). So, whilst there is little doubt that Fe distribution is an important factor in controlling primary production and climate, other mechanisms such as changes in oceanic circulation and sea-ice extent also play a significant role (*e.g.* Petit *et al.*, 1999; Behrenfeld *et al.*, 2006).

In addition to Fe, several first row transition metals (V, Cr, Mn, Co, Ni, Cu, Zn,) and some second row transition metals (Mo, Cd) are known to be essential for the efficient growth and functioning of marine primary producers (Table 1.1). These trace metals are often cofactors, or part of cofactors, in enzymes or structural elements in proteins (Morel and Price, 2003). As essential trace metals are actively assimilated by phytoplankton, this may be an important factor in controlling surface water concentrations and distributions in seawater (Bruland and Lohan, 2003). An interesting paradox in the oceans is that whilst planktonic microorganisms mediate the chemistry and cycling of biologically significant trace metals, the same metals exert an influence on the growth of the organisms and their cycling of the major nutrients (*e.g.* carbon and nitrogen). Such interaction results from the complex co-evolution of planktonic life forms and ocean chemistry (*e.g.* de Baar and La Roche, 2003; Saito *et al.*, 2003), and has resulted in a situation where biological productivity is maintained in an environment impoverished in essential elements, and where phytoplankton have evolved a number of novel uptake mechanisms operating at the limits

imposed by uptake kinetics (Morel and Price, 2003). Morel and Price (2003) emphasise this point by concluding their paper with the argument that these uptake mechanisms are refined such that,

"The biogeochemical cycles of trace metals in the oceans may thus have reached the limit of what is physically, chemically, and biochemically possible."

The chemical form and quantity of the metals required for phytoplankton growth is dependent on their evolutionary history and on their adaptations to metal availability, both of which vary widely between oceanic provinces (Peers and Price, 2006). A number of culture studies have found that the unchelated concentrations of several trace metals to be limiting phytoplankton growth, at the range estimated for surface seawater. The differential effects observed in different species implies that these metals exert an influence over the physiology and ecology of marine phytoplankton (Ho *et al.*, 2003 and references therein). The elemental cellular quotas of five eukaryotic phyla are shown in Figure 1.3, which clearly shows that Fe and Mn are quantitatively the most important trace metals in marine phytoplankton, being on average approximately an order of magnitude more abundant than Co, Cd, Cu, Mo and Zn. Of the fifteen species of phytoplankton investigated by Ho *et al.* (2003) significant interspecies variability of cellular trace metal quotas was found. In addition to apparent systematic differences in the composition of the different phyla, Ho *et al.*'s (2003) work illustrates the different cellular requirements for trace metals of various phytoplankton species. Thus, highlighting the potential for changes in community structure, changes that could in turn alter ecosystem functions, such as carbon fixation, which, given the current concerns over

climate change and elevated CO₂ concentrations is a vitally important ecosystem function (Emmerson and Huxham, 2002).

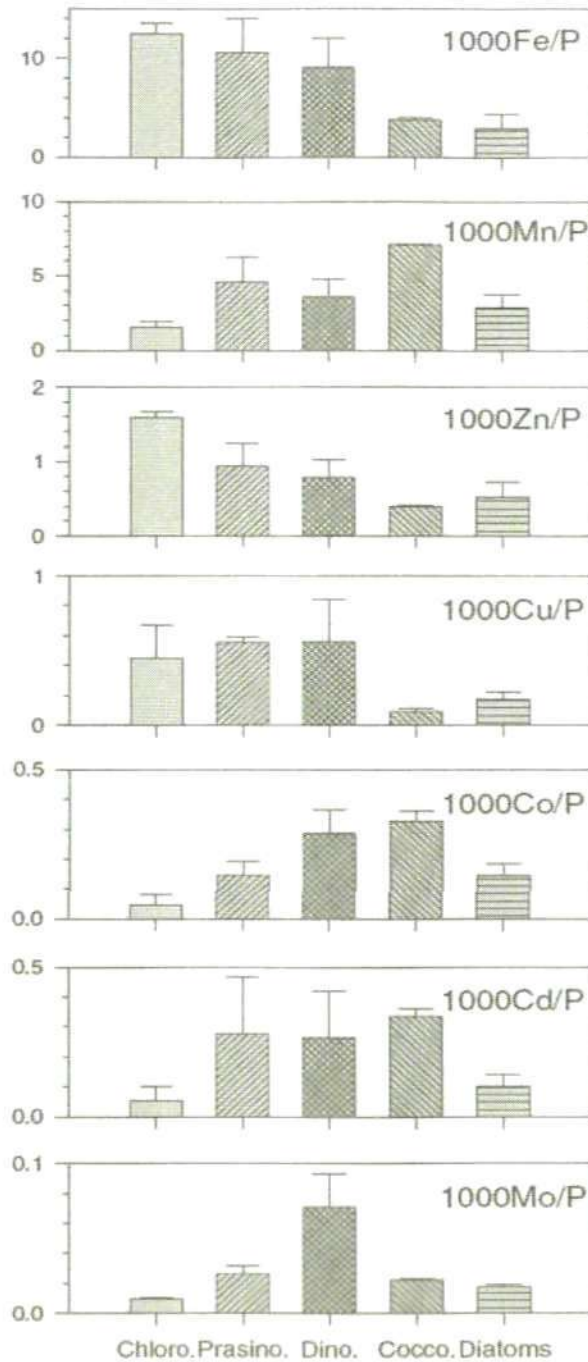


Figure 1. 3. Comparison of the average elemental quotas in five eukaryotic phytoplankton phyla. Elements are normalized to P (mmol/mol). For $n > 2$, the error bars represent 1SE; for $n = 2$, the error bars represent 1 average deviation. Chlorophyceae, $n = 3$, Dinophyceae, $n = 4$, Prymesiophyceae, $n = 2$, Bacillariophyceae, $n = 4$ (reproduced from Ho *et al.*, 2003).

The availability of essential trace metals, to phytoplankton assemblages in the remote open oceans, is further compounded by the fact that more than one element may limit growth, *e.g.* Fe and P have been demonstrated to co-limit nitrogen fixation in the eastern tropical North Atlantic (Mills *et al.*, 2004). Figure 1.4a illustrates how the numerous nitrogen transformations involve metalloenzymes. This requirement led Morel and Price (2003) to hypothesise that low metal availability may limit critical steps in the nitrogen cycle. In addition to the trace metal requirements of phytoplankton for nitrogen acquisition, the uptake of carbon and phosphorus is also a function of trace metal availability, principal requirements being shown in Figure 1.4b.

As well as indirectly influencing the carbon cycle, through the impacts on the nitrogen cycle, trace metal availability can have a direct effect on photosynthesis and respiration at both the cellular and ecosystem level. Given that trace metals play a fundamental role in biological processes in aquatic organisms (*e.g.* Howell *et al.*, 2003), and that aquatic organisms are involved in a range of ecosystem functions, slight shifts in their dynamics can have global consequences. Prediction of these consequences requires a comprehensive understanding of trace metal dynamics and the processes impacting on them. Thus, the key to understanding the role of the global ocean in global change lies in understanding the cycling and biological function of trace metals in the modern global ocean (de Baar and La Roche, 2003).

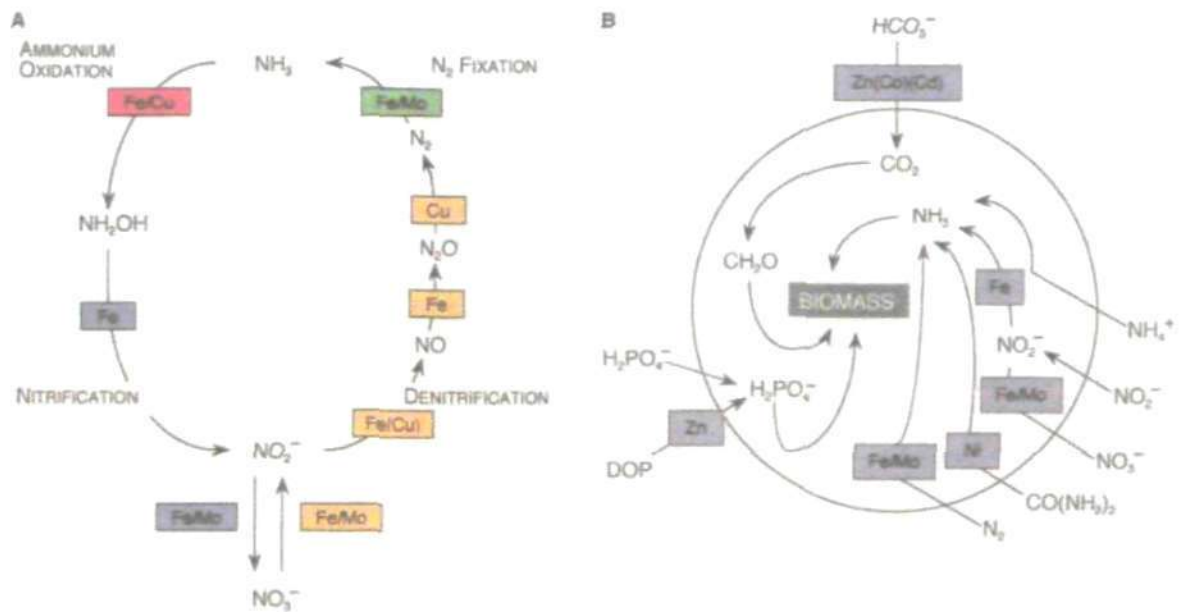


Figure 1. 4. (a) The main trace metal requirements for stages in the nitrogen cycle showing the metal cofactors at each enzymatically catalysed step. Each group of reactions is colour coded: nitrogen fixation (green); denitrification (orange); nitrification (blue) and ammonium oxidation (red). With the exception of Mo (surface concentration $0.1 \mu\text{M}$) all metals shown are depleted in surface waters. (b) The principal metal requirements for carbon, nitrogen and phosphorus acquisition and assimilation by marine phytoplankton (reproduced from Morel and Price, 2003).

1.2. Biological functions of cobalt and iron

Cobalt: Cobalt concentrations in the open ocean range from 4–120 pM, with many regions tending to the lower end of this scale (e.g. Knauer *et al.*, 1982; Martin *et al.*, 1989; Saito *et al.*, 2004). Saito *et al.* (2004) argue that the study of Co biogeochemistry in the oceans is complicated by two issues; (1) biochemical substitution of Co or Cd for Zn, and (2) the influence of the chemical speciation of Co, Zn and Cd on the bioavailability of these metals to phytoplankton. However, whilst some organisms (e.g. centric diatoms and coccolithophores) can substitute these three metals, there are others, particularly the

photosynthetic cyanobacteria (*Prochlorococcus* and *Synechococcus*), and some diatom species, that have an absolute requirement for Co (Sunda and Huntsman, 1995a; Saito *et al.*, 2002). Cobalt is a requirement for vitamin B₁₂ (cobalamin) synthesis. Vitamin B₁₂ is a biologically produced, Co-containing organometal compound that only select bacteria and archaea are able to synthesise *de novo*, thus all eukaryotes must either acquire it from the environment, or possess an alternative biochemistry with no requirement for vitamin B₁₂ (Bertrand *et al.*, 2007). However, as cellular quotas of vitamin B₁₂ tend to be very small ($\sim 0.01 \mu\text{mol} (\text{mol C})^{-1}$), Wilhelm and Trick (1995) argue that vitamin B₁₂ is not likely to represent a significant portion of the cellular Co. Yet, despite this low cellular quota, the limited data relating to the biogeochemistry of vitamin B₁₂ in the oceans suggests that this vitamin is involved in complex feedback interactions involving multiple environmental factors, and may also exist at limiting concentrations in seawater (Bertrand *et al.*, 2007; Panzeca *et al.*, 2008; King *et al.*, 2011).

Iron: Iron concentrations in the surface waters of the open ocean are typically < 1 nM, yet it plays a key role in the biochemistry and physiology of phytoplankton. Iron complexes have fundamental roles in intracellular respiration, and oxygenic and non-oxygenic photosynthesis where it is an essential component in the photosynthetic apparatus (photosystems I and II and cytochromes). Iron is a necessary enzymatic component in virtually all stages of the nitrogen cycle (Fig. 1.4a) and is required for the reduction of sulphate, and is a constituent of the enzyme ATP synthase (Jacobs and Worwood, 1974). Protein bound Fe-complexes are involved in a diverse array of metabolic

pathways, as they act as vital electron mediators (Falkowski and Raven, 1997). This multiplicity of uses has led Rue and Bruland (1995) to argue that Fe is the most important bioactive trace metal in the oceans. However, Fe is by no means the only essential bioactive element.

1.3. Biogeochemistry of cobalt and iron

1.3.1. The speciation of trace metals in seawater

Central to the determination of trace metal bioavailability, and where relevant toxicity, to phytoplankton is quantification of the chemical species present in seawater (Saito *et al.*, 2004), and thus it is of ecological relevance to determine the speciation, and fractionation of trace metals in natural waters. The factors controlling equilibrium speciation are (1) oxidation potential (Eh), (2) pH, (3) the presence of inorganic ligands (*e.g.* OH^- , CO_3^{2-}), and (4) the presence of organic ligand classes. In addition ionic strength, temperature and pressure are also important, as is the concentration and type of ligands present which are themselves a function of pH (Millero and Pierrot, 2002). The following section will address the issue of speciation twofold, describing complexation by inorganic and organic ligands as well as considering the redox speciation of Co and Fe.

The concentration of the free hydrated metal ion, $[M^{2+}]$, is known to strongly influence bioavailability. However, recent research has demonstrated that some organically complexed trace metals are also available to phytoplankton.

For instance, Fe bound to siderophores is readily available to phytoplankton (Hutchins *et al.*, 1999; Maldonado and Price, 1999). Siderophores are low molecular weight organic chelators with a very high and specific affinity for Fe(III) (the thermodynamically stable Fe species in oxic seawater). The synthesis of siderophores, by phytoplankton, is regulated by the concentration of the free hydrated Fe³⁺ ion in seawater, the function being to mediate microbial Fe-uptake of the predominant form of dissolved Fe in seawater (Maldonado and Price, 1999). Key to the argument of the importance of the biological role of Co is evidence documenting the production of strong, specific Co-chelators, both in the field (Saito *et al.*, 2005) and *in vitro* (Saito *et al.*, 2002). Morel and Price (2003) hypothesise that Co-ligands in surface waters are produced by cyanobacteria, and that these "cobalophores" are analogous to the production of siderophores for the chelation and uptake of organically complexed Fe.

It was in the 1980s that the first generally accepted convincing evidence for the organic complexation of metals, at concentrations typical of those occurring naturally in seawater, began to become available (Coale and Bruland, 1988; Bruland, 1989). Voltammetric analysis of seawater samples has demonstrated that > 98.5% Fe(III) (Gledhill and van den Berg, 1994; Rue and Bruland, 1995; Boyé *et al.*, 2006) and >90% Co (Ellwood and van den Berg, 2001; Saito and Moffett, 2001) in surface waters is organically complexed. However, the picture is complicated by the fact that natural organic metal-binding ligands are not a single entity, rather distinct classes of ligands exist with strong and relatively specific affinities for particular metals (Bruland and Lohan, 2003). At present

the chemical structures of few organic metal binding ligands in seawater have been fully structurally characterised (Barbeau *et al.*, 2001; Vraspir and Butler, 2009). Researchers have been able to determine stability constants for the formation of metal-organic ligand complexes without knowing the chemical structure of the ligands (Millero and Pierrot, 2002 and references therein). Trace metal-ligand reactions can be described by equation 1.1.



Equation 1.1

Equation 1.1 is a general equation for metal-ligand binding (modified from Nürnberg and Valenta, 1983), where X denotes inorganic ligands that form usually labile, mononuclear complexes with trace metals (the inorganic ligands that are commonly abundant and significant for trace metal speciation in seawater are Cl^- , OH^- , CO_3^{2-} , HCO_3^- and SO_4^{2-}), L denotes organic ligands with a strong and relatively specific affinity for a particular metal, and K_s is the stability constant.

Cobalt: The biogeochemistry of Co is believed to share a number of similarities with Fe (Saito and Moffett, 2002). Uncomplexed Co in seawater has similar redox chemistry to Fe, being present in the same two oxidation states under typical Eh and pH conditions. In common with Fe, the reduced Co^{2+} form is not thermodynamically stable in oxic seawater, and is rapidly oxidised to Co^{3+} . As for Fe^{3+} , Co^{3+} is poorly soluble owing to the precipitation of hydrolysis species,

and does not appear to accumulate in the deep, older waters of the Pacific like the nutrient-type trace metals, e.g. Zn. Although Co can exist in natural waters as Co^+ , Moffett and Ho (1996) found little evidence for its existence in seawater.

Iron: The oceanic chemistry of Fe is highly complex and, as yet, our understanding is incomplete (e.g. Rue and Bruland, 1995; Tortell *et al.*, 1999). The ferric (Fe^{3+}) form is thermodynamically stable, but insoluble, in oxic seawater, and therefore rapidly precipitates as $\text{Fe}(\text{OH})$ species. Although Fe^{2+} is soluble in seawater, it is rapidly (half-life in the order of a few minutes at $\sim\text{pH}$ 8.2) oxidised to Fe^{3+} in surface seawater (Elrod *et al.*, 1991). Insoluble Fe^{3+} consists largely of colloidal hydrolysis species, e.g. $\text{Fe}(\text{OH})_3$, which are rapidly scavenged out of the water column via coagulation and adsorption onto sinking particulate material. However, there are processes (e.g. photoreduction) that reduce Fe^{3+} to Fe^{2+} (Gledhill and van den Berg, 1995) in surface waters. Thus, it is necessary for organisms that require Fe for growth to have developed mechanisms to acquire the soluble, but unstable, Fe^{2+} needed for growth. One such important physiological response is that of the open ocean diatom, *Thalassiosira oceanica*. Under Fe-limiting conditions this species has the ability to reduce organically chelated Fe^{3+} , which may then be transported and assimilated for growth (Maldonado and Price, 2001).

In the Northeast Atlantic (a region not currently believed to be Fe-limited), Boyé *et al.* (2006) combined Fe speciation and phytoplankton data to conclude that the *in situ* production of organic ligands could be attributed to cyanobacteria

(*Synechococcus* spp. being numerically dominant). Thus, maintaining dissolved Fe in solution at a concentration far in excess of its solubility.

1.3.2. Open ocean surface concentrations

A selection of concentrations of dCo and dFe in the open ocean are presented in Tables 1.2 and 1.3. Note that the 'dissolved' pool is operationally defined. In some studies listed below it is defined as $< 0.2 \mu\text{m}$ and others $< 0.4 \mu\text{m}$. Both of these size fractions will include the truly dissolved fraction (operationally defined as $< 0.02 \mu\text{m}$). In the case of Fe, increases in the concentration of dFe are seen to follow increases in the concentration of colloidal Fe (Bergquist and Boyle, 2007). It is also a testament to the challenges associated with the sampling of deep waters that there are far fewer concentrations determined below 500 m than in surface waters.

Table 1. 2. A selection of dissolved cobalt concentrations in the open ocean (dissolved defined as either < 0.2 or < 0.4 μm).

Co Concentrations (pM)			
Ocean	Surface (0-10 m)	Depth (>500 m)	References
Atlantic			
Sargasso Sea (Station S)	18 - 44	20 - 43 (83) ^b	Jickells & Burton (1988)
Sargasso Sea (BATS)	17 - 73 (~44 m)		Saito and Moffett (2002)
W (N) Atlantic (BATS-coastal Massachusetts)	19 - 133		Saito and Moffett (2002)
NE Atlantic	33	31 - 41	Ellwood and van den Berg (2001)
NE Atlantic	19 - 45		Panzeca <i>et al.</i> (2008)
N & S (E) Atlantic (open ocean inc. gyres)	36 - 53 ^a		Bowie <i>et al.</i> (2002a)
N & S (E) Atlantic (upwelling & shelf)	47 - 93 ^a		Bowie <i>et al.</i> (2002a)
S (W) Atlantic (upwelling & shelf)	73 ^a		Bowie <i>et al.</i> (2002a)
Pacific			
NE Pacific (Gulf of Alaska)	<10 - >20		Martin <i>et al.</i> (1989)
NE Pacific (Central California shelf break)	109 - 119	24 - 49 (520-2350 m)	Knauer (1982)
N. Pacific (nr. Hawaii)	10 - 20	40 - 80	Noble <i>et al.</i> (2008)
Western Philippine Sea	95	22 - 30 (>1000 m)	Wong <i>et al.</i> (1995)
Southern Ocean			
S of Africa	5 - 59 (0-200 m)	25 - 73 (200-400 m)	Bown <i>et al.</i> (2011)
Sub-Antarctic Zone (S of Australia)	~10 - 30	~20 - 55	Ellwood (2008)
Ross Sea	31 - 51		Bertrand <i>et al.</i> (2007)

^aUnfiltered samples

^bValue in brackets is queried by Jickells and Burton (1988)

Table 1. 3. A selection of dissolved iron concentrations in the open ocean (dissolved defined as either < 0.2 or < 0.4 μm).

Fe Concentrations (nM)			
Ocean	Surface (0-10 m)	Depth (>500 m)	Reference
Global ocean averages			
N & S Pacific, N. Atlantic, Southern Ocean	0.07	0.76	Johnson <i>et al.</i> (1997)
Atlantic			
N. Atlantic Iceland Basin	<0.01 - 0.22		Nielsdottir <i>et al.</i> (2008)
N Atlantic (>51 °N)	0.09		Measures <i>et al.</i> (2008)
N Atlantic gyre (E)	0.2 - 1.2		Sarthou <i>et al.</i> (2003)
N Atlantic gyre (E)	0.1 - 0.4		Rijkenberg <i>et al.</i> (2008)
N Atlantic gyre (W = Sargasso Sea)	1 - 2 (summer); 0.1 - 0.2 (winter)		Sedwick <i>et al.</i> (2005)
Tropical N. Atlantic (4-18 °N)	1	2 (200-800 m)	Measures <i>et al.</i> (2008)
N (W) Atlantic	0.3 - 0.9		Bergquist and Boyle (2006)
S (W) Atlantic	0.2 - 0.7		Bergquist and Boyle (2006)
Pacific			
N. Pacific gyre	0.05 - 0.1		Nishioka <i>et al.</i> (2005)
N. Pacific gyre	0.2 - 0.7		Boyle <i>et al.</i> (2005)
Central N Pacific gyre	0.37	0.38 (500 - 4000 m)	Bruland <i>et al.</i> (1994)
Equatorial Pacific	0.02 (15 m)	0.4 - 0.5 (400 - 600 m)	Wu <i>et al.</i> (2007)
S Pacific gyre	0.09 - 0.2		Blain <i>et al.</i> (2007)

Southern Ocean			
Sub-Antarctic & polar fronts (Pacific Sector)	0.1 - 0.7		Lannuzel <i>et al.</i> (2010)
SOIREE station (Pacific Sector)	0.05 - 0.11		Boyd <i>et al.</i> (2000)
Polar front (Atlantic Sector)	0.2 - 0.3		de Jong <i>et al.</i> (1998)
Ross Sea	0.11 - 0.31		Bertrand <i>et al.</i> (2007)
Indian Ocean			
NW Indian Ocean	0.3	1	Saager <i>et al.</i> (1989)
Mediterranean			
Ligurian Sea	0.8 (Oct. 1994); ≤0.13 (May 1995)		Sarthou & Jeandel (2001)
Arabian Sea			
	1.5 (25 m)	1.7	Witter <i>et al.</i> (2000)
Red Sea			
Gulf of Aqaba	5.2 - 13 (Aug. 2003); 0.7 - 6.8 (Mar. 2004)		Chase <i>et al.</i> (2006)

As for other bioactive trace elements (*e.g.* Fe), surface depletion of dissolved Co has been observed (Saito and Moffett, 2002) (northwest Atlantic), yet conversely, others (*e.g.* Ellwood and van den Berg, 2001), report no such surface depletion (northeast Atlantic), suggestive of either a source, *e.g.* atmospheric deposition, or a mechanism preventing maximal uptake of Co in this region. However, Saito and Moffett (2002) found no obvious response between the summer maximum in aeolian dust deposition and Co concentration in surface waters in samples from the Bermuda Atlantic Time-Series station, BATS, although they acknowledge that this may have been a consequence of the positioning of the sampling mooring (at ~44 m) below the summer mixed layer. Furthermore, whilst some researchers found an inverse correlation between Co and salinity, suggestive of a continental weathering input, others found no such relationship (Saito and Moffett, 2002 and references therein).

In oceanic surface waters the maximum concentration of dissolved Fe is a function of the solubility of inorganic forms and the availability of organic complexing ligands, which promote greater solubility (Vink and Measures, 2001; Boyé *et al.*, 2006). Concentrations of Fe vary by two orders of magnitude across the surface of the world's oceans (Bowie *et al.*, 2006). Historically there has been some degree of variation in the dissolved metal concentrations reported, possible explanations for this discrepancy being attributed to inter-laboratory differences and/or technique sensitivities and to differences in sample preparation and storage time, as well as to natural variation. In recent years there have been a number of rigorous intercomparison exercises, *e.g.* *IRONAGES* (Bowie *et al.*, 2006) and *SAFe* (Johnson *et al.*, 2007) and

substantial progress towards an appropriate low concentration certified reference material for dissolved Fe in seawater has been made (Johnson *et al.*, 2007).

1.3.3. Vertical distributions

In order to discuss the depth profiles shown in Figures 1.5 and 1.6 it is necessary to consider them in terms of their chemical behaviour and distributions in the water column. Bruland and Lohan (2003) grouped trace metals into three principal categories conservative, nutrient and scavenged. Currently our knowledge of Fe distributions in the ocean exceed that of Co, therefore the following discussion reflects the state of the art and is thus biased.

Conservative behaviour: Metals that exhibit conservative behaviour maintain a relatively constant ratio with salinity, have oceanic residence times in excess of oceanic mixing times ($> 10^5$ years) and have weak interactions with other particles (e.g. molybdenum).

Nutrient-like: Distributions of these metals are dominated by the internal cycle of biological assimilation in surface waters, the export or transport of a proportion of this material out of the surface layer, followed by the oxidation and remineralisation of the majority of this material in deeper waters. Surface depletion, owing to assimilation by phytoplankton or adsorption to biogenic particles, followed by an increase with depth (regeneration owing to the decomposition or dissolution of sinking particles) is characteristic of this type of

behaviour. Furthermore, as nutrient-like metals are not readily scavenged in the deep ocean, their concentrations increase along the flow path of the oceanic deep waters. Thus, the older waters of the Pacific Ocean are enriched with nutrient-like metals with respect to those of the Atlantic, resulting in strong interbasin fractionation. Nutrient-like metals have intermediate oceanic residence times (10^3 - 10^5 years). A striking example of a trace metal with nutrient-like characteristics is Zn, the vertical profile of which typically shows a strong correlation with silicic acid. Thus, in the open ocean the vertical distribution of metals exhibiting nutrient-like behaviour is determined by their biological role as an essential element.

Scavenged: Metals with this type of vertical profile are particle-reactive elements with oceanic residence times much less than the turnover times of oceanic water ($\sim 10^2$ - 10^3 years). Particles are removed or recycled through particle adsorption or precipitation. Owing to continual particle scavenging, there tends to be no increase from the Atlantic to the Pacific, in fact concentrations may decrease along the deep water flow path as the Atlantic basin experiences greater dust deposition than the Pacific basin (Ellwood and van den Berg, 2001; Gao *et al.*, 2001). In general, the concentrations of these metals exhibit maxima near major sources, such as rivers, atmospheric dust, bottom sediments and hydrothermal vents. An example of a metal with this type of behaviour is aluminium.

In addition to the main three classifications of trace metal behaviour described above, Bruland and Lohan (2003) describe a further two groups. The first,

whose behaviour can be classed as a hybrid of those previously described (see below), and a second where the trace metal can exist in more than one chemical form, with significantly different distributions, such as germanium.

Hybrid: Several trace metals including Co and Fe have behaviours that are strongly influenced by both recycling and relatively intense particle scavenging. As with the nutrient-like metals, dissolved iron (dFe) may be depleted in remote surface waters, such as the HNLC regions, and appears to be regenerated at depth (to ~1000 m). However, in the oligotrophic central ocean gyres, especially those subject to high dust inputs, surface maxima of dFe have been observed, thus more closely resembling the profiles of scavenged-type elements (Bruland *et al.*, 1994; Johnson *et al.*, 1997). As the oceanic residence time of Fe is estimated to be 100-200 years, less than the oceanic mixing time, the older deep waters of the Pacific are not enriched with Fe relative to the Atlantic (Johnson *et al.*, 1997). At depths in excess of ~1000 m Fe does not exhibit an increase in concentration typical of deep water regeneration. Concentrations in deep water remain relatively constant, maintained by a balance between the remineralisation of sinking particles and particulate scavenging, and may be maintained by complexation with strong organic ligands (Johnson *et al.*, 1997). Based on the limited data available on Co distributions in seawater, Saito and Moffett (2002) hypothesised that, in common with Fe, Co can exhibit both scavenged and nutrient-like behaviour, although Co's importance as a micronutrient is arguably more subtle than that of Fe (Saito *et al.*, 2004).

In the open ocean Co has a relatively unique profile (Ellwood and van den Berg, 2001); generally low concentrations of between 10 and 40 pM (0.01-0.04 nM) are observed in surface waters (to ~200 m depth), the minimum concentration at ~100 m likely corresponding with the chlorophyll maximum, and maximal biological removal. In plots of lower resolution than Figure 1.5 this feature may be obscured. Maximal concentrations are observed in the upper thermocline (30-100 pM), coinciding with the oxygen minimum zone (Saito and Moffett, 2002), where release from sinking particles exceeds scavenging. The concentration then decreases with further depth to between 10 and 30 pM (Knauer *et al.*, 1982; Martin *et al.*, 1989) but remains fairly uniform below 500 m, a balance between particle scavenging and remineralisation. Such a profile is typified by Figure 1.5. Like dFe, dissolved Co (dCo) profiles do not show interbasin fractionation (Saito and Moffett, 2002).

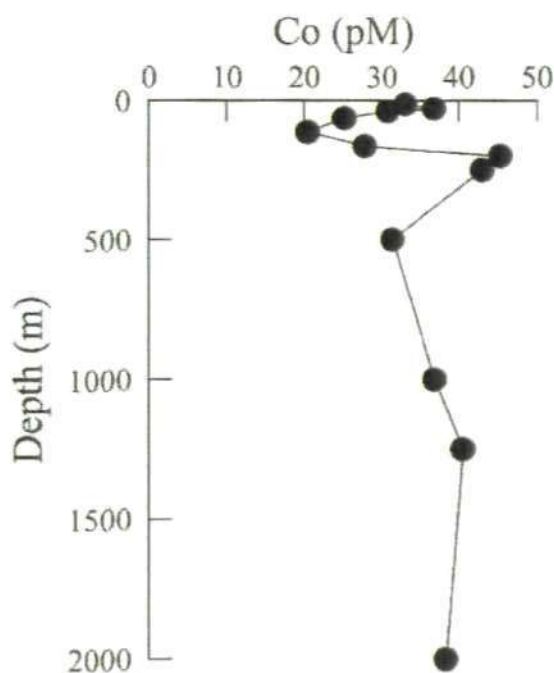


Figure 1.5. Vertical profile of dCo from the northeast Atlantic Ocean (reproduced from Ellwood and van den Berg, 2001).

Figure 1.6 shows vertical profiles of dFe from the HNLC high latitude North Atlantic and North Pacific. In this profile, the lowest concentrations of <0.2 nM are found in surface waters. Whereas, in deeper waters there is evidence for remineralisation and concentrations increase. At these depths concentrations are mediated by the biogeochemical controls of particle scavenging and remineralisation and below ~ 1000 m, where concentrations are fairly uniform, this represents a balance between these two processes. In contrast to in the oligotrophic central ocean gyres, particularly in areas of high aerosol dust inputs, dFe can exhibit a surface maximum (e.g. Martin *et al.*, 1989; Johnson *et al.*, 1997) and have profiles more analogous to a scavenged-type element. Bruland *et al.* (1994) attributed such a phenomenon (*i.e.* no surface depletion) to local seasonal conditions, where remineralisation of biogenic particles and nutrient regeneration dominates in the oligotrophic, surface mixed layer. In such systems, there is little new production (particulate organic matter export), owing to the strongly stratified water column that prevents vertical mixing and, thus, inputs of water enriched in macronutrients relative to the surface, and, by inference based on ^{234}Th scavenging data, a relatively low rate of reactive trace metal scavenging. Thus, conditions are favourable for accumulation of trace metals, such as Fe, from atmospheric deposition to the surface mixed layer.

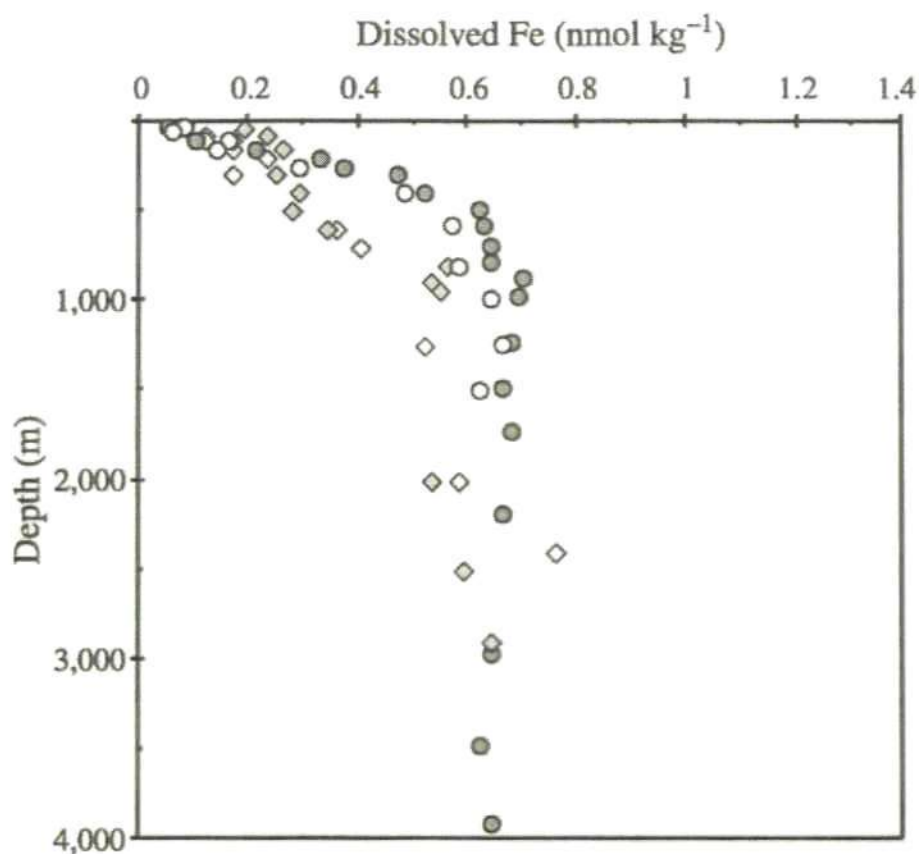


Figure 1. 6. Vertical profiles of dFe from high latitudes of the North Atlantic (diamonds) (59° 30' N, 20° 45' W; data from Martin *et al.*, 1993) and the North Pacific (circles) (50° N, 145° and 45° N, 142° 52' W; data from Martin *et al.*, 1989) (reproduced from Bruland and Lohan, 2003).

1.3.4. Supply of trace metals to the surface ocean

Constraints on primary production in the ocean can be divided into one of two factors; bottom-up (physicochemical processes which influence the adequate supply of essential macro- and micronutrients to the phytoplankton) or top-down (biotic) controls (Raven *et al.*, 2005). The bottom-up factors are directly related to physical processes and biogeochemical cycling. They may be further subdivided into (1) oceanic processes e.g. deep water circulation; upwelling regimes, (2) atmospheric deposition; wet and dry, (3) fluvial supply of

weathered continental material and (4) light stress, *i.e.* excessive or insufficient photosynthetically active radiation (PAR) or excess UV-B radiation.

1.3.5. Sources and sinks of trace metals to the ocean

In general, the sources and sinks of trace metals to the ocean (Table 1.4) are similar for all metals. The biogeochemical cycling of Fe is represented schematically in Figure 1.7. However, whilst the processes and mechanisms described are common to all trace metal cycling in the oceans, the relative importance and magnitude of these processes varies significantly between elements, and by location. For example, Bowie *et al.* (2002a) state that Fe concentrations are strongly dependent on the nature of input and removal mechanisms occurring in different water bodies, which vary between the ocean basins.

Table 1. 4. Sources and sinks of trace metals.

Sources	Sinks
Atmospheric deposition	Active assimilation by biota
Fluvial inputs	Passive scavenging onto SPM
Hydrothermal vent fluids	Sediments
Upwelling water/ vertical mixing	
Sediments	
Regeneration/remineralisation of particles at depth	

*SPM = suspended particulate matter

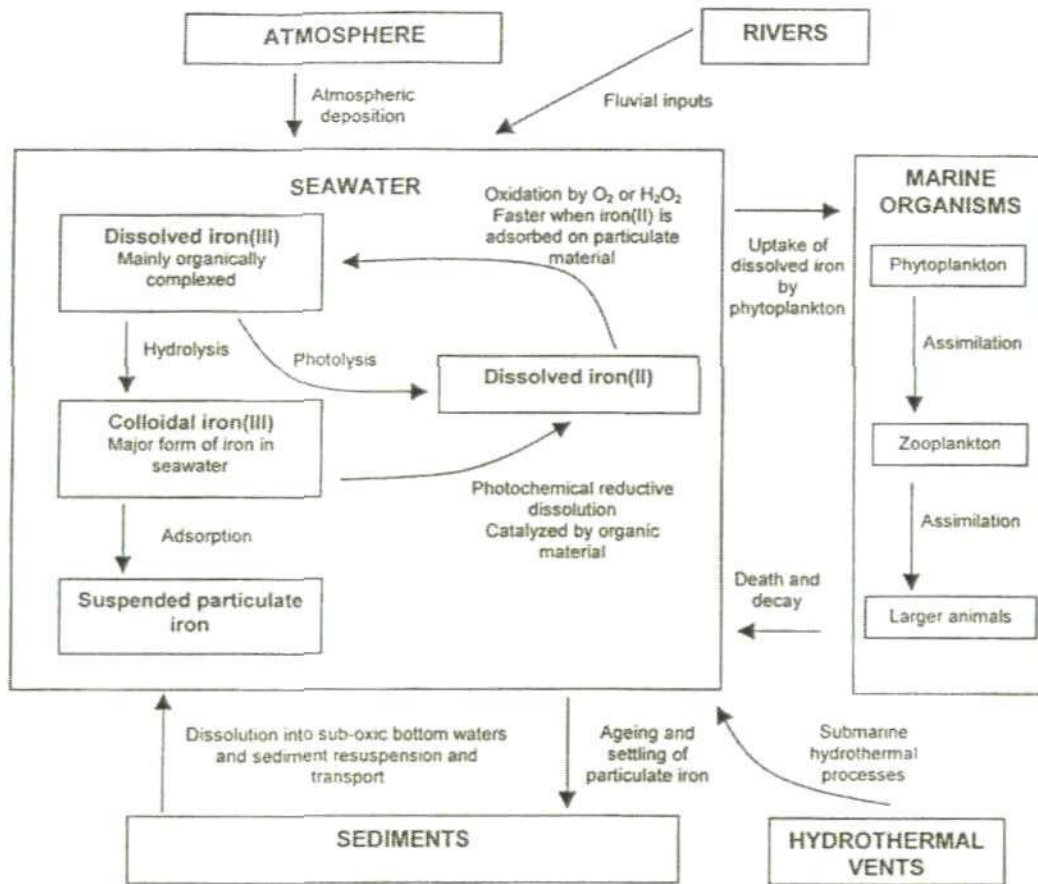


Figure 1. 7. Schematic diagram of the biogeochemical cycling of Fe in the ocean (reproduced from Achterberg *et al.* 2001).

1.3.5.1. Atmospheric deposition

Long-range transport and atmospheric deposition of dust is an important mechanism for the delivery of trace metals to the oceans. In regions of the ocean remote from continental input sources and hydrothermal vents, atmospheric deposition is critical to primary production, where this mechanism may be the only source of trace metals (Spokes *et al.*, 2001). Atmospheric deposition is typically greater in the Atlantic than Pacific Ocean, and in the northern hemisphere (Duce and Tindale, 1991; Gao *et al.*, 2001; Prospero *et al.* 2002). For instance, episodic dust storms originating in the Sahara Desert are

a significant source of Fe to oceanic surface waters (e.g. Prospero and Carlson, 1972; Prospero *et al.*, 1981; Prospero *et al.*, 2002)., an example of which can be seen by the intense dust event captured in Figure 1.9. Although at present the flux of Co to oceanic regimes is largely unknown, atmospheric inputs of Fe are better constrained, but are still subject to uncertainties of up to a factor of 10 in some regions (Mahowald *et al.*, 2005).

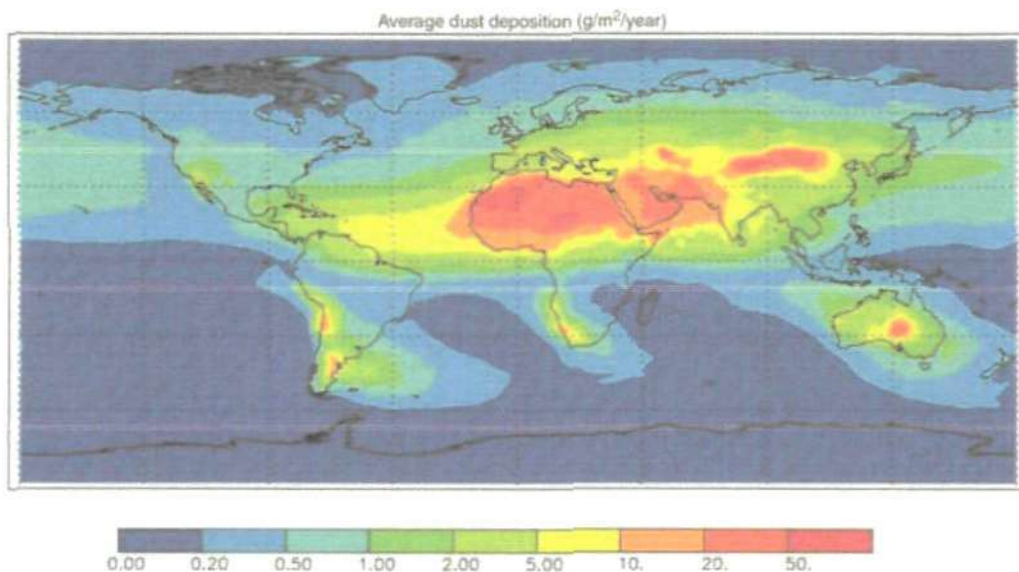


Figure 1. 8. Dust fluxes to the world's oceans based on a composite of three published modelling studies. The total atmospheric dust flux of $0.450 \text{ Tg year}^{-1}$ is distributed to the ocean basins as follows: North Atlantic 43%, South Atlantic 4%, North Pacific 15%, South Pacific 6%, Indian 25% and Southern Ocean 6% (reproduced from Jickells *et al.*, 2005).

Only a fraction of the trace metals associated with atmospherically transported dust are soluble (Table 1.5), and thus in a form available for uptake for primary production. Using a calculation, based on the degree of trace metal enrichment relative to crustal material, Chester *et al.* (1999) estimated the solubility of aerosols and demonstrated that whilst dry deposition is dominated by the particulate fraction, wet deposition of some trace metals (Cu and Pb) occurs predominantly in the dissolved phase which may be directly available to the

a significant source of Fe to oceanic surface waters (e.g. Prospero and Carlson, 1972; Prospero *et al.*, 1981; Prospero *et al.*, 2002)., an example of which can be seen by the intense dust event captured in Figure 1.9. Although at present the flux of Co to oceanic regimes is largely unknown, atmospheric inputs of Fe are better constrained, but are still subject to uncertainties of up to a factor of 10 in some regions (Mahowald *et al.*, 2005).

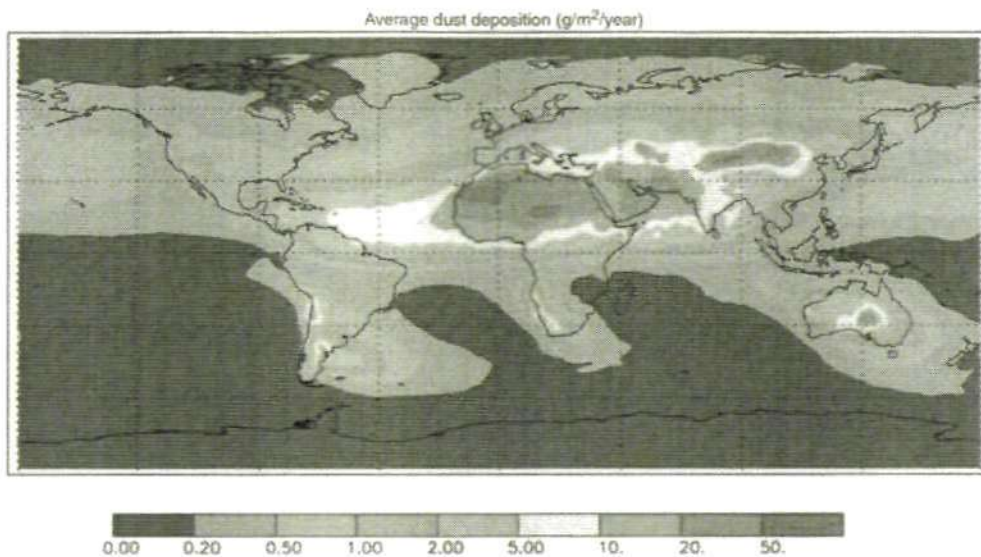


Figure 1. 8. Dust fluxes to the world's oceans based on a composite of three published modelling studies. The total atmospheric dust flux of $0.450 \text{ Tg year}^{-1}$ is distributed to the ocean basins as follows: North Atlantic 43%, South Atlantic 4%, North Pacific 15%, South Pacific 6%, Indian 25% and Southern Ocean 6% (reproduced from Jickells *et al.*, 2005).

Only a fraction of the trace metals associated with atmospherically transported dust are soluble (Table 1.5), and thus in a form available for uptake for primary production. Using a calculation, based on the degree of trace metal enrichment relative to crustal material, Chester *et al.* (1999) estimated the solubility of aerosols and demonstrated that whilst dry deposition is dominated by the particulate fraction, wet deposition of some trace metals (Cu and Pb) occurs predominantly in the dissolved phase which may be directly available to the

phytoplankton. Furthermore, trace metal solubility is a function of the mineral composition of the dust matrix, which in turn is a function of the provenance of the dust, alumino-silicates holding the metals most tightly bound to the dust matrix (Desboeufs *et al.*, 2005). Table 1.5 illustrates the relationship between composition of the dust matrix and the percentage of soluble trace metals in a model environment, clearly demonstrating the significant variation between particles of different mineral compositions.



Figure 1. 9. Saharan dust outbreak over the Canary Islands.

Saharan dust outbreak over the Canary Islands observed on 22/06/98 (available at: http://disc.sci.gsfc.nasa.gov/oceancolor/scifocus/oceanColor/sahara_dust.shtml)

Table 1. 5. Percentage solubility of selected trace metals from dust after a 120 min leach (UHP water acidified to pH 4.7 with H₂SO₄) (reproduced from Desboeufs *et al.*, 2005)

	Loess	AD	VFA	UP	PFA
Cd	Nc	10.1	Nc	96.6	37.6
Co	Nc	Nc	Nc	68.3	80.2
Cr	Nc	Nc	5.4	49.9	28.7
Cu	27.5	Nc	27.3	75.4	98.3
Fe	0.04	1.5	0.2	3.0	35.7
Mn	2.0	3.6	1.2	56.9	97.1
Ni	2.1	Nc	Nc	53.1	68.8
V	0.8	4.9	60.2	63.8	34.2
Zn	11	13.1	18.7	100	99.2

Nc: solubilities not calculated as dissolved concentrations were below the detection limit of the ICP-AES.

Loess: Loess (dust) from Cape Verde, selected as an analogue to Saharan aerosol particles. Diameter 2-20 µm, composition: alumino-silicate (quartz, feldspars, clays, pyroxenes); AD: Arizona Dust. Diameter 0.6-12 µm. Composition: quartz and clays; PFA: Porcheville Fly Ash. Diameter < 100 µm. Anthropogenic particles, principally graphite; VFA: Vichy Fly Ash. Diameter 2-100 µm. Anthropogenic particles, principally alumino-silicates; UP: Urban Particulate Matter. Diameter 30 nm-10 µm. Mixture of anthropogenic pollution and natural materials.

Although controls on dCo distributions in seawater are poorly constrained and understood (Saito and Moffett, 2002), surface maxima in the open ocean would suggest a predominantly atmospheric source, although an inverse correlation between dCo and salinity is indicative of a terrigenous source. Whilst examples of both these sources are described in the literature, it is of note that the relationship between measured concentrations of dCo in surface waters and observations, such as dust deposition events, were found to have no relationship (Saito and Moffett, 2002) suggestive that atmospheric deposition was not the predominant source of dCo to the Atlantic Ocean, near Bermuda.

1.3.5.2. Fluvial inputs

Fluvial inputs can provide a significant source of trace metals to surface waters adjacent to coasts, via the transport of weathered continental material, but is not a dominant source in remote open ocean regions. Trace metals are released from suspended particles, owing to the increased competition for binding sites with Mg^{2+} and Ca^{2+} ions in waters of increasing ionic strength. Despite this, the precipitation of major seawater ion chlorides (predominantly Ca^{2+} and Mg^{2+}) associated with trace metals, in the estuarine mixing zone, significantly reduces this input of trace metals that would otherwise have entered the marine system in the absence of such a transition zone (Turner and Millward, 2002). In laboratory studies using river water Sholkovitz and Copland (1981) found that dissolved trace metals (e.g. Co, Fe) exhibit colloidal properties, represented by the extent of coagulation in response to inorganic chloride complexes of major seawater ions. Coagulation, and subsequent precipitation, of inorganic chloride-trace metal complexes from destabilised river-borne colloids is an efficient mechanism for the removal of some trace metals, e.g. 80% Fe (Sholkovitz and Copland, 1981) from river water at seawater Ca^{2+} concentrations. However, this removal mechanism was not significant for Co with just 3% being removed (Sholkovitz and Copland, 1981). Sholkovitz and Copland (1981) found that interaction with dissolved organic carbon (DOC) was critical in determining whether trace elements will be removed (via precipitation of inorganic complexes), or held in the dissolved phase (via organic complexation) in the estuarine mixing zone. In addition to the DOC concentration, the extent to which trace metals are removed is also a function of the river flow rate, tidal cycle and the size of the suspended particle to which the trace metal is adsorbed, *i.e.* smaller sized particles are more likely to remain in

suspension during tidal cycles and at times of high flow rates, and thus escape the system.

1.3.5.3. Sediments and upwelling, vertical mixing and lateral transport

Although in open ocean environments trace metal supply to surface waters is believed to be dominated by atmospheric inputs (Duce and Tindale, 1991), there are a number of regions with low dust deposition (*e.g.* Southern Ocean, Bucciarelli *et al.*, 2001) and certain upwelling regimes (*e.g.* Peru and California upwelling, Saito *et al.* 2004; Bruland *et al.* 2005) for which the sedimentary flux is at least as significant as the atmospheric flux (Elrod *et al.*, 2004). In fact, a recent re-evaluation of Fe supply mechanisms indicates that sedimentary sources and atmospheric aerosol deposition supply similar contributions globally (Moore and Braucher, 2008). Vertical mixing and/or upwelling of deep waters have been shown to enhance sea surface concentrations of trace metals such as Fe and sustain productivity 100s of kms offshore (Elrod *et al.*, 2004). As neither Co nor Fe are significantly enriched in deep waters owing to their particle reactivity, upwelling at continental margins and lateral transport (via *e.g.* eddies, Johnson *et al.*, 2005; Ekman transport, Elwood *et al.*, 2008) provides a mechanism for surface supply that cannot be accounted for through budgets that overlook this source.

In the Santa Monica Basin, a region characterised by hypoxic bottom waters, dCo concentrations four times greater than at the surface were reported

(Johnson *et al.*, 1988), indicating significant sedimentary efflux. In hypoxic waters of the Peru upwelling, dCo associated with upwelling waters appears to be the dominant input source, and it is estimated that this source alone may be enough to supply 11% of the entire Pacific Ocean dCo inventory (Saito *et al.*, 2004). However, sediments can act as both a source and a sink of trace metals to the water column, and current data sets are insufficient to establish the extent to which upwelled dCo is recycled within surface and sub-surface waters and how much escapes to be returned to the sediments via association with particles.

There is also a question regarding the mechanism of benthic fluxes of dCo and dFe. A body of work (e.g. Johnson *et al.*, 1988; 1999; Elrod *et al.*, 2004; Saito *et al.*, 2004) indicates that the mode of supply differs for the two trace metals. Suboxic sediments have been shown to be a source of dCo to bottom waters (Sundby *et al.*, 1986), assumed to be from the release of dCo associated with Mn oxides (Saito *et al.*, 2004). However, in the Santa Monica Basin the high concentrations determined in hypoxic bottom waters (~124 pM at 879 m depth) were reduced to just 30 pM by 500 m depth, presumably due to particle scavenging, leading Johnson *et al.* (1988) to conclude that sedimentary sources did not supply surface waters of this region, yet more recent work by Elrod *et al.* (2004) has challenged this conclusion. In contrast to the Santa Monica Basin, in the Peru upwelling regime, where waters originate from the Equatorial Undercurrent which travels west across the surface of the Pacific basin (Toggweiler *et al.*, 1991), it is suggested that dCo from sedimentary sources is entrained to surface waters. Dissolved Fe, on the other hand, appears to be

supplied via release from suspended particles (Johnson *et al.* 1988), and thus incorporated into the Equatorial Undercurrent (Mackey *et al.* 2002).

1.3.5.4. Hydrothermal vent fluids

High temperature, metal-rich vent fluids are a major source of trace metals in the vicinity of vents. High concentrations of trace metals, including Co and Fe have been reported in the vicinity of hydrothermal vents as high temperature vent fluids are enriched with most metals by as much as 7-8 orders of magnitude (German and van Damm, 2003). As for other trace metal research, this area is dominated by studies of Fe. However, as Fe shares a similar redox chemistry to Co, the following discussion is likely pertinent for both these trace metals.

As hydrothermal iron precipitates rapidly on contact with seawater, hydrothermal vents have largely been overlooked as a source of dFe to the oceanic inventory. Yet hydrothermal vent fluids have been shown to be rich in organic Fe-binding ligands, therefore dFe may be stabilised against losses to the particulate phase via complexation at hydrothermal sites (Bennett *et al.*, 2008; Toner *et al.* 2009). A number of recent investigations have indicated that hydrothermal Fe may be an important source of oceanic dFe (Boyle *et al.*, 2005; Statham *et al.*, 2005; Bennett *et al.*, 2008; Toner *et al.*, 2009). In fact, Bennett *et al.* (2008) estimate that submarine venting may account for 12-22% of the global deep-ocean dissolved Fe budget. To this end, Tagliabue *et al.* (2010) initiated a series of model simulations to assess the hydrothermal contribution

to the oceanic dFe inventory. Their simulations indicated that the Southern Ocean is the region most sensitive to hydrothermal inputs, due to deep water ventilation, and that inputs of hydrothermal dFe increase productivity, augmenting carbon export by at least 5-15%. Furthermore, they argue that as hydrothermal dFe fluxes are constant over millennial timescales they may act to buffer the global dFe inventory against short-term fluctuations in dust deposition (decadal variability), concluding that this input term is necessary in order to assess the role of dFe sources that show variability on decadal or centennial timescales, *i.e.* sources that may be affected under climate change scenarios.

1.3.5.5. Regeneration of trace metals

As is true generally, Fe regeneration in the oceanic water column has been studied to a greater extent than Co, therefore it may be informative to describe the internal cycling of Co in terms of Fe cycling, due to the similarities in redox and speciation chemistry of the two elements. The process of internal recycling (*i.e.* within the water column) is of particular relevance to the nutrient-type bioactive trace metals (and to those elements that show aspects of nutrient-type behaviour *e.g.* Co and Fe). Both laboratory and field studies have demonstrated that zooplankton and bacterial grazers rapidly recycle Fe (Hutchins and Bruland, 1994; Barbeau *et al.*, 1996; Strzepek *et al.*, 2005). The high, specific cellular demand for Fe of numerous phytoplankton genera (*e.g.* Ho *et al.*, 2003) coupled with the rapid recycling of Fe within the microbial food-web has thus been termed the 'Ferrous wheel' by Kirchman (1996). In general it appears that Fe (and presumably other bioactive trace metals such as Co) is released as a result of microbial degradation and/or oxidation of carrier particles as they sink

through the water column (Bruland and Lohan, 2003). This results in higher concentrations being observed in intermediate and deep waters compared to the surface (except where inputs result in enrichment of sea surface concentrations, see Section 1.3.5.1). For Co, too, there is evidence for extremely efficient recycling in the upper water column, resulting in insignificant export fluxes of particulate Co (Noble *et al.* 2008; Bown *et al.*, 2011).

1.3.5.6. Removal mechanisms

For dCo an important removal mechanism in coastal waters is believed to be the oxidation of Co^{2+} to Co^{3+} (Moffett and Ho, 1996), via co-precipitation with Mn oxides, in the presence of manganese oxidising bacteria (Tebo *et al.*, 1984; Moffett and Ho, 1996). In contrast, in the surface waters of the oligotrophic Sargasso Sea, the main removal mechanism appeared to be dominated by biological uptake (Moffett and Ho, 1996). Description of this latter, biotic, removal mechanism is a significant development as, until recently, the prevailing view was that non-biological processes dominated the geochemical cycling of Co (Saito *et al.*, 2004). The major oceanic sinks of dFe are net biological uptake and scavenging by sinking particles (Blain *et al.*, 2007).

1.4. Co-limitation

It is the generally accepted convention in studies of nutrient limitation to ignore chemical conversions from one chemical state to another for the major nutrients (de Baar and La Roche, 2003). These authors argue that this approach is consistent with the paradigm of Liebig's Law of the Minimum whereby the growth of phytoplankton cells can only be limited by one nutrient at a time, aside from light. However, over the past twenty years it has been recognised that inorganic CO₂ (Riebesell *et al.*, 1993) and trace metals can act as limiting nutrients (*e.g.* Saito and Goepfert, 2008; Saito *et al.*, 2008). In contrast to the major nutrients, these micronutrients occur in numerous different chemical states under natural seawater conditions (see earlier sections), hence it is necessary to consider strictly chemical interconversions. Owing to the chemical speciation and many chemical forms in seawater of the various essential trace metals, and CO₂, an alternative approach is required, as Liebig-style limitation is not an environmentally realistic scenario. What is more, in a dynamic phytoplankton assemblage several elements could be limiting, or at least sub-optimal, for growth, owing to both the species composition and the various intracellular pathways that trace metals are involved in (de Baar and La Roche, 2003), coupled with the simultaneous scarcity of many nutrients (Saito *et al.*, 2008).

Based on mathematical formulations and visualisations Saito *et al.* (2008) propose that co-limitation (Table 1.6) can be categorised into one of three types.

Type I: independent nutrient limitation – this type of limitation describes two elements that are broadly speaking biochemically mutually exclusive, yet may occur in concentrations so low as to be potentially limiting, e.g. nitrogen and phosphorus. *Independent* is operationally defined in terms of the clear biochemical interactions of the other two types of co-limitation described by Saito *et al.* (2008), but these authors point out that, at the cellular level everything is related to some extent.

Type II: biochemical substitution co-limitation – describes two elements that can substitute for each other to fulfil the same biological role in an organism, e.g. Co for Zn in the enzyme carbonic anhydrase in eukaryotic phytoplankton (Sunda and Huntsman, 1995a; Saito *et al.*, 2002).

Type III: biochemically dependent co-limitation – describes a type of limitation in which the ability to acquire one element is inhibited by the absence or insufficient concentration of another, e.g. in some diatoms Fe uptake is inhibited by low Cu availability (Peers *et al.*, 2005).

Table 1. 6. Examples of potential nutrient co-limitation pairs in the marine environment (reproduced from Saito *et al.*, 2008).

Nutrient couple	Colimitation type (targeted enzyme)		Example refs. ^a
Zinc and cobalt (Cyanobacteria)	0 or I	Only one nutrient/independent	a,b
Nitrogen and phosphorus	I	Independent	c
Nitrogen and light	I	Independent	d
Nitrogen and carbon	I	Independent	d
Iron and cobalt	I	Independent	e
Iron and zinc	I	Independent	f
Iron and phosphorus	I	Independent	g
Iron and vitamin B ₁₂	I	Independent	h
Zinc and cobalt (eukaryotic phytoplankton)	II	Biochemical substitution (CA) [*]	b,i
Zinc and cadmium (diatoms)	II	Biochemical substitution (CA) [*]	j
Iron and Manganese (or Ni, or Cu-Zn)	II	Biochemical substitution (SOD) [*]	k
Zinc and cobalt (hypothesized)	II	Biochemical substitution (AP) [*]	l,m
Iron on light	III	Dependent	n
Zinc on phosphorus	III	Dependent (AP) [*]	f
Cobalt on phosphorus	III	Dependent (AP) [*]	m
Zinc on carbon	III	Dependent (CA) [*]	j
Cobalt on carbon	III	Dependent (CA) [*]	j
Cadmium on carbon	III	Dependent (CA) [*]	k
Copper on iron	III	Dependent (FRE and MCO) [*]	o
Iron on nitrate	III	Dependent (NR) [*]	p
Iron on nitrogen (N ₂ fixation)	III	Dependent (NIF) [*]	q
Molybdenum on nitrogen (N ₂ fixation)	III	Dependent (NIF) [*]	r
Nickel on urea (nitrogen)	III	Dependent (urease)	s
Copper on amines	III	Dependent (amine oxidase)	t

^{*} CA, carbonic anhydrase; SOD, superoxide dismutase; AP, alkaline phosphatase; FRE, ferric reductase; MCO, multicopper oxidase; NR, nitrate reductase; NIF, nitrogenase.

^a Example references: a, Saito *et al.* 2002; b, Sunda and Huntsman 1995a; c, Benitez-Nelson 2000; d, Heim and Sand-Jensen 1997; Riebesell *et al.* 1994; e, Saito *et al.* 2005; f, Franck *et al.* 2003; Wisniewski 2006; g, Mills *et al.* 2004; h, Bertrand *et al.* 2007; i, Morel *et al.* 1994; Yee and Morel, 1996; j, Price and Morel 1990; k, Tabares *et al.* 2003; Wolfe-Simon *et al.* 2005; l, Shaked *et al.* 2006; m, Sunda and Huntsman 1995a; n, Boyd *et al.* 2001; Maldonado *et al.*, 1999; Sunda and Huntsman 1997; o, Peers *et al.* 2005; Robinson *et al.* 1999; p, Raven 1988, 1990; Maldonado and Price 1996; q, Falkowski 1997; Berman-Frank *et al.* 2001; r, Howarth and Cole 1985; s, Price and Morel 1991; t, Palenik and Morel 1991.

1.5. Study area

The Atlantic Ocean is the second largest of the five major ocean basins (only the Pacific is larger). It encompasses all of the major marine ecological province types described by Longhurst (1998), from polar to tropical, oligotrophic gyre to coastal upwelling. Due to global air mass circulation, the Atlantic Ocean receives the greatest inputs of mineral dust (a significant source of trace metals to the open ocean; Duce and Tindale, 1991), predominantly from the Sahara (*e.g.* Prospero and Carlson, 1972; Prospero *et al.*, 1981), but there is also an anthropogenically influenced source of dust from North America/Asia that contributes to the total aerosol deposition flux (Sedwick *et al.*, 2007; Sholkovitz *et al.*, 2009). Owing to the distribution of the major continental land masses, the North Atlantic receives greater aerosol dust inputs than the South.

Trace metal studies of the Atlantic Ocean benefit from a legacy of time-series data. Situated in the Sargasso Sea, in the western North Atlantic, the Bermuda Atlantic Time-Series (BATS) station has provided data over the past few decades, and enabled regional scale studies to elucidate many aspects of marine Fe biogeochemistry, *e.g.* the role of aerosol provenance in solubility of aerosol Fe (Sedwick *et al.*, 2007). On a basin-wide scale the Atlantic Meridional Transect (AMT) (<http://www.AMT-uk.org/>), has occupied hydrographic sections between 50 °N - 50 °S allowing the mapping of trace metal distributions, including Co and Fe (*e.g.* Bowie *et al.*, 2002a). Since 1995, nineteen AMT cruises have been undertaken. In addition, there are several other major international oceanographic programmes that regularly conduct studies in the Atlantic Ocean, *e.g.* Climate Variability and Predictability (CLIVAR) (*e.g.* Measures *et al.*, 2008), Surface Ocean Lower Atmosphere Study (SOLAS) (*e.g.* Rijkenberg *et al.*, 2008), providing a wealth of ancillary data, as well as trace metal studies that can be used for comparison and validation. However, in contrast to Fe and Al, in particular, relatively little is known about the biogeochemical cycling of Co in the marine environment. Therefore, research conducted in the Atlantic Ocean provides an excellent opportunity to build on the work of previous oceanographic campaigns and further our understanding of Co biogeochemistry.

1.6. Aims and Objectives

The aim of the work presented in this thesis was to investigate sources of Co to the Atlantic Ocean and the impacts that they have on the biogeochemical cycling of Co in the different provinces of the Atlantic Ocean. In order to do this

a flow injection technique, using chemiluminescence detection (FI-CL), was optimised so that it was suitable for measuring picomolar (pM) concentrations of total dissolved Co in samples from open ocean regimes. Cobalt data, in conjunction with other hydrographic parameters, from three research cruises to different regions in the Atlantic are presented. *FeAST-6* was a small-scale study located in the Sargasso Sea in the western North Atlantic gyre, *INSPIRE* was also a small-scale study, this time located in the eastern North Atlantic gyre, whereas, *AMT-19* was a large-scale meridional transect from ~ 50°N - 50°S that sampled across diverse biogeochemical provinces (based on Longhurst, 1998), including two subtropical gyres and the equatorial upwelling regime.

Therefore, the key objectives were:

- (1) Optimisation of a sensitive, robust automated FI-CL system for the detection of total dissolved Co (pM) in open ocean samples, suitable for both shipboard and laboratory use (Shelley *et al.*, 2010).
- (2) To establish whether UV-irradiation of samples is a necessary pre-treatment in order to accurately determine total dissolved Co and submit data to the GEOTRACES Intercalibration Committee.
- (3) To submit the results of the UV-irradiation investigation to the GEOTRACES intercalibration to improve reporting of total dissolved Co concentrations.
- (4) To investigate if atmospheric deposition is a significant source of Co to surface waters (Shelley *et al.*, submitted).

- (5) To investigate the impacts of trace metals (Co, Cu, Fe, Zn) on biological rates (nitrogen fixation, primary production, heterotrophic bacterial production) (Turk *et al.* 2011).
- (6) To investigate sources and the biogeochemical cycling of Co in the upper water column (< 200 m) of the Atlantic Ocean across diverse biogeochemical provinces.
- (7) Interpretation of the Co data in conjunction with other hydrographic parameters to further our understanding of its biogeochemical cycling in the Atlantic Ocean and publish the results in peer reviewed journals.

In order to present the results from the stated aims and objectives, this thesis will be presented in the following format:

Chapter 2 – Describes the analytical methods employed during this study. The first section of this chapter describes the FI-CL method used for the determination of dissolved Co (dCo) in seawater samples, and has been published in *Limnology and Oceanography: Methods* (Shelley *et al.*, 2010). It is followed by a section describing a similar FI-CL technique for the determination of dissolved Fe (dFe) in seawater samples. The final section of this chapter details a technique for the determination of dissolved Cu (dCu) based on off-line preconcentration which uses ICP-MS as the detection system.

Chapter 3 – Results are presented from the *FeAST-6* cruise to the Sargasso Sea (31 - 24 °N) in June 2008. The purpose of this research was to establish

whether deposition of aerosol dust is a significant source of Co in this region. The results of this work are presented in conjunction with dFe and dAl (dissolved aluminium), Co and Fe solubility from aerosol dusts and biological data. This chapter is based on a paper that has been submitted to *Global Biogeochemical Cycles* for publication.

Chapter 4 – This chapter describes the author's contribution to the cruise, Investigation of Near Surface Production of Iodocarbons: Rates and Exchanges (*INSPIRE*) cruise. This cruise took place in the tropical Northeast Atlantic (26–16°N) from Nov.–Dec. 2007, and was part of the UK-SOLAS programme. During this cruise bioassays were conducted to investigate trace metal (Co, Cu, Fe, Zn) limitation of nitrogen fixation, primary production and heterotrophic bacterial production. The results of this study have been published in a co-authored paper in the *IMSE Journal* (Turk *et al.*, 2011).

Chapter 5 – In contrast to the two regional studies described in Chapters 3 and 4, this chapter presents dCo results from a large-scale meridional transect from 50°N–50°S (Falmouth, UK to Punta Arenas, Chile) that sampled diverse biogeochemical provinces as part of the Atlantic Meridional Transect programme (cruise *AMT-19*). The sources of Co to the different provinces are described and discussed in the context of the physico-chemical and biological factors that influenced dissolved Co distributions in the upper water column (< 200 m). Data from this cruise will be prepared as a paper for submission to *Marine Chemistry*.

Chapter 6 – The final chapter includes conclusions and recommendations for future research directions based on the findings presented in the previous chapters.

Chapter 2

Analytical Methods

2.1. Introduction

The extremely low (picomolar) concentrations of Co in open ocean waters presents a significant analytical challenge. In particular, the lack of highly-sensitive techniques suitable for shipboard use has hindered studies relating to its distribution and biogeochemical behaviour. Due to the ubiquitous sources of contamination and low concentrations of Fe (sub-nanomolar) in seawater, studies of this element are also very challenging. The presence of various metal components in research vessels, laboratories and manufactured items presents the constant threat of contamination. However, technological advances since the mid-1970s, combined with ultra-clean sampling and sample handling practices (Achterberg *et al.*, 2001), have enabled the accurate determination of these very low concentrations. The desire to better understand the biogeochemical cycling of bio-active trace elements, such as Co and Fe, in the ocean has created a demand for reliable protocols and sensitive, precise, accurate and rapid techniques suitable for ship- and laboratory-based use, and are currently being used to determine dissolved Co and Fe as part of the international GEOTRACES programme (www.ldeo.columbia.edu/res/pi/geotraces).

2.2. Background

2.2.1. Flow Injection Analysis

Flow injection systems are particularly well suited to oceanographic analyses, since they are portable and robust, contain relatively simple and inexpensive components, and offer analytical determinations over a dynamic range of as much as three orders of magnitude (Xu *et al.*, 2005). Modern FI systems are

capable of high sensitivity, although the limits of detection vary with the method of detection and the analyte in question. Flow injection systems can also be coupled with towed, trace-metal clean sampling devices, enabling the near-real time determination of trace metals in surface ocean waters (Bowie *et al.*, 2002b; Bruland *et al.*, 2005). In addition, FI methods are ideal for kinetic catalytic methods which use the analyte of interest as a reaction catalyst, resulting in highly sensitive analytical techniques (Resing and Mottl, 1992; Measures *et al.*, 1995; Aguilar-Islas *et al.*, 2006).

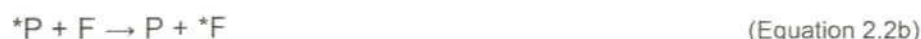
Flow injection manifolds can be coupled with different (portable) detection systems for the determination of trace metals. Examples of which are: flow injection using chemiluminescence detection (FI-CL) (Sakamoto-Arnold and Johnson, 1987; Cannizzaro *et al.*, 2000; Shelley *et al.*, 2010); flow injection using spectrophotometric detection (FI-spec) (Measures *et al.*, 1995; Sedwick *et al.*, 1997; Lohan *et al.*, 2006); flow injection using fluorimetric detection (FI-FI) (Ren *et al.*, 2001; Brown and Bruland, 2008). In addition, FI manifolds can also be coupled with laboratory-based instruments such as ICP-MS. The main advantage of ICP-MS detection over the portable technologies described above is the capability for simultaneous multi-element detection (*e.g.* Milne *et al.*, 2010). However, ICP-MS instrumentation is not portable, and therefore, is not suitable for use onboard research vessels.

Owing to the extremely low concentrations of dCo, dFe and dCu in open ocean waters (dCo = 4–120 pM, *e.g.* Knauer *et al.*, 1982; Martin *et al.*, 1989; Saito *et*

et al., 2004; $d\text{Fe} = 0.02\text{--}2$ nM, Landing and Bruland, 1987; Martin *et al.*, 1990; Measures and Vink, 1999; de Baar and de Jong, 2001; $d\text{Cu} = 0.5\text{--}3.5$, Boyle *et al.*, 1981) and the complexity of the seawater matrix (which contains the major seawater ions at concentrations up to 10^9 greater than $d\text{Co}/d\text{Fe}/d\text{Cu}$), it is essential to include a preconcentration step and separate the analyte from the major seawater cations. This can be done by incorporating a column containing a chelating resin into the FI manifold. Traditionally, the preconcentration resin of choice for the FI analysis of trace metals has contained 8-hydroxyquinoline (8-HQ) as the chelating group. Resin-immobilised 8-HQ is attractive, as it has a strong affinity for binding a number of trace metals of interest in seawater (Landing *et al.*, 1986). However, as resin-immobilised 8-HQ is not commercially available, it needs to be synthesised (Landing *et al.*, 1986; Dierssen *et al.*, 2001), which produces resins of varying quality. Hence commercially available chelating resins are preferable, since the quality of the resins is reproducible, and such resins have been successfully used in FI systems (*e.g.* Aguilar-Islas *et al.*, 2006; Lohan *et al.*, 2006) and combined with ICP-MS detection (Lohan *et al.*, 2005; Sohrin *et al.*, 2008; Milne *et al.*, 2010). Commercially available resins that have been used for the determination of trace metals in seawater include an NTA-type chelating resin for Fe and Cu (Lohan *et al.*, 2005), an EDTA-type resin for Al, Cd, Co, Cu, Fe, Mn, Ni, Pb and Zn (Sohrin *et al.*, 2008), and Toyopearl resin, which contains tridentate iminodiacetate functional groups, for Al, Cd, Co, Cu, Mn, Ni, Pb and Zn (Warnken *et al.*, 2000; Ndung'u *et al.*, 2003; Aguilar-Islas *et al.*, 2006; Brown and Bruland, 2008; Milne *et al.*, 2010).

2.2.2. Chemiluminescence

In this study, a FI manifold was coupled with chemiluminescence detection (FI-CL). Chemiluminescence (CL) is the emission of light (luminescence) by a substance as a result of undergoing a chemical reaction. This reaction does not involve a significant increase in temperature. Detection of CL requires relatively simple instrumentation (a photon multiplier tube, PMT) in comparison with absorption techniques as no light source is required. Due to its high sensitivity, wide dynamic range and speed of response, CL is a popular detection method (Lin and Yamada, 2003). Chemiluminescence emission occurs mainly during oxidation reactions or free-radical recombination. The general reaction scheme for luminescence emission is described by Equations 2.1–2.3: Flow injection-chemiluminescence (FI-CL) techniques utilise a chemical reaction to quantitatively determine an analyte's concentration following its reaction with a chemiluminescent dye. Thereby, the reaction between an analyte (*e.g.* Co or Fe) and reagents produces a product (P) that is in an excited state (*P) (Equation 2.1). Decay of the electronically excited *P to a lower energy state produces light-emitting photons ($h\nu$) (Equation 2.2a). Alternatively, the energy may be transferred to a fluorophore (F), which is usually a more efficient emitter (Equation 2.2b). When *F decays to a lower energy state, light emitting photons are emitted (Equation 2.3). The emitted photons are detected by a PMT, and the quantum yield is a function of the concentration of the analyte.



Cobalt – The reaction that produces chemiluminescence by the Co-enhanced oxidation of pyrogallol (1,2,3-trihydrobenzene) or gallic acid (3,4,5-trihydroxybenzene) (both polyhydric phenols) in a basic medium (pH 9–11, Slawinski, 1971) is a modification of the Trautz-Schorigen reaction (TSR) (Figure 2.1). In this reaction CL is produced in the spectral range 560–850 nm. Spectrometric (Bowen, 1964) and chemical data (Kearns, 1971) has suggested the formation of oxygen free radicals, although details of the mechanism and the exact nature of the chemiluminescence emitters is not clear. Discussion of a study by Stieg *et al.* (1977) in which gallic acid was oxidised to produce CL provides a basis for understanding the light emission process of the TSR. The oxidation of gallic acid (I) (when the functional group, R, is a carboxyl group) proceeds as a gradual multi-stage process, involving coloured intermediates (II) and (III). The final oxidation products (IV – VIII) are tropolone, oxalate and a brown, low-molecular weight, water soluble polymer (P) of unknown structure. Carbon dioxide (CO₂) and molecular O₂ (O₂* in Figure 2.1) are also generated. Bowen (1964) reported a narrow, red emission band at 630 nm, assigning it to molecular O₂, and a much weaker blue emission band in the range 440–510 nm which he assigned to the radiative deactivation of molecular O₂ and the excited state anions of caboxylic acids, resulting from the oxidative cleavage of

polyphenols. One of the intermediate products that has been identified is 2,3,4,6-tetra-hydroxy-5H-cycloheptabenzene-5-one-purpurogallin (PPG), which itself undergoes oxidation to produce CL (Slawinski, 1971).

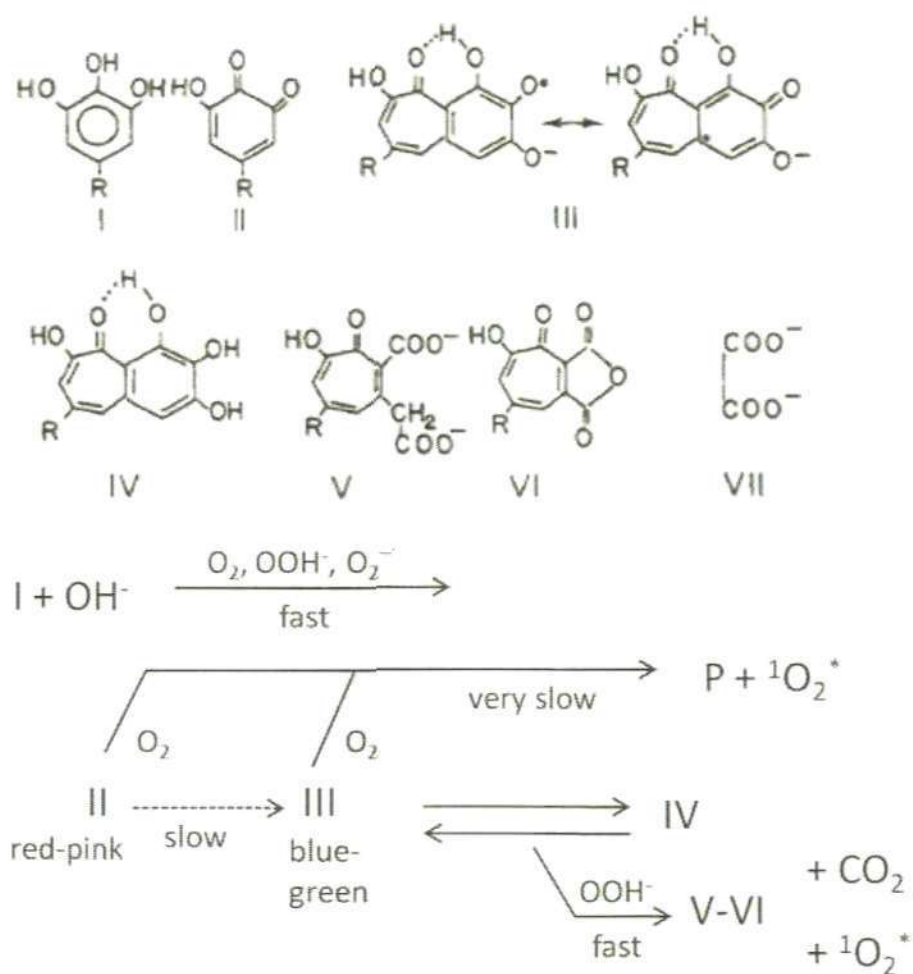


Figure 2. 1. The Trautz-Schorigen Reaction (the oxidation of pyrogallol), where R = COOH or COO (adapted from Slawinska and Slawinski, 1977).

Iron – For the determination of dFe in seawater, one of the most sensitive chemiluminescent dyes is luminol (5-amino-2,3-dihydrophthalazine-1,4-dione) (Achterberg *et al.*, 2001). The major CL-generating mechanism for luminol oxidation in aqueous solution has been proposed to occur in three basic steps (Merényi *et al.*, 1990) and is summarised in Figure 2.2.

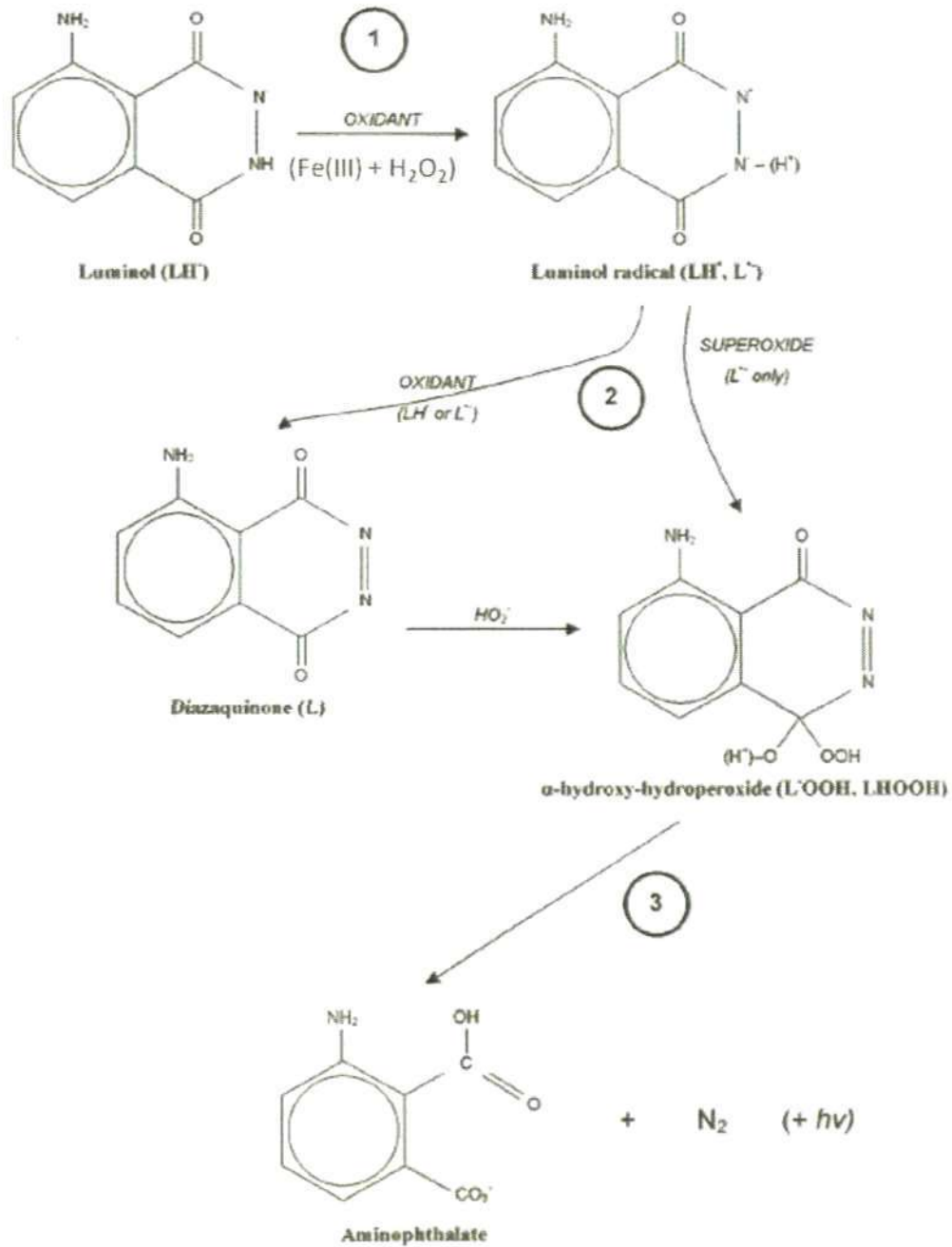


Figure 2. 2. The major steps in the oxidation of luminol (adapted from Rose and Waite, 2001).

The primary oxidation of luminol to the luminol radical (reaction 1, Figure 2.2) in the Fe(III) method of Obata *et al.* (1993) and de Jong *et al.* (1998) likely occurs through OH^\cdot or its radical derivatives which are produced during the oxidation of Fe(II) by H_2O_2 . The formation of the key intermediate α -hydroxy hydroperoxide (α -HHP) (reaction 2, Figure 2.2) is propagated through the oxidants O_2 and O_2^\cdot (formed from the initial oxidation of luminol). The final decomposition step (reaction 3, Figure 2.2) and generation of CL is dependent on the prototropic state of α -HHP (pK 8.2, Merényi *et al.*, 1990) and subsequently depends on pH. The optimum reaction pH is > 9.5 (de Jong *et al.*, 1998). Following preconcentration onto a chelating resin at pH 3.0–4.0, the luminol CL reaction provides an effective and highly sensitive method for determining low concentrations (sub-nanomolar) of total dissolved Fe, as Fe(III), in seawater (Obata *et al.*, 1993; de Jong *et al.*, 1998; de Baar *et al.*, 2008).

2.2.3. Dissolved Co and Fe

The measurement of trace metal species in seawater samples is frequently operationally defined by the sample pre-treatment process and the analytical technique employed. In this study, the dissolved fraction was determined. This is frequently operationally defined by the pore size of the filtration process, *e.g.* < 0.2 or $< 0.45 \mu\text{m}$. In reality this cut-off contains both the truly dissolved (soluble fraction) and colloidal fractions.

In addition to filtration techniques, acidification of samples affects the fractionation of Fe (and likely Co, which has similar redox chemistry). Therefore, when comparing concentrations it is important to note the size fraction being

reported and the sample preparation method (acidification and period of storage). A range of pHs have been suggested for stored samples; pH 3 (Obata *et al.*, 1993), pH 2 (Sarhou and Jeandel, 2001; Bowie *et al.*, 2002a), pH 1.7 (Lohan *et al.*, 2005). The range of pHs for sample preparation has resulted from investigations into the recovery of leachable Fe present in colloidal material contained in the filtered fractions. Lohan *et al.*, 2005 and Ussher *et al.*, 2005 demonstrated that in samples stored for > 1 week some of the dissolved Fe is reduced to Fe(II). In techniques that determine dissolved Fe as Fe(II), it is necessary to add a reducing agent to ensure full reduction of Fe(III) to Fe(II) (Bowie *et al.*, 1998). In contrast, in techniques that determine dissolved Fe as Fe(III) the addition of H₂O₂ is required as an oxidising agent prior to analysis. Recent studies have demonstrated that acidification of seawater samples to < pH 1.8 is required to release all Fe from colloids and Fe-binding ligands (Lohan *et al.*, 2005; Johnson *et al.*, 2007) and to achieve a stable sample within hours of collection. For dissolved Co, it appears that acidification to this pH is not adequate to fully release organically-bound Co and samples need an additional UV-irradiation step (Vega and van den Berg, 1997; Shelley *et al.*, 2010).

In this study, total dissolved cobalt (II + III) (dCo) and iron (II + III) (dFe) are defined as the fraction which passes through a 0.2 µm filter (*INSPIRE*, *AMT-19*) and 0.45 µm (*FeAST-6*) and determined after acidification (≤ pH 1.8, HCl) and storage for at least one month.

2.3. Aims and objectives

The aim of the work described in this chapter was to:

1. Develop a FI-CL method capable of determining dCo in open-ocean waters (4–120 pM). Therefore, the target detection limit was ≤ 4 pM and accuracy was $> 95\%$. This technique was validated by determination of dCo in SAFe reference samples, and was used to map surface concentrations and investigate water column distributions of dCo in the Atlantic Ocean, with a view to identifying input sources of this element (Chapters 3 and 5).
2. Develop a FI-CL method for the determination dFe (based on Obata *et al.*, 1993, de Jong *et al.*, 1998; de Baar *et al.*, 2008) in bioassays to investigate trace metal limitation of microbial processes affecting the nitrogen cycle in the tropical Northeast Atlantic Ocean (Chapter 4). The target detection limit was 0.02 nM with $> 95\%$ accuracy. This technique was validated by determination of dFe in SAFe reference samples.
3. Develop a FI technique using ICP-MS detection for the determination of dCu (based on Milne *et al.*, 2010) in bioassays to investigate trace metal limitation of microbial processes affecting the nitrogen cycle in the tropical Northeast Atlantic (Chapter 4). The target detection limit was 0.1 nM with $> 95\%$ accuracy. This technique was validated by determination of dCu in SAFe and GEOTRACES reference samples.

2.4. Determination of dCo in seawater using FI-CL

2.4.1. Introduction

Earlier FI-CL techniques have been used for the determination of dCo in estuarine and coastal seawater samples (Sakamoto-Arnold and Johnson, 1987; Cannizzaro *et al.*, 2000). In order to preconcentrate and separate the analyte (dCo) from the major seawater cations, these earlier methods used resin-immobilised 8-HQ. In this study, dCo was quantified from the CL signal produced by the oxidation of pyrogallol in the presence of the surfactant cetylammmonium bromide (CTAB) and hydrogen peroxide in a basic medium (Cannizzaro *et al.*, 2000). However, as dCo in open ocean waters is 1-2 orders of magnitude lower than observed in coastal waters significant modifications to the Cannizzaro *et al.* (2000) method were required. The first of these was the replacement of resin-immobilised 8-HQ with the commercially available chelating resin Toyopearl AF-Chelate 650M. This resin has a non-swelling hydroxylated methacrylic polymer base bead (Toyopearl HW-65) derivatised with iminodiacetate (IDA) functional groups (Brown and Bruland, 2008) with a high affinity for binding cobalt at pH 5-6 (Willie *et al.*, 1998; 2001). The second modification was the use of acidified ammonium acetate (pH 4) to condition the resin column prior to the sample loading, and to rinse the column after sample loading as the presence of the major seawater cations causes a significant interference on the CL signal produced by Co (Sakamoto-Arnold and Johnson, 1987). Thus, the use of an ammonium acetate rinse step, which removes more of the loosely-bound major cations than a UHP water rinse, increases the sensitivity of the reaction. In addition, column conditioning ensures the resin is close to the optimum pH prior to sample loading, which improves analyte retention. However, the most significant modification was the incorporation of a

UV-irradiation step of the acidified seawater samples, in order to determine total dCo, rather than an operationally-defined dissolved fraction. Additional minor modifications to the Cannizzaro *et al.* (2000) method included an increase in the acid eluent strength, thus requiring an increase in reaction buffer concentration, and a reduction in the reaction temperature.

The focus of the study described here was the analysis of dCo in open-ocean seawater, for which no FI method has been developed to date. The recent launch of the international GEOTRACES programme, which aims to determine trace metal concentrations in oceanic regions, requires accurate methods which are also highly sensitive. At present there is no certified reference material (CRM) that is representative of the extremely low concentrations of dCo in open ocean waters, *e.g.* the NASS-5 CRM (National Research Council of Canada) contains dCo at a concentration up to 20-fold greater than typical of oceanic surface water concentrations. Therefore, in addition to the determination of dCo in NASS-5, the accuracy of the FI-CL method described here was assessed and verified using acidified Pacific seawater reference samples from 1000 m depth from the SAFe program (Johnson *et al.*, 2007).

2.4.2. Materials and procedures

A schematic diagram of the flow injection manifold used is shown in Figure 2.3; it consists of an 8-channel peristaltic pump (Minipuls 3, Gilson), two micro-electronically actuated 6-port, 2-position injection valves (VICI, Valco Instruments), a photomultiplier tube (PMT, Hamamatsu H 6240-01) containing a

quartz glass spiral flow cell (internal volume 130 μL ; Baumbach and Co.) and a thermostatic water bath (Grant). The peristaltic pump tubing used was 2-stop accu-ratedTM PVC (Elkay). All other manifold tubing was 0.8 mm i.d. PFA Teflon (Cole-Parmer). The FI manifold had one mixing coil (1.85 m) and one reaction coil (5 m). The reaction coil was constructed by 'French-knitting' 5 m of 0.8 mm i.d. PFA Teflon tubing using a four pronged knitting spool. Two acrylic columns (internal volume 70 μL), with porous HDPE frits (BioVion F, 0.75 mm thick), were incorporated in-line; one on the sample-buffer line to remove trace-metal impurities from the buffer solution, and a second for the preconcentration of dCo and removal of the cations from the seawater sample matrix. Both columns were filled with Toyopearl AF-Chelate-650M resin (Tosohaas). The direction of flow through the clean-up column was one-way, so it was necessary to reverse the column at the end of each day to prevent the resin becoming compacted. This was not required for the sample preconcentration column, which was loaded and eluted in opposing flow directions. The T-piece prior to the 1.85 m mixing coil, the mixing coil itself and the 5 m reaction coil were maintained at 60 °C by placing them inside a thermostatic water bath (Grant). The data acquisition module (Ruthern Instruments) and valve control software (LabVIEW v. 7.1) were operated using a laptop computer (Dell). To minimise contamination, all sample handling was carried out in a Class-100 clean bench. The FI system was flushed daily and after any configuration changes (such as pump tube or reagent replacement) with 1 M HCl solution.

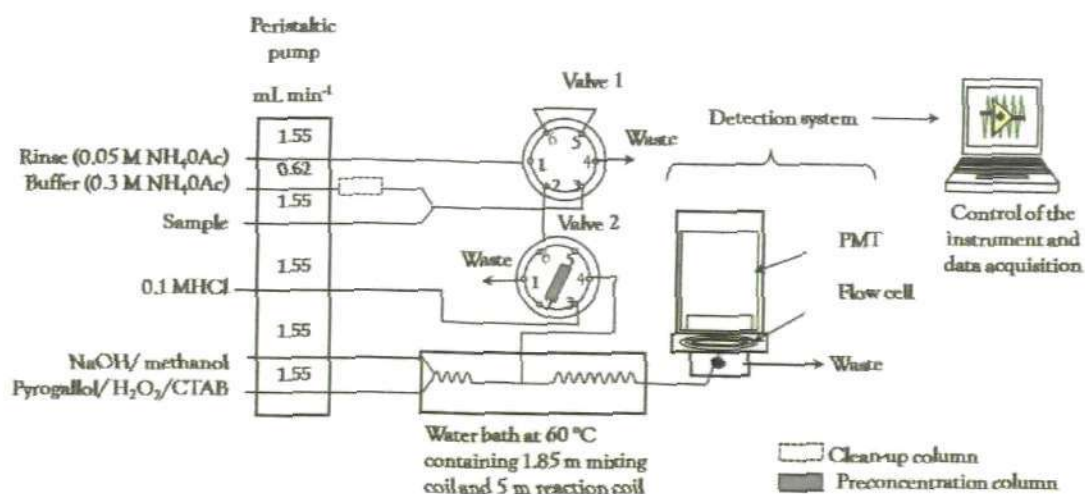


Figure 2. 3. FI-CL manifold configuration for the determination of dCo in seawater.

2.4.2.1. Reagents

Unless otherwise stated, all chemicals were obtained from Fisher Scientific, and used as received. All solutions were prepared inside a Class-100 clean bench using ultra high purity (UHP) water (≥ 18.2 M Ω cm, Elgastat Maxima). The eluent, 0.1 M hydrochloric acid (HCl), was prepared by diluting 8.8 mL of 10 M ultra-pure sub-boiling distilled HCl (SpA, Romil) to 1 L in UHP water. The 0.05 M ammonium acetate column rinse and conditioning solution was prepared by dissolving 3.8 g of ammonium acetate crystals in 1 L of UHP water and adjusting to pH 4 with 3.8 mL of 10 M ultra-pure HCl (SpA, Romil). The 0.3 M ammonium acetate sample buffer solution was also prepared in UHP water from ammonium acetate crystals (23.11 g L⁻¹), and the acidified seawater samples buffered on-line to between pH 5.2 and 5.5 by mixing with this solution. The 0.17 M sodium hydroxide (NaOH) reaction buffer solution was prepared by dissolving sodium hydroxide (NaOH) pellets (6.7 g L⁻¹) in 1 L of solution (20 % v/v methanol (HPLC grade), 80% v/v UHP water). The 50 mM pyrogallol reagent was prepared by sonicating 6.30 g of pyrogallol and 9.12 g of

cetyltrimethylammonium bromide (CTAB) in UHP water; when the pyrogallol and CTAB were fully dissolved, 58.4 mL of 35% hydrogen peroxide (H_2O_2) was added and the solution diluted to 1 L with UHP water. As the pyrogallol solution is reportedly only stable for 48 h (Cannizzaro, 2001, PhD thesis, University of Plymouth), this reagent was prepared daily as required.

2.4.2.2. Procedures

The peristaltic pump (Minipuls 3, Gilson) was set at 5.50 rpm to attain the flow rates shown in Figure 2.3. Following stabilisation of the baseline (typically 30 - 45 min), with valve 1 and valve 2 in position B, acidified ammonium acetate was passed through the preconcentration column for 40 s. Valve one was then switched to position A and a buffered sample was loaded onto the preconcentration column for 300 s. Valve 1 was then switched to position B, and the preconcentration column rinsed for 40 s with the acidified ammonium acetate solution. After this rinse step, valve 2 was switched to position A for 90 s, and the eluent (0.1 M HCl) was passed over the chelating resin in the opposite direction to that of the loading phase, thus eluting the cobalt from the preconcentrating resin into the reagent stream that was then carried to the PMT detector. In total, one complete analytical cycle took 7.8 min. During the load and rinse phases, the eluting acid bypassed the column and mixed with the other reagents to produce the baseline signal.

The analytical system was calibrated daily by simple linear regression of standard curves. Stock standard solutions were prepared in acidified UHP

water by serial dilution of a 17 mM Co atomic absorption standard solution (Spectrosol). Working standards (additions of 12.5 - 75 pM) were prepared in acidified low trace metal seawater (Atlantic Ocean surface seawater collected from 28°51'S, 4 °41'W; dCo = 13.7 ± 2.7 pM). Standards were run at the beginning and end of each programme of analysis in triplicate, and concentrations calculated from peak heights. Standard curves were linear ($r^2 > 0.99$) up to concentrations of 2 nM.

2.4.3. Assessment

2.4.3.1. On-line chelating resins

The commercially available Toyopearl chelating resin was compared with resin-immobilised 8-HQ, which has been used in previous FI-CL methods for Co determination (Sakamoto-Arnold and Johnson, 1987; Cannizzaro *et al.*, 2000). Figure 2.4 shows the FI elution profiles for (A) resin-immobilised 8-HQ and (B) Toyopearl resin. The same analytical conditions were used for both resins to allow a direct comparison. The use of Toyopearl provided consistently higher sensitivity and sharper elution profiles, e.g. for a 50 pM Co standard addition to seawater (Figure 2), use of Toyopearl gave a peak height of 1.28 mV, compared with 0.59 mV with the use of resin-immobilised 8-HQ.

A comparison of the characteristics of the two resins is presented in Table 2.1. One of the advantages of Toyopearl is the greater binding capacity of this resin compared with resin-immobilised 8-HQ (25-45 µeq mL⁻¹ versus 10 µeq mL⁻¹, respectively). The 'breakthrough capacity' (defined as the concentration of Co

sorbed to the resin before 5% of the total concentration of the analyte in the eluant was detected) of the two resins (profiles not shown) was determined using inductively-coupled plasma optical emission spectroscopy detection (ICP-OES, Varian 725-ES). An acidified 10 μM Co solution (pH 1.7) was buffered to pH 5.2 and loaded onto a column containing a preconcentration resin (either Toyopearl or 8-HQ). Cobalt in the column eluent was continuously monitored by ICP-OES at an emission wavelength of 238.9 nm. The Toyopearl resin retained 25.3 nM Co before the 5% breakthrough limit was exceeded, compared with 13.4 nM Co for the resin-immobilised 8-HQ. Therefore, Toyopearl was selected as the preferred chelating resin for this method.

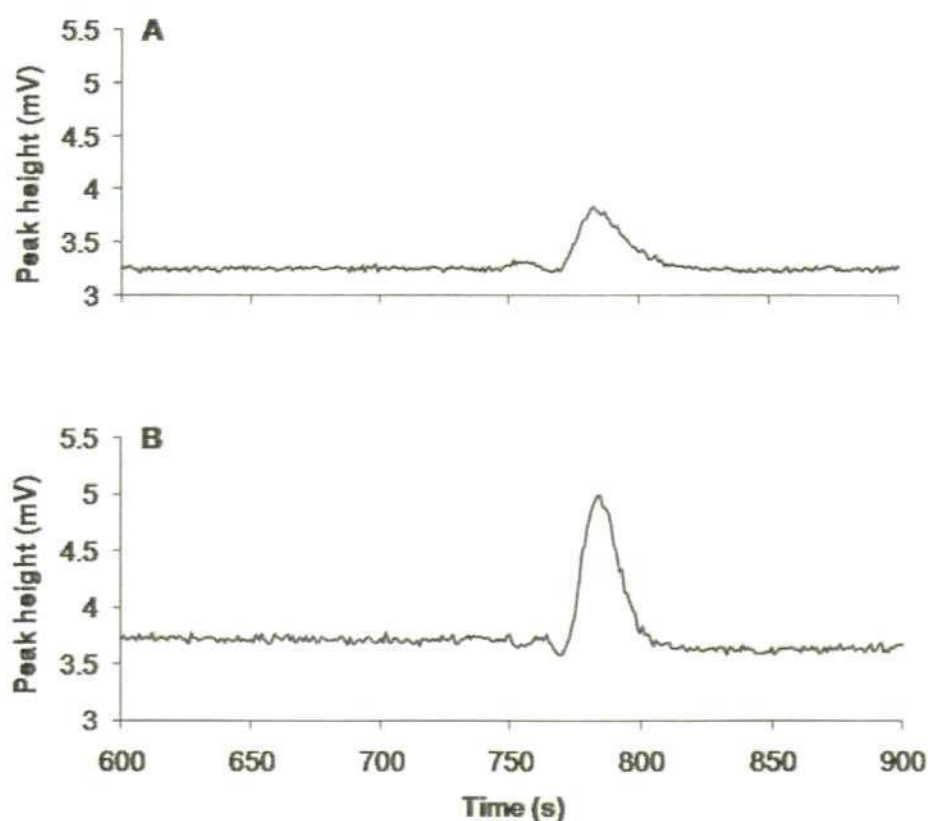
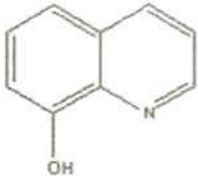
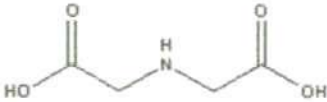


Figure 2. 4. Effect of two different chelating resins on sensitivity and elution profiles for a 50 pM standard in seawater: (A) resin-immobilized 8-hydroxyquinoline and (B) Toyopearl AF-Chelate-650M.

Table 2. 1. Comparison of 8-HQ and Toyopearl resin characteristics.

	8-HQ ^a	Toyopearl AF-Chelate-650 M ^b
Bead	HW-75F	HW-65
Chelating group	8-hydroxyquinoline (8-HQ)	Iminodiacetic acid (IDA)
Chelating group structure		
Capacity	10 $\mu\text{eq mL}^{-1}$	25-45 $\mu\text{eq mL}^{-1}$
Particle size	32-63 μm	65 μm
Pore size	>1000 Å	1000 Å
Exclusion limit	50 MDa	5 MDa

^a = Landing *et al.* (1986)

^b = Tosoh Bioscience (2008)

2.4.3.2. Reaction conditions

Column loading pH - Using ICP-MS as a detection system, Willie *et al.* (1998; 2001) demonstrated that Toyopearl AF-Chelate 650M quantitatively preconcentrated Co from seawater over the pH range 5.0 - 6.0. In the present study, the optimum pH range for the quantitative preconcentration of dCo from seawater samples was found to be in the range of 5.2 - 5.5. Seawater samples were buffered in-line with 0.3 M ammonium acetate solution. Ammonium acetate buffers effectively within the pH range 3.8 - 5.8 ($\text{pK}_a = 4.8$), and is therefore suitable for this FI-CL method. A critical component of dCo determination is characterization of the blank, even very low level contamination ($\leq 10 \text{ pM}$) of reagents can obscure the accuracy of a data set. As the buffer is loaded on the column for the same period as the sample, any dCo in the buffer

solution could constitute a significant contribution to the blank (Willie *et al.*, 1998). Therefore, a 'clean-up column', packed with Toyopearl resin, was placed in the sample buffer line prior to the sample preconcentration column, in order to remove any dCo that might be present in the buffer solution.

Column conditioning and rinse step - Previous FI-CL methods employing resin-immobilised 8-HQ for dCo determination (Sakamoto-Arnold and Johnson, 1987; Cannizzaro *et al.*, 2000) have used UHP water as a column rinse solution, and did not use a column-conditioning step. However, previous FI methods that have employed the Toyopearl chelating resin have included a column-conditioning step using a buffer with a pH similar to that of the in-line buffered seawater sample to ensure an optimum pH in the resin column prior to sample preconcentration, thus resulting in quantitative recovery of the analyte during the sample loading step (Aguilar-Islas *et al.*, 2006; Brown and Bruland, 2008). This column-conditioning step removes any residual acid that remains from the previous sample elution step, and ensures that the resin is no longer in the protonated form, which might otherwise reduce retention of the analyte and thereby lessen the sensitivity of the method. However, when using Toyopearl resin it is necessary to match the pH of the rinse solution (which combines with the reagent stream) to the pH of the eluting acid (which combines with the reagent stream). Failure to match the pH of the rinse solution and acid eluent leads to a depression in the baseline prior to the analytical peak, which can result in a significant reduction in sensitivity, as demonstrated for the FI method for analysis of dFe in seawater described by Lohan *et al.* (2006). Willie *et al.* (2001) demonstrated that a 0.1 M ammonium acetate rinse solution, buffered in

the range of pH 3 - 5, was sufficient to eliminate seawater matrix components whilst still retaining the analyte on the Toyopearl chelating resin. Investigations during this study found that a further reduction in strength of this ammonium acetate rinse solution to 0.05 M did not result in reduced sensitivity, so this lower concentration was used. Thus the column-conditioning and rinse steps were incorporated in the analytical cycle to remove sea salt and excess acid from the preconcentration column prior to the sample loading and elution steps.

Eluting acid concentration - A range of ionic strengths of eluting acid are reported in the literature for FI systems using chelating resins for the preconcentration of dCo from seawater. For example, Cannizzaro *et al.* (2000) used 0.05 M HCl to elute dCo from an 8-HQ chelating resin, whereas Hurst and Bruland (2008) used a much stronger 1 M HCl solution to elute dCo from Toyopearl resin. However, Hurst and Bruland (2008) used a system with ICP-MS detection, which is considerably less sensitive to pH fluctuations than CL detection. In this study it was essential to maintain an optimum reaction pH of 10.35 ± 0.2 . A reaction pH outside of this range resulted in changes to the baseline signal and significantly reduced sensitivity; *e.g.*, at pH 10.6 the signal for a 25 pM Co addition was reduced by ~ 44%. It would not have been feasible to achieve an optimum reaction pH of 10.35 if using 1 M HCl as the acid eluent. To determine a suitable eluent strength while maintaining this reaction pH, eluents of 0.05 M, 0.1 M and 0.5 M HCl were investigated, with standard additions of 25 - 75 pM Co in seawater. Increasing the acid concentration from 0.05 M (Cannizzaro *et al.*, 2000) to 0.1 M HCl resulted in the rapid elution of dCo from the Toyopearl resin and produced sharp sample peaks with CL detection, although there was no further improvement in peak shape

between 0.1 and 0.5 M HCl. The increase in the eluting acid concentration (from 0.05 to 0.1 M HCl) required that the concentration of the NaOH solution was increased from 0.15 M to 0.17 M, in order to achieve the optimum reaction pH of 10.35.

Matrix effects and interferences - An investigation of the potential suppression of the dCo CL signal by the major seawater cations was conducted by directly injecting solutions containing 9.9 nM dCo in UHP water spiked with the chloride salts of Na, K, Ca and Mg for 300 s (*i.e.* without a preconcentration step). These Co solutions were spiked with NaCl (10.7 g L⁻¹ Na), KCl (0.387 g L⁻¹ K), CaCl₂ (0.413 g L⁻¹ Ca), or MgCl₂ (1.29 g L⁻¹ Mg). A control solution contained dCo and no added salts. Between each injection, a solution of 0.05 M HCl (SpA, Romil) was injected for 120 s to rinse the previously injected solution.

With respect to the CL signal of the control dCo solution, the alkaline earths produced the strongest reduction in CL (51% and 55% reduction in signal for calcium (Ca) and magnesium (Mn) respectively, Figure 2.5). This significant reduction in CL, combined with a 44% signal reduction in the presence of sodium (Na) ions, illustrates the need for a matrix elimination step to remove the major seawater cations prior to the reaction and detection of the analyte. Although, the major seawater cations have low CL quantum yields in the pyrogallol reaction, their concentrations are sufficiently high in seawater that the resulting CL signal overwealms the CL signal produced due to the presence of Co (Sakamoto-Arnold and Johnson, 1987). Further, Sakamoto-Arnold and Johnson (1987) demonstrated that the interference caused by the major seawater cations cannot be masked by the addition of complexing agents, such

as sodium citrate, sodium fluoride or EDTA, to the reagents. Thus, it is necessary to remove the major seawater cations from the matrix in order to determine Co in seawater by the CL oxidation of pyrogallol.

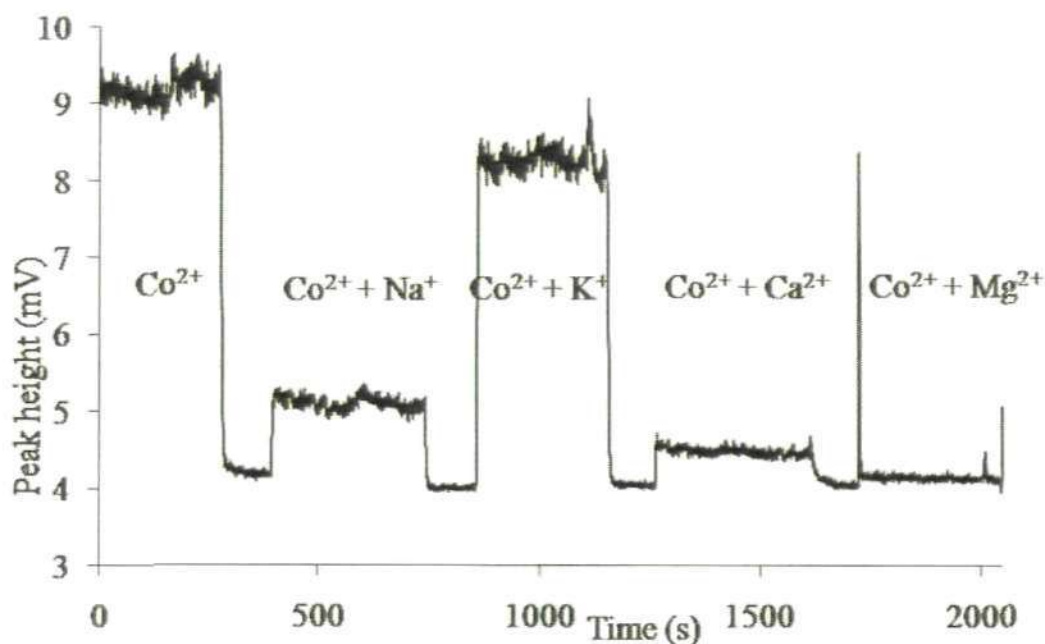


Figure 2. 5. Effect of the major seawater cations on the chemiluminescence signal (0.5 M Na⁺, 0.01 M K⁺, 0.01 M Ca²⁺ and 0.05 M Mg²⁺).

For the analysis described here, the on-line preconcentration column must ideally have a low affinity for the major ions in seawater, whilst quantitatively retaining the analyte on the resin. Elimination of the seawater ions can be achieved by rinsing the column with a dilute ammonium acetate solution prior to eluting the analyte with HCl. However, even with the inclusion of this rinse step, some residual seawater ions still serve to reduce the sensitivity of the method. By comparing standard additions of dCo to seawater versus UHP water (12.5 - 75 pM), a 35% reduction in sensitivity was observed for standards prepared in seawater (data not shown). Consistent with this finding, is the lower detection

limit for standards prepared in UHP water compared with those prepared in seawater (Table 2.2).

The potential for interference by the metal ions Ag^+ , Fe^{3+} , Cu^{2+} , Pb^{2+} , Mn^{2+} and Cd^{2+} , in the determination of Co^{2+} in seawater of the pyrogallol reaction was investigated by Cannizzaro *et al.* (2000). Of the ions tested, only Ag^+ was found to cause a detectable interference. However, as these interference experiments were conducted using trace metal concentrations 50x that of open water, it was concluded that this species (Ag^+) was unlikely to interfere with dCo analysis given the extremely low dissolved concentrations of dissolved Ag in open ocean seawater (≤ 0.7 pM, Flegal *et al.*, 1995).

Reaction temperature - Chemiluminescence reactions are sensitive to temperature, with the rate of reaction typically doubled for every 10 °C increase in temperature. Cannizzaro *et al.* (2000) used a reaction temperature of 80 °C, however, optimisation experiments during this study showed that a reaction temperature of 60 °C provided good sensitivity. The advantages of working at this lower temperature are twofold. First, by working below the boiling point of methanol (64.7 °C), the formation of bubbles in the NaOH/methanol reagent stream is avoided. Second, the use of this lower reaction temperature reduces evaporation losses from the thermostatic bath, thus avoiding the need to top it up (and potentially alter the reaction temperature) during the analysis.

2.4.4. Sample treatment for the determination of total dissolved cobalt

2.4.4.1. UV-irradiation

Similar to several other bioessential trace metals in seawater, a large fraction (>90%) of dCo is complexed by uncharacterized organic ligands (Ellwood and van den Berg, 2001). When using cathodic stripping voltammetry or cation-exchange liquid chromatography with luminol chemiluminescence detection (LC-CL) as the analytical method, it is well established that it is necessary to breakdown these ligands in order to achieve full recovery of total dCo (CSV: Donat and Bruland, 1988; Vega and van den Berg, 1997; Saito and Moffett, 2001; Noble *et al.*, 2008 and LC-CL: Boyle *et al.*, 1987). As the degree of retention of organically-bound Co by chelating resins is unknown, investigations were conducted to establish whether it was necessary to UV-irradiate seawater samples prior to the determination of dCo by FI-CL. Previously-acidified samples collected from 1000 m depth in the North Pacific subtropical gyre (30° N, 140° W) as part of the Sampling and Analysis of Iron (SAFe) program (Johnson *et al.*, 2007) were analysed to allow comparison between samples with and without UV-pretreatment. Acidified SAFe samples were UV-irradiated in acid-washed quartz vials for 3 h using a 400 W medium-pressure Hg lamp (Photochemical Reactors). After UV-irradiation, samples were decanted into acid-clean LDPE bottles and then left for 48 h prior to analytical determination, in an effort to eliminate UV-generated free radicals that might otherwise interfere with the CL reaction. The concentration of dCo determined in UV-irradiated SAFe seawater samples was 40.9 ± 2.6 pM ($n = 9$), which was almost double the concentration measured in non-irradiated samples (25.4 ± 1.2 pM, $n = 8$). The results of this experiment demonstrate conclusively that UV-

irradiation is essential for the determination of dCo in acidified seawater by FI-CL.

There is evidence for the presence of strong, Co-binding organic ligands in seawater that have a stability constant (K_s) of $10^{16.3 \pm 0.9}$ (Saito and Moffett, 2001; Saito *et al.*, 2005) compared with the reported K_s value of $10^{13.08}$ for strong Fe(III)-binding ligands in seawater (Rue and Bruland, 1997). However, in contrast to organic Fe complexes, which appear to fully dissociate when seawater samples are acidified to pH 1.7 (Lohan *et al.*, 2005), the results of this and earlier UV-irradiation experiments using other analytical techniques (e.g. Donat and Bruland, 1988; Vega and van den Berg, 1997; Noble *et al.*, 2008; Milne *et al.*, 2010) indicate that organic Co complexes do not completely dissociate at pH 1.7.

Although IDA-based resins such as Toyopearl are able to selectively complex free metal ions and other metal species that are thermodynamically- and kinetically-labile, they may be unable to extract metals bound to strong organic ligands. Where it is necessary to increase pH to ≥ 5 prior to the preconcentration step, such as is the case for FI-CL analysis of acidified samples, some of the metal analyte may become recomplexed to form thermodynamically- or kinetically-inert complexes (in terms of chelation by the resin) with organic ligands present in the sample, and thus pass through the column without being retained on the resin. Unless the dissolved organic material (DOM) that contains these ligands is destroyed (e.g., by UV-irradiation),

such organic complexation may result in trace metal analytes not being fully retained by the preconcentrating resin (Ndung'u *et al.* 2003), and hence the determination of only the labile (rather than total) dissolved concentrations of trace metals such as Co.

2.4.4.2. Addition of a reducing agent

The pyrogallol-FI-CL method described here determines dCo by reducing the thermodynamically- and kinetically-labile Co fraction to Co(II). The SAFe samples were collected and acidified to pH 1.7 in 2004. Lohan *et al.*, (2005) reported that the longer a sample was acidified, the greater the percentage of Fe that exists as Fe(II). Noting the similarity between the redox speciation of Fe and Co in seawater (both are present in the +2 and +3 oxidation states under typical seawater conditions), Co may similarly tend towards Co(II) in acidified seawater. However, in order to verify that the reduction of Co(III) to Co(II) was complete in this method, an experiment was conducted to investigate the effect of incorporating a strong reducing agent in the reaction scheme. A buffered 0.04 M solution of sodium sulphite (NaSO_3) solution was prepared by dissolving 0.202 g of NaSO_3 in 30 mL UHP water plus 10 mL of 0.4 M ammonium acetate buffer, to ensure no changes in the sample pH that could affect the sensitivity of the CL reaction. Prior to use, this solution was passed through two columns in series containing Toyopearl resin, in order to remove trace metal impurities; the first 10 mL of the purified NaSO_3 solution was discarded, and the following 30 mL was collected and left for at least 24 h to stabilise before spiking the acidified SAFe seawater with 25 μL per 10 mL of sample. Samples were then left at least 8 h, to allow time for the reduction of Co(III) to Co(II), before dCo was determined by FI-CL. The samples used in this experiment were not UV-

irradiated. Using a *t*-test, no significant difference ($p = 0.06$) was observed between samples with and without NaSO_3 addition (25.4 ± 1.2 pM and 30.5 ± 1.7 pM respectively; $n = 8$), suggesting that the method effectively determines all dCo in previously acidified seawater samples.

Saito *et al.* (2005) described natural Co-binding ligand complexes with stability constants greater than $10^{16.8}$ (c.f. $10^{11.48}$ - $10^{13.08}$ for Fe-binding ligands in seawater; Rue and Bruland, 1995), and reported that addition of excess Ni(II) ions did not liberate organically-complexed Co. On this basis it was argued that organically-bound Co was present as Co(III) complexes: a further parallel with Fe biogeochemistry, since dFe is thought to exist mainly as organically complexed Fe(III) in seawater (*e.g.* Rue and Bruland, 1995). Acidification of samples may dissociate these organic complexes, releasing Co(III), which is then reduced to Co(II) over time, thus explaining the apparent lack of effect of the added reducing agent (see above). However, if this was the case, one would predict no increase in dCo determined after UV irradiation, which is inconsistent with the results presented here. This then implies that it is it may not be the redox chemistry of Co that is preventing complete recovery of dCo from acidified seawater samples on the Toyopearl resin, but rather that the acidified samples contain organic ligands that complex dCo upon readjustment of the sample pH (Ndung'u *et al.*, 2003; Saito *et al.*, 2005).

The addition of a reducing agent resulting in no difference in dCo concentrations has been previously reported by Vega and van den Berg (1997). However, their results contrast with results of a similar study by Donat and Bruland (1988) using sodium borohydride (NaBH_4) as the reducing agent, who

found that it was still necessary to add a reducing agent even after samples had been UV-irradiated, in order to fully recover dCo. Vega and van den Berg (1997) argue that the reason for this contrast may result from the less extensive UV-irradiation step employed by Donat and Bruland (1988). As no difference was observed between samples with and without addition of a reducing agent, it suggests that the samples in this study contained Co(II).

Without UV-irradiation, the dCo concentration in the SAFe D2 reference samples was 38% lower. A similarly reduced concentration was observed by Donat and Bruland (1988) in their non-UV-irradiated samples, using CSV. However, the key differences between this study and Donat and Bruland's (1988) was the addition of a reducing agent to samples following UV-irradiation. It is therefore important to investigate the amount of time necessary to UV-irradiate open ocean samples prior to analysis using SAFe or GEOTRACES reference samples. In addition, further insights might be gained by investigating the redox state of complexed Co during the analytical process.

2.4.5. Analytical figures of merit

The accuracy of the method was assessed using SAFe seawater reference samples. The key analytical parameters are shown in Table 2.2. Of particular interest is the improvement in detection limit of this FI-CL method compared with a previously published FI method (the average detection limit of this new method was 4.5 pM, *c.f.* ~8 pM for the method of Sakamoto-Arnold and

Johnson, 1987), and the wide dynamic range of this method (over three orders of magnitude, ~4.5–2000 pM).

Table 2. 2. Key analytical parameters.

Parameter	This study	Literature values
Detection limit (seawater)	4.5 pM	~ 8 (Sakamoto-Arnold & Johnson 1987)
Detection limit (UHP water)	3.8 pM	5 (Cannizzaro <i>et al.</i> 2000)
Linear range	3.8–2000 pM	5–850 pM (Cannizzaro <i>et al.</i> 2000)
Blanks	4.2 ± 1.5 pM	
RSD ($n = 3$)	≤4%	

2.4.5.1. Blanks and detection limits

For this FI-CL method, the major contribution to the blank was from the addition of the ammonium acetate sample buffer. Whilst Cannizzaro *et al.* (2000) found no detectable signal from the added ammonium acetate buffer, this was not the case in the present work. The extremely low concentrations of Co in the open ocean samples analysed in this study required a five-fold increase in loading time compared with that used for estuarine samples (300 s versus 60 s, respectively). Since the sample buffer and sample are loaded simultaneously, any Co present in the buffer potentially contributes to the analytical signal. Therefore, a clean-up column (containing Toyopearl resin) was added to the sample buffer line to reduce the amount of Co loaded onto the preconcentration column. In common with other flow injection techniques, the manifold blank was determined by running an analytical cycle without the sample (*e.g.* loading the sample buffer only onto the preconcentration column, Bowie and Lohan, 2009), resulting in a concentration of 4.2 ± 1.5 pM ($n = 21$). The detection limit was calculated as the dCo concentration corresponding to three times the standard

deviation of the blank, resulting in a detection limit of 4.5 pM ($n = 21$) in seawater.

2.4.5.2. Accuracy and precision

The accuracy of previous methods determining dCo in seawater have been assessed using the North Atlantic Surface Seawater (NASS; National Research Council of Canada) certified reference material (CRM). In this study, a concentration of 208 ± 30 pM for dCo was determined in NASS-5, which is within the certified range (187 ± 51 pM). This result is within error, and is consistent with the results of Vega and van den Berg's (1997) determination of dCo in UV-irradiated NASS-2. Like NASS-2, NASS-5 has a large standard deviation, and has a mean concentration that is up to 20 times greater than typical open-ocean surface concentrations of dCo. Therefore, the combination of a large uncertainty and high dCo concentration renders this CRM unsuitable with respect to the determination of dCo in open-ocean surface waters. Consequently, an alternative low-level dCo reference sample was analysed to assess the accuracy and precision of this FI-CL technique. The concentration of dCo was determined in acidified seawater samples ('D2') collected from 1000 m depth in the North Pacific as part of the SAFe program (Johnson *et al.*, 2007). Sample collection details are described by Johnson *et al.* (2007). The dCo concentrations for the SAFe D2 reference samples after UV-irradiation (40.9 ± 2.6 pM; $n = 9$) are in excellent agreement with results obtained for the same sample by other analytical techniques which also used a UV-pretreatment step (43 ± 3.2 pM, <http://es.ucsc.edu/~kbruland/GeotracesSaFe/kwbGeotracesSaFe.html>). The SAFe D2 sample was UV-irradiated and analysed by this FI-CL technique together with all seawater samples for which data are presented here,

in order to verify the accuracy of the method. The analytical precision of the method was determined from repeat analyses of the SAFe D2 reference sample, yielding an uncertainty of $\pm 4\%$ expressed as relative standard deviation on the mean ($n = 9$). Samples that were not UV-irradiated were also in excellent agreement with the consensus values for non-UV-treated SAFe D2 samples (this study = 25.4 ± 1.2 pM; $n = 8$, SAFe D2 non-UV = 26.9 ± 4.7 pM).

From the data already submitted to the intercalibration website it has become apparent that a UV-irradiation step is necessary to determine dCo in the SAFe reference samples. However, at present there is too much spread in the dCo values for the SAFe reference samples, and further work needs to be conducted to investigate optimal UV-irradiation parameters (Bruland pers.comm.). As additional laboratories continue to submit data for SAFe and GEOTRACES reference samples, using UV-pre-treatment, confidence in the consensus values will increase.

2.4.6. Discussion and recommendations

The UV-irradiation experiment represents an important analytical development in the analysis of dCo in seawater, in that it demonstrates the absolute requirement for UV-irradiation to liberate organically complexed Co in acidified samples prior to FI-CL determination of dCo. Previous FI-CL methods (and other analytical techniques) that did not include this step may only have determined dissolved labile Co (as defined by Noble *et al.*, 2008). The use of the commercially available resin Toyopearl AF-Chelate-650M improves the

reproducibility of the method and simplifies the preparation of the analytical system, as there is no need to synthesise the chelating resin. The introduction of a resin-conditioning step (acidified ammonium acetate rinse) also led to increased sensitivity. In addition to highlighting the need to UV-irradiate seawater samples and the advantages of using a column conditioning step, this method also demonstrates the importance of effective sample buffering, both for the pH at which the sample is loaded onto the chelating resin column (pH 5.2–5.5), and the reaction pH of the combined reagent stream as it enters the detector (pH 10.35 ± 0.2). In this method, incorrect buffering results in a significant reduction of sensitivity.

The FI-CL method presented here is selective, has a low detection limit (4.5 pM), and is portable making it an ideal method for determining dCo in open ocean regimes. The suitability of this method for shipboard use enables the mapping of dCo distributions whilst at sea, which make this technique an attractive analytical tool for examining high-resolution spatial and temporal trends in the oceanic distribution of dCo. Although CSV can be used to determine dCo at sea, FI methods are generally less time-consuming. Given that Co is an essential micronutrient for carbon acquisition for certain key phytoplankton genera (*e.g. Prochlorochooccus, Synechococcus*), it is important to attain high quality data to further our understanding of the biogeochemical cycling of this element in marine waters.

The relative simplicity and low risk of contamination make this method well suited for use in the laboratory and for shipboard analyses. The implementation

of an automated sample selection valve could further reduce the risk of contamination associated with transferring the sample line from one sample to the next. In this study, the preconcentration columns were fabricated according to Cannizzaro *et al.* (2000). Commercially available columns potentially improve the reliability and reproducibility of the separation/preconcentration step by minimising leakage and contamination. Such columns have successfully been used in other FI applications (*e.g.* Aguilas-Islas *et al.*, 2006; Lohan *et al.*, 2006), and would likely be suitable for application in this method.

Owing to the absence of a suitably low concentration certified reference material for dCo, it is recommended that SAFe and GEOTRACES seawater reference samples be used for quality assurance when analysing open ocean samples. The consensus values of the SAFe reference seawater materials are now available at: www.geotraces.org/Intercalibration.html#standards_certified_refs and <http://es.ucsc.edu/~kbruland/GeotracesSaFe/kwbGeotracesSaFe.html>. The GEOTRACES values are soon to be published on the same two websites. However, a cautionary note must be added at this point with regards to the dCo numbers. A UV-irradiation step is necessary to determine dCo in the SAFe reference samples. However, at present there is still too much variation in the values, even after UV-irradiation to make a definitive conclusion. Consequently more research needs to be performed to evaluate the intensity and duration of the UV pre-treatment required to release all the Co for the various analytical methods. Therefore, although there is a slight caveat attached to the accuracy of the dCo values, the use of these low metal, open-ocean reference materials is strongly advocated as they will likely benefit scientists determining dCo and

other trace elements in much the same way as they have done for the determination of dFe in seawater.

2.5. Determination of dFe in seawater using FI-CL

2.5.1. Introduction

In common with the dCo FI-CL technique described in the previous section, the sub-nanomolar concentrations of dFe in open ocean waters requires a preconcentration and separation step. The recovery of Fe on to a preconcentration resin is pH dependent. For example, operationally defined, labile dissolved Fe(III) is recovered on resin-immobilised 8-HQ at pH 3–4.2, whereas at pH 5.2–6 Fe(II) and Fe(III) are quantitatively recovered (Obata *et al.*, 1993). Similarly, Toyopearl resin has successfully been used for the recovery of dFe from seawater in the same pH range (de Baar *et al.* 2008). In this study, dFe was determined as Fe(III).

2.5.2. Materials and procedures

In this study the FI-CL technique developed by Obata *et al.* (1993), and later modified by de Jong *et al.* (1998) and de Baar *et al.* (2008) was used for the determination of dFe. A schematic diagram of the flow injection manifold is shown in Figure 2.6. The same components used in the Co FI-CL system (see Section 2.6) were used in the manifold of the Fe FI-CL system. Briefly, an 8-channel peristaltic pump (Minipuls 3, Gilson), two micro-electronically actuated 6-port, 2-position injection valves (VICI, Valco Instruments), a photomultiplier tube (PMT, Thorn EMI) containing a quartz glass spiral flow cell (internal volume 130 μ L; Baumbach and Co.) with 1.1 kV power supply (DPS55, Astec)

and a thermostatic water bath (Grant). The 2-stop accu-rated™ PVC (Elkay) peristaltic pump tubing and manifold tubing (0.8 mm i.d.; Cole-Parmer), mixing coil, reaction coil, preconcentration and clean-up columns were the same as previously described for the Co FI-CL system (Section 2.6). Both the mixing coil and reaction coil were maintained at 35 °C by placing them inside a thermostatic water bath (Grant). The data acquisition module (Ruthern Instruments) and valve control software (LabVIEW v.7.1) were controlled via a laptop computer (Dell). To minimise contamination, all sample handling was carried out in a Class-100 clean bench, and prior to use the FI system was flushed daily with 1 M HCl solution.

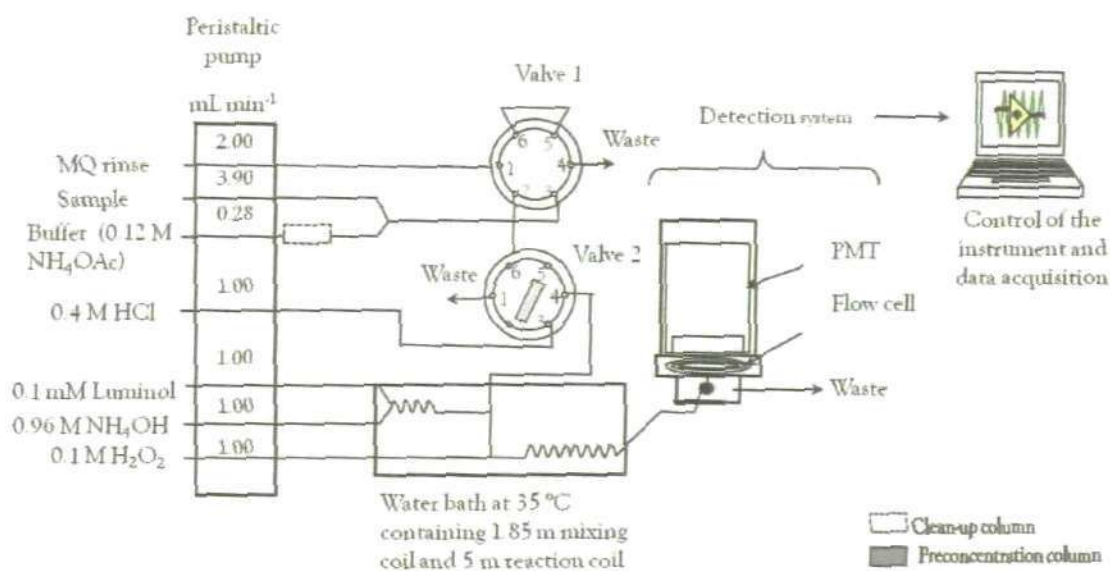


Figure 2. 6. FI-CL manifold configuration for the determination of dFe in seawater.

2.5.2.1. Reagents

Unless otherwise stated, all chemicals were obtained from Fisher Scientific and used as received. All solutions were prepared inside a Class-100 clean bench using ultra high purity (UHP) water (≥ 18.2 M Ω cm, Elgastat Maxima); reagent concentrations are shown in Table 2.3. The rinse solution was UHP water. The

eluent, 0.4 M hydrochloric acid (HCl), was prepared by diluting 41.1 mL of 10 M ultra-pure sub-boiling distilled HCl (SpA, Romil) to 1 L in UHP water. The 0.12 M ammonium acetate sample buffer solution was prepared in UHP water by diluting 25 mL of 2 M ammonium acetate stock solution (30 mL SpA acetic acid (Romil) + 70 mL SpA ammonia solution (Romil) + 150 mL MQ) per 100 mL with UHP water and adjusting to pH 5.2 with acetic acid. The acidified seawater samples were buffered in-line to between pH 3 and 3.5 by mixing with this solution. The 0.96 M ammonia solution (NH₄OH) (Romil) reaction buffer was prepared by diluting 168.13 mL NH₄OH in 1 L UHP water, to attain the reaction pH of 9.8-10. The 0.1 mM luminol reagent was cleaned off-line by dissolving 0.177 g luminol in 10 mL UHP water to give a 0.1 M stock. Next 1 mL of luminol stock was diluted in 1 L of UHP water and 73 µL of triethylenetetramine (TETA) (60%) was added. The 0.1 mM luminol solution was then passed through a column containing acid-cleaned Chelex-100 beads to minimise trace metal impurities that might otherwise reduce the sensitivity of the system. The first 200 mL of cleaned luminol was discarded and the remaining 800 mL retained for use after a standing period of 24 h.

Table 2. 3. Reagent concentrations and analytical cycle timings used in this study (following modifications by de Baar *et al.*, 2008).

Rinse	UHP water; 2.0 mL min ⁻¹
Buffer	0.12 M NH ₄ OAc (adjusted to pH 5.2 with NH ₄ OH, samples buffered to pH 3-3.5)
Eluent	0.4 M HCl
Luminol	0.1 mM
NH ₄ OH	0.96 M
H ₂ O ₂	0.1 M
Load	210 s (13.7 mL sample vol.)
Rinse	40 s
Elute	90 s
Resin	Toyopearl AF- Chelate-650M

2.5.2.2. Procedures

The peristaltic pump (Minipuls 3, Gilson) was set at 7.0 rpm to attain the flow rates shown in Figure 2.6. Following stabilisation of the baseline (typically 30–45 min), with valve 1 and valve 2 in position B, the rinse solution (UHP water) was passed through the preconcentration column for 40 s. Valve one was then switched to position A and a buffered sample (pH 3.0–3.5) was loaded onto the preconcentration column for 210 s. Valve 1 was then switched to position B, and the preconcentration column rinsed for 40 s with UHP water. After this rinse step, valve 2 was switched to position A for 90 s, and the eluent (0.4 M HCl) was passed over the chelating resin in the opposite direction to that of the loading phase, thus eluting the Fe from the preconcentrating resin into the reagent stream that was then carried to the PMT detector. In total, one complete analytical cycle took 6.3 min. During the load and rinse phases, the eluting acid bypassed the column and mixed with the other reagents to produce the baseline signal.

The analytical system was calibrated daily by simple linear regression of standard curves, an example of which is shown in Figure 2.7. Stock standard solutions were prepared in acidified UHP water by serial dilution of a 17.9 mM Fe atomic absorption standard solution (Spectrosol). Working standards (additions of 0.2–1.5 pM) were prepared in acidified low trace metal seawater (Atlantic Ocean surface seawater collected from 28° 51' S, 4 ° 41' W; dFe = 0.14 ± 0.02 nM). Calibrations were run at the beginning and end of each programme of analysis, and concentrations calculated from peak heights.

Standard curves were linear ($r^2 > 0.99$) over the calibration range, where $y = 0.8496x + 0.008$.

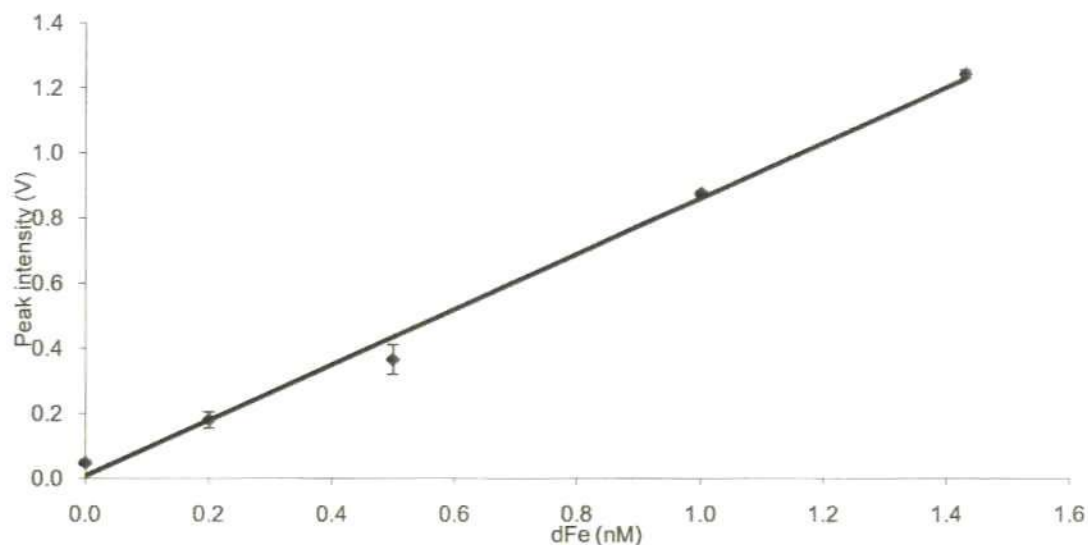


Figure 2. 7. Example of a calibration curve with standard additions of 0.2–1.5 nM dFe.

2.5.3. Analytical figures of merit

2.5.3.1. Blanks and detection limits

In common with the Co FI-CL method described in the previous section, blank signals were generated by running a complete analytical cycle without a sample. Any Fe present in the buffer potentially contributes to the analytical signal. Therefore, a clean-up column (containing Toyopearl resin) was added to the sample buffer line to reduce the amount of Fe loaded onto the preconcentration column. This resulted in blank concentrations of 0.03 ± 0.005 nM ($n = 6$). The detection limit was calculated as the dFe concentration corresponding to three times the standard deviation of the blank, resulting in a detection limit of 0.01 nM ($n = 6$) in seawater.

2.5.3.2. Accuracy and precision

The accuracy of this technique was assessed using reference samples ('S' surface seawater and 'D2' collected from 1000 m depth) from the SAFe programme (Johnson *et al.*, 2007). The dFe concentrations for the SAFe reference samples ($S = 0.09 \pm 0.02$ nM, $D2 = 0.95 \pm 0.01$ nM; $n = 3$) are in excellent agreement with results obtained for the same sample by other analytical techniques ($S = 0.094 \pm 0.008$ nM, $D2 = 0.923 \pm 0.029$ nM, <http://es.ucsc.edu/~kbruland/GeotracesSaFe/kwbGeotracesSaFe.html>). In order to verify the accuracy of the method The SAFe S and D2 samples were analysed with all seawater samples using this FI-CL technique for which data are presented in this thesis (Chapter 4). The analytical precision of the method was determined from repeat analyses of the SAFe reference samples, yielding an uncertainty of ± 1.4 % expressed as relative standard deviation on the mean ($n = 3$) (SAFe D2).

2.5.4. Discussion

The Fe FI-CL method presented here is selective, has a low detection limit (0.01 nM), and is portable, making it an ideal method for determining near real-time concentrations of dFe in open ocean regimes. The suitability of this method for shipboard use enables the mapping of dFe distributions while at sea, which makes this technique an attractive analytical tool for examining high-resolution spatial and temporal trends in the oceanic distribution of dFe. However, the system still requires further optimisation as occasionally sensitivity was poor leading to over-estimation of concentrations of dFe in the SAFe reference samples. Incorrect sample buffering or reaction pH leads to a

reduction in sensitivity. This problem could be overcome by preparing fresh sample buffer or NH_4OH solution. Additionally, investigation into the most suitable rinse solution needs further consideration. The Fe FI-CL system is likely to benefit in the same way as the Co FI-CL system in terms of sensitivity by replacing the UHP rinse solution with a weak, acidified ammonium acetate solution.

2.6. Three pump FI-CL system for the determination of dCo and dFe

The Co FI-CL and Fe FI-CL systems shared many similarities (Figures 2.5 and 2.6). Apart from the Co FI-CL system having an additional reagent line, the only practical difference between the two systems was the chemistry in terms of the choice of reagents, each being specific to one analyte (Co or Fe). Therefore, it was relatively simple to adapt the FI system for use for either Co or Fe. An additional modification that was adopted for later analytical runs was the use of a FI system that used three peristaltic pumps, rather than the one originally used. The advantage of working with three pumps was that they could be controlled separately via the computer software, enabling the sample, buffer and rinse pumps to be switched off when not in use, thereby reducing sample volume and buffer/rinse usage. The first stage was to load the buffered sample onto the preconcentration resin. When loading was complete the sample pump was turned off and the rinse pump on. The switching valve allowed flow to the column from these two pumps to be controlled. Next, the injection valve was switched enabling the eluent to flow over the preconcentration column in the opposite direction, thus eluting the analyte into the reagent stream prior to

detection. The reagent and eluent pump remained on throughout the analytical cycle in order to maintain a constant baseline. Using the example of the Co FI-CL system shown in Figure 2.5, Figure 2.8 highlights the difference between the one and three pump systems; *i.e.* the use of three pumps (colour coded in Figure 2.8) and the replacement of valve 1 with a switching valve.

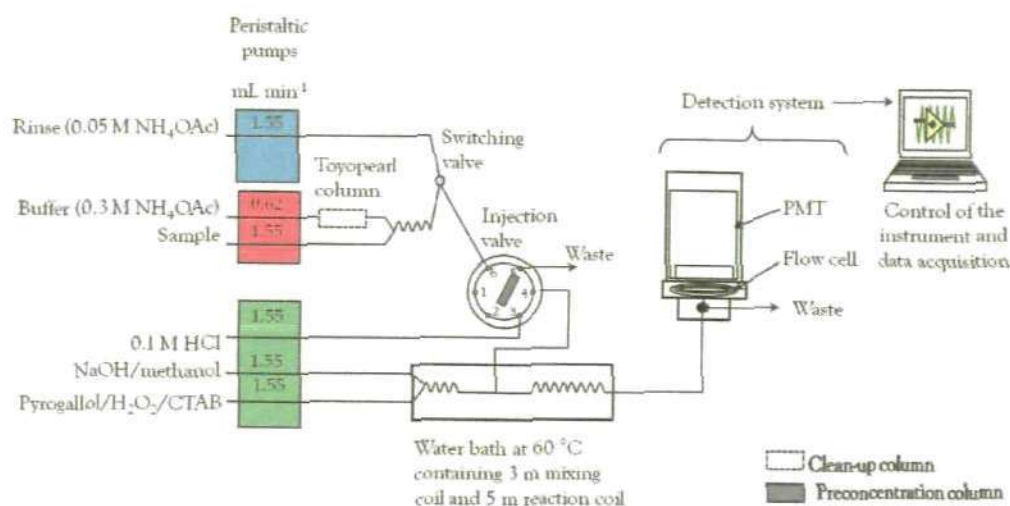


Figure 2. 8. Three-pump flow injection manifold for the determination of dCo. The three pumps are coloured thus: rinse pump = blue, sample pump = red, reagent and eluent pump = green.

In terms of sensitivity, there was some improvement as the gain was set at x400 when using the one-pump system for dCo determination, and x200 when using the three-pump system, without any loss of sensitivity. However, the temperature in the laboratory was approximately 10 °C higher when the three-pump system was in use (an increase from 22 to 32 °C). Even though the reaction and mixing coils were maintained at 60 °C, it is possible that the increase in ambient temperature was responsible for the increased sensitivity, rather than the change from a one pump to a three pump system, as the CL reaction is sensitive to temperature fluctuations. Therefore, the main advantage

that can be attributed to use of a three pump system is the reduction in sample and reagent volumes. Despite this advantage, it is recommended that analysis conducted at sea be undertaken using a one-pump system, as it is easier to programme and has less components.

2.7. Determination of dCu using ICP-MS with off-line pre-concentration

2.7.1. Introduction

A major advantage of using ICP-MS is the capability for multi-element detection. However, the high salinity of open ocean samples can result in substantial salt precipitation and build-up on the cones. Furthermore, the analyte signal may be masked due to polyatomic interferences. As a consequence direct sample injection is not practical, and sample pre-treatment is required to remove the high salinity matrix. This may be achieved either by dilution of the sample (Field *et al.*, 1999) or by separation/pre-concentration (alternatively termed extraction in the literature) techniques (Ndung'u *et al.*, 2003; Milne *et al.*, 2010). The extremely low concentrations of trace metals in open ocean samples prohibits further dilution of samples due to instrumental detection limits. Therefore, pre-concentration and separation of the trace metal analytes from the seawater matrix is recommended when using ICP-MS detection for open ocean samples. As previously stated (section 2.6), this can be achieved through a number of approaches. Due to its successful application in previous techniques (*e.g.* Brown and Bruland, 2008; de Baar *et al.*, 2008; Milne *et al.*, 2010; Shelley *et al.*, 2010), the one favoured in this study was the use of the iminodiacetate (IDA)-

based chelating resin, Toyopearl. The following section presents details of this ICP-MS technique with off-line preconcentration for the determination of dCu in bioassays using open ocean seawater. This technique was chosen as it was the aim to simultaneously detect dissolved Fe and Zn in addition to Cu.

2.7.2. Materials and procedures

A schematic diagram of the flow injection manifold used for the off-line preconcentration is shown in Figure 2.9; it consists of 3 4-channel peristaltic pumps (Minipuls 3, Gilson), a micro-electronically actuated 6-port, 2-position injection valve (VICI, Valco Instruments) and a two position switching valve (Cole-Parmer). All peristaltic pump tubing used was 2-stop (grey-grey) silicone (Elkay), except for the sample-buffer line which was 2-stop Accu-rated PVC (orange-white) (Elkay). All other manifold tubing was 0.8 mm i.d. PFA Teflon (Cole-Parmer). Two acrylic columns (internal volume 70 μ L), with porous HDPE frits (BioVion F, 0.75 mm thick), were incorporated; one on the sample-buffer line to remove trace-metal impurities from the buffer solution, and a second for the preconcentration of dCu and removal of the cations from the seawater sample matrix. Both columns were filled with Toyopearl AF-Chelate-650M resin (Tosohaas). The valve control software (LabVIEW v. 7.1) was operated using a laptop computer (Dell). To minimise contamination, all sample handling was carried out in a Class-100 clean bench. The FI system was flushed daily with 1 M HCl solution. This system was not fully automated. During sample loading, the eluent flowed through the sample collection line to rinse it and the solution went to waste. However, as soon as the injection valve switched direction into the elute phase of the analytical cycle, the sample line was manually placed into

a sample collection vial (2 mL polypropylene cryogenic vial, Nalgene) for sample collection.

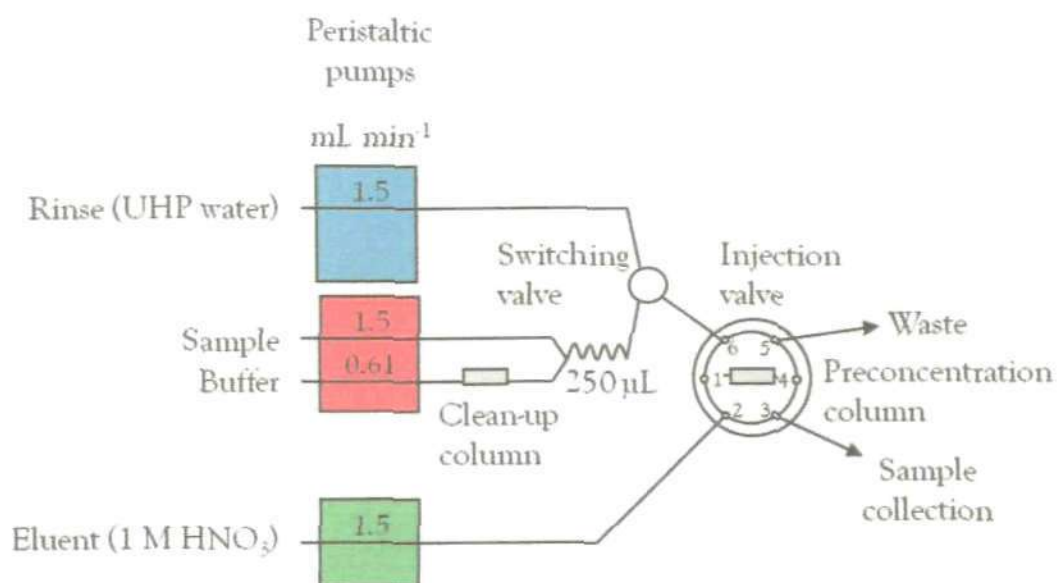


Figure 2. 9. Manifold configuration for the off-line pre-concentration of total dissolved copper.

2.7.2.1. Reagents

All solutions were prepared inside a Class-100 clean bench using ultra high purity (UHP) water ($\geq 18.2 \text{ M}\Omega \text{ cm}$, Elgastat Maxima). The eluent, 1.0 M nitric acid (HNO_3), was prepared by diluting 92.7 mL of 10 M ultra-pure sub-boiling distilled HNO_3 (SpA, Romil) to 1 L in UHP water. The sample buffer solution was prepared from a 2 M ammonium acetate stock: 70 mL ammonium solution (SpA, Romil) + 30 mL acetic acid (SpA, Romil) + 150 mL UHP water. The 0.3 M ammonium acetate sample buffer solution was prepared by diluting 12.5 mL of the 2 M ammonium acetate stock per 100 mL UHP water. The buffer solution was mixed with the acidified seawater samples on-line to attain pH 5.5–6. If

required the pH of the buffer solution was adjusted with acetic acid in order to attain the correct pH of the buffered sample.

2.7.2.2. Procedures

For the off-line preconcentration the peristaltic pumps (Minipuls 3, Gilson) were set at 15.0 rpm to attain the flow rates shown in Figure 2.9. Following a 1 M HCl rinse and then a MQ rinse, each for ~15 min, the sample line was filled with the sample, next the sample was loaded onto the preconcentration column for 900 s. Thus, 22.5 mL sample was loaded on to the column. The next stage was to rinse the column with UHP water for 60 s (1 mL). Following the rinse, the injection valve was switched so that the eluent (1 M HNO₃) flowed across the column in the opposite direction. At the same time the sample collection line was placed in a 2 mL polyethylene cryogenic vial (Nalgene) to collect the sample. The elution stage took 60 s, but the sample was collected for 90 s, to ensure that all the eluted analyte was collected and that there was a suitable volume collected for ICP-MS detection. Collection of 1.5 mL of sample resulted in a fifteen-fold concentration factor. The final stage was a second 60 s MQ rinse (which ran to waste).

Dissolved Cu was determined in the preconcentrated samples by quadrupole ICP-MS (Thermo X-Series 2, Hemel Hempstead). The ICP-MS parameters used are shown in Table 2.4. The collision cell was not used for the final concentrations reported in Chapter 4, but was used initially whilst investigating

dFe and dZn recovery from reference samples. This was to minimise polyatomic interferences such as $^{40}\text{Ar}^{16}\text{O}^+$ on $^{56}\text{Fe}^+$.

Table 2. 4. ICP-MS parameters for the determination of dissolved Cu in seawater samples following off-line extraction.

Instrument	Thermo Scientific X-series 2 ICP-MS
Matrix	1 M HNO ₃
Eluent	Argon
Forward Power	1.4 kW
Coolant gas	13.0 L min ⁻¹
Auxiliary flow	0.8 L min ⁻¹
Plasma Flow	15 L min ⁻¹
Nebulizer flow	0.85 L min ⁻¹
Nebulizer	Glass concentric
Spray Chamber assembly	ESI PC ³
Dwell time (ms)	10
Mass : charge ratio (m/z)	⁶³ Cu, ⁶⁵ Cu, ¹¹⁵ In
Optimisation	Multi-element standard containing 10 µg L ⁻¹ Ba, Be, Bi, Ce, Co, In, Li, Ni, Pb and U.
Collision cell 7% H ₂ in He*	3.5 mL min ⁻¹

*Collision cell not used for dCu concentrations reported in Chapter 4

The analytical system was calibrated daily by simple linear regression of standard curves. Stock standard solutions were prepared in UHP water weekly or daily (first dilution weekly, subsequent dilutions daily) by serial dilution of 15.7 mM Cu, 17.9 mM Fe and 15.3 mM Zn atomic absorption standard solutions (Romil). Mixed working standards (additions of 14–112 ppt Cu, Fe and Zn) were prepared in 1 M HNO₃ (SpA, Romil). An internal standard of 10 ppt indium (In) was added to all standards and samples. Standards were run at the beginning of each analytical run in triplicate, and concentrations calculated from ¹¹⁵In-corrected counts. Standard curves were linear ($r^2 > 0.99$) for the range of standard additions used in this study, where $y = 129.82x + 4685.4$ (Figure 2.10).

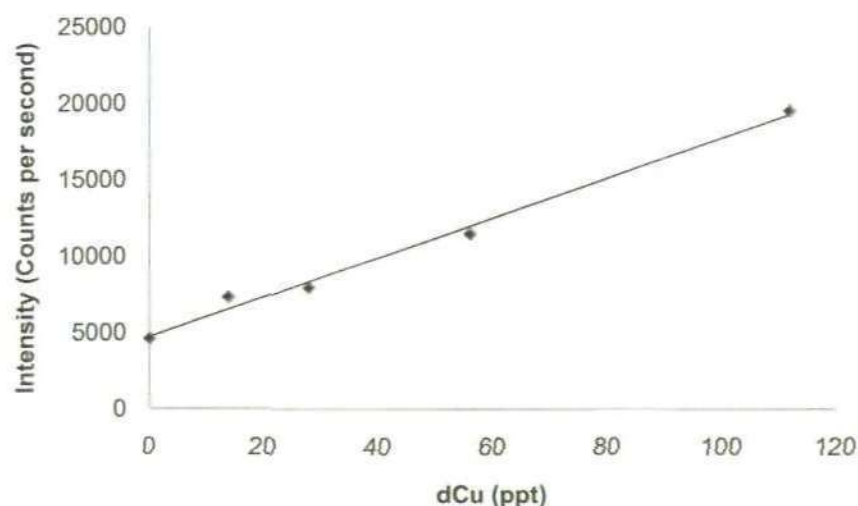


Figure 2. 10. An example of a calibration curve of standard additions of dCu (collision cell off) by ICP-MS with off-line preconcentration (error bars of ± 1 sd).

2.7.3. Analytical figures of merit

2.7.3.1. Blanks and detection limits

The blank signal was generated by running a complete analytical cycle without loading a sample. This approach was able to determine the contribution the sample-buffer (0.3 M ammonium acetate) and the eluent (1 M HNO₃) had on the analytical signal. As for the FI-CL techniques described in sections 2.6 and 2.7, the sample-buffer line had a clean-up column (containing Toyopearl resin) incorporated in-line to remove any trace metal impurities that may have otherwise interfered with the signal. This resulted in dCu blanks of 0.28 ± 0.004 nM. The detection limit was calculated as the dCu concentration corresponding to three times the standard deviation of the blank, resulting in a detection limit of 0.01 nM ($n = 3$) in seawater.

2.7.3.2. Accuracy and precision

The concentration of dCu in acidified surface seawater samples from the *SAFe* (S) (Johnson *et al.*, 2007) and *GEOTRACES* (GS) programmes was determined to assess the accuracy of this technique. Concentrations of dCu determined in the surface reference samples were in good agreement with results obtained for the same samples by other analytical techniques which also did not incorporate a UV-irradiation step (K. Bruland, pers. comm.) This study: *SAFe* S = 0.40 ± 0.01 nM, GS = 0.74 ± 0.01 nM, reference samples: *SAFe* S = 0.55 ± 0.04 nM, GS = 0.6–0.7 nM. The reference samples were analysed by ICP-MS together with the preconcentrated samples from the bioassays from the *INSPIRE* cruise, and the results are presented in Chapter 4. The analytical precision of the method was determined from repeat analyses of the surface water reference samples (*SAFe* S and *GEOTRACES* GS), yielding an uncertainty of $\pm 2.3\%$ expressed as relative standard deviation on the mean ($n = 3$).

2.7.4. Discussion and recommendations

As part of the analytical cycle, a survey run of each sample was undertaken prior to analysis. Despite the off-line preconcentration and separation step, this revealed that very high levels of sodium (Na) (10^8 cps compared to 10^4 for Cu, 10^{5-6} for Fe, and 10^{3-5} for Zn depending on the isotope) were retained on the resin after the rinse step and eluted with the analytes of interest (Cu, Fe and Zn). Repeat analysis of blank samples during an analytical run for dCu showed no significant change in concentration, indicating that Na build-up on the cones was not causing interferences with recovery. Discussions with Dr Angela Milne during the optimisation process revealed that comparable counts of Na were

detected using a similar ICP-MS method (isotope dilution, Milne *et al.*, 2010), and that when an ammonium acetate rinse was used no increase in sensitivity was observed.

Initially the aim was to be able to determine dCu, dFe and dZn simultaneously. In order to do this the PVC peristaltic pump tubing (Elkay) that was used for the FI-CL applications used in this study was replaced by silicone tubing (Elkay) as this was found to reduce the Zn blanks (Milne *et al.*, 2010). In addition, early investigations used a collision cell (gas flow rate 3.5 mL min^{-1}) to reduce polyatomic interferences, and a range of concentration factors were investigated (x12, x15, x20). However, recovery of dFe was generally poor and inconsistent. On occasions the 'correct' consensus value was attained (GEOTRACES (GD) this study = $0.94 \pm 0.01 \text{ nM}$, consensus value = $0.92 \pm 0.02 \text{ nM}$). However, dFe recovery was inconsistent, often being significantly greater than the consensus value. In contrast, dZn recovery was up to an order of magnitude too low and occasionally below the limit of detection. Unfortunately, time constraints prohibited further optimisation of this technique to allow simultaneous recovery of these three trace metals. Therefore, it was decided to concentrate on the determination of dCu, as dFe could be determined by FI-CL and determination of dZn is notoriously problematic. Consequently, dCu measurements were made without the collision cell because of the greater degree of sensitivity afforded.

The contribution of the blank to the signal of dCu was relatively high (0.28 ± 0.004 nM), comprising 59.5% of the zero addition standard (acidified seawater, 0.47 ± 0.007 nM). Fortunately, the sensitivity was such that this ICP-MS technique was able to accurately determine dCu in GEOTRACES reference samples. However, future work should concentrate on reducing the concentration of dCu in the blank. This might be possible by increasing the volume of Toyopearl resin in the clean-up column. Additionally, further optimisation work is required to enable simultaneous detection of dFe and dZn (and dCu). In order to do this future analytical runs will need to be conducted with the collision cell on.

Chapter 3

Controls on Dissolved Cobalt in Surface Waters of the Sargasso Sea

3.1. Introduction

Cobalt (Co) is an important micronutrient for marine phytoplankton (Morel *et al.*, 1994; Croft *et al.*, 2005). While it is widely accepted that iron (Fe) limits phytoplankton growth over large areas of the surface ocean (*e.g.* Coale *et al.*, 1996; Boyd *et al.*, 2000), there is increasing evidence which suggests other trace elements such as Co may limit or co-limit algal growth in some oceanic regions (Saito *et al.*, 2008). Indeed, a number of recent studies have recognised the importance of Co in influencing phytoplankton dynamics in the open ocean (*e.g.* Saito *et al.*, 2002; 2004; 2005; Bertrand *et al.*, 2007; Panzeca *et al.*, 2008; Saito and Goepfert, 2008).

Cobalt is required for the synthesis of vitamin B₁₂ by marine prokaryotes. Vitamin B₁₂ is a biologically produced, Co-containing organometallic compound that is only produced by certain bacteria and archaea, hence eukaryotes must either acquire it from the environment, or possess an alternative metabolism with no vitamin B₁₂ requirement (Bertrand *et al.*, 2007). Cobalt is also a co-factor in the enzyme carbonic anhydrase (CA), which is required by marine phytoplankton for inorganic carbon acquisition (Lane and Morel, 2000). Some eukaryotic phytoplankton are able to substitute Co or cadmium (Cd) for zinc (Zn) in CA but there are some marine phytoplankton, such as the cyanobacteria *Prochlorococcus* and *Synechococcus*, which have an absolute requirement for Co (Sunda and Huntsman, 1995a; Saito *et al.*, 2002). Given that *Prochlorococcus* is thought to be the most abundant autotroph in the ocean (Partensky *et al.*, 1999) and accounts for a significant proportion of global photosynthesis (Goericke and Welschmeyer, 1993; Campbell *et al.*, 1994),

there is a need to understand the potential role of Co in controlling the growth and distribution of this organism. In addition, there is emerging evidence that some forms of alkaline phosphatase (AP), a metalloenzyme that facilitates acquisition of phosphorus (P) from the dissolved organic phosphorous (DOP) pool (Cembella *et al.*, 1982), may contain Co as a metal cofactor (Gong *et al.*, 2005) rather than Zn (*e.g.* Plocke *et al.*, 1962). Expression of AP is of particular importance in the North Atlantic Subtropical Gyre, where up to 30% of primary production may be supported by the DOP pool (Mather *et al.*, 2008). Jakuba *et al.* (2008) have also provided evidence for important linkages in the biogeochemical cycles of Co, Zn and P in the phosphorous-poor surface waters of the Sargasso Sea. At present, however, the biogeochemical cycling of Co and the extent to which this trace element may influence the phytoplankton community in the surface ocean are not well understood.

In seawater the biogeochemistry of Co and Fe share a number of similarities; both metals have vertical distributions that are strongly influenced by biological uptake, recycling and scavenging (Saito and Moffett, 2002). Vertical concentration profiles of dissolved Co and Fe can be considered as a hybrid of 'nutrient-type' and 'scavenged-type' (Noble *et al.*, 2008; Boyd and Elwood, 2010). Furthermore, the chemical speciation of dissolved Co and Fe in seawater is similar; both have similar redox chemistries (both are present in the 3+ oxidation state under oxic conditions) and their speciation is dominated by organic complexation. For example, Ellwood and van den Berg (2001) found that when Co-binding ligands were present in excess of total dissolved cobalt (dCo), all of the dCo was organically bound. Similarly, > 99% of total dissolved iron (dFe) in seawater has been shown to be complexed by organic ligands in

seawater (Gledhill and van den Berg, 1995; Rue and Bruland, 1997; van den Berg, 1995).

Dissolved Co concentrations in open ocean surface waters are extremely low (~4-120 pM, e.g. Knauer *et al.*, 1982; Martin *et al.*, 1989; Saito *et al.*, 2004), with remote ocean regions tending towards the lower end of this range. In the Sargasso Sea, for instance, dCo concentrations < 20 pM are reported (Jickells and Burton, 1988; Saito and Moffett, 2002). In surface waters at the Bermuda Atlantic Time-series Study station (BATS, 31°N, 64°W), Saito and Moffett (2002) reported a significant depletion of sea-surface dCo (annual mean 20 ± 10 pM) relative to concentrations below the euphotic zone (~30-40 pM). These workers observed no clear relationship between the summer maximum in aeolian dust deposition and surface dCo concentrations, leading them to conclude that atmospheric deposition was not an important control on dCo in surface waters of the Sargasso Sea. This conclusion stands, in marked contrast to the situation for dissolved Fe, for which there is evidence of significant aeolian input to the Sargasso Sea surface waters (Wu and Boyle, 2002; Sedwick *et al.*, 2005). However, at a more northerly station in the North Atlantic Ocean (40°N 23°W), Ellwood and van den Berg (2001) have reported dCo enrichment in the surface mixed layer, (34 ± 3 pM at < 40 m) relative to deeper waters in the photic zone (25 ± 4 pM at 65-165 m). The vertical profiles observed are suggestive of either a surface source, such as aerosol deposition, and/or variation in the rate of removal of dCo as a function of depth.

Located in the western North Atlantic subtropical gyre, the Sargasso Sea is well situated for studying the impact of atmospheric deposition on the distribution of

trace metals in the surface ocean, owing to the atmospheric and oceanographic time-series observations that have been collected in the region over several decades. The atmospheric observations have shown that aerosols over Bermuda and the surrounding ocean region are typically dominated by air masses carrying North African mineral aerosols ('Saharan') during the summer and early autumn months, whereas aerosols carried from North America, Asia and Europe are more abundant during the late autumn and spring (e.g. Duce and Hoffman, 1976; Chen and Duce, 1983; Arimoto *et al.*, 1995, 2003; Moody *et al.*, 1995; Huang *et al.*, 1999; Smirnov *et al.*, 2002). Recent work by Sedwick *et al.* (2007) and Sholkovitz *et al.* (2009) in the Bermuda region suggests that aerosols associated with North American air masses contain a greater proportion of anthropogenic combustion products as well as Fe that is more readily water soluble, relative to the Saharan dust that is carried in air masses from North Africa.

The atmospheric transport of mineral aerosols (dust) is thought to provide a major source of dissolved Fe to open ocean surface waters (Duce and Tindale, 1991; Jickells *et al.*, 2005). At present, however, it is uncertain whether aeolian deposition represents a significant source of dissolved Co to surface waters of the open ocean. If aerosol deposition is a significant source of Co to surface waters, differences in the operational solubility associated with aerosols of different composition/provenance (Sedwick *et al.*, 2007) and/or the extent of atmospheric processing may be significant (Mackie *et al.*, 2005, 2006; Baker *et al.*, 2006; Baker and Jickells, 2006). Here we gain insight into the biogeochemical cycling of Co in the surface ocean, by examining trace metal data obtained for water-column samples, underway surface-water samples and

aerosol samples collected along a meridional section of the Sargasso Sea to the south of Bermuda in June 2008.

3.2. Methods

3.2.1. Study area

Samples were collected aboard the RV *Atlantic Explorer* during the *FeAST-6* cruise, which included a meridional transect of the Sargasso Sea from the BATS region at $\sim 31^\circ\text{N}$ southward to $\sim 24^\circ\text{N}$ from 5-18 June 2008. In terms of the flux and source of aerosols to the Sargasso Sea, June is a transitional month with large variations in Fe loading and V/Al ratios (an indicator of the amount of anthropogenic aerosols present in the bulk aerosol) (Sholkovitz *et al.*, 2009). In the later summer months (July-Sept.) Saharan sources dominate dust supply and the quantity of dust deposited over the region is typically higher compared to the preceding months (where aerosol supply is lower and characterized by higher V/Al ratios) (Arimoto *et al.*, 1995; Huang *et al.*, 1999; Gao *et al.*, 2001; Sholkovitz *et al.*, 2009). The cruise track was chosen to include water column sampling stations that were located both within and between mesoscale eddies, according to satellite sea level altimetry analyses. Information on the location and mesoscale circulation associated with each water-column sampling station is provided in Table 3.1.

Table 3. 1. Details of water-column trace metal sampling stations occupied during *FeAST-6*.

Station	Date	Lat ($^\circ\text{N}$)	Long ($^\circ\text{W}$)	Eddy context
K1	06/06/2008	31.48	62.75	Cyclone
K2	09/06/2008	28.93	64.44	Anticyclone
K3	10/06/2008	27.50	64.50	Between eddies
K4	13/06/2008	25.63	63.88	Anticyclone
K5	14/06/2008	24.00	63.88	Between eddies

3.2.2. Seawater sample collection and treatment

Water column samples - Water column samples were collected for trace metals analysis from five stations (K1–K5) along the north-south transect (Fig. 3.1, Table 3.1). Samples were collected in modified 5 L Teflon-lined external closure Niskin-X samplers (General Oceanics Inc.) deployed on a Kevlar line (Sedwick *et al.*, 2005). The surface seawater (0-1 m depth) samples for the water column profiles were collected in 1 L wide-mouth low density polyethylene bottles (LDPE, Nalgene) mounted on the end of a ~5 m bamboo pole, which was extended from the ship's stern for sample collection whilst backing slowly into the wind. Upon recovery, seawater samples were filtered inside a shipboard Class-100 clean container laboratory, through a 0.4 µm pore Supor Acropak filter capsule (Pall Corp.) that was pre-rinsed with ~5 L of ultrapure deionized water (> 18 MΩ cm, Barnstead Nanopure) followed by several hundred mL of each sample (Niskin-X samples), or through 0.4 µm pore Poretics polycarbonate membrane filters (surface sample only) mounted in a Savillex Teflon PFA filtering assembly (Sedwick *et al.*, 2005). The filtered seawater samples were acidified to 0.024 M with ultrapure HCl (SpA Romil for Al and Co analysis; Seastar Baseline for Fe analysis) prior to analysis, and stored in rigorously acid-cleaned Nalgene LDPE bottles (Sedwick *et al.*, 2005; Shelley *et al.*, 2010).

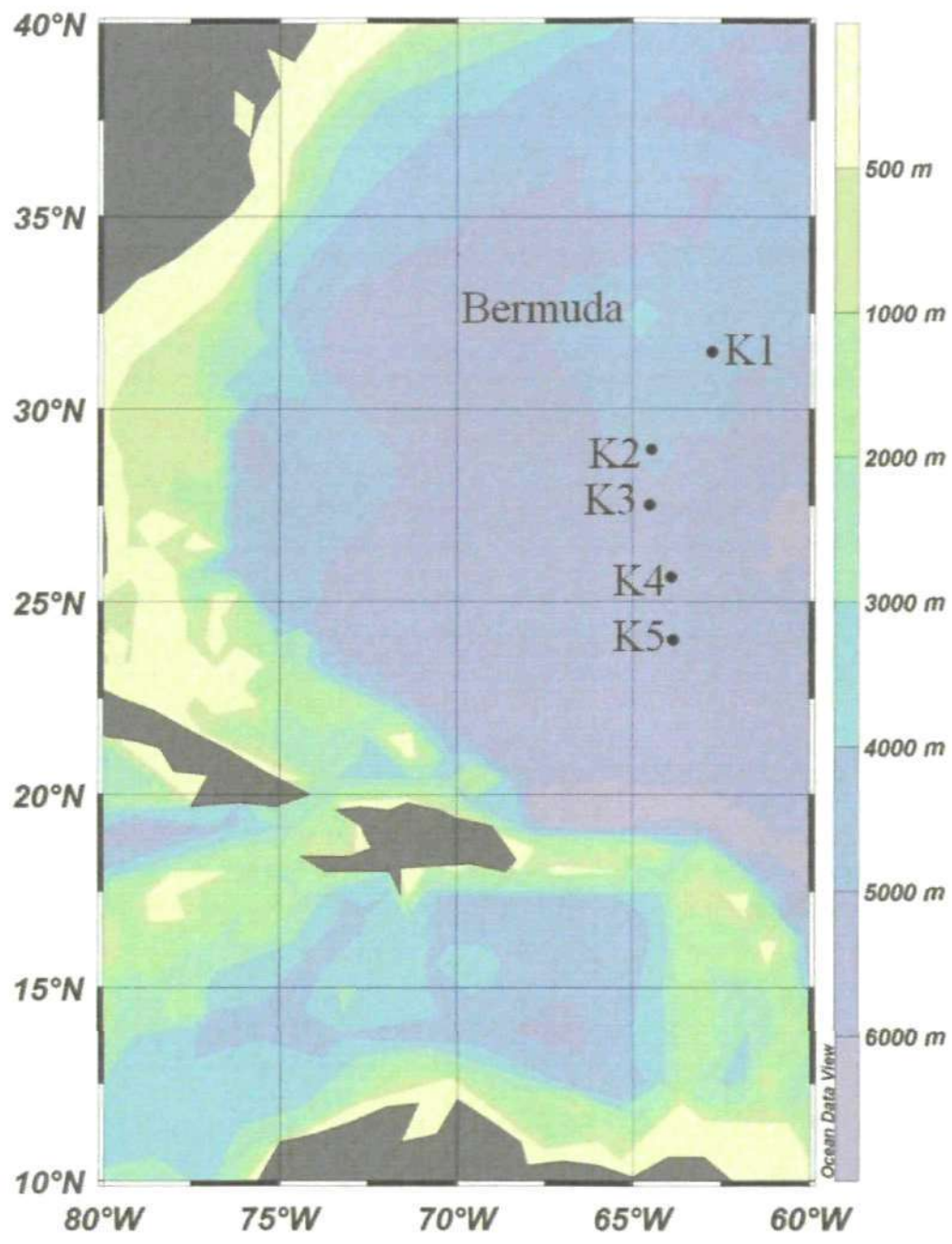


Figure 3. 1. FeAST-6 cruise track (June 2008) in the Sargasso Sea showing, from north to south, stations K1–K5.

Underway surface samples – In order to investigate lateral variations in surface waters, concentrations of dissolved Co, Fe and Al, in near-surface seawater samples were collected during four transects between the water column

sampling stations. Water was pumped from ~5 m depth directly into a shipboard 'clean bubble' using a trace-metal clean towfish sampler (Bruland *et al.*, 2005). During these transects, water samples were collected every hour, thus providing water near-surface samples at spacings of ~12 km. The underway seawater samples were filtered in-line through a 0.4 µm pore Supor Acropak filter capsule (Pall Corp.) and then acidified to ~0.024 M with ultrapure HCl and stored in LDPE bottles, as described for the water column samples.

Determination of trace metals in seawater samples – Both dCo and dFe were determined by flow injection analysis with in-line preconcentration. For the determination of dCo, the flow injection manifold was coupled with a photomultiplier tube and dCo was determined in UV-irradiated samples by means of chemiluminescence, as described by Shelley *et al.* (2010). Dissolved Fe was determined by flow injection analysis with spectrophotometric detection modified from the method of Measures *et al.* (1995), as described by Sedwick *et al.* (2008). Dissolved Al was determined by flow injection analysis using micelle-enhanced fluorimetric detection using Brij-35 as the surfactant instead of Triton-X 100 (Resing and Measures, 1994; Brown and Bruland, 2008).

Accuracy of the analytical methods used for the determination of dCo, dFe and dAl was assessed through the analysis of reference seawater samples from the SAFe and GEOTRACES programs. For dCo, the method used in this study yielded 40.9 ± 2.6 pM for SAFe reference seawater D2, versus the consensus value of 43.1 ± 3.2 pM and 73 ± 3 pM for the GEOTRACES reference sample GD versus the consensus value of 68 ± 13 pM. For dFe, the method used in this study yielded 0.11 ± 0.01 nM and 0.97 ± 0.06 nM for SAFe reference

seawater S1 and D2, versus consensus values of 0.097 ± 0.043 nM and 0.91 ± 0.17 nM respectively. For dAl, the method used in this study yielded 28.8 ± 2.7 nM and 17.3 ± 2.5 nM for GEOTRACES reference seawater GD and GS, versus consensus values of 28 ± 1 nM and 18 ± 1 nM respectively (consensus values for the SAFe and GEOTRACES seawater are listed at, <http://www.es.ucsc.edu/~kbruland/GeotracesSaFe/kwbGeotracesSaFe.html>).

Aerosol sample collection and treatment – Aerosol samples were collected at sea during the FeAST-6 cruise using low volume pumps (air flow rate $\sim 2 \text{ m}^3 \text{ h}^{-1}$) that pulled air through acid-cleaned 47 mm diameter filter membranes mounted in downward-facing filter heads fitted with polyethylene rain shields (Véron and Church, 1997; Sedwick *et al.*, 2007). The filter heads were positioned on a 7 m high sampling tower located forward of the ship's bridge. Samples were collected while the ship was slowly underway into the wind, over periods of ~ 6 -12 hours. Two filter types were deployed in parallel: Millipore HA filters (0.45 μm nominal cutoff size) for the analysis of bulk aerosol composition, and Poretics polycarbonate membranes (0.4 μm pore size) for aerosol leaching experiments (see below).

Processing and analysis of aerosol samples – For determination of bulk aerosol composition, the aerosol-laden Millipore HA filter halves were treated with a 1:3 (v/v) mixture of 48% (w/w) hydrofluoric acid solution and 70% (w/w) nitric acid solution at 80°C for one day in the laboratory at the University of Delaware. Any filter residue was removed following dissolution of the aerosol particles, then the solution was heated to dryness. The digestion residue was re-dissolved in 1 M nitric acid. Total Co, Fe and Al were determined by inductively-coupled plasma

mass spectrometry (ICP-MS; Finnegan Element2). It is assumed that the Co, Fe and Al measured in the aerosol digest solutions account for both the labile and refractory fractions of these elements in the bulk aerosol, thus allowing calculation of 'total aerosol' concentrations in units of pM m^{-3} air (for total Co) or nM m^{-3} air (for total Fe and total Al) using the total volume of air passed through each aerosol filter sample. As there is currently no representative standard for trace metals in oceanic aerosol material, the accuracy of trace metal recovery from aerosol digests is validated by duplicating the widely published crustal weight ratio of Fe/Al (0.6) in dust samples from near Bermuda (Arimoto *et al.* 1995; T. Church, pers. comm.). During this study, Fe/Al was 0.6 ± 0.099 .

The fractional solubility of aerosol Co and Fe ($\% \text{Co}_s$ or $\% \text{Fe}_s$) in this study was estimated using a modification of the flow-through deionized water leaching protocol of Buck *et al.* (2006). In this study, 250 mL of ultrapure deionized water ($> 18 \text{ M}\Omega \text{ cm}$ resistivity, pH ~ 5.5 , Barnstead Nanopure) was passed through an aerosol-laden polycarbonate filter membrane held in a Savillex Teflon PFA filtering assembly (Sedwick *et al.*, 2007). The aerosol leaches were conducted under a Class-100 laminar flow hood within 6 hours of sample collection. The filtrate (leachate) was immediately transferred into a 125 mL LDPE bottle and acidified to $\sim 0.024 \text{ M}$ with Seastar Baseline ultrapure hydrochloric acid. Dissolved Co and Fe were subsequently determined in the leachate solutions by ICP-MS and flow injection analysis, respectively, as described by Sholkovitz *et al.* (2009). Blank solutions were prepared by passing 250 mL of deionized water over clean polycarbonate filter membranes that had been mounted on the shipboard sampling tower without running the pumps. Fractional solubility is operationally defined as the aerosol

concentration of soluble aerosol Co or Fe as calculated from dCo and dFe in the leachate solutions, expressed as a percentage of the total aerosol Co or Fe as calculated from analysis of the filter digest solutions (Sedwick *et al.*, 2007).

3.2.3. Air mass back trajectories

Five day air mass back trajectories were simulated for each sampling location using the NOAA Air Resources Laboratory Hybrid Single-Particle Lagrangian Integrated Trajectory model (HYSPLIT) (<http://ready.arl.noaa.gov/HYSPLIT.php>) (Draxler and Rolph, 2010; Rolph, 2010). Arrival heights of 200 m and 1500 m were selected; the 1500 m arrival height was chosen to include the Saharan Air Layer, which typically delivers Saharan dust to the American continent in summer at altitudes of ~1.5-6 km (Prospero and Carlson, 1972; Prospero *et al.*, 1981), whereas the 200 m arrival height was chosen to represent aerosols carried within the marine boundary layer.

3.2.4. Enumeration of phytoplankton groups

Three groups of picophytoplankton were enumerated by A. Macey (National Oceanography Centre, Southampton) using a FACSort flow cytometer (Becton Dickinson, Oxford, U.K.). For the flow cytometry analysis, 1.8 mL whole seawater samples were fixed with 1% paraformaldehyde and incubated at 4 °C for 24 h before freezing and storage at -80 °C. *Prochlorococcus*, *Synechococcus* and picoeukaryote cells were identified and enumerated using group-specific side scatter, along with orange (585 ± 21 nm) and red (> 650 nm) autofluorescence properties (Olson *et al.*, 1993). Multifluorescent beads (0.5

μm) were added to all samples at known concentrations to enable enumeration using syringe pumped flow cytometry (Zubkov and Burkill, 2006).

3.3. Results and Discussion

3.3.1. Hydrographic and biogeochemical observations

In the Sargasso Sea, the region between 25°N and 32°N forms a transitional zone between permanently stratified oligotrophic waters in the subtropical convergence zone south to seasonally oligotrophic waters in the north (Steinberg *et al.*, 2001). In the BATS region near 31°N, convective mixing to depths of 150-300 m during late autumn through early spring replenishes surface waters with macronutrients, which are subsequently depleted to nanomolar concentrations between April and October, when the surface mixed layer depth shoals to less than 20 m (Steinberg *et al.*, 2001). Net surface flow in our study region is dominated by southwesterly geostrophic circulation, whereas westerly-propagating mesoscale eddies dominate surface ocean circulation over sub-seasonal timescales (Siegel *et al.*, 1999; Steinberg *et al.*, 2001; McGillicuddy *et al.*, 2007).

Hydrographic data (temperature, salinity and in-situ fluorescence) from the FeAST-6 water column sampling stations are shown in Figure 3.2. The surface mixed layer depth (MLD) was ~ 10 m along the entire transect, which is typical of this ocean region in the northern summer. Dissolved nitrate and phosphate were depleted to concentrations below 50 nM (data not shown) to depths of ~ 100-150 m at all water column sampling stations. In addition, a subsurface

chlorophyll maximum was observed at ~ 150 m depth at each station along the cruise track (Fig. 3.2). Low salinity features were observed at the surface at all stations indicating significant rainfall prior to the cruise. This was supported by weekly rainfall data from the Tudor Hill atmospheric observatory that showed highest rainfall in our records in April and May 2008 which was just prior to the cruise.

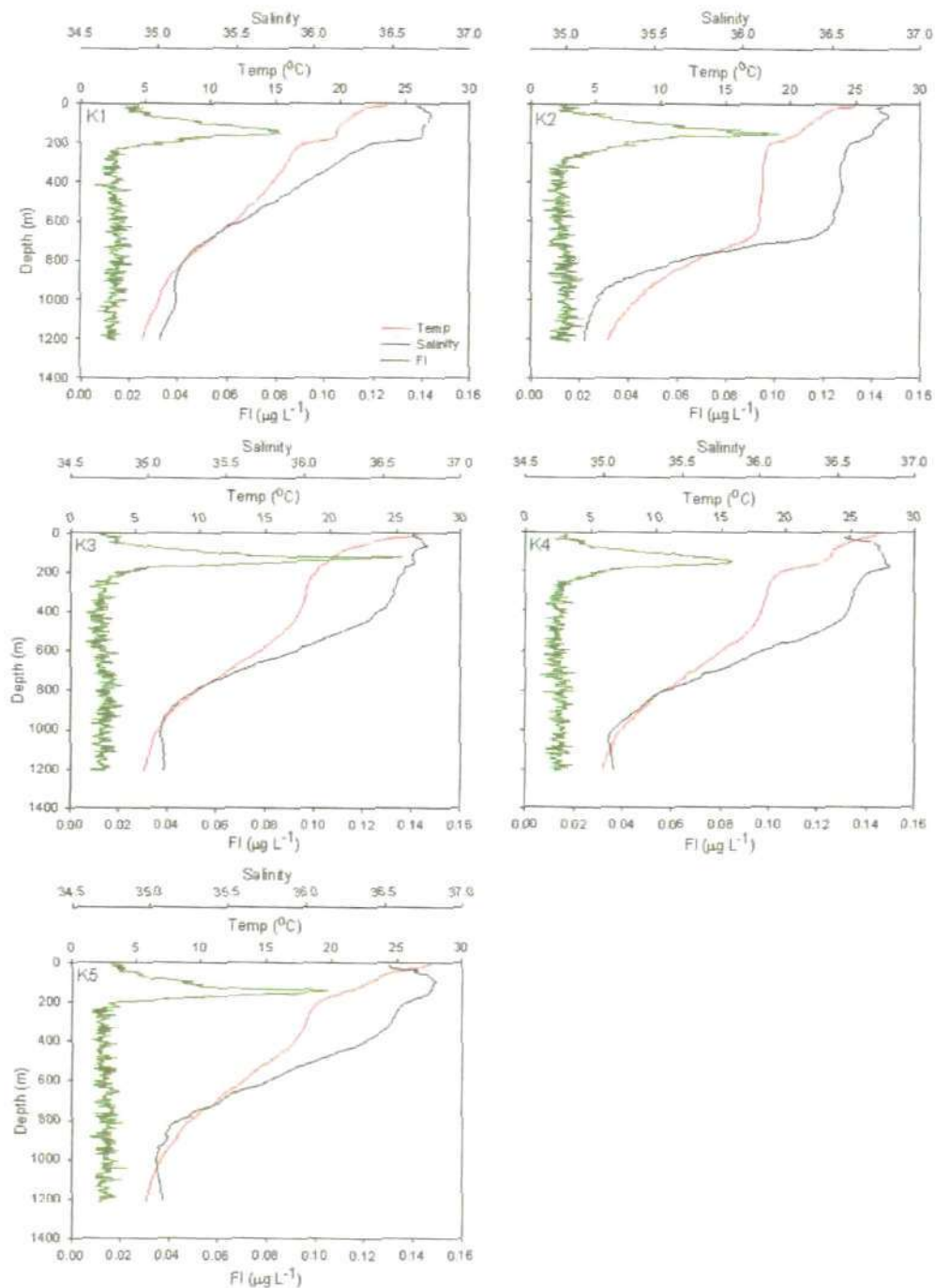


Figure 3. 2. Vertical profiles of temperature ($^{\circ}\text{C}$), salinity and chlorophyll-a (fluorescence; $\mu\text{g L}^{-1}$).

The distribution of dCo at Station K1 (31.48°N, 62.75°W), which was located close to the BATS station (31.67°N, 64.17°W), shows excellent agreement with the dCo profile reported by Milne *et al.* (2010) which was sampled from a similar position 17 days later as part of the GEOTRACES Intercalibration programme. Dissolved Co concentrations from these two profiles was 27 ± 2 pM at 25 m, 54 ± 2 pM at 500 m and 75 ± 7 pM at 1000 m (Fig 3.3). The dCo concentrations in these two profiles were determined by different techniques (this study FI-CL, Shelley *et al.*, 2010 and ICP-MS with offline preconcentration, Milne *et al.*, 2010). The excellent agreement between these two profiles indicates the suitability of these two techniques for the determination of dCo in seawater samples.

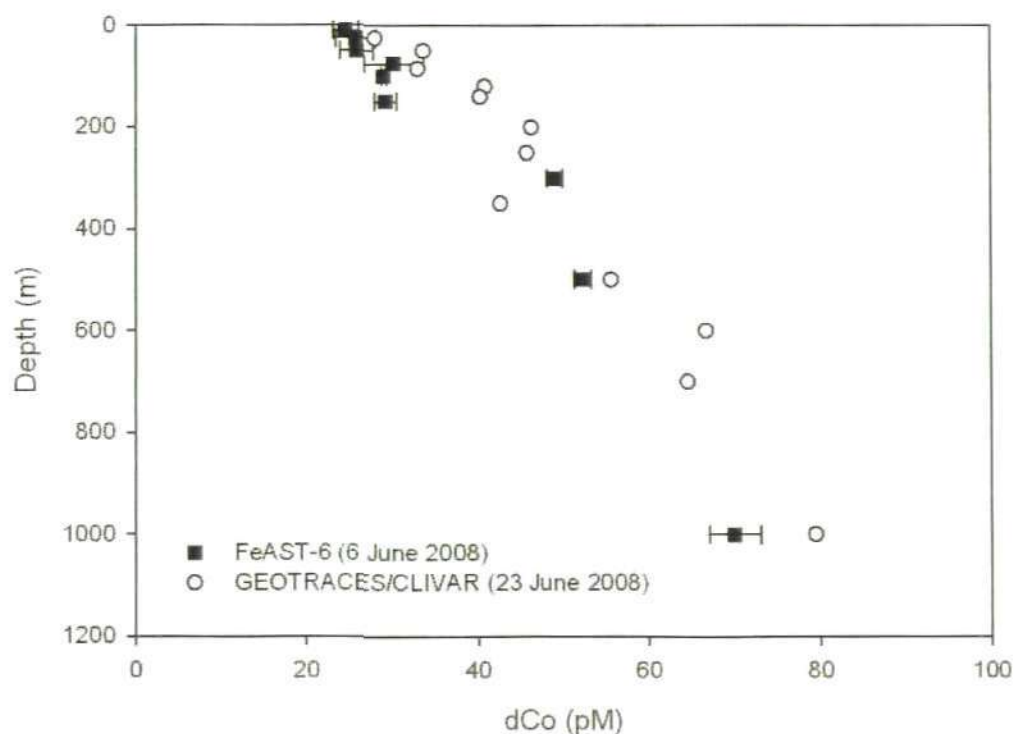


Figure 3. 3. Comparison of vertical profiles of dCo in the vicinity of BATS (31.67°N, 64.17°W), sampled during the *FeAST-6* cruise (black squares) and the GEOTRACES Intercalibration II cruise.

3.3.2. Surface transects

Surface transects were undertaken to investigate the relationship between dCo, dFe and dAl in surface waters. The north-south (N-S) surface distributions of dCo, dFe and dAl along the cruise track from ~31°N to 24°N are shown in Figure 3.4. All three trace metals displayed significant lateral variability (dCo = 18-63 pM, dFe = 0.3-1.6 nM, dAl = 14-43 nM), both within and between the four underway transects, which likely reflects the mesoscale surface circulation, variable small-scale inputs and the expected north to south increase in dust deposition. In regions remote from mineral aerosol sources, surface dAl concentrations are typically less than 1 nM (Jickells *et al.*, 1994; Measures and Vink, 2000). Given that the residence time of Al in surface waters of the Sargasso Sea is estimated to be in the region of 6.5 years with the highest flux in late summer (Jickells *et al.*, 1994; Han *et al.*, 2008), the surface dAl data from this study suggest significant dust deposition to the Sargasso Sea.

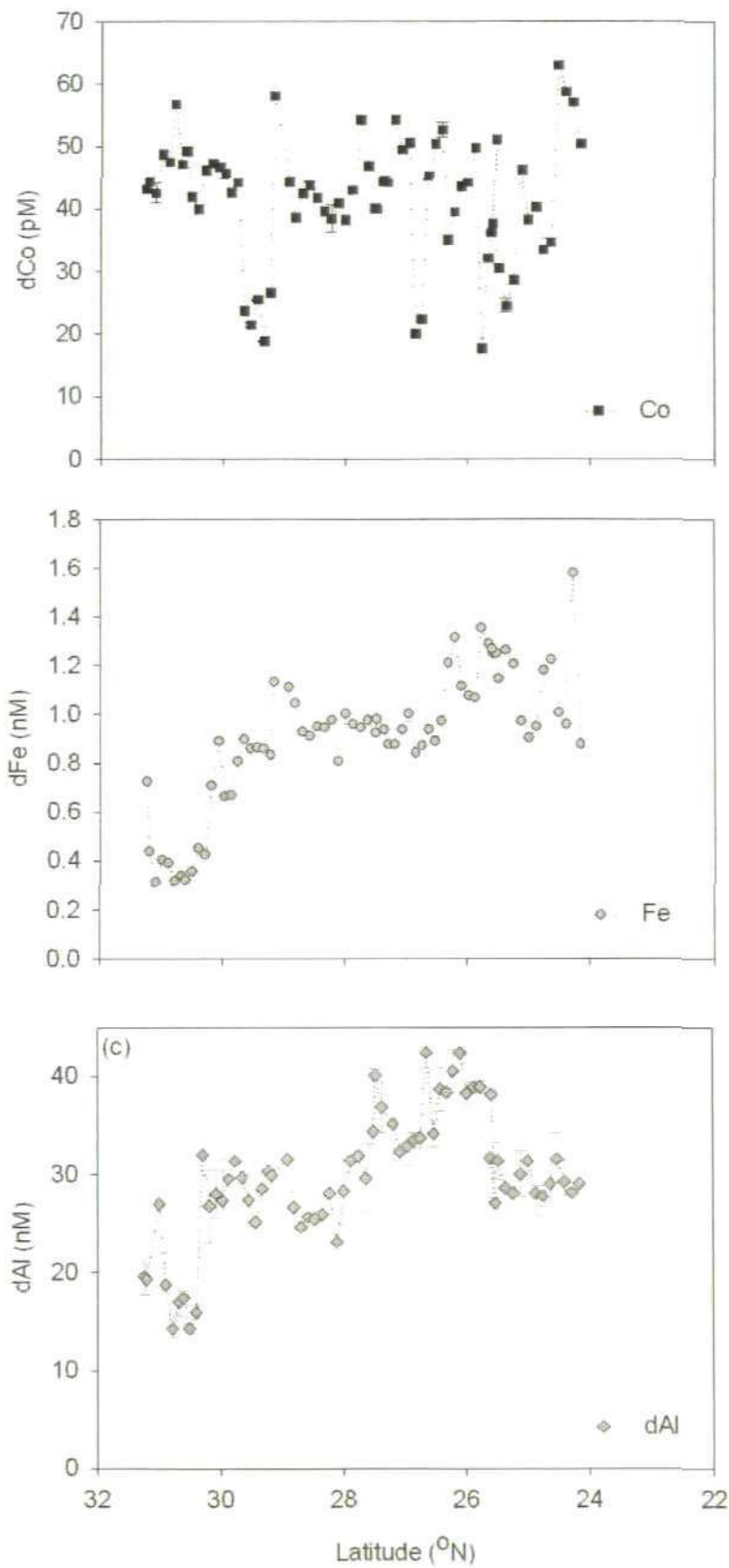


Figure 3. 4. Surface concentrations of dCo (± 1 sd), dFe (determined by P. Sedwick) and dAl (± 1 sd, determined by P. Cabedo-Sanz) from 31-24° N during FeAST-6.

Over the subtropical North Atlantic Bergquist and Boyle (2006) noted that there is much less of a north-south gradient in surface dFe than would be expected based on the steep (10x) aerosol deposition gradient. This possibly reflects the higher solubility of aerosol Fe in the north, relative to further south (under the Saharan plume), where lower aerosol Fe solubility might lessen the impact of high dust deposition (E. Boyle, pers.comm.). Thus, the poor correlation between sea surface concentrations of dFe (or dAl) versus *in situ* aerosol deposition flux in the western North Atlantic gyre reported by Bergquist and Boyle (2006) was attributed to the difference in surface residence times of dFe and dAl (214–291 days for dFe compared to 3–6.5 years for dAl (Orlans and Bruland, 1986; Jickells *et al.*, 1994; Jickells, 1999) and the scarcity of atmospheric deposition samples for the open-ocean. The study by Bergquist and Boyle (2006) covered a larger area and extended into the tropics. During *FeAST-6* (~31–24°N) the significant co-variation between dFe and dAl in surface waters (correlation coefficient = 0.63, $p = 1.92 \times 10^{-8}$, $n = 65$) represents an ~ 3x north-south increase in dFe and dAl concentrations and this is consistent with the expected gradient in aerosol dust deposition (based on Jickells *et al.*, 2005).

In the surface waters of the Sargasso Sea, dCo has an even shorter estimated residence time than dFe (dCo = 117 days, Saito and Moffett, 2002). Thus, the absence of a correlation between dCo (Fig. 3.4a) and dAl (Fig. 3.4c) concentrations (correlation coefficient = 0.08, $p = 0.54$, $n = 65$), may reflect the relatively minor importance of aeolian Co input, higher solubility of Co in the north of our study region, and/or the shorter residence time of dCo compared to dFe and dAl. Although there was no correlation between surface dCo and dAl concentrations, the vast majority of surface samples had dCo concentrations

(mean 42 pM) greater than the reported regional annual average of 20 ± 10 pM (Jickells and Burton, 1988; Saito and Moffett, 2002), indicative of a source to surface waters.

3.3.3. Fractional solubility of aerosol cobalt and iron

To quantify *in situ* dry deposition of dCo, ship-board aerosol samples were collected between the stations. The total aerosol Co loading in the samples ranged from 5.4-11.0 $\mu\text{g Co m}^{-3}$ which resulted in air-sea fluxes of 4.7-9.5 $\text{ng m}^{-2} \text{d}^{-1}$ (Table 3.2a). Assessment of the % soluble Co in the aerosols by DI-water leaches showed that most of the Co delivered to the surface ocean during FeAST-6 was soluble (75-100%). This was substantially higher than the solubility of aerosol Fe (5-45%).

Table 3. 2. (a) Aerosol Co and (b) Fe fluxes and fractional solubility during FeAST-6 (low dust deposition). Note that the calculated solubility for one sample in Table 3.2a was 115%, but it has been corrected to reflect maximum possible solubility. This analytical artefact is likely due to the extremely low concentrations of Co (5-15 $\mu\text{g Co m}^{-3}$ air) in the bulk aerosol (c.f. Fe 10-28 Fe ng m^{-3} air).

(a)	Total aerosol Co loading ($\mu\text{g Co/m}^3$ air)	Deposition velocity (m/s)	Total Co Flux _{dry} ($\mu\text{g/m}^2/\text{d}$)	%Co _S	Soluble Co flux ($\mu\text{g/m}^2/\text{d}$)	Soluble Co flux (pmol/m ² /d)
9 June 2008	0.00000544	0.01	0.00470	93	0.00435	74
10 June 2008	0.00001058	0.01	0.00914	100	0.00914	155
12 June 2008	0.00001102	0.01	0.00952	75	0.00712	121
14 June 2008	0.00000401	0.01	0.00346	79	0.00274	47
16 June 2008	0.00001050	0.01	0.00907	78	0.00712	121

(b)	Total aerosol Fe loading ($\mu\text{g Fe/m}^3$ air)	Deposition velocity (m/s)	Total Fe Flux _{dry} ($\mu\text{g/m}^2/\text{d}$)	%Fe _S	Soluble Fe Flux _{dry} ($\mu\text{g/m}^2/\text{d}$)	Soluble Fe Flux _{dry} (nmol/m ² /d)
9 June 2008	0.0115	0.01	9.936	9	0.865	15.5
10 June 2008	0.0105	0.01	9.07	45	4.061	72.7
12 June 2008	0.0133	0.01	11.49	36	4.150	74.3
14 June 2008	0.0276	0.01	23.85	5	1.210	21.7
16 June 2008	0.0163	0.01	14.08	10	1.384	24.8

Although there have been laboratory studies that have investigated the dissolution of Co from end member dust types (Thuróczy *et al.*, 2010), few studies have determined the fractional solubility of Co in marine aerosols. The fractional solubility estimates from this study (Table 3.2) suggest a much greater fractional solubility for aerosol Co (75-100%) than for anthropogenic end member dusts (0.8%). This suggests that atmospheric processing (*e.g.* particle 'sorting', exposure to low pH in clouds, photochemical reactions) increases the solubility of Co in transit from continental sources and therefore plays a key role in effecting the flux of Co to the open-ocean. For instance, aerosol particles are exposed to ~10 condensation/evaporation cloud cycles (cloudwater can have very low pH due to H₂SO₄ and HNO₃ uptake and SO₂ oxidation) before removal via wet deposition (rainfall) (Spokes *et al.*, 1994).

In this study the highest Co solubility (100%) was associated with the lowest Fe loading (10 ng m⁻³). Iron solubility in the BATS region has been found to vary inversely as a function of the total Fe loading on the bulk aerosol, with differences in the relative solubility and total aerosol Fe loadings being attributed to the origin and composition of the aerosol particles (Sedwick *et al.*, 2007). Low Fe loadings and relatively high solubilities have been found in aerosols carried in air masses that have passed over North America/Asia/Europe (Sedwick *et al.*, 2007). Our data from shipboard aerosol sampling suggest that the aerosols sampled during *FeAST-6* contained a significant proportion of non-Saharan particles. Indeed, air mass back trajectory simulations indicate a predominantly North American origin (Fig. 3.5).

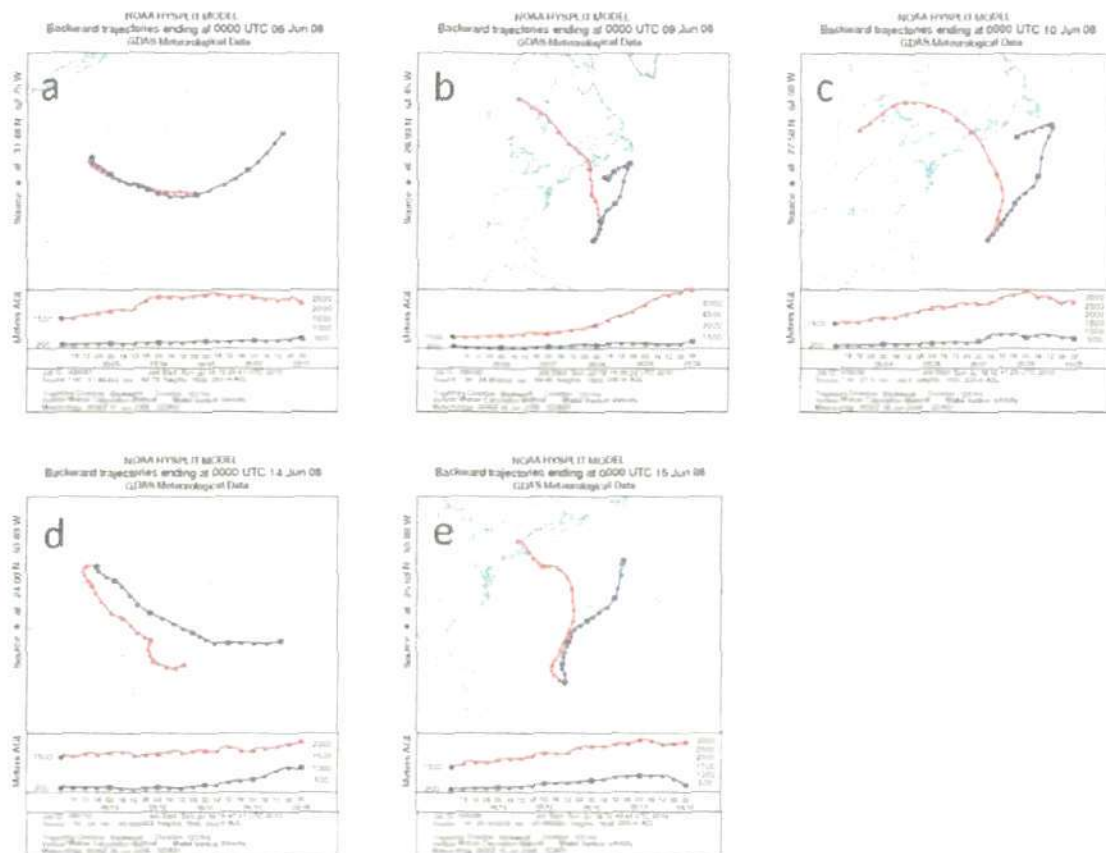


Figure 3. 5. Five day air mass back trajectory simulations (HYSPLIT model) for stations during FeAST-6 showing (a) K1, Atlantic maritime (a 10 day back trajectory indicated no contact with major land masses within the modelled period); (b) K2, North American; (c) K3, North American; (d) K4, Atlantic maritime (a 10 day back trajectory indicated a Saharan origin) and (e) K5, North American end members.

Total aerosol Fe loadings can be used to estimate the dry deposition flux of total aerosol Fe (total Fe F_{dry}) (Arimoto *et al.*, 1985). Using a similar approach the dry deposition flux of total aerosol Co (total Co F_{dry}) can be estimated according to Equation 1:

$$\text{total Co } F_{dry} = C_a \times V_d \quad (\text{Equation 1})$$

where C_a is the total aerosol Co loading ($\mu\text{g m}^{-3}$ air) and V_d is the dry deposition velocity of the Co-bearing aerosol particles. In this study V_d is assumed as a constant 0.01 m s^{-1} , consistent with the dry deposition flux calculations of Fe to the Sargasso Sea used by Sholkovitz *et al.* (2009). As there is a 30-fold increase in V_d from sub-micron particles (0.001 m s^{-1}), to mineral dust (0.01 m s^{-1}), to large sea-salt particles (0.03 m s^{-1}), and the assigned values of V_d for each particle type is only known within a factor of 2-3, it has been noted that there is a significant uncertainty associated with the assumption of constant V_d (Arimoto *et al.*, 2003). As a result the dry deposition fluxes presented here have an uncertainty of at least a factor of three.

By multiplying the dry deposition flux of total Co by the estimate of the percentage of soluble Co (%Co_S), the deposition flux of soluble aerosol Co (soluble Co F_{dry}) can be estimated according to Equation 2:

$$\text{soluble Co } F_{\text{dry}} = (C_a \times V_d) \times (\% \text{Co}_S \times 0.01) \quad (\text{Equation 2})$$

Taking the range of soluble Co F_{dry} in Table 2a ($47\text{-}155 \text{ pmol dCo m}^{-2} \text{ d}^{-1}$) we estimate that between 0.4 and 1.4 pM of dCo could be supplied to the mixed layer (assuming a MLD of 20 m) over a 6 month period of stratification, if dust supply remained consistently low. This rate of accumulation is unlikely to contribute to the short-term variability in surface dCo, and indicates that aerosol input of dCo during this study was very low. As the dry deposition flux of Fe during this study was very low ($1\text{-}4 \mu\text{g m}^{-2} \text{ d}^{-1}$) compared to the annual range at Bermuda ($0.1\text{-}10\,000 \mu\text{g m}^{-2} \text{ d}^{-1}$) (Sholkovitz *et al.*, 2009), the mean value for soluble Co F_{dry} ($0.006 \mu\text{g m}^{-2} \text{ d}^{-1}$) during *FeAST-6* can be assumed to be a

conservative lower limit. Using the same calculation and the soluble Fe F_{dry} value in Table 3.2b, accumulation of Fe over a six month period is estimated at 0.2- 0.7 nM.

An earlier cruise to the study area, *FeATMISS-I* (22 July-6 Aug. 2003, Tables 3.3a and b), took place during a period of high aerosol deposition (e.g. mean Fe dry deposition flux during *FeATMISS-I* was $1040 \mu\text{g m}^{-2} \text{d}^{-1}$, Table 3.3b). The total aerosol loading of Co at this time was over two orders of magnitude higher than during *FeAST-6*, which resulted in a total flux of $0.35\text{-}0.89 \mu\text{g m}^{-2} \text{d}^{-1}$ (Table 3.3a). Interestingly the % solubility of Co in these samples ranged from 8-10%, again consistent with the negative relationship between solubility and aerosol Fe loading.

Table 3. 3. (a) Aerosol Co and (b) Fe fluxes and fractional solubility during *FeATMISS-1* (high dust deposition).

(a)	Total aerosol Co loading ($\mu\text{g Co/m}^3$ air)	Deposition velocity (m/s)	Total Co Flux _{dry} ($\mu\text{g/m}^2/\text{d}$)	%Co _s	Soluble Co flux ($\mu\text{g/m}^2/\text{d}$)	Soluble Co flux (pmol/m ² /d)
01-02 Aug 2003	0.00104	0.01	0.89856	10	0.09077	1540
03-04 Aug 2003	0.00100	0.01	0.86400	8	0.07306	1240
04-05 Aug 2003	0.00041	0.01	0.35424	10	0.03497	593

(b)	Total aerosol Fe loading ($\mu\text{g Fe/m}^3$ air)	Deposition velocity (m/s)	Total Fe Flux _{dry} ($\mu\text{g/m}^2/\text{d}$)	%Fe _s	Soluble Fe Flux _{dry} ($\mu\text{g/m}^2/\text{d}$)	Soluble Fe Flux _{dry} (nmol/m ² /d)
01-02 Aug 2003	1.563	0.01	1350.432	1.1	14.855	266.0
03-04 Aug 2003	1.554	0.01	1342.656	0.44	5.908	105.8
04-05 Aug 2003	0.495	0.01	427.68	1.1	4.704	84.2

The flux during this period results in the estimated increase of 5-14 pM in dCo, accumulated over the six months of strong stratification. Assuming a mean accumulation rate of 10 pM and the mean surface dCo during *FeAST-6* (41 pM), this suggests that the soluble Co dry deposition flux could account for ~ 25% of the mixed layer dCo reservoir. Changes in rates of accumulation could contribute to the short-term variability in surface dCo concentrations. Similarly, the rate of Fe accumulation using *FeATMISS-I* soluble Fe F_{dry} (Table 3.3b) yields higher accumulation rates (0.8-2.4 nM); highlighting the importance of dry deposition as the predominant source of Fe to the Sargasso Sea.

Deposition flux calculations provide a snapshot, however, may not be regionally or seasonally representative due to the inhomogeneous and episodic nature of aerosol dust inputs. Furthermore, our estimates of dust deposition do not include wet deposition, as no rain events were sampled during the cruise. Due to the relatively low pH in rainwater, and the strong pH dependency of metal solubility, wet deposition may be equally or more important in delivering certain trace metals to the open ocean (Helmert and Sorensen, 1995; Jickells, 1999; Baker *et al.*, 2007). Similar to dry deposition, rainfall over the ocean is patchy and sporadic. For Fe, wet deposition is estimated to represent 30% of the total atmospheric deposition flux to the BATS region (Tian *et al.*, 2008; Sholkovitz *et al.*, 2009). In contrast, recent evidence shows that Co atmospheric flux is dominated by wet deposition (~ 85% in the years 2007-8, Church *et al.* in prep.). Using the estimate of 85% wet versus dry deposition and assuming the same percentage solubility as the aerosols determined here, the supply of dCo to the summer mixed layer (20 m) would therefore result in an additional supply of 2-8 pM in 2008 and 57 pM in 2003. These results indicate that wet deposition

is a large source of dCo to surface waters in this region. The two months preceding this cruise (April-May 2008) were the wettest in our records from Bermuda. The large variability in dCo concentrations seen in surface water transects may be residuals of rain showers during this time period.

3.3.4. Factors influencing the vertical distribution of cobalt

Comparison of the vertical profiles (Figure 3.6) showed differences in the vertical trace metal distributions between the different types of mesoscale eddy. In particular, Station K1 showed differences in its dCo, dFe and dAl distributions compared to the other stations. This is possibly due to its location inside a cyclonic eddy (Table 3.1). Whilst eddy-associated upwelling may not be a major source of hybrid or scavenged-type trace metals to the euphotic zone, as these elements are not greatly enriched in deep waters, there is evidence to suggest that the highly efficient remineralisation of particulate Co in cyclonic eddies may provide an alternative source of Co to the upper water column (Noble *et al.*, 2008). However, further studies in the Sargasso Sea would need to be undertaken to investigate whether this is a general characteristic of dCo behaviour in cyclonic eddies.

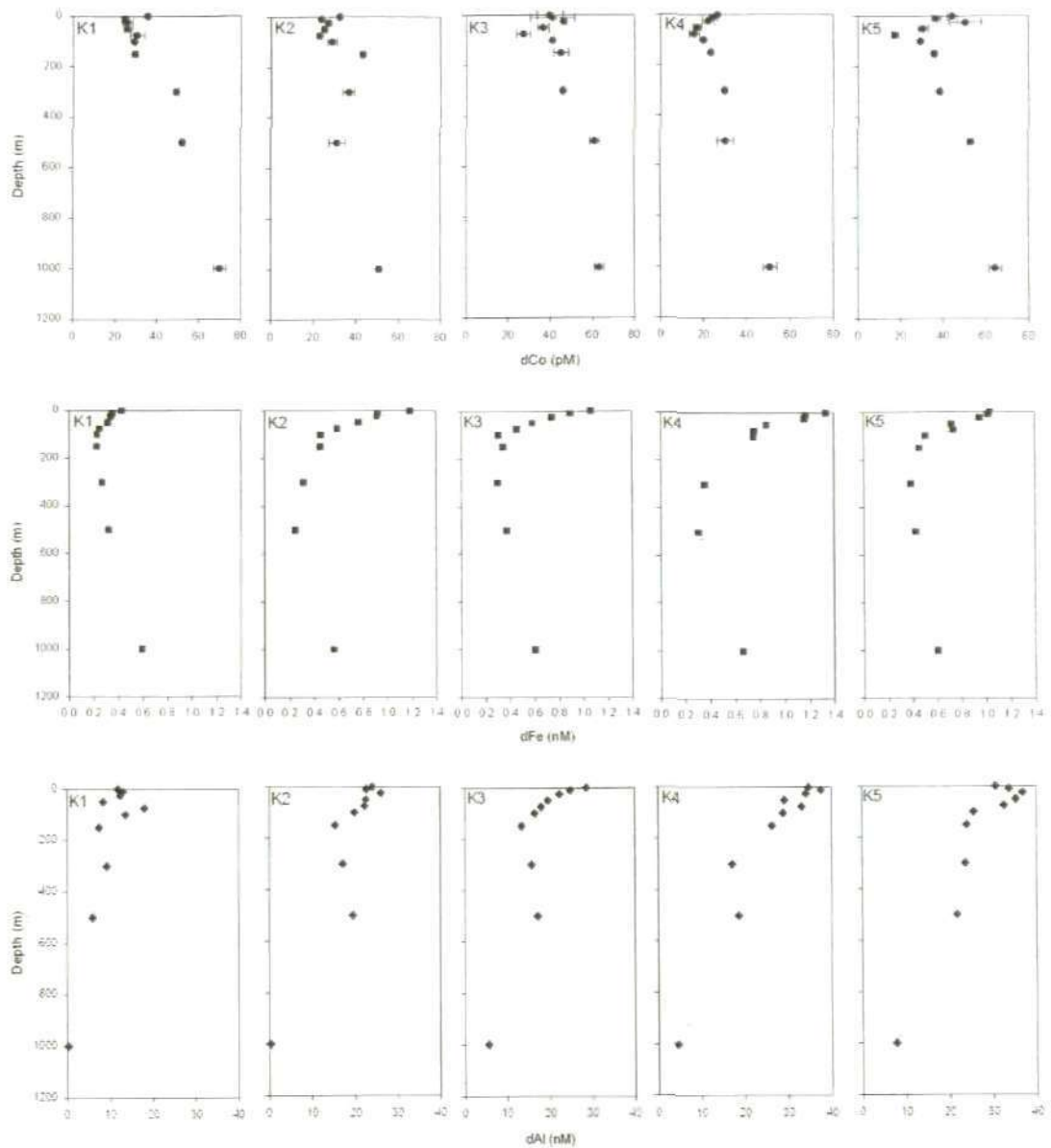


Figure 3. 6. Vertical profiles of dCo (pM), dFe (nM) and dAl (nM) at stations K1-K5.

At all sampling stations dFe and dAl displayed surface enrichment (0.4-1.3 nM dFe; 12-35 nM dAl; Fig. 3.6), indicative of atmospheric inputs and removal from subsurface waters via biological uptake and/or particle scavenging. There was a general north-to-south (stations K1-K5) increase in surface dFe and dAl concentrations consistent with those observed in the surface transects. For dAl, a typical scavenged-type vertical distribution was observed, with lowest concentrations observed at the maximum sampling depth 1000 m (0.4-8 nM).

Such scavenged-type profiles are characteristic of dAl in both the North Atlantic and North Pacific Oceans, although sea surface concentrations are 8-40 times lower in the Pacific due to lower dust inputs to that region (Orlans and Bruland, 1986). For dFe, the vertical profiles suggest a combination of scavenged and nutrient-type behaviour, (*i.e.* hybrid behaviour). Sedwick *et al.* (2005) have reported similar vertical distributions and concentrations for dFe in this region during summer 2003. The dFe concentrations at 1000m depth (0.6 ± 0.04 nM) are consistent with the global average for ocean waters at depths below 500 m (0.76 ± 0.25 nM) as compiled by Johnson *et al.* (1997).

Like dFe, dCo also displayed a hybrid-type vertical distribution, with higher concentrations (~ 36 pM) observed in surface waters (Fig. 3.6) and a minimum (~ 23 pM) near the chlorophyll maximum (75-100m) and increasing with depth (~ 60 pM at 1000 m). As discussed above, dCo was not highly enriched in surface waters relative to waters below the euphotic zone and there was no clear north-to-south concentration gradient, in contrast to the distributions of dFe and dAl. These observations have important implications regarding the principal supply mechanism of dCo to surface waters in the Sargasso Sea. In particular, the absence of a surface dCo maxima and the lack of a north-to-south increase in surface dCo concentrations could imply that atmospheric deposition is not a significant source of dCo to surface waters of the Sargasso Sea, at least during the early summer. Indeed, given that surface dCo concentrations were similar to values measured at 200-300 m depth, this might suggest that dCo is supplied to surface waters by convective overturning during the winter and early spring (Saito and Moffett, 2002).

Due to the very low concentrations of dCo in the open ocean, Noble *et al.* (2008) posit that for surface concentrations of dCo to correlate with aeolian inputs there would either need to be much higher aeolian inputs or for Co to have a much higher solubility than Fe in seawater. To date there has been no data published describing the concentration of Co in marine aerosol dust in conjunction with the determination of the fractional solubility of aerosol Co. As discussed above, the cruise data from *FeAST-6* revealed significant differences in the surface distributions of dCo and dFe, despite the geochemical similarities between these two elements in terms of their oxidation states and organic complexation in seawater. Differences in the fractional solubility of Co and Fe and net fluxes of wet and dry deposition offer one plausible explanation for the observed differences in surface water distributions of dCo and dFe.

While Co has a much higher aerosol solubility than Fe (75-100% and 5-45% respectively) we observed no obvious relationship between surface concentrations of dCo and dAl (a proxy for dust deposition) during *FeAST-6*. A shortcoming of Co fluxes and residence time estimates to-date has been the lack of wet deposition measurements. However, the recent rain measurements in the BATS region revealed that the majority of the atmospheric Co flux is from wet deposition (*ca.* 85%), whereas for both Fe and Al dry deposition is the principle atmospheric source (Tian *et al.* 2008; Church *et al.*, in prep.).

Therefore, if it is assumed that wet deposition was the dominant source of dCo to surface waters in the study region, it is likely that the amount of rainfall is a major cause of the spatial variability observed in these surface waters. Though no significant correlation between dCo and salinity was observed, the low salinity features consistently found in the mixed layer provides further evidence

for this. Furthermore, the disparity caused by wet and dry deposition fluxes could account for the lack of correlation between dCo and dFe observed in the surface data reported here.

Once Co and Fe enter the euphotic zone, concentrations of dCo and dFe are subject to solubility limits and biological control (primarily in terms of dissolved organic Co/Fe-binding ligand availability). In surface waters of the Sargasso Sea, Fe-binding ligands exceed dFe concentrations (Cullen *et al.*, 2006, Cullen *et al.*, in prep.), thus keeping Fe in solution in excess of its solubility. In contrast, Saito and Moffett (2001) found that dCo concentrations exceeded Co-binding ligand concentrations. We have shown here that Co is highly soluble in DI leaches. Hence, if Co-binding ligands are always saturated in surface waters, then excess soluble Co(II) is likely to be rapidly oxidised to insoluble Co(III) or scavenged from the upper water column.

The minimum dCo observed near the chlorophyll maximum at all stations suggests that biological removal is exerting a control on the vertical distribution. This is consistent with Moffett and Ho (1996) who concluded that the removal of dCo in the euphotic zone is dominated by biological uptake. Sedwick *et al.* (2005) noted concomitant dFe minima and fluorescence maxima pointing to removal of dFe via particle scavenging and/or active uptake by phytoplankton. However, these authors suggest an alternative explanation for dFe minima at this depth, which is that it is a relict feature, reflecting the low dFe concentrations of the deeper mixed layer of the preceding winter-spring season. Thus, they argue that subsurface minima of dFe (and presumably other

bioactive trace metals, such as dCo), do not simply reflect repartitioning between the dissolved and sinking suspended particulate pools.

If we assume that surface waters are not always saturated in terms of Co solubility, the resultant vertical distribution of dCo can then be hypothesised to be dominated by (i) atmospheric deposition or (ii) upwelling and convective mixing. This study has shown that atmospheric deposition (wet + dry) results in estimated dCo inputs of 6-67 pM to the surface mixed layer during summer. These concentrations are similar to the range observed for dCo in the surface transects (18-60 pM). On the other hand, the concentrations of dCo between 150-400 m that could be entrained into the euphotic zone during winter mixing is 40-60 pM which is also similar to what is observed in surface waters.

Using calculations based on Duce (1986) the advective upwelling flux was calculated from the difference between the average dCo concentrations at 100 and 150 m and particulate Co concentrations (Huang and Conte, 2009) in the study area (Table 3.4). This calculation demonstrates that vertical advective supply of dCo from below the euphotic zone contributes an amount of dCo to surface waters similar in magnitude to the soluble dry deposition flux (1.7-1430 pmol m⁻² d⁻¹, compared to 47-1540 pmol m⁻² d⁻¹ for dry deposition). Given that Co is supplied to the BATS region at a wet:dry deposition ratio of 85:15% (Church *et al.*, in prep.) this result further highlights the importance of wet deposition as a source of dCo to the Sargasso Sea, which is likely to dominate overall. Prior to this study atmospheric fluxes (wet + dry) were unknown and it had been suggested that convective mixing with deeper waters during the winter months was the primary supply of dCo to the euphotic zone (Saito and

Moffett, 2002). Our data show that the surface water dCo distributions may reflect a combination of both of these sources.

Table 3. 4. Input of dCo from below the euphotic zone. Advection-diffusion calculation of flux F ; $F = WR + K_z(dx/dz)$, where W = vertical velocity, R = mean concentration of dCo at 100 m during FeAST-6, K_z = eddy diffusivity; dx/dz = gradient of dCo over 100-150 m depth range.

Vertical velocity; w (m/day)	Mean concentration of dissolved metal at 150 m; $R(Z)$ (nmol/m ³)	Eddy diffusivity; K_z (m ² /day)	Gradient over 100-150 m depth range nM/m ⁴ ; dx/dz	Upwelling flux; F (nmol/m ² /day)	"Upwelling flux"; F (pmol/m ² /day)
0-0.04 ^a	30.8 ^b	1.7-10 ^a	0.001 ^c	0.0017-1.43	1.7-1430

^aDuce (1986) and references therein

^bFeAST-6

^cDerived from dCo at 100 m (3 $\mu\text{mol/m}^2$; FeAST-6) and particulate Co (0.03 $\mu\text{mol/m}^2$; Huang and Conte, 2009) and $R(z)$

3.3.5. Phytoplankton ecology

In line with observations that removal of dCo in the euphotic zone of the Sargasso Sea is dominated by biological uptake (Moffett and Ho, 1996), minimum concentrations (16-28 pM) occurred at 75 m, roughly coincident with maximum abundances of *Prochlorococcus* (mean = 3.1×10^6 cells mL⁻¹), an example of which is shown in Figure 3.6a. Below this depth dCo concentrations increased, with profiles conforming to a more nutrient-like distribution (Fig. 3.6), as has previously been reported for dCo in this region (Saito and Moffett, 2002). At depths below the subsurface chlorophyll maximum (SCM) there was a net increase of dCo and dFe.

Euphotic zone minima of dFe (~100 m) were always deeper than the dCo minima, and were approximately coincident with the SCM and highest abundances of picoeukaryotes (570 cells mL⁻¹) at ~100-150 m. A high cellular demand for dFe results in rapid removal of this element from surface waters, and an inverse relationship between dFe concentration and phytoplankton abundance has been observed, resulting in minima coincident with the SCM. In terms of biomass, the SCM tends to be dominated by eukaryotic phytoplankton. The inverse relationship between picoeukaryotic phytoplankton abundance and dFe distributions was evident throughout the euphotic zone in this study (at depths < 150 m); station K1 being the exception. Similarly, there appears to be an inverse relationship between dCo concentrations and *Prochlorococcus*, a genera with an absolute cellular requirement for Co (Fig. 3.7), suggesting that Co too may play a role in structuring the phytoplankton community in the Sargasso Sea.

Given the absolute cellular requirement for Co of the numerically dominant *Prochlorococcus*, as well as biological utilisation by key eukaryotic phytoplankton groups, it follows that a significant proportion of dCo removal is dominated by biological uptake. For a population of 10⁵ cells mL⁻¹ of *Prochlorococcus* growing at 0.4 d⁻¹ in the Sargasso Sea (Mann and Chisholm, 2000), Saito *et al.* (2002) estimated that 0.3 pM L⁻¹ d⁻¹ of dCo would be incorporated into new cells, which is a significant proportion of the dCo reservoir in the Sargasso Sea. In this study *Prochlorococcus* populations were an order of magnitude more abundant, numbering 10⁶ cells mL⁻¹. Following these calculations, which were based on particulate Co (pCo) concentrations in surface waters of 1.5 μM Co M⁻¹ C (Sherrell and Boyle, 1992) and 53 fg C cell⁻¹

(Campbell *et al.*, 1994), we estimate that $3 \text{ pM L}^{-1} \text{ d}^{-1}$ of dCo would be incorporated into new cells, therefore accounting for an even larger removal from the dCo reservoir.

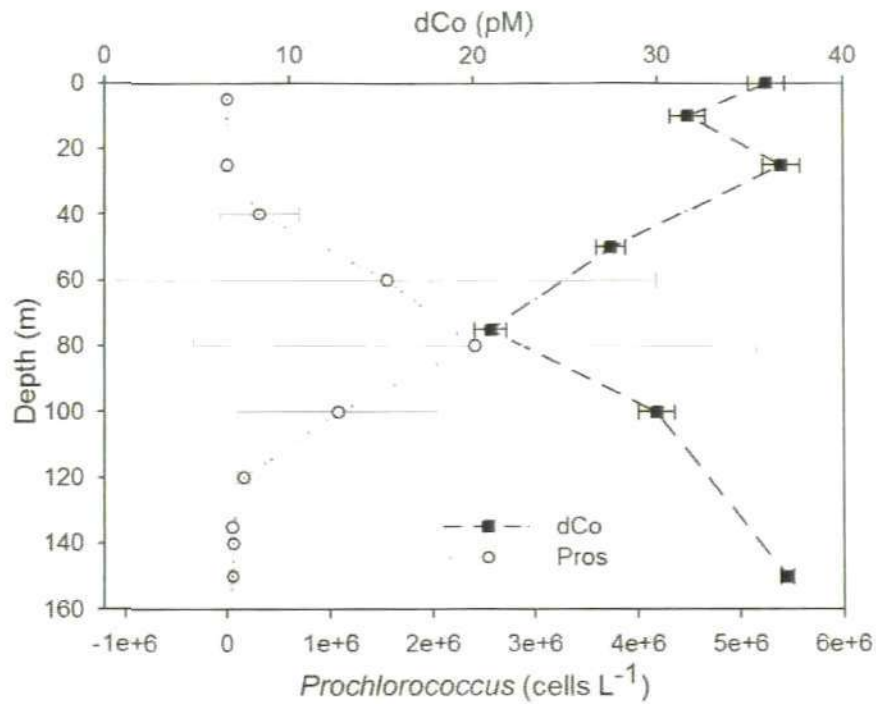


Figure 3. 7. *Prochlorococcus* (Pros) abundance (cells mL^{-1}) versus dCo concentration (pM). An inverse correlation during FeAST-6 (Pearson's Product Moment correlation coefficient = -0.996 where $p = 0.0003$) in the uppermost 150 m was observed. The data is an average ($\pm 1\text{sd}$) for stations K2-K5. There was no relationship between *Prochlorococcus* abundance and dCo at station K1; reasons for this are addressed in the discussion.

In order to prevent Co limitation, due to the specific biological demand of *Prochlorococcus*, Co must be recycled rapidly and/or replenished from an alternative source. Regeneration will be facilitated by the labile association of Co with the particulate phase (pCo), as indicated by the absence of significant pCo export (reported by Noble *et al.* (2008), at a similarly oligotrophic location).

In the Sargasso Sea the concentration of pCo is estimated at only ~2.6% that of dCo (Sherrell and Boyle, 1992), whereas particulate Fe (pFe) concentrations are equivalent to dFe (Jickells, 1999), which suggests that Fe is more particle reactive than Co and/or Co is more efficiently recycled in the upper water column of the Sargasso Sea. This work has highlighted some key differences in the geochemistry of dCo and dFe, but in order to characterize the dominant supply route(s) of Co to the Sargasso Sea it will be necessary to conduct further studies. In particular, sampling occurring immediately after and during dust deposition events would be expected to clarify the role of atmospheric deposition as a source of Co to surface waters.

3.4. Conclusions

The extremely labile association of Co with aerosol particles, results in atmospheric deposition being an important source to the Sargasso Sea. In this study the operational solubility of Co (8-100%) was significantly higher than Fe (0.44-45%). In common with Fe, Co solubility varies as a function of the Fe loading of the bulk aerosol. The covariation between dAl and dFe in surface waters (correlation coefficient = 0.63, $p = 1.92 \times 10^{-8}$, $n = 65$) indicates that dust was the predominant source of dFe to surface waters, with a general north-south increase in dust loading observed. Estimates of wet deposition of Co based on solubility data presented here and elemental fluxes from the BATS region clearly show the importance of this source and provide an explanation as to why there was no clear pattern between sea-surface dCo and aerosol dust loading.

In terms of the vertical distribution of dCo, atmospheric deposition and winter mixing both appear to supply Co to the euphotic zone. The extent to which one dominates over the other will be dependent on whether dissolved Co binding-ligands are always saturated in the surface mixed layer and the influence this has on the residence time. Clearly, the principal sources of Co to surface waters in open ocean environments requires further investigation to elucidate input pathways alongside increased measurements of Co binding ligands. The role of winter mixing can be examined by conducting seasonal studies and by comparison with vertical profiles in tropical regions which are less impacted by seasonal mixing.

Chapter 4

The Impact of Trace Metal (Co, Cu and Fe) Additions on Productivity and Nitrogen Fixation Rates in the Tropical Northeast Atlantic Ocean

4.1. Introduction

As marine phytoplankton account for approximately 50% of global photosynthesis (Falkowski, 1994; Field *et al.*, 1998) it is important to understand the processes mediating their growth. The availability of dissolved inorganic carbon, major nutrients (N, P and Si), and trace elements (*e.g.* Co, Cu, Fe, Zn) are key factors in determining growth rates in marine phytoplankton. Trace metals are required by marine phytoplankton for numerous enzymatic intracellular functions (Morel and Price, 2003), examples of which can be found in Table 1.1 (Chapter 1). It is now well established that low Fe concentrations limit primary production in the major high nutrient, low chlorophyll (HNLC) regions and can regulate phytoplankton processes in a number of other oceanic settings (de Baar *et al.*, 2005; Boyd and Ellwood, 2010). As well as requiring inorganic micronutrients (*e.g.* Co, Fe), phytoplankton require numerous organic cofactors for growth, an example of which is vitamin B₁₂ (a Co-containing molecule) (Provasoli and Carlucci, 1974). Recent work by King *et al.* (2011) has demonstrated that CO₂ and vitamin B₁₂ interactively influence growth rates, carbon fixation and trace metal requirements in the subarctic diatom, *Attheya sp.* Similarly Zn is a cofactor in alkaline phosphatase, an enzyme required to acquire organic phosphorus (Dyhrman and Palenik, 2003). Copper serves as a micronutrient to phytoplankton in the electron transport protein, plastocyanin (Peers and Price, 2006) and other enzymes required for growth (Maldonado *et al.*, 2006), although there is also empirical evidence that Cu toxicity may play a role in structuring phytoplankton communities (Moffett *et al.*, 1997; Mann *et al.*, 2002; Paytan *et al.*, 2009). These studies highlight that relationships between

phytoplankton and trace metals (Cu Co Fe and Zn) involve complex feedbacks and multiple environmental factors.

In the oligotrophic subtropical gyres both nitrogen and, to a lesser extent, phosphorus are considered limiting to phytoplankton growth (Smith, 1984; Tyrell, 1999; Wu *et al.*, 2000). However, biological nitrogen (N) fixation (the reduction of atmospheric N₂ to biologically available ammonium) is an important source of N for phytoplankton communities and can increase the nitrate inventory of the ocean, thus increasing primary production (Gruber and Sarmiento, 1997; Karl *et al.*, 1997; Mahaffey *et al.*, 2003; Mills *et al.*, 2004). In the oligotrophic North Atlantic, N₂ fixation may fuel 50% of the export production (Gruber and Sarmiento, 1997). Nitrogen fixation is carried out by a limited, but diverse, range of diazotrophs which use both the nitrogenase enzyme (NifH) and a heterotetrameric molybdenum-iron protein (NifDK) (Zehr *et al.*, 2003; Zehr and Paerl, 2008; Saito *et al.*, 2010). These enzymes and proteins both require Fe; NifH requires 4 Fe atoms and NifDK 8 Fe atoms, resulting in a high cellular demand for Fe by diazotrophs (Kustka *et al.*, 2003; Saito *et al.*, 2010). Recent observations have shown a direct link between the supply of Fe and N₂ fixation along a latitudinal transect in the Atlantic (Moore *et al.*, 2009). In addition to low Fe, low phosphorus (P) availability is also thought to limit N₂ fixation rates and diazotroph growth (Berman-Frank *et al.*, 2001; Sañudo-Wilhelmy *et al.*, 2001; Kustka *et al.*, 2003; Mills *et al.*, 2004). It has become clear that no one factor controls marine N₂ fixation rates and that nitrogenase activity is determined by a combination of variables that differ depending on the geographic region and diazotroph community composition (Mahaffey *et al.*, 2005).

The focus of this chapter is on the impact of trace metal (Co, Cu and Fe) additions on primary production and N₂ fixation rates in the tropical Northeast Atlantic Ocean. This project was undertaken during the UK-SOLAS research cruise, 'Investigation of Near-Surface Production of Iodocarbons: Rates and Exchanges' (*INSPIRE*), to the tropical Northeast Atlantic (16–26°N) and subsequent sample analysis in the laboratory at the University of Plymouth. Shipboard bioassays were conducted in order to investigate the limitation of microbial processes (primary productivity, heterotrophic bacterial productivity, N₂ fixation).

4.1.1. Aims and Objectives

The aim of the present research was to investigate the role of four bioactive trace metals (Co, Cu, Fe and Zn) on microbial processes (e.g. N₂ fixation, primary production, heterotrophic bacterial productivity) in the euphotic zone of the subtropical Northeast Atlantic Ocean. In order to achieve this goal, shipboard bioassays were undertaken onboard the UK Natural Environment Research Council's vessel, *RRS Discovery*. To measure the extremely low (*i.e.* sub-nanomolar) concentrations of the dissolved trace metals (operationally defined as < 0.2 µM) in the bioassays, suitable analytical methods were developed (Chapter 2). The key objectives of this study were:

1. To design shipboard incubation experimental protocols to investigate the effects of trace metals (Co, Cu, Fe, Zn) limitation of microbial processes (N₂ fixation, primary production and heterotrophic bacterial production) in the subtropical Atlantic Ocean.

2. To determine the uptake rates of trace metals (Co, Cu, Fe, Zn) by the ambient phytoplankton community in shipboard bioassays over 48 h.
3. To investigate trace metal (Co, Cu, Fe, Zn) uptake in relation to N₂ fixation, primary production and heterotrophic bacterial productivity.

4.2. Methods

4.2.1. Study region

Shipboard incubation experiments were conducted aboard the *RRS Discovery* during the *INSPIRE* cruise (D325) between 13th of November 2007 and the 18th of December 2007. Six stations of differing levels of primary productivity; high (0.30 ± 0.16 mg chl m⁻³), medium (0.11 ± 0.007 mg chl m⁻³) and low (0.07 ± 0.02 mg chl m⁻³) were occupied in the subtropical Northeast Atlantic (16–26°N; Figure 4.1 and Table 4.1) for a duration of four days each. Stations A–D were located in the vicinity of the Cape Verde Islands (~16–17°N, 23°W), which are situated ~500 km off the east coast of Senegal. Stations E and F (20°N, 25°W and 26°N, 24°W) were located further north and offshore (Fig. 4.1).

This region was selected as the study area owing to its proximity to the UK-SOLAS atmospheric sampling station on the island of Sao Vicente, Cape Verde. Macro-nutrient (N and P) concentrations are generally depleted in surface waters, but can be influenced by filaments from coastal upwelling off the coast of West Africa that transfer nutrient-rich waters into the nutrient-depleted surface waters of the North Atlantic gyre (Pastor *et al.*, 2008). All stations sampled during the *INSPIRE* cruise were positioned in the oligotrophic

subtropical North Atlantic gyre. This region experiences high annual aerosol dust inputs ($\sim 0.190 \text{ Tg year}^{-1}$; Jickells *et al.*, 2005), which supplies both Fe and P to surface waters, primarily from the arid and desert regions of Northwest Africa (Prospero *et al.*, 2002). Previous studies in the subtropical North Atlantic and the equatorial North Atlantic have documented the presence of diverse N_2 -fixing cyanobacteria and bacteria (Langlois *et al.*, 2005, 2008; Goebel *et al.*, 2010). In addition, recent studies have shown the importance of Fe and P availability to these diazotrophs (Mills *et al.*, 2004; Moore *et al.*, 2009).

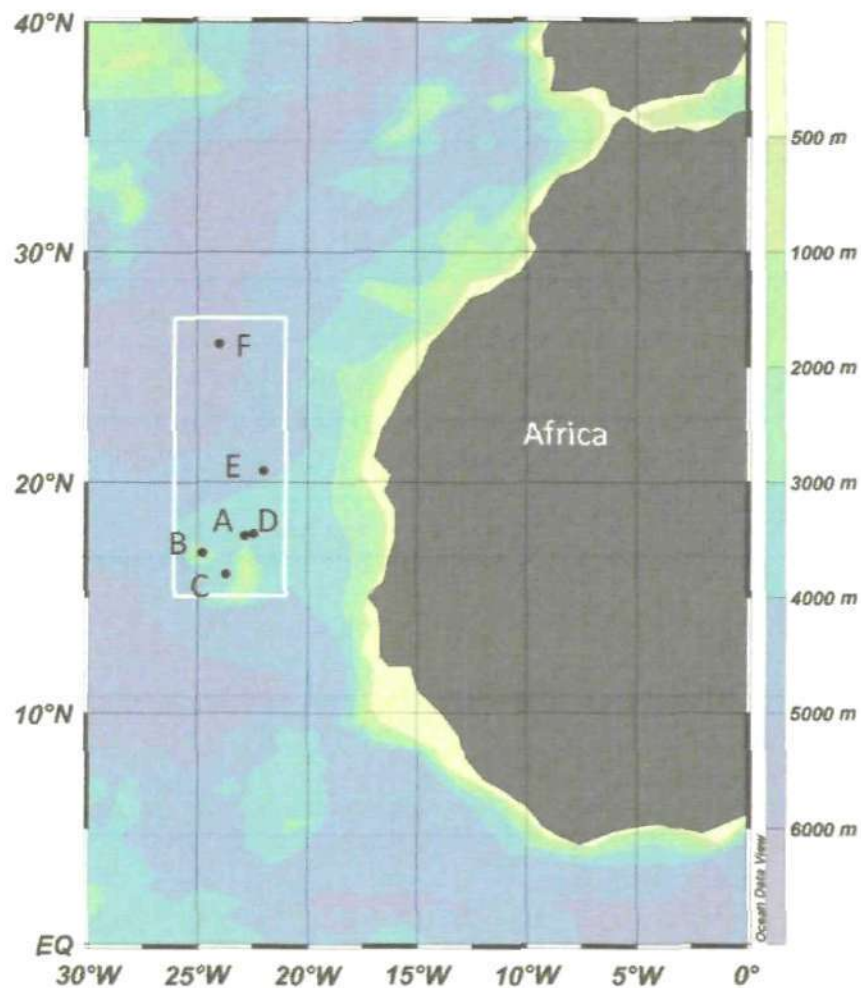


Figure 4. 1. The INSPIRE cruise stations, with stations A – F marked. The area inside the white box corresponds with the boxed area in Figure. 4.2.

Table 4. 1. Chlorophyll-a concentration and position of stations sampled during the *INSPIRE* cruise.

Station	Chl-a (mg m ⁻³)*	Position	
A	0.10 ± 0.001	17.8°N, 22.8°W	
B	0.41 ± 0.020	16.9°N, 24.8°W	Near UK-SOLAS atmos. sampling site
C	0.19 ± 0.040	16.0°N, 23.7°W	Coastal; W. of Boa Vista Island
D	0.11 ± 0.005	17.7°N, 22.8°W	Near Station A
E	0.08 ± 0.021	20.5°N, 25.0°W	
F	0.05 ± 0.002	26.0°N, 24.0°W	

*Chl-a data kindly provided by A. Rees, Plymouth Marine Laboratory (PML), where Stations B and C, A and D, and E and F were located in regions of relatively high, medium and low chl-a concentrations respectively.

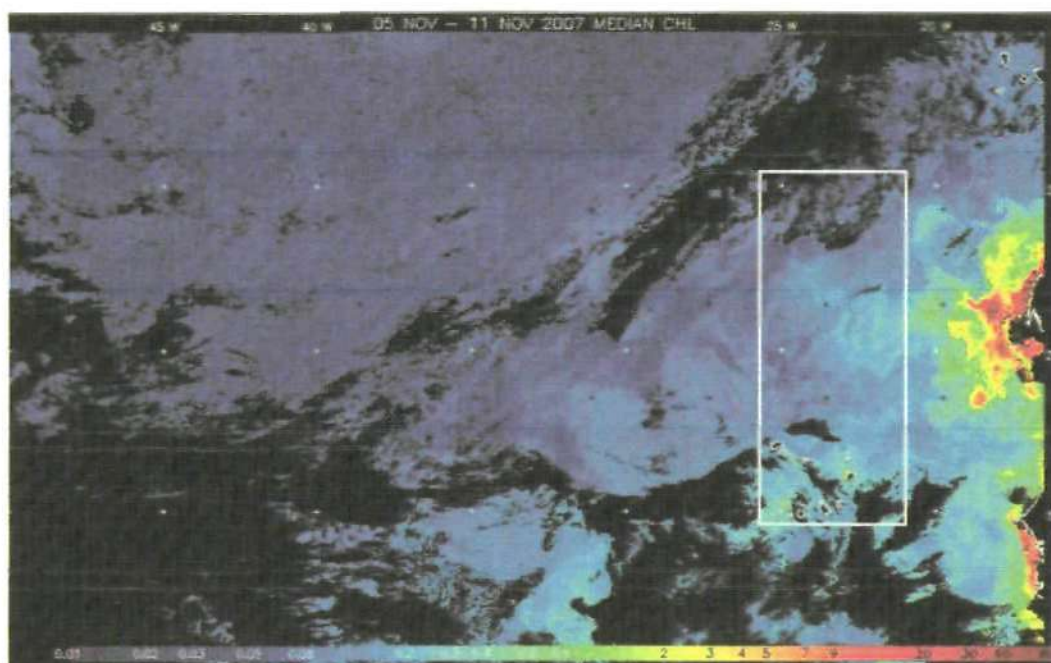


Figure 4. 2. Seven day composite satellite (MODIS) image of chlorophyll ($\mu\text{g L}^{-1}$) for the week prior to the start of the *INSPIRE* cruise. The locations of the six stations were selected based on this image. Chl-a concentrations were initially determined from a range of satellite data (MODIS, SeaWiFS and MERIS) provided by the NERC Earth Observation Data Acquisition and Analysis Service (NEODAAS <http://www.neodaas.ac.uk/>) at PML. The area inside the white box corresponds to that in Figure 4.1.

As stations were occupied over four days, it was important that stations of relatively homogeneous chlorophyll levels were sampled. Therefore, waters that were clearly associated with the Mauritanian upwelling (identified as the red/orange region off the coast of West Africa in Fig. 4.2) were avoided. However, the spiral shaped features characteristic of eddies, are clearly identifiable in the study region (centre of white box in Fig. 4.2), reflecting the dynamic nature of this area.

4.2.2. Sampling and ship-based bioassays

Initially, the position of the six stations to be occupied during *INSPIRE* were selected based on chlorophyll-*a* concentrations determined from near-real time satellite images (Fig. 4.2), provided by the NERC Earth Observation Data Acquisition and Analysis Service (NEODAAS, <http://www.neodaas.ac.uk/>) at Plymouth Marine Laboratory (PML). In Figures 4.1 and 4.2 the area inside the white rectangle corresponds to the same location. Seawater was collected for the trace metal addition bioassays (Co, Cu, Fe, Zn) from a depth of 55% surface photosynthetically active radiation (PAR). PAR was determined using a Fast Repetition Rate Fluorometer (FRRF; Chelsea Instruments) fitted with PAR scalar irradiance sensors (PML 2-pi) configured to measure downwelling and upwelling radiation. In order to calculate the light-attenuation coefficient (PAR), the downward irradiance was measured throughout the water column. The FRRF was mounted on the optics rig which was deployed at solar noon prior to the first day of the bioassays. Seawater was sampled using an underway fish fitted with acid washed (10% HCl) PFA (Cole Parmer) tubing. The PFA tubing was connected to Teflon tubing which directly delivered seawater to the clean

container by means of a diaphragm pump (Almatec A-15) fitted with Teflon components.

While slowly steaming (2 knots) the fish was positioned at a depth of approximately 2 m, outside the wake of the ship, to minimise possible contamination from the ship's hull (de Jong *et al.*, 1998). Upon arrival at station, the fish was lowered to 55% PAR and an acid-washed 120 L HDPE carboy was rinsed thoroughly with seawater supplied via the fish, prior to being filled with seawater for the bioassay experiments. All seawater for the bioassays was collected before dawn, and the 120 L HDPE carboy was surrounded by black plastic to prevent exposure to light which would have initiated photosynthesis before the start of the experiment. The unfiltered water was then homogenised by gentle shaking and decanted into 18 acid-washed 4.6 L polycarbonate bottles (Fig. 4.3). Polycarbonate bottles were chosen as adsorption of Fe to vessel walls was found to be less than for other materials, such as HDPE (Fischer *et al.* 2007). The polycarbonate bottles were spiked with trace metals, 0.5 nM Co, 2 nM Cu, 2 nM Fe, 1 nM Zn, and a mixture of all four metals at the same concentrations. The metal additions were prepared from serial dilution of stock standard solutions of: $\text{CoCl}_2 \cdot 6\text{H}_2\text{O}$; $\text{CuCl}_2 \cdot 2\text{H}_2\text{O}$; $\text{FeCl}_3 \cdot 6\text{H}_2\text{O}$ and $\text{ZnCl}_2 \cdot \text{H}_2\text{O}$ (Fisher). The final working standards were prepared in UHP water acidified to pH 2 with ultra-high purity HCl (Optima, VWR). All treatments were carried out in triplicate. Initial (T_0) and control (T_{48}) bottles received no metal additions. Additionally, at stations D and F, a nitrate and ammonium (referred to as '+N') spike was added in combination with the trace metal spike, as these waters were confirmed as N-limited following ship-board determination of

macronutrients by E.M.S. Woodward. The concentration of the N additions were determined based on the Redfield ratio of 16N:1P (Redfield, 1934) using the *in situ* concentration of phosphate at the respective station. The N additions were calculated to give a ratio of 1 nitrate : 2 ammonium to account for substrate preferences within the phytoplankton community.

For Station D, *in situ* nitrate was < 5 nM and phosphate was 80 nM. Therefore, the N addition was made up of 400 nM nitrate and 800 nM ammonium.

For station F, *in situ* nitrate was < 5 nM and phosphate was 5 nM. Therefore, the N addition was made up of 25 nM nitrate and 50 nM ammonium.

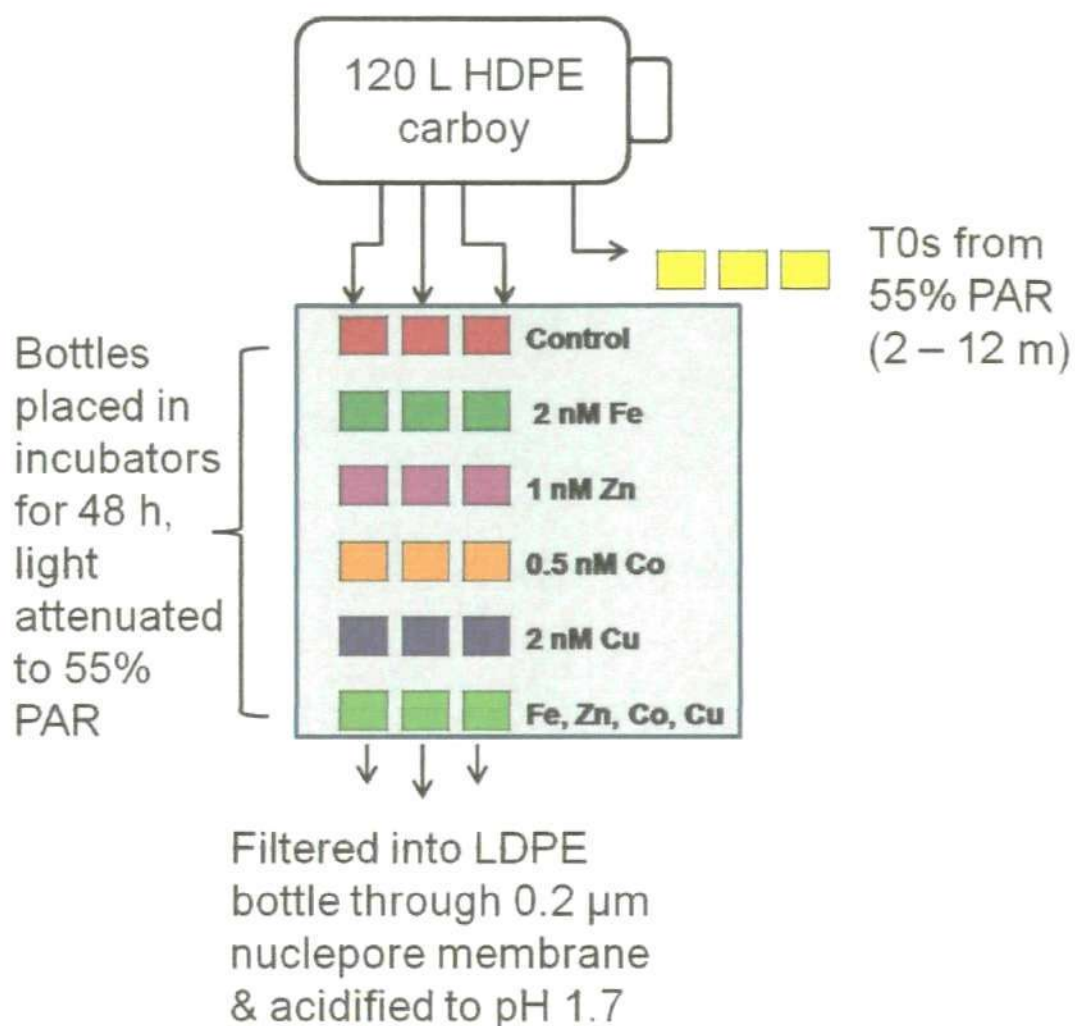


Figure 4. 3. Experimental design for the 48 h incubation experiment - each coloured block represents a 4.6 L polycarbonate incubation bottle, with incubations repeated in triplicate. At stations D and F the final treatment (Co, Cu, Fe and Zn) was substituted for additions of nitrate and ammonium (+N addition) to give a final bottle concentration of 16N :1P based on the *in situ* concentrations of phosphate at T_0 .

To prevent ingress of water, and other possible contaminants from the incubation tanks, the incubation bottle lids were sealed with super-88 electrical tape. All bottles, with the exception of the T_0 bottles, were incubated before dawn and covered with blue filmed lids to attenuate light levels to approximate *in situ* levels (*i.e.* 55% PAR). At night the incubator lids were covered with black plastic to prevent the deck lights illuminating the tanks, thus simulating a natural diel cycle as some ubiquitous phytoplankton genera have been shown to exhibit circadian rhythms (*e.g.* Kondo *et al.*, 1994). Water in the incubators was maintained at ambient temperature by a means of a flow-through system continually supplied by local surface seawater. The incubations took place over a 48 h period. The T_0 controls were not incubated, and sub-samples for trace metal determination were immediately decanted into acid-clean 250 mL LDPE bottles and vacuum filtered (max. 200 mbar) through acid-washed 0.2 μm nuclepore track-etched polycarbonate membranes, using a Savillex filtration system fitted with Teflon components (Fig. 4.4), into acid-clean 125 mL LDPE bottles. Samples were then acidified to 0.024 M (\sim pH 1.7) with triple distilled HCl (SpA, Romil) inside a class 100 laminar flow hood. Samples were acidified to \sim pH 1.7 as, at this pH, the Fe complexed by organic ligands dissociates, an important consideration as the natural seawater matrix is not organic free (Lohan *et al.*, 2005). Acidification of seawater samples to \sim pH 1.7 thus allows determination of the operationally-defined total dissolved Fe, rather than just the labile fraction. Following acidification, the samples were triple zip-lock bagged for storage and transport back to the University of Plymouth.

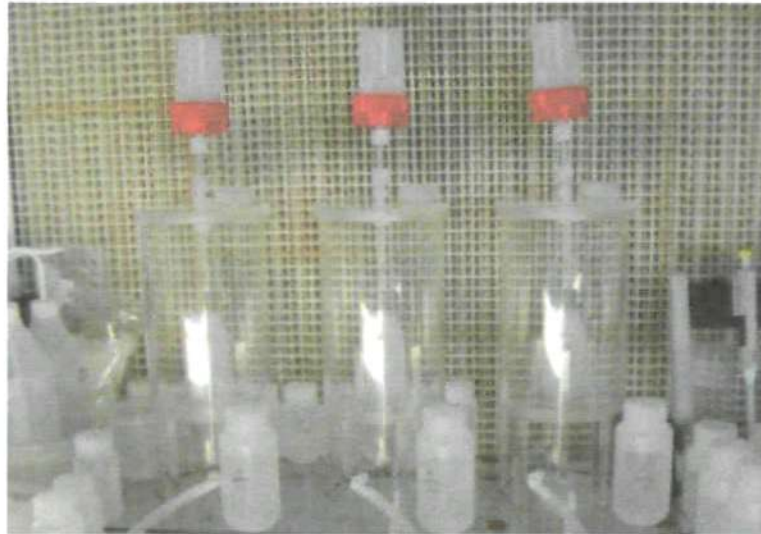


Figure 4. 4. The vacuum filtration system. The vacuum pump is not shown as it was positioned outside the laminar flow hood.

Before dawn on day 2 (T_{48}) of the incubation experiments, the 4.6 L bioassay bottles were removed from the incubators and brought into the clean van. The bottles were rinsed 3x with UHP water and gently shaken before sub-sampling commenced (Fig. 4.5). Between each use the filtration system was rinsed liberally with UHP water, followed by 1 M HCl, rinsed again with UHP, and finally with some of the seawater sample that was to be filtered next. A new, previously acid-washed (20% HCl) 0.2 μm nuclepore track-etched polycarbonate membrane was used for filtration of each sample. The samples were filtered and acidified as described above. Chlorophyll-*a* concentrations were determined at T_0 by acetone extraction of 0.2 μm nuclepore track-etched polycarbonate membranes after filtration of 220 mL of seawater sample, following the method of Welschmeyer (1994). Determination of dissolved trace metals was not carried out on board ship; samples were returned to the University of Plymouth for analysis in the laboratory. For the purpose of this study dissolved metals were operationally-defined as those which passed through a 0.2 μm nuclepore track-etched polycarbonate membrane. Colloidal

metals were not directly considered during this study, but would be included within the operationally-defined dissolved fraction.

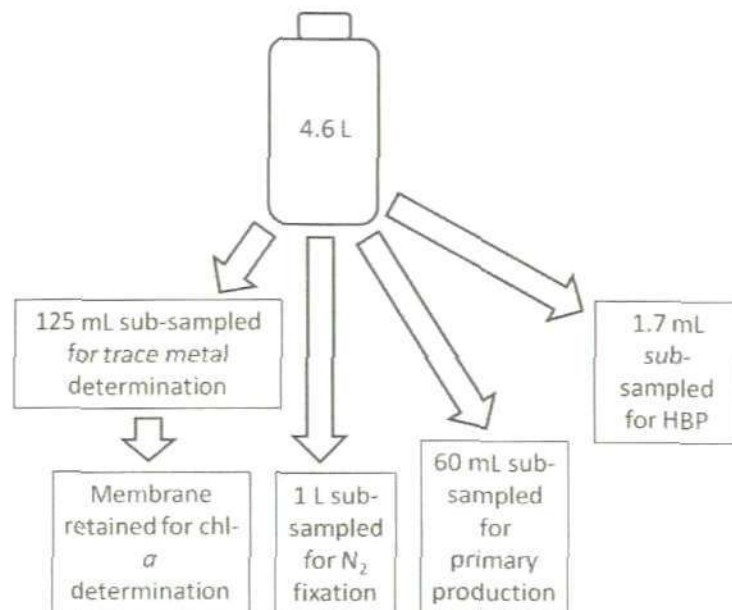


Figure 4. 5. Sub-sampling protocol for the 4.6 L incubation bottles at T₄₈ (HBP = heterotrophic bacterial production). To minimise the possibility of sample contamination, sub-sampling for trace metal (Co, Cu, Fe, Zn) determinations occurred before sub-sampling for the other parameters shown. Sub-samples were collected in triplicate; the extra volume was used for rinses while sub-sampling.

Deck-based bottle experiments are frequently used as a convenient way to control environmental conditions, while trying to approximate *in situ* conditions as closely as possible. However, they are closed systems, cut off from a ready supply of nutrients (from the ocean and/or the atmosphere), thus their use may have an effect on community production. The present study was designed to incorporate rate measurement incubations (frequently made over a 24 h period to represent a diel cycle, e.g. Mills *et al.*, 2004) and trace metal addition

incubations, where 7 days is a frequently used period, as it allows the phytoplankton and bacterial assemblage to adapt and respond to the experimental conditions. As rate measurements and trace metal concentrations were determined from the same incubation bottles, it was necessary to make these rate measurements after trace metal sub-sampling had occurred to minimise the possibility of sample contamination. Thus, the bioassays were incubated for 48 h prior to the commencement of rate determination experiments. The 48 h incubation period was chosen as Mills *et al.* (2004) found it to be sufficiently long for the fast-growing subtropical phytoplankton and bacterial assemblage to respond to the addition of Fe (and N and P).

4.2.3. Analytical techniques

Co: FI-CL

Dissolved Co was determined from the bioassay samples using the FI-CL technique described in Chapter 2 and Shelley *et al.* (2010).

Fe: FI-CL

Dissolved Fe was determined using a modified version of the FI-CL method of Obata *et al.* (1993), details of which can be found in Chapter 2.

Cu, Fe and Zn: ICP-MS

Dissolved Cu was determined by ICP-MS (Thermo Scientific X-series 2) following off-line pre-concentration on to a chelating resin, Toyopearl AF-Chelate 650 M. This technique was based on the isotope dilution method of Milne *et al.* (2010), but used standard additions to quantify trace metal

concentrations instead of isotope dilution. Dissolved Cu recovery from the GEOTRACES (GS) and SAFe (Surface) reference seawater samples showed good agreement with the consensus values (this study GS = 0.7 ± 0.01 nM, SAFe S = 0.4 ± 0.01 nM versus consensus values of GS = 0.6 ± 0.1 and SAFe S = 0.5 ± 0.1 nM). The aim was to simultaneously determine dFe and dZn in addition to dCu. However, recovery of dFe and dZn was incomplete. Using the GEOTRACES (GS and GD) and SAFe (Surface) reference seawater samples dZn, recovery was typically < 50% of the consensus values. For example, the concentration of dZn determined in a GD reference sample was 0.57 ± 0.01 nM versus the consensus concentration of 1.4 ± 0.45 nM. Dissolved Zn in the GS samples is extremely low (consensus value = 0.14 ± 0.09 nM), and was below the limit of detection (0.39 nM). For dFe, the reference samples had concentrations which exceeded the GEOTRACES reference sample consensus values of GS = 0.47 ± 0.03 ; GD = 0.97 ± 0.05 . The extremely low concentrations of dFe in the SAFe surface sample (0.09 ± 0.02 nM) were below the instrumental detection limit (0.29 nM). Therefore, only dCu values are reported using this ICP-MS technique; further details of which can be found in Chapter 2.

The poor analytical performance for dFe determination may be due to the fact that a collision cell, which reduces polyatomic interferences, such as the ArO^+ dimer which causes an interference on the ^{56}Fe isotope, was not used during ICP-MS detection. In this study, use of the collision cell reduced the detection limit of dCu to below the lower end of the concentration range of the reference samples. Therefore, the collision cell was not used; the erroneously high dFe

values reported for the reference samples were a result of interferences on the Fe isotopes. Dissolved Fe was, therefore, determined using FI-CL, as described in Chapter 2.

The reason for the incomplete recovery of Zn cannot be accounted for by interferences, and does not appear to be a response to the absence of a collision cell. The poor sensitivity may have resulted in the reporting of apparently incomplete recovery. This may have been due to high naturally-occurring Zn levels or contamination of the seawater medium in which the standard additions were prepared. The seawater used for standard preparation was collected from 50 m depth in the remote South Atlantic Ocean (37.9°S, 41.1°W), it is unlikely that high naturally-occurring dZn would have been observed in this seawater. Furthermore, comparison of the intensity (In-normalised counts per second; cps) of this seawater and the GEOTRACES reference seawater samples (GS and GD, which were collected from 10 and 1000 m depth respectively at 31.8°N, 69.7°W) shows that the intensity of the signal was close to that of the GD reference seawater sample which contains 1.6 ± 0.4 nM Zn (1248 cps for the zero addition standard versus 544 cps for GS and 1677 cps for GD), suggesting low-level contamination for Zn in the seawater used for sample preparation in this study. Further studies using seawater containing lower dZn concentrations would be expected to yield an improvement in sensitivity, and thus more accurate reporting of the dZn content of the reference samples.

Macronutrients

Macronutrients were determined within two hours of sample collection by E.M.S. Woodward (PML) using a segmented flow colorimetric autoanalyser (Bran and Luebbe AAIII Autoanalyzer). Nanomolar (nM) nitrate, ammonium and phosphate and μM silicate were determined following the methods described in Woodward and Rees (2001). The detection limit for the nM nutrients (N and P) was 20 nM and 0.1 μM for silicate.

Primary production

Primary production (as the rate of carbon uptake) was determined by J.L. Dixon (PML) at T_{48} for all samples (except for the T_0 sample, which was determined without being incubated) following Poulton *et al.* (2006). Briefly, at T_{48} , 60 mL of seawater was sub-sampled from each incubation bottle, and distributed into polycarbonate bottles and amended with $\sim 10 \mu\text{Ci } ^{14}\text{C}$ labelled NaHCO_3 . Experiments were terminated by filtration (HCl-fumed, 0.2 μm Supor 200 membrane filters) prior to onboard liquid scintillation counting (Packard Tri-Carb 3100).

Heterotrophic bacterial production

Heterotrophic bacterial production was determined by J.L. Dixon (PML) at T_{48} for all samples (except for the T_0 sample). ^3H -leucine (^3H -leu) was incorporated into bacterial protein in seawater sub-samples following the method of Smith and Azam (1992). Samples of 1.7 mL were inoculated with 25 nM ^3H -leu (7 μL) and incubated in the dark at *in situ* water temperature ($\sim 25^\circ\text{C}$) for 1 h. Experiments were terminated by addition of 100 μL trichloroacetic acid (TCA)

(5% final concentration). The incorporated ^3H was extracted following the procedures outlined in Smith and Azam (1992), and the concentration determined by liquid scintillation counting (Packard Tri-Carb 3100).

Nitrogen fixation

Nitrogen (N_2) fixation was determined by A.P. Rees (PML). At the end of the incubation experiments (T_{48}), seawater was sub-sampled from the 4.6 L polycarbonate incubation bottles by decanting into triplicate 1 L polycarbonate bottles, which were then injected with 2 mL of 99% $^{15}\text{N}_2$ introduced to each bottle through a butyl septum using a gas-tight syringe. The 1 L bottles were then returned to the deck-board incubators (with the light-attenuating filters removed) for a further 6 h. Six h incubations were chosen to provide a gross N_2 fixation rate to correspond with samples collected for molecular analysis. Experiments were terminated by filtration onto 25 mm GF/F filters (Millipore). The filters were dried onboard at 50 °C for 12 h and pelleted into tin capsules, then stored over silica-gel desiccant until return to PML. Particulate N and ^{15}N atom% was measured using continuous-flow stable isotope mass spectrometry (PDZ Europa 20-20) at PML following the method of Owens and Rees (1989), with rates and ^{15}N enrichment determined according to Montoya *et al.* (1996). Background ^{15}N content of particulate material was determined from unamended 1 L aliquots of seawater filtered immediately after collection.

4.3. Results and Discussion

The impact of trace metal additions (Co, Cu, Fe and Zn) on the rates of primary production, heterotrophic bacterial production and N₂ fixation at the six stations occupied during the *INSPIRE* cruise are discussed in the following section. The N₂ fixation rates in ship-based bioassays conducted during *INSPIRE* are discussed primarily in association with dFe concentrations. All trace metal determination was conducted by the author, and all other analyses are credited to the appropriate researchers. The dFe and N₂ fixation data have been published in a co-authored paper in the *ISME Journal* (Turk *et al.*, 2011; see publications section).

4.3.1. Macronutrients

Macronutrients (nitrate, ammonium, phosphate and silicate) were determined at T₀ from water sampled from 55% PAR (2–11 m; Table 4.2). Nitrate concentrations were generally low, but ranged from below detection to 661 nM at Station B (Table 4.2). Although the coastal station (station B) can clearly be identified by its higher nitrate signature (which ranges from sixfold higher nitrate than at Station C to two orders of magnitude higher than at Stations A, E and F), all stations sampled during *INSPIRE* were oligotrophic and had low N/P ratios (< 1.3; Table 4.2), indicating potential N-limiting conditions consistent with the observations of Mills *et al.* (2004). Phosphate concentrations were similarly low (15–117 nM), but did not relate to proximity to the coast in the same way as nitrate concentrations did. Silicate concentrations were consistently low across all stations ($0.8 \pm 0.1 \mu\text{M}$). At stations D and F, N-limitation was confirmed by ship-board determination of nitrate and phosphate by E.M.S. Woodward prior to

initiation of the incubations. Therefore, at these two stations N-additions were made simultaneously with trace metal additions. All macronutrient concentrations during *INSPIRE* were consistent with previous measurements of surface waters in the tropical NE Atlantic Ocean (e.g. Mahaffey *et al.*, 2003; Mather *et al.*, 2008).

Table 4. 2. Nitrate, ammonium, phosphate and silicate at T_0 , from CTD bottle depths (m) corresponding to 55% photosynthetically active radiation (PAR).

Station	55% PAR (m)	CTD bottle depth (m)	Nitrate (nM)	Ammonium (nM)	Phosphate (nM)	Silicate (μ M)	N:P
A	9	9	1	7	68	0.9	0.01
B	2	2	661	30	108	0.9	6.1
C	2	2	120	124	91	0.8	1.3
D	9	9	11	6	117	0.8	0.09
E	11	13	2	14	81	0.6	0.02
F	11	13	1	5	15	0.8	0.06

4.3.2. Primary production

Primary production rates ($\text{mg C m}^{-2} \text{ h}^{-1}$) were estimated in terms of the incorporation of radio-labelled sodium bicarbonate ($\text{NaH}^{14}\text{CO}_3$) into particulate material (Poulton *et al.*, 2006). Therefore, the terms primary production rate and carbon fixation rate are used interchangeably in this report. The present study was conducted in the North Atlantic gyre, where rates of autotrophic carbon fixation at T_0 of $0.82\text{--}2.57 \text{ mg C m}^{-2} \text{ h}^{-1}$ were observed. In the Atlantic Ocean subtropical gyres rates of carbon fixation vary over a wide dynamic range ($0.75\text{--}15 \text{ mg C m}^{-2} \text{ h}^{-1}$; Marañón *et al.*, 2003), and are considerably more variable than phytoplankton biomass (in terms of total chl-a). This variability has been linked to fluctuations in the supply of inorganic N and P (Pérez *et al.*, 2005). In this study, the range of carbon fixation at T_0 corresponded to the lower

end of the dynamic range from previous studies across the six stations sampled.

Regardless of the rate of primary production at the start of the experiment (T_0), the rates of primary production decreased by at least 50% over the 48 h (T_{48}) of the incubation at all stations (Fig. 4.6). The only stations where an increase in the rate of productivity was observed with respect to the control (T_{48}) were the two stations where the trace metal spikes had been augmented with N-additions (stations D and F). As primary production rates were not significantly higher in any trace metal + N spikes compared to the N only spikes, this suggests that the observed increases in productivity were a response to alleviation of N-limitation rather than relief of trace metal limitation. These findings are in general agreement with the observations of Mills *et al.* (2004), who argued that algal growth in the NE Atlantic was proximately N-limited. Mills *et al.* (2004) went on to demonstrate that once N-limitation was alleviated additions of P and Fe further increased productivity, the largest increase being observed when N, P and Fe were added simultaneously.

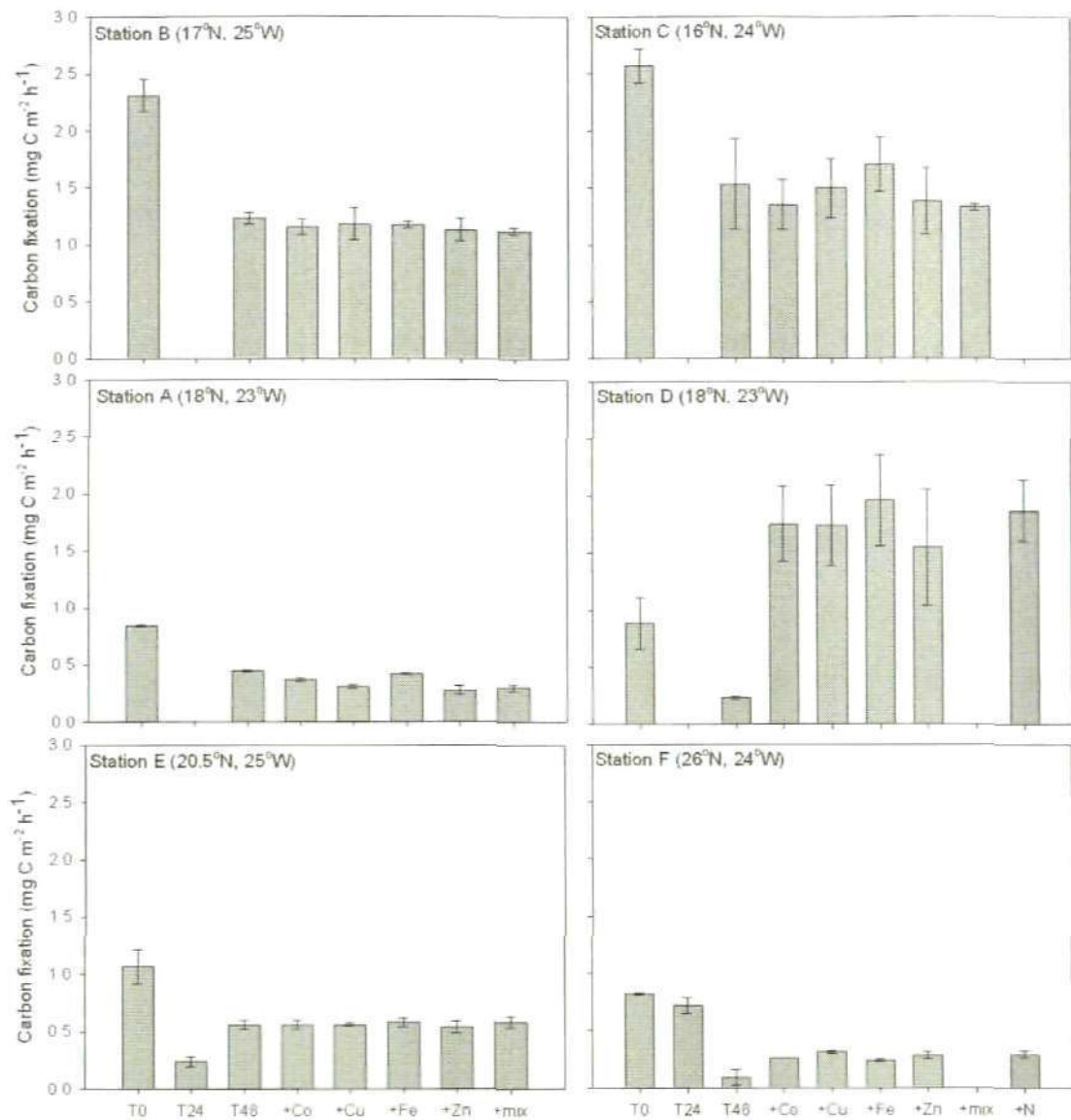


Figure 4. 6. Primary production as determined by ^{14}C uptake rates ($\text{mg C m}^{-2} \text{ h}^{-1}$) in bioassays conducted during *INSPIRE*, where Stations B and C were in regions of high chl-*a*, A and D medium chl-*a* and E and F low chl-*a*. At Stations D and F, nitrogen additions (+N) were added to all trace metal treatments so that +Co = Co+N, +Cu = Cu+N, +Fe = Fe +N and +Zn = Zn+N and the mixed metal treatment was replaced by a +N only treatment. Carbon fixation rates kindly provided by J. Dixon (PML).

All stations sampled during the INSPIRE cruise were found to be N-limited and Stations A, D, E and F, in particular, were extremely oligotrophic (nitrate = 1–11 nM, phosphate = 15–117 nM) (Table 4.2). At such low concentrations of phosphate (15–117 nM) it is likely that relief of N-limitation would have shifted the system to towards P-limitation, and is consistent with the findings of both Mills *et al.* (2004) and Moore *et al.* (2009). Therefore, even if one of the trace metals had been a co-limiting factor no response to the trace metal additions would be expected without concomitant N and P additions.

4.3.3. Heterotrophic bacterial production

Heterotrophic bacterial productivity (HBP) at T_0 ranged from $3.6 \times 10^{-5} \text{ mg C L}^{-1} \text{ h}^{-1}$ at Station C to $5.6 \times 10^{-6} \text{ mg C L}^{-1} \text{ h}^{-1}$ at station F (Fig. 4.7). At the two most remote stations (E and F) the rate of HBP was within the range reported by Zubkov *et al.* (2000) for the subtropical gyres ($4.2\text{--}8.3 \times 10^{-6} \text{ mg C L}^{-1} \text{ h}^{-1}$). At the other stations (A–D), HBP was an order of magnitude higher, perhaps due to proximity to the Cape Verde Islands. At Station A there was no observed response to metal additions on HBP rates relative to the control, T_{48} , (ANOVA, $p = 0.98$), although HBP rates were reduced by ~30 % from $2.58 \times 10^{-5} \text{ mg C L}^{-1} \text{ h}^{-1}$ at T_0 to $1.80 \times 10^{-5} \text{ mg C L}^{-1} \text{ h}^{-1}$ after 48 h (T_{48}) (Fig. 4.7). In contrast, at Station D, there was no significant difference between T_0 , T_{24} and T_{48} (ANOVA, $p = 0.10$, mean = $2.0 \times 10^{-5} \pm 5.6 \times 10^{-6} \text{ mg C L}^{-1} \text{ h}^{-1}$), but there was a response to addition of N (nitrate and ammonium), with a 57% increase in the rate of HBP observed (from $2.05 \times 10^{-5} \text{ mg C L}^{-1} \text{ h}^{-1}$ at T_{48} to $3.57 \times 10^{-5} \text{ mg C L}^{-1} \text{ h}^{-1}$ in the +N treatment). As stations A and D were at approximately the same location (18°N , 23°W), and confirmed as N-limited in terms of Redfield stoichiometry, this

data further suggests proximal N-limitation of primary production in this region; the increase in HBP being a response to increased primary production following alleviation of N-limitation.

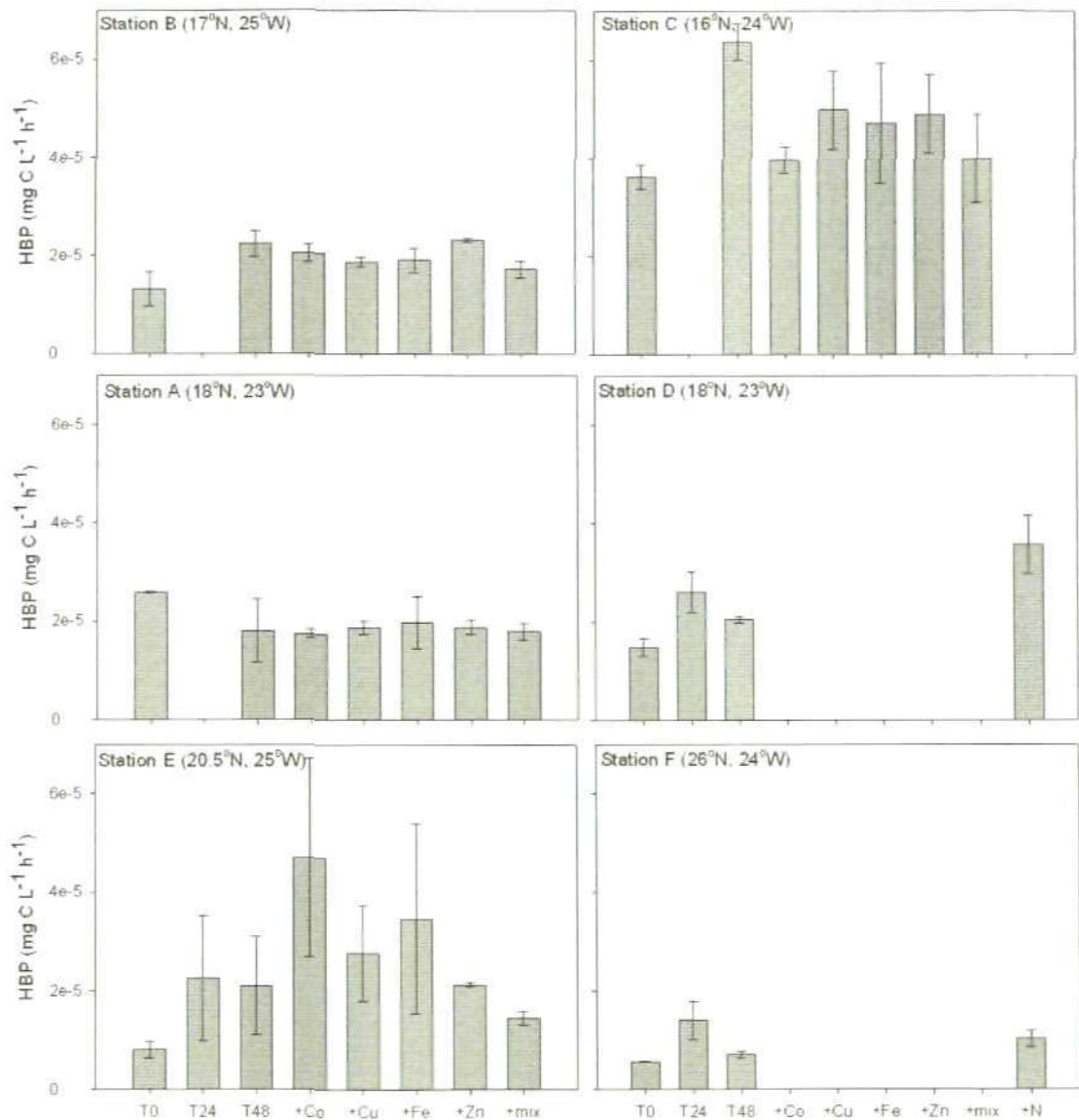


Figure 4. 7. Heterotrophic bacterial productivity (HBP) rates ($\text{mg C L}^{-1} \text{h}^{-1}$) in bioassays conducted during *INSPIRE*, where Stations B and C were in regions of high chl-a, A and D medium chl-a and E and F low chl-a. At Stations D and F, nitrogen additions (+N) were added to all trace metal treatments so that +Co = Co+N, +Cu = Cu+N, +Fe = Fe +N and +Zn = Zn+N and the mixed metal treatment was replaced by a +N only treatment. HBP data kindly provided by J. Dixon (PML).

At Station B there was no significant response to trace metal additions with respect to T_{48} (t -test, $p = 0.05$), except for the mixed addition which resulted in ~30% reduction in HBP. At the other high chlorophyll-*a* station, the coastal Station C, where the highest rates of HBP were observed ($3.6 \times 10^{-5} \text{ mg C L}^{-1} \text{ h}^{-1}$), there was a negative effect from the addition of individual trace metals and from the mixed metal addition. Therefore, data from these two stations provides no evidence for trace metal limitation. At the low chl-*a* Station E there was also no observed effect (ANOVA, $p = 0.09$). As observed at Station D, the addition of N to bioassays from Station F also increased the rate of HBP, again indicating the knock-on effect of N-limitation of primary production on HBP in the North Atlantic gyre. In this study, there was no evidence for trace metal limitation without relief from N- (and possibly P-) limitation.

4.3.4. Dissolved Co and Cu

Dissolved Co and Cu concentrations in the bioassays are presented in Figures 4.8 and 4.9 and Tables 4.3 and 4.4. At stations A–F, in the bottles that had not received additions of 0.5 nM Co, all dCo concentrations were within error of the control (T_{48}) (where A = 27 ± 1 pM, B = 27 ± 2 pM, C = 35 ± 3 pM, D = 46 ± 8 pM, E = 21 ± 3 pM, F = 13 ± 3 pM; Fig. 4.8). There was also no statistical difference between T_0 and the control, T_{48} , indicating no significant removal of dCo after 48h (T_{48}) (t -test, $p = < 0.05$). Where 0.5 nM dCo had been added (+Co and +mix treatments), drawdown varied from 71–72% (stations A, B, C and F) to 58% and 37% (stations E and D respectively) (Table 4.3).

Dissolved Co concentrations in surface waters of the North Atlantic gyre are extremely low (generally between 0.02 and 0.04 nM, Chapter 5). In this study, spikes of 0.5 nM dCo were added (+Co and mixed metal additions), and between ~ 0.15 and 0.35 nM dCo was removed from solution. The phytoplankton assemblage during *INSPIRE* was dominated by *Prochlorococcus* (G. Tarran, pers. comm.), given this genus' absolute cellular requirement for Co it is likely that they accounted for the majority of the observed dCo uptake. However, Saito *et al.* (2010) state that they are not aware of any examples of luxury Co uptake by phytoplankton, likely because open ocean dCo concentrations are so low. Furthermore, as the incubation bottles were polycarbonate, adsorption onto the bottle walls was assumed to be minimal. Assuming no luxury uptake of dCo, the most likely explanation for the 'additional' (in excess of cellular requirements) removal of dCo from the bioassays is via extra-cellular adsorption.

Table 4. 3. Concentrations of dCo in the bioassay bottles that had been treated with additions of 0.5 nM (500 pM) dCo and at T_0 .

Station	T_0 (pM)	T_0 + addition (pM)	+Co (pM)	+mix (pM)	Mean (pM)	dCo removed (pM)	% removal	N addition
A	28	528	153	152	153	376	71	N
B	24	524	154	151	153	372	71	N
C	35	535	147	150	149	387	72	N
D	37	537	338		338	199	37	Y
E	20	520	225	214	220	301	58	N
F	12	512	146		146	366	71	Y

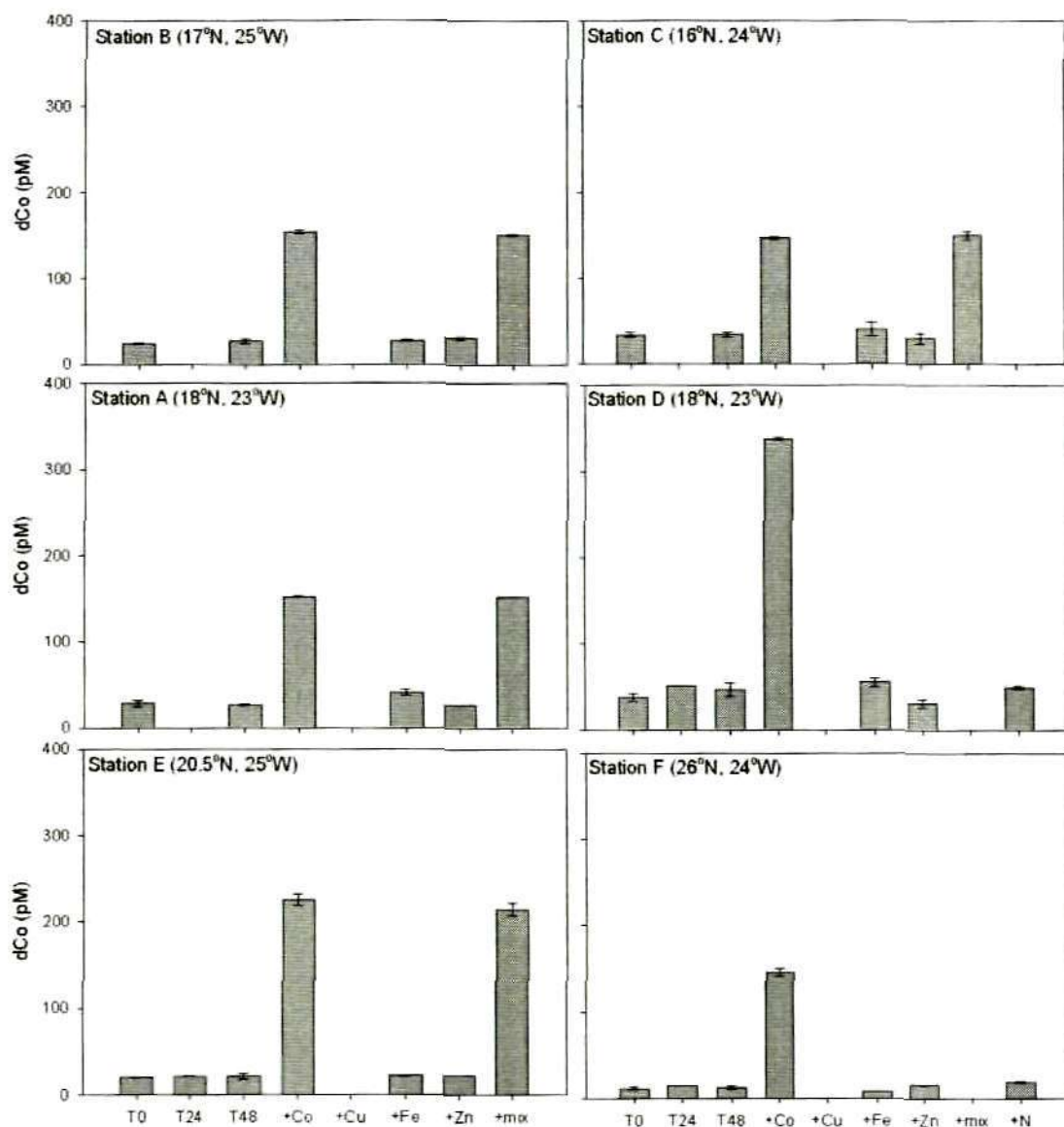


Figure 4. 8. Dissolved Co (pM) in bioassays conducted during *INSPIRE*, where Stations B and C were in regions of high chl-*a*, A and D medium chl-*a* and E and F low chl-*a*. At Stations D and F, nitrogen additions (+N) were added to all trace metal treatments so that +Co = Co+N, +Cu = Cu+N, +Fe = Fe +N and +Zn = Zn+N and the mixed metal treatment was replaced by a +N only treatment.

For dCu, the T₀ concentrations were remarkably consistent between stations (0.4 ± 0.1 nM), as were the final concentrations in all bottles without 2 nM dCu

additions (0.4 ± 0.05 nM) (Fig. 4.9 and Table 4.4). In addition, the bottles with 2 nM dCu additions (+Cu and +mix treatments) from stations A-E (1.4 ± 0.1 nM) also displayed remarkable similarity in concentrations. This resulted in a similarly consistent amount of dCu removal in incubations from these five stations ($42 \pm 3\%$). Only at Station F, the station with the lowest macronutrient concentrations, did the amount of dCu removal differ, with 63% removed during the 48 h incubation.

An interesting aspect of Cu biogeochemistry is that even at very low concentrations of the free cupric ion phytoplankton growth can be inhibited (cupric ion activities as low as 10 pM inhibited growth in *Prochlorococcus*, Brand *et al.*, 1986). Brand *et al.* (1986) hypothesised that even at the concentrations of dCu naturally found in upwelling regimes (1.5 nM Cu in the nearby Guinea Dome, centred at $\sim 10^\circ\text{N}$, Pohl *et al.* 2010), just to the south of our study area, cupric ion activity may be sufficiently high to inhibit growth of the cyanobacteria, *Prochlorococcus* and *Synechococcus*. In this study, 2 nM treatments of dCu were added to the bioassays and, given that the biomass in the Atlantic gyres is dominated by *Prochlorococcus* (e.g. Poulton *et al.*, 2006), dCu may have impacted on phytoplankton growth. However, in bottles with dCu additions primary production rates varied little from the bottles containing the other trace metal additions (Fig. 4.6), indicating that this concentration of dCu did not appear to have a negative effect on cyanobacteria growth.

As for dCo, the addition of N did not appear to be a controlling factor on the degree of dCu removed from solution. However, in contrast to dCo, the greatest

amount of dCu removal occurred at the two most oligotrophic stations (E and F), which suggests dCu at the most oligotrophic stations in the eastern North Atlantic gyre may be present at (co-)limiting concentrations. Due to Cu-dependent Fe transport systems in some phytoplankton (Maldonado *et al.*, 2006), dCu may be being drawn down to a greater extent at these two stations in order facilitate Fe uptake where dFe availability is low, or to facilitate luxury uptake of Fe if conditions are non-limiting (Sunda and Huntsman, 1995b).

Table 4. 4. Concentrations of dCu in the bioassay bottles that had been treated with additions of 2 nM dCu and at T₀.

Station	T ₀ (nM)	T ₀ + addition (nM)	+Cu (nM)	+mix (nM)	Mean (nM)	dCu removed (nM)	% removal	N addition
A	0.4	2.4	1.4	1.4	1.4	1.0	42	N
B	0.5	2.5	1.4	1.4	1.4	1.0	42	N
C	0.4	2.4	1.5	1.5	1.5	0.9	37	N
D	0.3	2.3	1.4		1.4	0.9	41	Y
E	0.4	2.4	1.3	1.3	1.3	1.1	46	N
F	0.4	2.4	0.9		0.9	1.5	63	Y

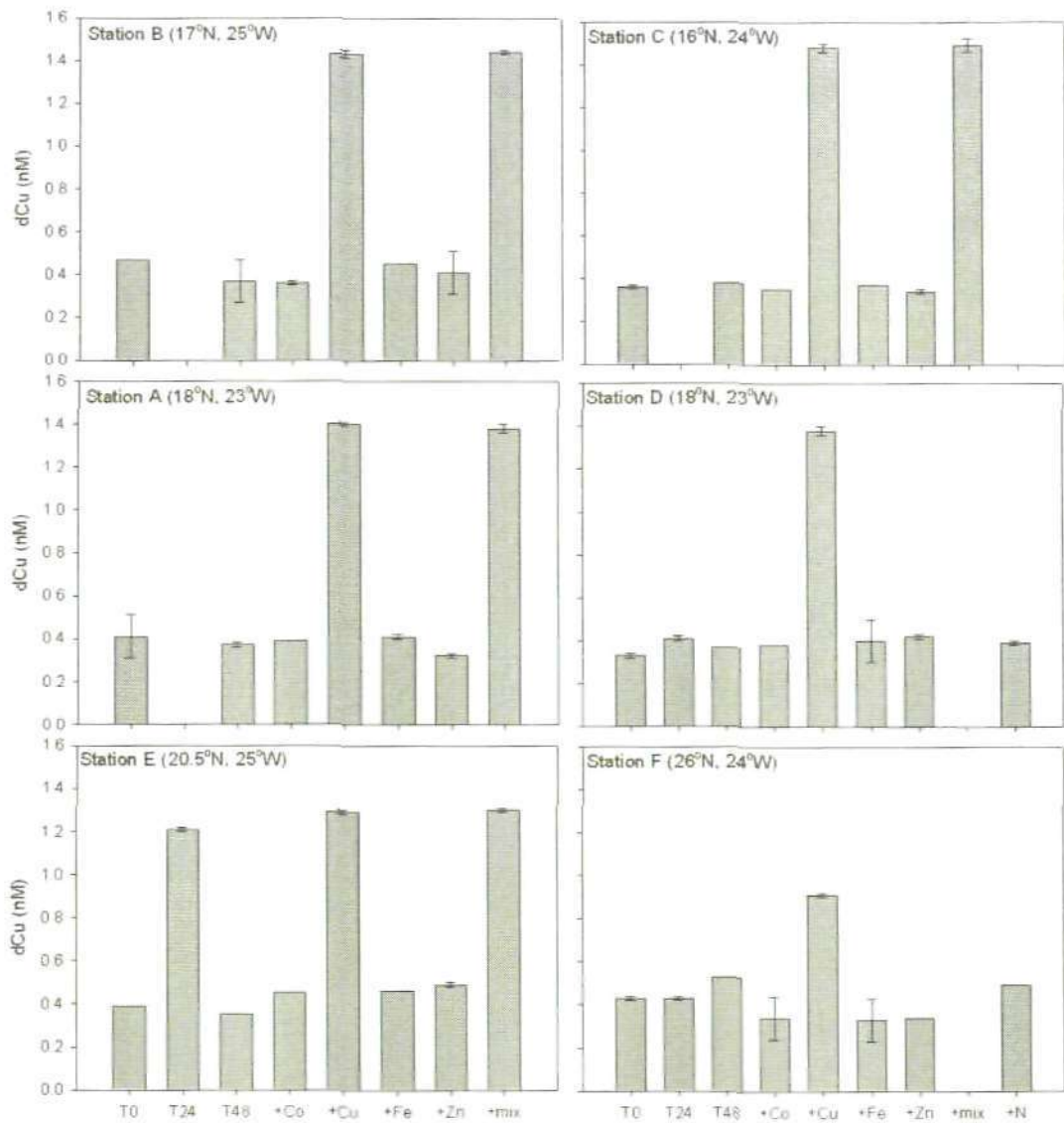


Figure 4. 9. Dissolved Cu (nM) in bioassays conducted during *INSPIRE*, where Stations B and C were in regions of high chl-*a*, A and D medium chl-*a* and E and F low chl-*a*. At Stations D and F, nitrogen additions (+N) were added to all trace metal treatments so that +Co = Co+N, +Cu = Cu+N, +Fe = Fe +N and +Zn = Zn+N and the mixed metal treatment was replaced by a +N only treatment.

4.3.5. Dissolved Fe and N₂ fixation

There are some differences between the N₂ fixation rates presented here and the data presented in Turk *et al.* (2010). This is because the N₂ data presented

in this chapter refers to rates obtained from N₂ fixation experiments conducted after 48 h trace metal incubation experiments, whereas Turk *et al.* (2010) discuss N₂ fixation rates from separate incubations conducted in seawater not augmented with trace metals from the same six stations occupied during the *INSPIRE* cruise. This difference does not change the overall conclusion reached by Turk *et al.* (2010), that dFe availability exerts a significant control on N₂ fixation rates in the Northeast Atlantic Ocean.

Surface water dFe concentrations during this study (0.3–0.6 nM at T₀; Table 4.5 and Fig. 4.10) were within the range (0.1–1.2 nM) previously reported for surface waters of this region (Sarhou *et al.*, 2003; Rijkenberg *et al.*, 2008; Ussher *et al.*, 2010), with the exception of Station A (1.5 nM). Five-day air mass back trajectories, simulated using the HYPSPPLIT transport and dispersion model (Draxler and Rolf, 2010; Rolph, 2010) (data not shown), indicate the presence of dust (a major source of Fe to surface waters) over the study area (Fig. 4.11) immediately prior to the commencement of sampling at Station A on 13/11/07. While this may have accounted for the slightly higher concentrations of dFe in surface waters at Stations B–F compared to the concentration range of 0.1–0.4 nM reported by Rijkenberg *et al.* (2008), it is unlikely to have resulted in the very high dFe concentrations reported here for Station A. In this instance sample contamination is suspected for two reasons; 1) the concentration of dFe at Station D (0.3 ± 0.01 nM), which was located close to Station A, was found to be fivefold lower than at Station A (1.5 ± 0.01 nM), and 2) Rijkenberg *et al.* (2008) sampled in this region both before and after a dust deposition event and

reported only small increases in surface dFe concentrations, from 0.20 ± 0.03 nM ($n = 125$) to 0.25 ± 0.03 ($n = 17$).

Table 4. 5. Dissolved Fe and N₂ fixation rates at T₀.

Station	dFe (nM)	st dev	N ₂ fixation (nM N L ⁻¹ h ⁻¹) ^a	Position	
A	1.5 ^b	0.01	1.47	17.8°N, 22.8°W	
B	0.6	0.03	9.77	16.9°N, 24.8°W	Nr UK-SOLAS atmos sampling site
C	0.4	0.01	0.69	16°.0N, 23.7°W	W. of Boa Vista Island
D	0.3	0.01	0.06	17.7°N, 22.8°W	Near Station A
E	0.4	0.03	0.09	20.5°N, 25.0°W	
F	0.6	0.01	0.06	26.0°N, 24.0°W	
SAFe D2 ^c	0.95	0.01		consensus = 0.92 ± 0.06 nM	

^aData kindly provided by A. Rees (PML)

^bSample contamination suspected

^cDetails of the SAFe reference samples can be accessed at: <http://www.es.ucsc.edu/~kbruland/GeotracesSaFe/kwbGeotracesSaFe.html>

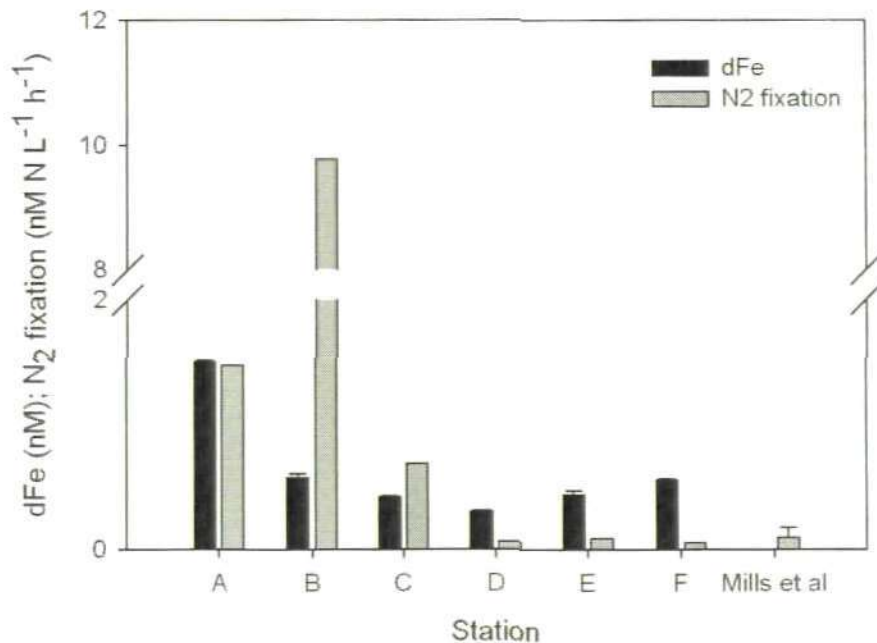


Figure 4. 10. Dissolved Fe concentrations (black bars) and N₂ fixation rates (grey bars) at T₀ (N₂ fixation rates kindly provided by A. Rees, PML), plus the N₂ fixation rates in non-amended seawater (*i.e.* no N, P or Fe additions) reported in Mills *et al.* (2004) at stations ~ 800 km south of our study area.

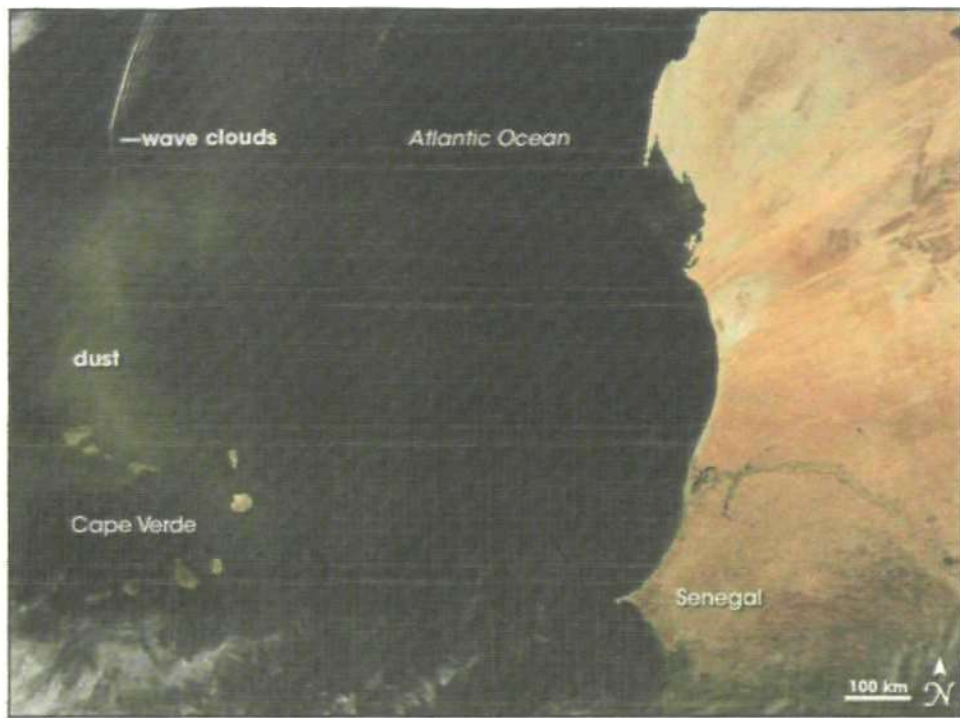


Figure 4. 11. Saharan dust over the Cape Verde Islands in early November 2007 after a few days of dust storm activity off the west coast of Africa. This image was taken on 10/11/07 by NASA's Moderate Resolution Imaging Spectroradiometer (MODIS). Sampling on the *INSPIRE* cruise commenced on 13/11/07. Image available at: <http://earthobservatory.nasa.gov/NaturalHazards/view.php?id=19326> (accessed 23/02/11).

Iron (and phosphate) availability has been hypothesised to limit or co-limit N_2 fixation (Berman-Frank *et al.*, 2001; Karl *et al.*, 2002; Mills *et al.*, 2004). In this study, Stations A and B had both the highest N_2 fixation rates (1.5 and 9.8 $nM N L^{-1} h^{-1}$ respectively), and the highest dFe concentrations (1.5 and 0.6 nM respectively) (Table 4.5). Although N_2 fixation rates of similar magnitude have been reported in the Eastern Mediterranean (5.3 $nM N L^{-1} h^{-1}$; Rees *et al.*, 2006), N_2 fixation rates at Stations A, B and also C (1.47, 9.77 and 0.69 $nM N L^{-1} h^{-1}$ respectively) were relatively high in comparison to those reported by Mills *et al.* (2004) (0.01–0.17 $nM N L^{-1} h^{-1}$) in the tropical North Atlantic ~ 800 km south of our study area where Fe and P were found to be limiting or co-limiting algal growth. While these results may reflect N_2 fixation rates in the Northeast tropical

Atlantic Ocean at the time of this study, it is likely that the high rate of N_2 fixation reported for samples from Station A was a response to Fe contamination that occurred during the incubation or sample handling process, particularly as phosphate was so low at this station (68 nM). On the other hand, if the dFe concentrations were sufficiently high to meet the enzymatic Fe requirements of diazotrophy (0.6 and 0.4 nM dFe at Stations B and C respectively) the relatively high rates of N_2 fixation observed at Stations B and C may be a true reflection of N_2 fixation in this region at this time. The higher ammonium concentrations observed at Stations B and C (30 and 124 nM respectively) relative to the other stations (5–14 nM) could result from the higher N_2 fixation rates at Stations B and C. The rates of N_2 fixation at Stations B and C were comparable to those reported in Fe- and P-amended waters by Mills *et al.* (2004), which suggests that these stations were not Fe- (or P-) limited at the time of this study, perhaps due to their proximity to the Cape Verde Islands. Nitrogen fixation rates at T_0 at Station D-F (0.06–0.09 nM $N L^{-1} h^{-1}$) were comparable to the rates reported in Mills *et al.* (2004) in non-amended waters.

In addition to the high rates of N_2 fixation calculated at T_0 , the N_2 fixation rates from trace metal amended bottles at Stations A and B were also an order of magnitude greater than at the other four stations (Fig. 4.12). These two stations were not close to each other (or rather other stations were closer), they had different initial (T_0) concentrations of dCo, dCu and macronutrients (N and P) and, very different dFe concentrations, as well as different diazotrophic community structure (Fig.4.13). As previously discussed, the reasons for the high rates of N_2 fixation at Station A (> 1.5 nM $N L^{-1} h^{-1}$) are likely a response of the diazotroph community to high dFe (*i.e.* contamination) in the incubation

bottles. However, at Station B sample contamination is not suspected, and it was at this station that the highest rates of N_2 fixation were observed (5.1–18.4 $nM N L^{-1} h^{-1}$), although relative to the control (T₄₈) the addition of trace metals had a suppressing effect on N_2 fixation rates (Fig. 4.12).

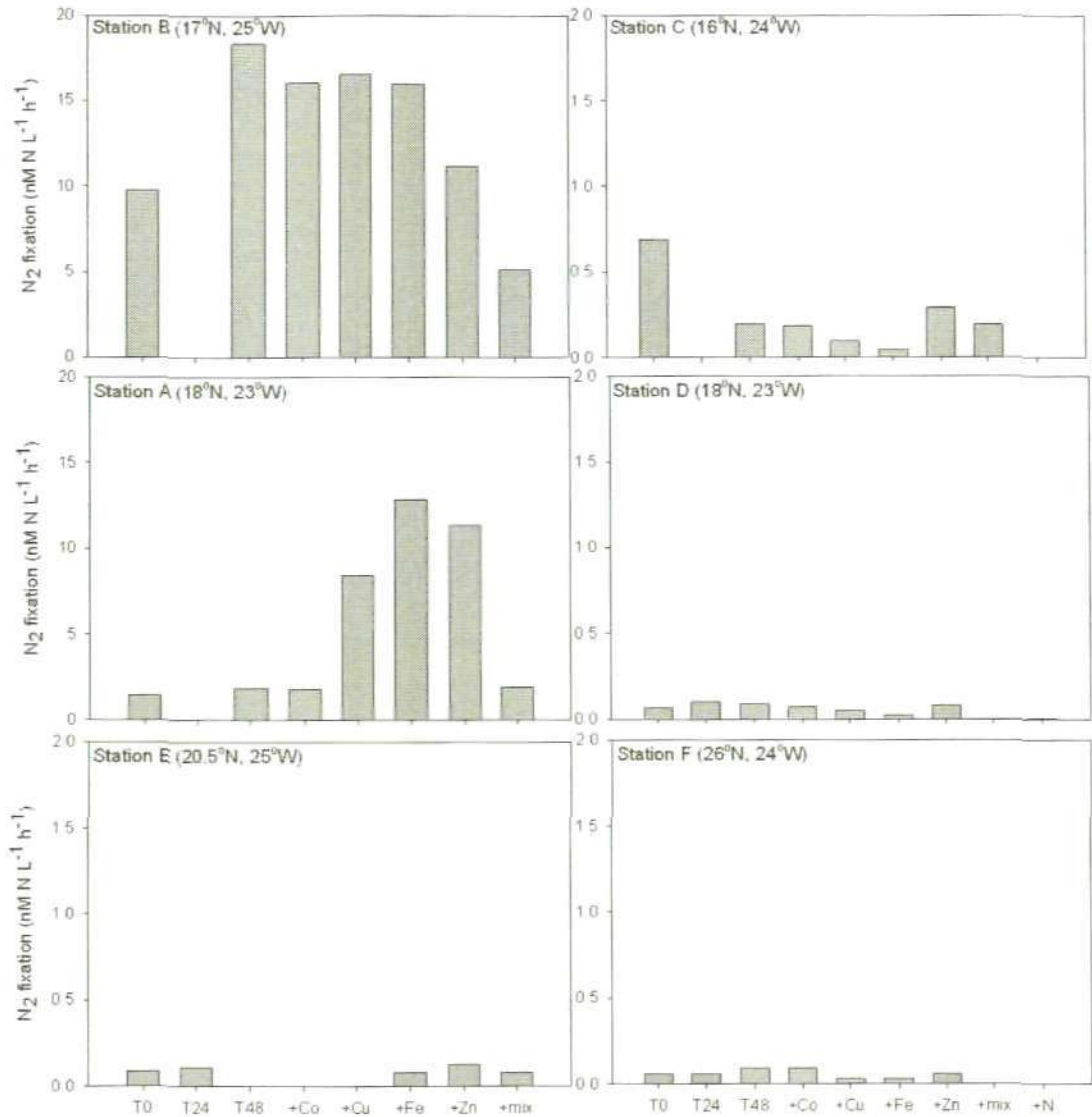


Figure 4. 12. N_2 fixation rates ($nM N L^{-1} h^{-1}$) in bioassays conducted during INSPIRE where Stations B and C were in regions of high chl-*a*, A and D medium chl-*a* and E and F low chl-*a*. At Stations D and F, nitrogen additions (+N) were added to all trace metal treatments so that +Co = Co+N, +Cu = Cu+N, +Fe = Fe +N and +Zn = Zn+N and the mixed metal treatment was replaced by a +N only treatment. Note that the scale is x10 higher for Stations A and B compared with Stations C–F. Data kindly provided by A. Rees (PML).

At both Stations B and A, the unicellular cyanobacteria UCYN-A, dominated diazotroph community structure, although *Trichodesmium* also made a significant contribution (> 25%) to the assemblage at Station B (Fig. 4.13). Indeed, Goebel *et al.* (2010) reported high abundances of UCYN-A near the Cape Verde Islands, and based on modelled rates, concluded UCYN-A was responsible for the majority of N₂ fixation in this region. Although no overall correlation was found between UCYN-A *nifH* expression and N₂ fixation rates ($r^2 = 0.12$, $p = 0.09$, $n = 25$) in surface water samples analysed for *nifH* gene expression from these six stations (see Supplementary Table 1 in Turk *et al.* 2010), these findings suggest that UCYN-A contributed to the high N₂ fixation rate measured in incubated seawater from Stations A and B. However, complex environmental interactions mean that high UCYN-A *nifH* transcript abundance does not always correlate to high rates of N₂ fixation. The diazotroph community at Stations D and E were also overwhelmingly dominated by UCYN-A (Fig. 4.13), but had much lower (by an order of magnitude) rates of N₂ fixation than at Station B (and A), which suggests that the interplay of other factors, such as the availability of trace metals (in addition to dFe), macronutrients (P and N), and hydrography (*e.g.* temperature, salinity, ocean currents) either directly or indirectly influence N₂ fixation in this region by influencing diazotroph ecology.

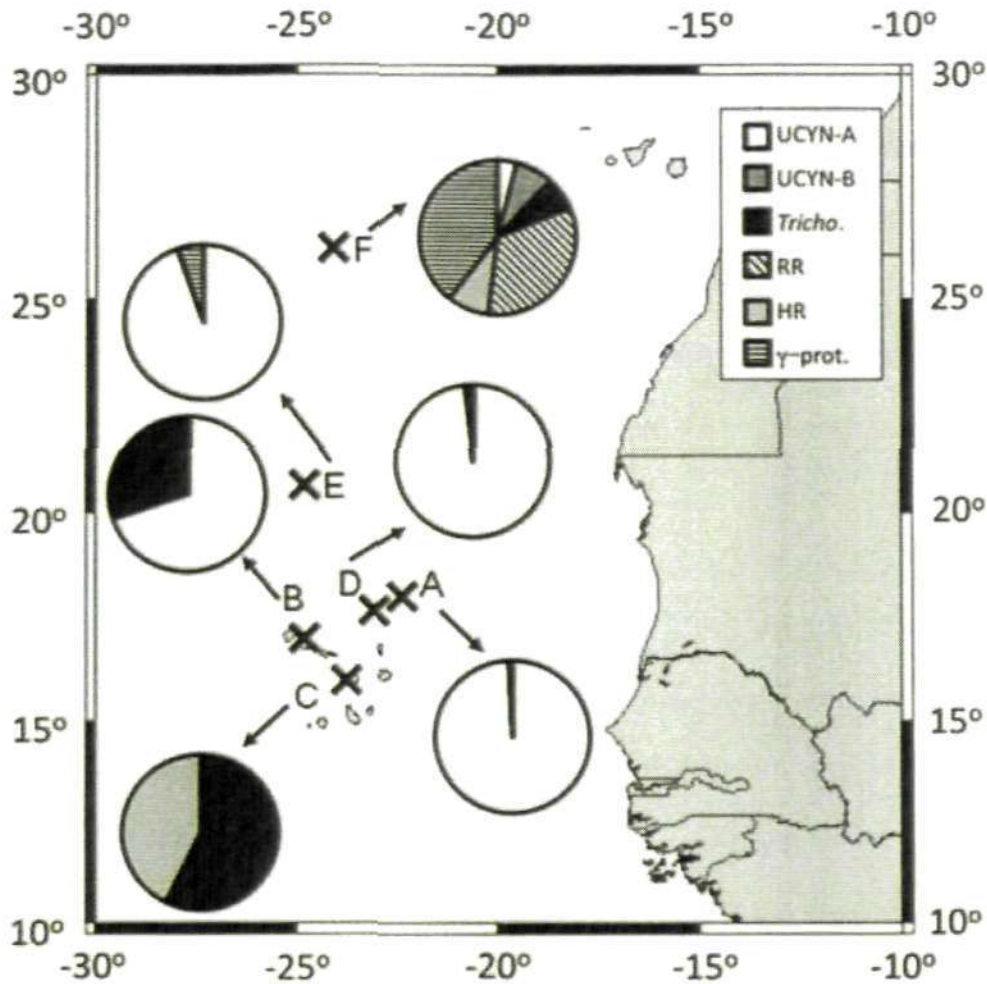


Figure 4. 13. Relative contribution of individual diazotrophs to overall *nifH* gene expression quantified from surface waters at stations during *INSPIRE*, where UCYN-A and UCYN-B represent two separate groups of unicellular diazotrophs, *Tricho.* is *Trichodesmium*, RR and HR are two strains of the diazotrophic symbiont, *Richelia intracellularis* (associated with the diatoms *Rhizosolenia* and *Hemiaulus hauckii* respectively) and γ -prot are proteobacteria. (Figure reproduced from Turk *et al.*, 2011).

Rates of N_2 fixation in the dFe-contaminated samples from Station A confirm the importance of dFe availability on high rates of diazotrophy in this region. As additions of dCu and dZn increased N_2 fixation by x 8 and x 11 with respect to the control (Fig. 4.12), it appears that these two trace metals have a synergistic

effect on N₂ fixation when dFe is abundant (in this case 1.5 nM dFe), although this effect was negated by addition of dCo. Neither the +Co addition nor the mixed trace metal addition (that contained dCo) had any effect on N₂ fixation compared to the control. At the remaining stations (B, C, D, E and F), without inadvertently high dFe augmentation, trace metal additions had little to no effect on N₂ fixation rates, where an effect was observed it was as a suppression of N₂ fixation (Fig. 4.12).

Nitrate depletion in the mixed layer has been shown to strongly influence diazotroph community structure. For the vast majority of diazotrophs nitrate-depletion is a pre-requisite for high rates of N₂ fixation in surface waters (Langois *et al.*, 2005). Trace metal incubations from two stations during *INSPIRE* (Stations D and F) were supplemented with inorganic N (nitrate and ammonium) additions. Nitrogen fixation rates at these two stations (both 0.06 nM N L⁻¹ h⁻¹) were comparable to the similarly N-amended samples of Mills *et al.* (2004), and were the lowest observed in this study. In bottle incubations with N additions there are two explanations for the inhibition of N₂ fixation; 1) physiological inhibition of nitrogenase activity by high inorganic N concentrations, 2) competitive inhibition of diazotrophs by other microorganisms that compete with the diazotrophs for the limited Fe and P resources on relief of N-limitation. At present it is unknown which of these two scenarios dominate.

Although both Fe and phosphate are hypothesised to limit or co-limit N₂ fixation (Berman-Frank *et al.*, 2001; Sañudo-Wilhelmy *et al.*, 2001; Karl *et al.*, 2002; Mills *et al.*, 2004), linear regressions indicate that the only parameter that N₂ fixation could be correlated with was temperature ($r^2 = 0.37$, $P = 0.001$, $n = 25$),

consistent with Langois *et al.* (2005). There was no correlation with either dFe (when Station A is discarded) or phosphate, nor could any of the other environmental parameters measured be correlated to N₂ fixation rates.

It is important to note that a recent study by Mohr *et al.* (2010) has shown that the ¹⁵N-tracer method developed by Montoya *et al.* (1996) used here and widely throughout the scientific community may underestimate N₂ fixation rates. Mohr *et al.* (2010) determined that bubble injections of ¹⁵N₂ gas are slow to equilibrate using traditional shipboard incubation techniques, which has a significant impact on calculations used in determining N₂ fixation rates. As such, the timing of ¹⁵N₂ injections relative to peak nitrogenase activity in diel studies can have a variable impact on measured N₂ fixation rates. It is unclear as to what extent our current understanding of global N₂ fixation rates will be altered as the community adopts the modified technique developed by Mohr *et al.* (2010) to address this underestimation.

4.4. Conclusions and recommendations

All stations were N-limited during the *INSPIRE* cruise. In terms of rates of primary production, the only response to trace metal additions occurred in conjunction with N-additions. The response to an N only addition indicated that the observed increase in primary production was a response to alleviation of N-limitation, rather than to any of the trace metal additions. In terms of HBP, there was also no evidence of trace metal limitation. While the highest rates of N₂ fixation occurred in bottles with the highest dFe concentrations, additions of N reduced the rate of N₂ fixation.

The apparent lack of biological response to trace metal additions in the present study are consistent with the observation that phytoplankton growth in the North Atlantic gyre is proximally N-limited, and that alleviation of N-limitation shifts the system towards P-limitation (Mills *et al.*, 2004; Moore *et al.*, 2009). In order to confirm N and P co-limitation of primary and heterotrophic bacterial production, it would be necessary to carry out concomitant N, P and trace metal additions. Such additions would then allow any biological response to Co, Cu, Fe or Zn to be determined. An additional modification to the experimental design would be to conduct longer trace metal incubations to allow the phytoplankton to adapt and respond to the experimental conditions. Measurements of primary and heterotrophic bacterial production and N₂ fixation rates may need to be determined in parallel incubations under the same experimental conditions. This would allow incubations to be terminated at the same time, while allowing the necessary manipulations required for the rate measurements (*e.g.* introduction of radio-labelled carbon) to be made without risk of contaminating the samples for trace metals. Further experiments that take these factors into consideration are recommended in order to investigate the impact of increases in trace metal availability on fundamental biological parameters in a time of increasing uncertainty about changes in supply of the macronutrients, N and P.

Chapter 5

Dissolved Cobalt Distributions in Surface Waters During an Atlantic Meridional Transect (*AMT-19*)

5.1. Introduction

Cobalt (Co) is essential for phytoplankton growth (Morel *et al.*, 1994; Saito *et al.*, 2002; Sunda and Huntsman, 1995a; Timmermans *et al.*, 2001). It is required for the synthesis of vitamin B₁₂ by marine prokaryotes, and is the metal co-factor in some forms of the metalloenzyme carbonic anhydrase, which is required for inorganic carbon acquisition (Sunda and Huntsman, 1995a; Saito *et al.*, 2002). In addition, there is evidence for Co-based forms of alkaline phosphatase, the enzyme that facilitates use of the organic phosphorus pool (Gong *et al.*, 2005). Evidence of a correlation with phosphate in the upper water column is also emerging as a common feature across diverse oceanic regimes (Bown *et al.*, 2011; Noble *et al.*, 2008; Saito and Moffett, 2002; Saito *et al.*, 2010). In terms of its chemistry in seawater Co shares a number of similarities, such as redox behaviour, with iron (Fe) but is geochemically quite distinct (Shelley *et al.*, submitted).

The sources of Co to surface waters are thought to be similar to sources of Fe, that is from deposition of aerosol dusts, lateral advection of continental material (from fluvial systems and continental slope sediments), vertical advective supply in upwelling regimes, hydrothermal vents and remineralisation from sinking particles (*e.g.* Bown *et al.*, 2011; German and van Damm, 2003; Johnson *et al.*, 1988; Knauer *et al.*, 1982; Noble *et al.* 2008; Saito *et al.*, 2004; Saito and Moffett, 2002; Sholkovitz and Copland, 1981; Toggweiler *et al.*, 1991). The main removal mechanisms are biological uptake and particle scavenging (*e.g.* Saito and Moffett, 2002). The relative importance and impact of the input/removal mechanisms is spatially and temporally variable and remains poorly constrained

over large areas of the global ocean due to a lack of data from the open ocean compared to the macronutrients. Thus, our current understanding of Co biogeochemistry is incomplete.

The Atlantic Ocean receives large amounts of water and sedimentary run-off from river systems (the Amazon, Congo and Rio de la Plata being the largest) and large areas underlie a path of high atmospheric aerosol deposition from the arid regions of NW Africa (Carlson and Prospero, 1972). Gross circulation of Atlantic upper waters is dominated by two large anticyclonic subtropical gyres. The Atlantic Meridional Transect (*AMT*) cruise tracks (~50°N– 50°S) provide an excellent opportunity to resolve surface distributions and upper water column profiles of trace elements, such as Co, through regions of diverse inputs and removal mechanisms as they traverse a range of contrasting oceanic provinces, which are characterised by similar chemical, biological and/or physical properties (Longhurst, 1998).

There are few published data sets from large-scale studies that report distributions of dissolved Co in the Atlantic Ocean (Bowie *et al.*, 2002a; Bown *et al.*, 2011; Pohl *et al.*, 2010), an issue that is currently being addressed by the GEOTRACES programme (www.geotraces.org). Across diverse open-ocean regimes, *e.g.* the Northeast Pacific Ocean (Knauer *et al.*, 1982; Martin *et al.*, 1989), Sargasso Sea (Saito and Moffett, 2002); Peru Upwelling region of the tropical South Pacific Ocean (Saito *et al.*, 2004), Atlantic sector of the Southern Ocean (Bown *et al.*, 2011) dCo concentrations are extremely low, ranging from 4–120 pM. To date, dissolved iron (dFe) has been measured on eight of the

twenty *AMT* cruises (Bowie *et al.*, 2002a; Ussher *et al.*, in prep.; Wyatt *et al.*, in prep.), whereas dissolved Co (as total dissolvable Co, TdCo) has only been measured on two (*AMT-3* and *AMT-6*, Bowie *et al.*, 2002a). More recently, dissolved Co (dCo) has been measured on another Atlantic meridional cruise (*ANT XXIII/I*) from Vigo, Spain to Cape Town, South Africa as part of the GEOTRACES programme (Pohl *et al.*, 2010).

In this chapter, the upper water column (< 200 m) distributions of dCo along a north-south meridional transect in the Atlantic Ocean are presented. This transect included contrasting biogeochemical provinces, such as the two oligotrophic gyres and the equatorial upwelling regime, as well as contrasting areas of high and low aerosol deposition and fluvial inputs. The data set presented here is one of only two large-scale data sets of dCo (< 0.2 μm) distributions, covering a distance of ~ 12,000 km in the Atlantic Ocean. The dCo data are discussed in the context of the biogeochemical and physical properties of the different biogeochemical provinces in order to interpret the distribution and behaviour of dCo in the upper water column of the Atlantic Ocean between ~ 50°N and 50°S.

5.2. Materials and Methods

5.2.1. Sampling

Twenty two water column profiles were sampled during the *AMT-19* cruise (13/10/09–28/11/09) from Falmouth, UK to Punta Arenas, Chile, on board the *RRS James Cook* (Fig. 5.1). In this gyre-centred cruise, stations were sampled from five biogeochemical provinces: (1) the North Atlantic Drift Region (NADR,

49–38°N); (2) the eastern North Atlantic Gyre (NATL-E, 38–12° N); (3) the Western Tropical Atlantic (WTRA, 12°N–10°S); (4) the South Atlantic Gyre (SATL, 10–32°S) and (5) the South Subtropical Confluence (SSTC, 33–38°S), based on the provinces described by Longhurst (1998). In this study, the distribution of salinity, temperature, dissolved Co (dCo) and macronutrients (nitrate and phosphate) were used to identify the province boundaries (Table 5.1). As the province boundaries drift seasonally, the assigned boundaries are subject to small-scale variations. For example, the seasonal shift in the boundaries of the subtropical gyres results in a southward displacement of the NADR–NAST boundary during northern spring from 40–36°N, and a northward displacement of the SSTC–SATL boundary during southern spring from 37–33°S (Longhurst, 1998). In addition, the intertropical convergence zone (ITCZ), a region subject to high annual rainfall that forms the boundary between the atmospheric hemispheres, migrates seasonally from ~5°N in northern winter to ~10°N in the summer (Sultan and Janicot, 2000).

Table 5. 1. Description of the biogeochemical provinces sampled during *AMT-19* (adapted from Longhurst, 1998).

Oceanic region	Biogeochemical province	Acronym	Latitudinal range
Open NE Atlantic	North Atlantic Drift Region ($n=3$)	NADR	55/56–38° N
Open-ocean gyre	North(east) Atlantic Gyre ($n=9$)	NATL-E	38–12° N
Tropical W Atlantic	Western Tropical Atlantic ($n=4$)	WTRA	12° N–10° S
Open-ocean gyre	South Atlantic Gyre ($n=3$)	SATL	10–33° S
SW Atlantic mixing zone	South Subtropical Convergence ($n=3$)	SSTC	33–55° S

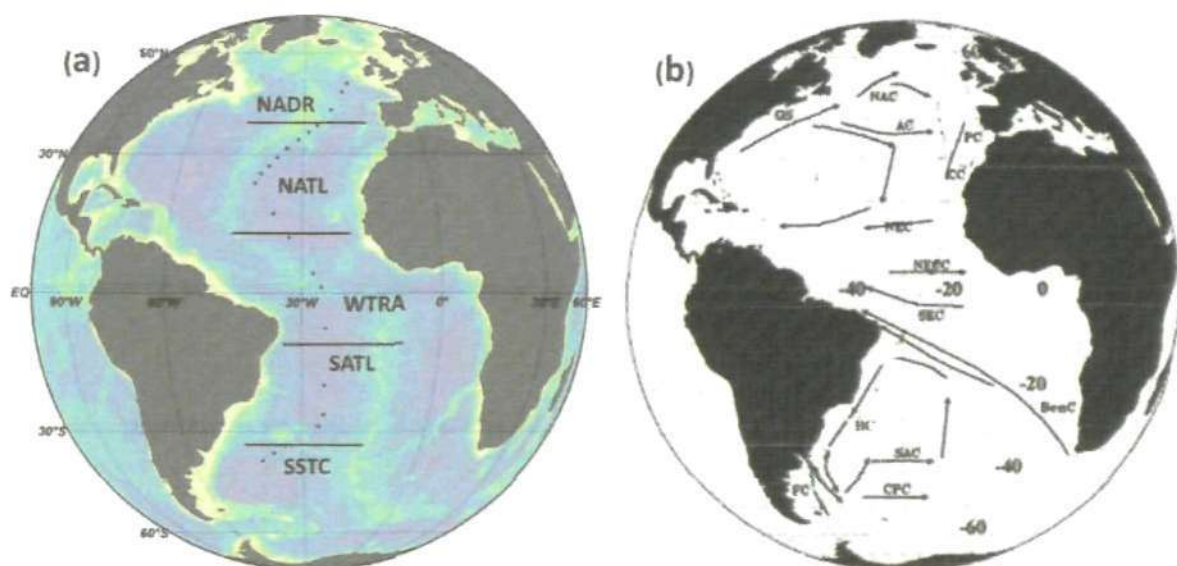


Figure 5. 1. AMT-19 (a) cruise track, showing the water column sampling stations and the biogeochemical provinces (adapted from Longhurst, 1998): North Atlantic Drift (NADR), North Atlantic Gyre (NATL), Western Tropical Atlantic (WTRA), South Atlantic Gyre (SATL), and surface currents of the Atlantic Ocean, where: AC = Azores Current, BenC = Benguela Current, BC = Brazil Current, CC = Canary Current, CPC = Circumpolar Current, FC = Falklands Current, GS = Gulf Stream, NAC = North Atlantic Current, NEC = North Equatorial Current, NECC = North Atlantic Counter Current, PC = Portugal Current, SAC = South Atlantic Current, SEC = South Equatorial Current (adapted from Aiken *et al.*, 2000).

Seawater samples for the determination of dCo were collected from customised 24 x 10 L trace metal clean Teflon coated OTE water sampling bottles, fitted with silicone O-rings and plastic coated external springs, attached to a trace metal-free titanium CTD rosette. Samples for macronutrients were collected from ten depths from each CTD deployment; from the titanium CTD rosette to correspond with dCo sampling, and additionally from standard 20 L Niskin bottles fitted to a stainless steel CTD rosette (Seabird), thus providing high resolution profiling along the cruise track.

All ship-based trace metal sample handling was conducted in a positive-pressure clean van. Seawater samples were filtered into acid-cleaned low density polyethylene (LDPE) bottles (Nalgene) using a Sartobran 300 filter capsule (Sartorius) with a 0.2 μm cut-off, and acidified to pH 1.7–1.8 (0.024 M) with ultraclean HCl (Romil SpA) inside a class-100 laminar flow hood. Samples were then double zip-lock bagged for storage prior to return to the home laboratory for determination of dCo.

5.2.2. Dissolved cobalt determination

Due to the extremely stable organic complexation of Co in seawater, a number of studies have demonstrated the requirement to UV irradiate samples prior to determination of the operationally-defined dissolved fraction (Donat and Bruland, 1988; Saito and Moffett, 2001; Shelley *et al.*, 2010; Vega and van den Berg, 1997), rather than the labile fraction. Dissolved Co was determined in UV-irradiated seawater samples in the clean room facility (ISO 9001) at the University of Plymouth, UK by flow injection with chemiluminescence detection (Shelley *et al.*, 2010). Briefly, the flow injection manifold was coupled with a photomultiplier tube, and dCo was determined in UV-irradiated samples (3 h; 400 W medium-pressure Hg lamp, Photochemical Reactors) from the chemiluminescence produced from the catalytic oxidation of pyrogallol (1,2,3-trihydroxybenzene). During all analytical runs UV-irradiated SAFe D2 and GEOTRACES GD reference samples were analysed. The concentrations of dCo $\pm 1s$ were: SAFe D2 ($n = 9$), this study 49.5 ± 2 pM, consensus value 43.1 ± 3.2 pM, consensus range 41–49 pM; GD ($n = 9$), this study 73 ± 3 pM, consensus value 68 ± 13 pM. The consensus values are available at:

[http://www.es.ucsc.edu/~kbruland/GeotracesSaFe/kwbGeotraces SaFe.html](http://www.es.ucsc.edu/~kbruland/GeotracesSaFe/kwbGeotraces%20SaFe.html).

Typically, blank values were 4 ± 1 pM ($n = 24$), with a detection limit of 3 pM (3s blank).

5.2.3. Ancillary measurements

Inorganic macronutrients (nitrite + nitrate, phosphate, silicate) were determined in fresh samples (analysed within 3–4 h of collection) onboard using a 5-channel segmented flow analyser (Bran and Luebbe, AAll AutoAnalyzer) following standard spectrophotometric procedures (Grashoff *et al.*, 1983) modified by (Woodward *et al.*, 1999). Detection limits for were 0.01 μ M nitrate + nitrite (hereon referred to as nitrate) and phosphate, and 0.1 μ M for silicate.

Phytoplankton; *Prochlorococcus*, *Synechococcus*, pico-eukaryotes (coccolithophores, cryptophytes) and nano-eukaryotes were enumerated using a Becton Dickinson FACSort flow cytometer equipped with an air-cooled laser providing blue light at 488 nm (Tarran *et al.*, 2006).

A Seabird 911+ CTD was fitted with dual pumped temperature and conductivity sensors, both pairs were mounted on the CTD rosette. Dissolved O₂ was measured using a Seabird SBE 43 O₂ sensor mounted on the rosette. Salinity and dissolved O₂ measurements were calibrated using ship-board determinations of discrete seawater samples. Salinity was calibrated using an Autosal 8400B salinometer (Guideline), and dissolved O₂ by automated Winkler titration with photometric end-point detection (Carritt and Carpenter, 1966).

Fluorescence and irradiance were determined using an Aquatraka MkIII fluorometer and Alphatraka MkII transmissometer (Chelsea Instruments) respectively. Sampling depths were determined by reference to the *in situ* fluorescence, temperature, salinity and irradiance (400–700 nm) profiles, to include 97%, 55%, 33%, 14%, 1% and 0.1% irradiance levels. Ship-board fluorimetric determinations of total chlorophyll-*a* (chl-*a*) were made following the methods of Welschmeyer *et al.* (1994); filtration of 250–500 mL seawater (Whatman GF/F, nominal pore size 0.7 μm), extraction in 10 mL of 90% acetone (HPLC grade) in the dark for 18–20 h at 4 °C, followed by measurement of chlorophyll fluorescence on a TD-700 fluorometer (Turner Designs) and calibrated against a chl-*a* standard (Sigma).

Dissolved Co concentrations and can be found in the Appendix. Ancillary data and a full station list is available at: <http://www.bodc.ac.uk/projects/uk/AMT/>.

5.3. Results and Discussion

5.3.1. Hydrography

The biogeochemical province boundaries identified in Figure 5.1a for AMT-19 are based on Longhurst (1998), and are as follows: the North Atlantic Drift Province (NADR) is bounded to the south by the bifurcation of the northeasterly flow of the North Atlantic current (see Fig. 5.1b for Atlantic Ocean surface currents) and the southeasterly flow of the Azores Current, at $\sim 40^\circ\text{N}$, thus forming the boundary with the North Atlantic Subtropical Gyre Province (NAST). The southern boundary of NAST is the Subtropical Convergence (STC), which is weakly defined by a series of largely sub-surface thermal fronts. The eastern component of NAST (NAST-E) is defined by the offshore Canary Current and

separated from the western component by the southerly edge of the Azores Current, and further south, the mid-Atlantic Ridge. To the south of NAST is the North Atlantic Tropical Gyral Province (NATR), which is comprised of the North Atlantic gyre south of the STC. The southern extent of NATR is formed by the limit of the westerly flow along the thermocline ridge marked by the convergence of the North Equatorial Current/North Equatorial Countercurrent, at 10–12°N. In this study NAST and NATR are combined to form the North Atlantic Gyre Province (NATL) for consistency with the southern gyre (SATL). The southern extent of the Western Tropical Atlantic Province (WTRA) is marked by the northern edge of the seasonally varying flow of the South Equatorial Current (SEC). In turn, the SEC forms the South Atlantic Gyre Province (SATL). The northern and southern boundaries of the dynamic South Subtropical Convergence Province (SSTC) are formed by the Subtropical Convergence (~ 35°S), and Antarctic Polar Front (~ 55°S) respectively.

During October 2009, the water column in the Northeast Atlantic (~ 30–50° N) had a mixed layer depth of 45–50 m. In the western tropical Atlantic Province (WTRA, ~ 12°N–10° S) equatorial upwelling water was identified, with colder, lower salinity water than in the adjoining gyres penetrating well into the euphotic zone (Fig. 5.2). As observed in earlier *AMT* studies (Robinson *et al.*, 2006), a gradual decline in temperature was observed across the southern gyre (SATL), such that south of ~ 33° S the upper water column (0–200 m) was thermally homogeneous (~ 16 °C). The salinity minimum associated with the Intertropical Convergence Zone (ITCZ) is clearly visible in surface waters between ~ 7–11°N (Fig. 5.2 bottom panel).

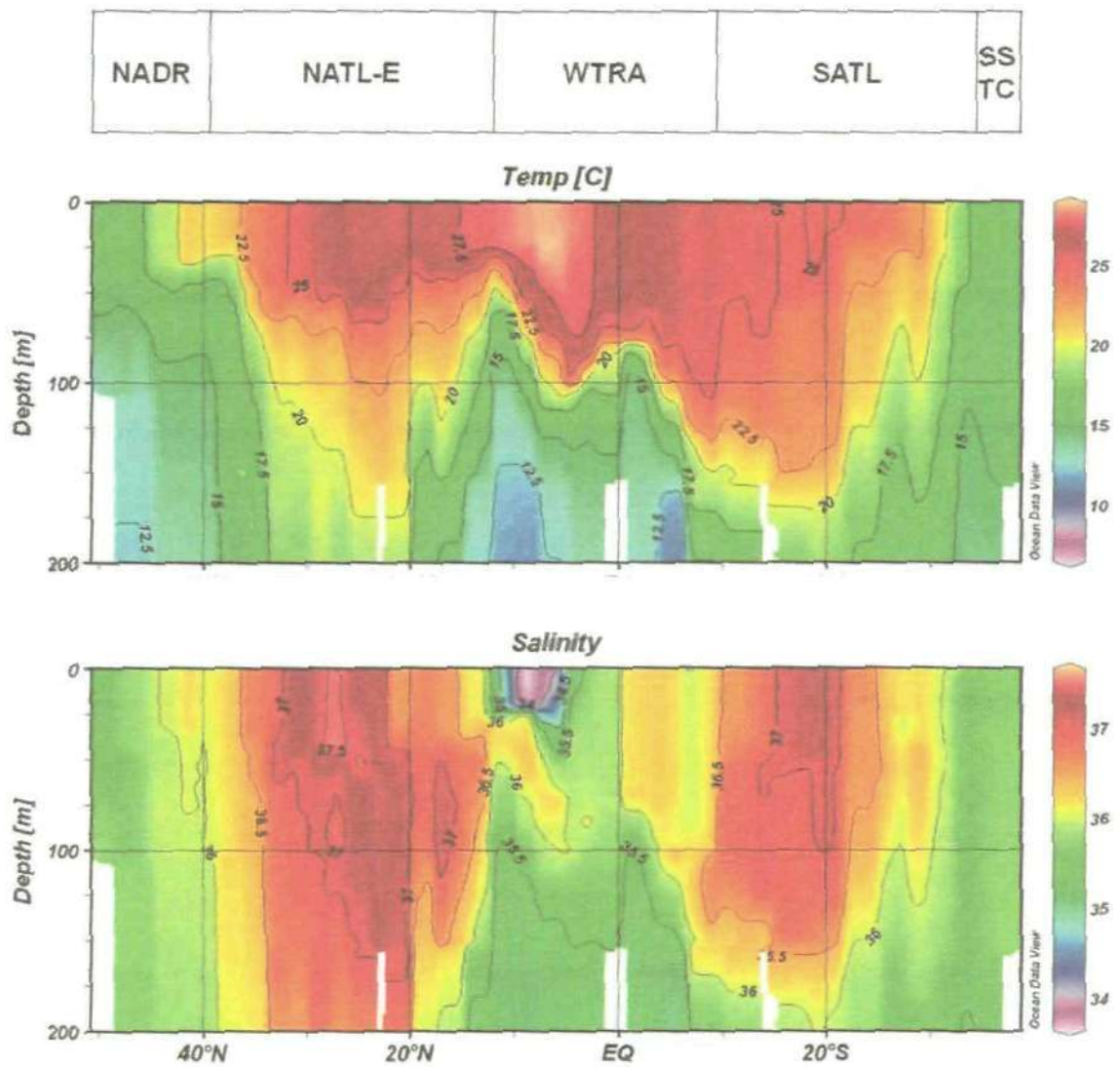


Figure 5. 2. North– south distributions of temperature (top) and salinity (bottom) during AMT-19, with the biogeochemical provinces marked above (refer to Table 5.1 for acronyms).

5.3.2. North-south distribution of macronutrients in the upper water column (< 200 m)

Macronutrient (nitrate, phosphate and silicate) concentrations are shown in Figure 5.3. For all three macronutrients, the highest concentrations were observed in the equatorial upwelling. This is consistent with other gyre-centred *AMT* cruises (e.g. *AMT-16*, Ussher *et al.* in prep.). In some areas of the SATL, macronutrient concentrations were depleted in surface waters to concentrations below the instrumental detection limit (nitrate and phosphate = 0.01 μM , silicate = 0.1 μM) (visible as blank patches in the contour plots of Fig. 5.3), which is due to a combination of downwelling, driven by wind forcing, and biological utilisation. In the case of nitrate, surface waters of the southern region of the WRTA is also depleted to below the limit of detection, as the thermocline creates a barrier to vertical diffusion (note that phosphate and silicate concentrations are also extremely low in this highly productive region). The boundary of the WRTA and the SATL is marked by strong gradients in the concentrations of the macronutrients, with very low concentrations of nitrate (< 2.5 μM), phosphate (< 0.25 μM) and silicate (< 1 μM) observed throughout the upper water column of the SATL. Although the data set is incomplete at present, previous *AMT* cruises (e.g. *AMT-16*, Ussher *et al.* in prep.) have noted higher concentrations of phosphate in the SATL compared with the NATL-E. This has been attributed to lower biological utilisation of phosphate in the SATL due to low dFe availability in this region. Annually, the South Atlantic receives only 4% of the global atmospheric dust flux, compared with 43% for the North Atlantic (Fig. 1.8; Jickells *et al.*, 2005), and results in lower concentrations of dFe in the SATL compared with the NATL-E (Ussher *et al.*, in prep.; Wyatt *et al.*, in prep.).

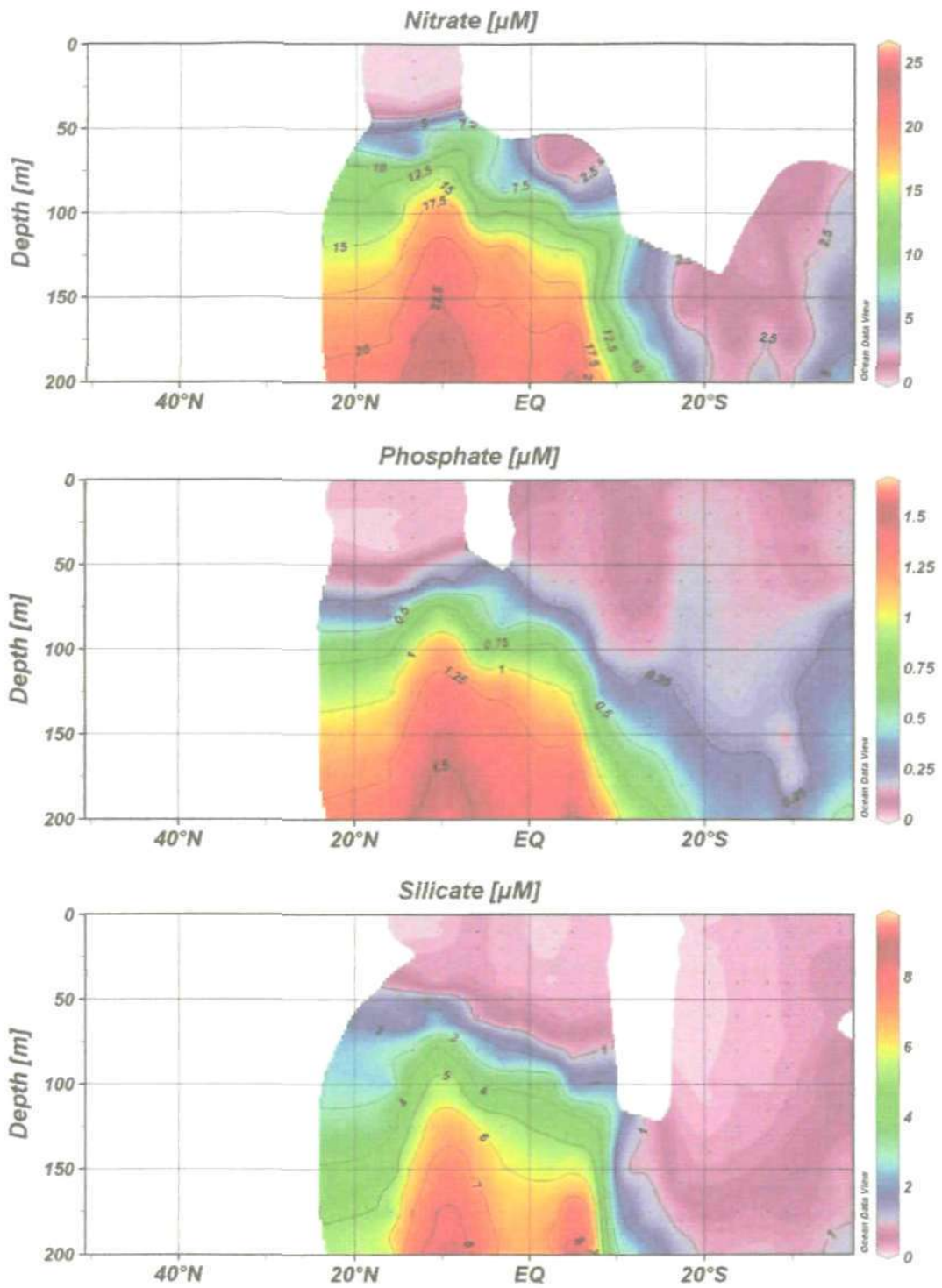


Figure 5. 3. Concentrations of macronutrients (nitrate, phosphate and silicate) during AMT-19 from $\sim 16^{\circ}\text{N}$ – 38°S . The blank regions in the Southern hemisphere reflect concentrations below the instrumental detection limit (nitrate and phosphate = $0.01 \mu\text{M}$, silicate = $0.1 \mu\text{M}$), the blank regions in the Northern hemisphere will be filled when the data becomes available.

Macronutrient determination by C. Harris (PML).

A correlation between dCo and phosphate concentrations in the upper water column, indicative of the nutritive role of Co, is emerging as a consistent oceanographic feature across diverse oceanographic settings, such as the subarctic Pacific (Martin *et al.*, 1989; Sunda and Huntsman, 1995a), South Atlantic Ocean (Saito and Moffett, 2002), Peru upwelling (Saito *et al.*, 2004), tropical Pacific (Noble *et al.* 2008), Atlantic sector of the Southern Ocean (Bown *et al.*, 2011) and Ross Sea (Saito *et al.*, 2010). In regions where upper water column dCo and phosphate distributions are decoupled, a minimum productivity threshold (which can vary significantly between regions) is proposed below which dCo and phosphate removal is not at a near-constant ratio (Bown *et al.*, 2011; Noble *et al.*, 2008; Saito and Moffett, 2002; Saito *et al.*, 2010). During AMT-19, no relationship between dCo and phosphate at depths \leq the subsurface chlorophyll maximum (SCM depth: NATL = \sim 100 m, WTRA = \sim 60 m; SATL = \sim 150 m; SSTC = 50 m) was observed ($r^2 = 0.04$, $n = 27$) (Nb. incomplete data set \sim 16°N - 38°S only). In this large-scale meridional transect diverse hydrographic regimes, over a wide range of productivity (< 0.01 – 0.55 mg chl-*a* m⁻³) were sampled. Therefore, it is more appropriate to consider provinces or even stations on an individual basis. For example, at 1.3°N, 25.8°W (WTRA) phosphate concentrations at depths shallower than the SCM were 0.01–0.03 μ M. At 70 m (the approximate depth of the SCM and nitricline) phosphate was 0.11 μ M, increasing sharply to 0.96 μ M at 100 m (below the depth of the SCM/nitricline). At this station, at depths \leq the SCM (\sim 75 m), a strong correlation with phosphate was observed (*e.g.* $r^2 = 0.91$, $n = 4$).

5.3.3. North-south distributions of dCo in the upper water column (< 200 m)

Dissolved Co concentrations in the upper water column (< 200 m) of the Atlantic Ocean (~50°N to 38°S) are shown in Figure 5.4. The boundaries of the gyre regions (NATL-E and SATL) were characterised by sharp dCo gradients, maintained by the water mass movements that delineate the biogeochemical province boundaries. In Figure 5.4 dCo distributions are overlaid with isopycnals, which shows good agreement between dCo distributions and density gradients, indicating the role of water mass movement in dCo distributions. Dissolved Co concentrations in the gyres were the lowest observed during *AMT-19*, with concentrations in the NATL-E approximately 50% less than in the SATL (~ 20 and 40 pM respectively).

Dissolved Co concentrations in the water column of the NATL-E were both more homogenous and lower (25 ± 12 pM, 16–29°N) than at comparable latitudes in the SATL (54 ± 18 pM, 19–28°S). In both gyres dCo concentrations were higher at the surface than in underlying waters, due to biological uptake and/or external inputs, with concentrations increasing below ~ 100 m. This feature is particularly clear in the NATL-E. In the NATL-E the increase in dCo concentrations occurred below the subsurface chlorophyll maximum (SCM at ~ 100 m), suggesting Co recycling below this depth, whereas in the SATL lateral advection of Co-enriched WTRA water is an important additional source of dCo (Fig. 5.4). The low dCo waters of the gyres (NATL-E and SATL) were separated by the WRTA. In this upwelling region high dCo concentrations (> 60 pM) were observed roughly coincident with a region of low dissolved O₂ (< 150 μM). Dissolved Co distributions in the upper water column during *AMT-19* followed

the same general trends as previous Atlantic meridional investigations (Bowie *et al.*, 2002a; Pohl *et al.*, 2010).

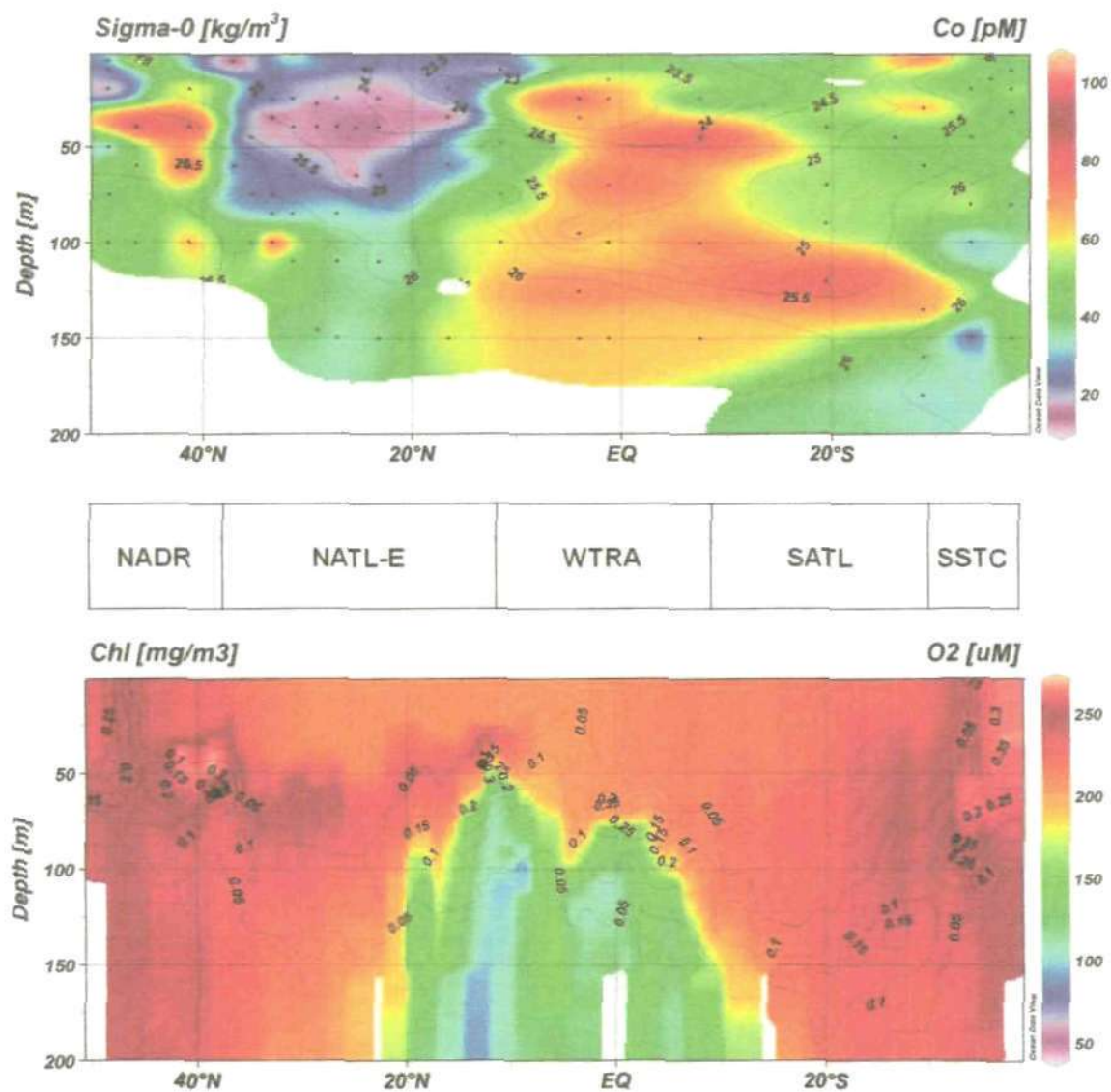


Figure 5. 4. The north-south distribution of dCo (pM) overlaid with potential density (kg m^{-3}) (top panel) and O_2 (μM) overlaid with chl-a (mg m^{-3}) (bottom panel) during AMT-19.

Dissolved Co profiles in the open ocean are described as having hybrid-type distributions, as concentrations are influenced by both biological uptake and scavenging processes. As only upper water column (< 200 m depth) distributions are reported here profiles are not discussed in terms of nutrient-,

scavenged- or hybrid-type distributions (Bruland and Lohan, 2003). Total chlorophyll concentrations are plotted overlying the dissolved O₂ concentration in Figure 5.4, and shows the variability in depth of the SCM during AMT-19. In general, the SCM was positioned at the base of the thermo- and haloclines, which effectively form a barrier to vertical nutrient diffusion. In the Atlantic Ocean the SCM is commonly positioned just above the nitracline (defined as the depth at which nitrate concentrations = < 0.1 μM) (Letelier *et al.*, 2004). Thus, basin-scale variability in the depth of the SCM can be interpreted as a function of nitricline depth, with the notable exception of the equatorial region (of the Atlantic Ocean), where the two are found at similar depths (Poulton *et al.*, 2006).

NADR – In the region of the Porcupine Abyssal Plain (PAP) fixed point observatory, located at ~ 49.0°N, 16.5°W, highly variable water column dCo concentrations (15–89 pM) were observed, with the highest concentrations (> 80 pM) between 40 and 60 m depth (Fig. 4). These high subsurface dCo concentrations were observed just below the surface mixed layer (~ 40 m, Fig. 5.5a) and followed the 26 kg m⁻³ isopycnal (Atlantic Central Water has a potential density of 25.8–27.1 kg m⁻³, Stramma *et al.*, 2005) (Fig. 5.4, top panel) to ~ 40°N, 23°W. This is consistent with the conclusions of Ellwood and van den Berg (2001), who observed higher concentrations of dCo with increasing proximity to the continental margin. The sediments of the western European continental shelf are the most likely source of Co to this province.

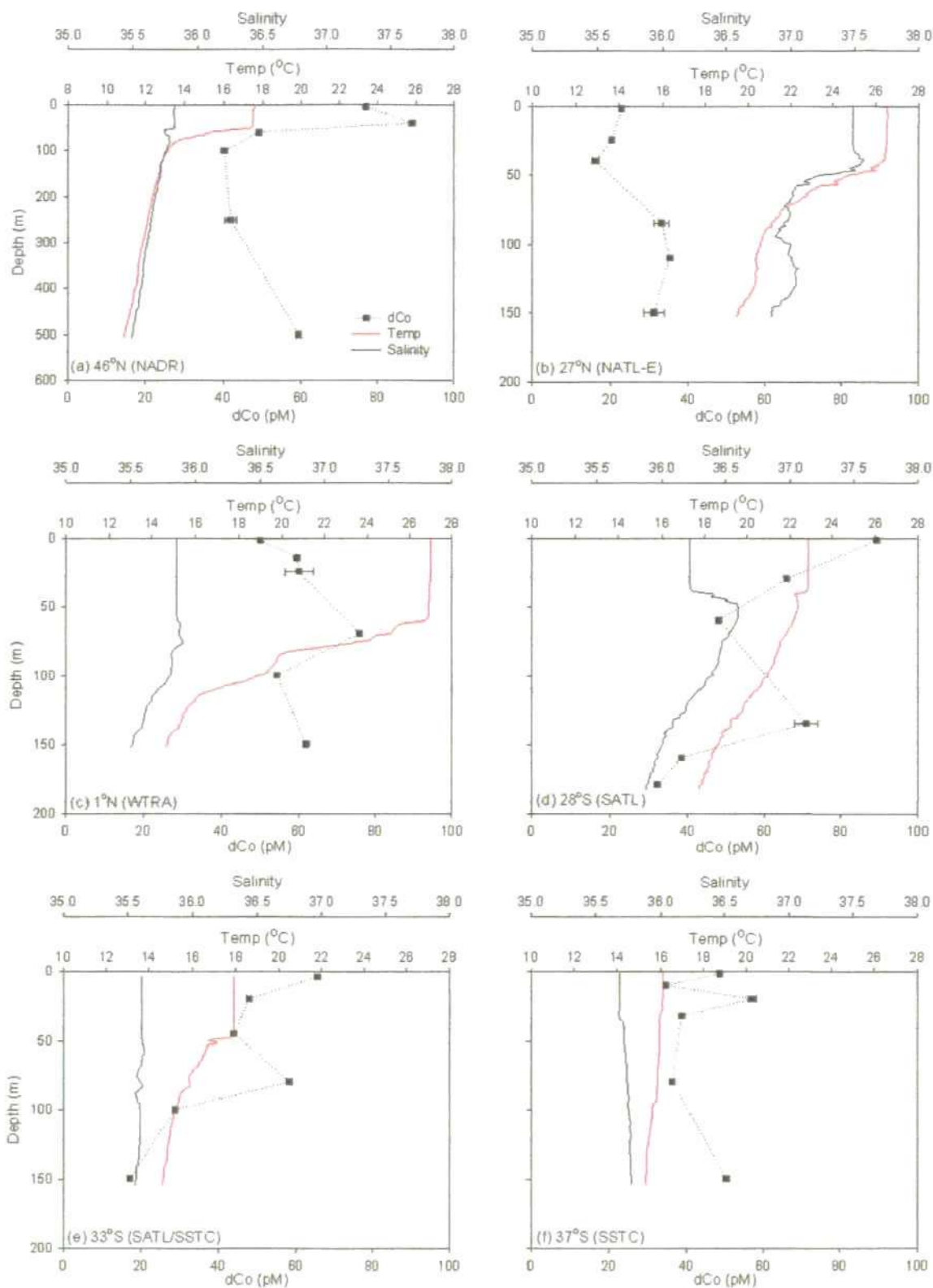


Figure 5. 5. Examples of vertical profiles of dCo, temperature and salinity from different biogeochemical provinces: (a) NADR, (b) NATL-E, (c) WTRA, (d) SATL, (e) SATL/SSTC, (f) SSTC. Note that the depth in Figure 5.5(a) differs from the other profiles.

NATL-E – During AMT-19, waters of this province were characterised by low productivity (province mean = $0.03 \text{ mg chl-a m}^{-3}$) and low dCo concentrations (province mean = $25 \pm 17 \text{ pM}$). The lowest dCo concentrations were observed in this province, forming a broad band of very low dCo $< 20 \text{ pM}$ between 10 and 50 m depth (Fig. 5.4). In this province, the area to the south of $\sim 25^\circ\text{N}$ is subject to high annual dust loadings ($0.194 \text{ Tg year}^{-1}$; Jickells *et al.*, 2005), supplied predominantly from the arid and desert regions of North Africa (Carlson and Prospero, 1972). Aerosol dust of this provenance, frequently termed *Saharan*, is a significant source of trace metals, such as Fe and Al, to surface waters of this province (Duce and Tindale, 1991). Although atmospheric dust as a source of Co to surface waters has been alluded to (e.g. Bowie *et al.*, 2002a; Knauer *et al.* 1982; Wong *et al.*, 1995), there is little direct evidence to suggest that dust deposition is the predominant input flux to the remote Atlantic Ocean. For example, despite being located close to the region of maximum dust deposition, Figure 5.5b shows that there was just 7 pM difference between surface dCo ($23 \pm 1 \text{ pM}$) and the minimum concentration at 40 m ($16 \pm 1 \text{ pM}$), which suggests that aerosol dust deposition is not a significant source of Co to this region. Indeed, the very low concentrations of dCo in this province may be a reflection of biological uptake in a region where phytoplankton community structure is dominated by *Prochlorococcus* (Poulton *et al.*, 2006; $1.5\text{--}3.7 \times 10^5 \text{ cells mL}^{-1}$ in this study) in the absence of a significant source of Co. The very strong inverse relationship between dCo and salinity ($r^2 = 0.86\text{--}0.95$) at some stations in this province, particularly those in the centre of this region ($\sim 27\text{--}29^\circ\text{N}$) suggests a continental source of Co transported along isopycnals (Fig. 5.4, bottom panel).

WTRA –This province was characterised by high dCo (> 60 pM). In common with other upwelling regimes high concentrations of dissolved Co, Fe and macronutrients have all been reported in this region (Bowie *et al.*, 2002a; Pohl *et al.*, 2010; Ussher *et al.*, in prep; Wyatt *et al.*, in prep). Although, in contrast to the macronutrients, high concentrations of dCo were observed in the mixed layer (< ~ 60 m), which either suggests that the thermocline is not such an effective barrier to vertical diffusion of dCo or, far more likely, the functional shift in phytoplankton community structure from being picoplankton-dominated (predominantly *Prochlorococcus*) to nanoplankton-dominated (predominantly eukaryotes) (this study; Poulton *et al.*, 2006; Tarran *et al.*, 2006) results in lower biological requirements for dCo in this province than in the neighbouring gyres.

The temperature plot in Figure 5.5c clearly shows colder water (< 16 °C) at shallower depths than in the neighbouring gyre regions (NATL-E and SATL). Relatively cold water is characteristic of upwelling regimes due to the vertical transport of deep water. As shown in Figure 5.3 there is a sharp gradient in macronutrient concentrations below the mixed layer, such that upwelling water is enriched with macronutrients compared with the surface. Thus, upwelling regimes tend to support high rates of primary production. Indeed, primary production is typically threefold higher in the equatorial upwelling compared with the adjacent nutrient-deplete gyres, although only moderate increases in chl-*a* and biomass are observed (Pérez *et al.*, 2006) (Fig. 5.4).

Oxygen is produced during algal respiration; conversely microbial degradation of sinking organic matter has high O₂ demands. Thus, the highest

concentrations of chl-*a* ($> 0.4 \text{ mg m}^{-3}$) did not coincide with the highest O_2 concentrations, but rather were observed in relatively low- O_2 water ($\sim 160 \text{ } \mu\text{M}$; Fig. 5.4). In this province as a whole, the SCM was positioned just above the $150 \text{ } \mu\text{M}$ O_2 horizon, biological consumption resulting in low O_2 concentrations below the SCM (Fig. 5.4, bottom panel). Where high O_2 utilisation and weak oceanic ventilation are combined they create conditions conducive to the formation of an oxygen minimum zone (OMZ). In the eastern equatorial Atlantic a broad OMZ is known to extend west from the eastern boundary at $\sim 100\text{--}900$ m depth (Karstensen *et al.*, 2008). During AMT-19, the $150 \text{ } \mu\text{M}$ oxicleine was positioned just below the base of the thermo- and haloclines (Fig. 5.5c), which separated the O_2 -rich tropical surface water from O_2 -poor Atlantic Central Water (Karstensen *et al.*, 2008).

In the eastern North Atlantic the core of the OMZ is located between the equatorial current system and the North Equatorial Current (NEC) (see Fig. 1b for surface currents), in the shadow zone (a poorly ventilated region at the equatorial edge of the North Atlantic gyre) of the eastern boundary (Stramma *et al.*, 2005). The upwelling Guinea Dome is centred between 9°N , 25°W (in northern summer) and 10.5°N , 22°W (in northern winter; Siedler *et al.*, 1992). The NEC, equatorial currents and Guinea Dome form a cyclonic (anticlockwise) gyre (Stramma and Schott, 1999), thereby providing a mechanism for the offshore transport and subsequent upwelling of O_2 -poor waters that have interacted with reducing sediments at the eastern boundary. Wallace and Bange (2004) describe an OMZ of $< 50 \text{ } \mu\text{M}$ O_2 centred at ~ 400 m depth, and a less-pronounced oxygen minimum at the base of the thermocline at $60\text{--}150$ m.

They attributed the deeper OMZ to offshore advection of O₂-poor waters that had interacted with reducing sediments at the continental margin, whereas the shallower, weaker OMZ was attributed to enhanced remineralisation in a region with a shallow mixed layer (~ 60 m during *AMT-19*) and high biological productivity. This is consistent with the high concentrations of nitrate (8–27 μM), phosphate (0.7–1.8 μM) and dCo (64 ± 12 pM) that were observed in conjunction with O₂-poor (≤ 150 μM) sub-surface waters in this province, and with the arguments that particulate Co remineralisation is extremely efficient in the euphotic zone (Noble *et al.*, 2008), thus representing a significant flux of dCo to surface waters in this region.

Release of trace metals during biological consumption results in high dCo (this study; Pohl *et al.*, 2010) and high dFe (Measures *et al.*, 2008; Ussher *et al.*, in prep; Wyatt *et al.* in prep.) concentrations in this upwelling region. In a study near the Hawaiian Islands, Noble *et al.* (2008) noted that Co export was very low, hypothesising that Co was very efficiently recycled within the water column. During microbial degradation, dCo is released from sinking particulate matter at a depth coincident with nearly complete particulate organic carbon (POC) remineralisation and is subsequently resupplied to the euphotic zone via upwelling (Noble *et al.* 2008). This is consistent with the dCo budgets calculated by Bown *et al.* (2011), who found that in order to close their budgets it was necessary to include a significant flux of remineralised Co. This tight euphotic zone recycling of Co is analogous to the so-called microbial ferrous wheel described for Fe by Kirchman (1996), where heterotrophic bacteria, the first component of the microbial loop account for a large fraction of the

mineralisation of sinking POC, live on the dissolved organic matter released by many processes in the water column.

During this study, one station was sampled in the ITCZ (11.5°N, 32.6°W; Fig. 5.6), which is located within the WTRA province, just to the north of the centre of the upwelling Guinea Dome). At this station, dCo concentrations in water \leq 10 m were low (20 ± 5 pM) increasing to 59 ± 2 pM by 100 m depth. The increase in dCo concentrations occurred at depths deeper than the mixed layer (~ 40 m) coincident with decreases in temperature and dissolved O_2 , suggesting a source of dCo in upwelling waters. In addition, the low concentrations of dCo in surface waters most likely reflects the high cellular demand for Co of the phytoplankton assemblage at this station compared to other stations in this province. Although, upwelled waters are reportedly dominated by eukaryotic nanoplankton (Poulton *et al.*, 2006; Tarran *et al.*, 2006) the abundance of *Prochlorococcus* (a genera with a absolute cellular Co requirement) was approximately threefold greater at this station than at the next station south (3×10^5 cells mL^{-1} versus 1×10^5 cells mL^{-1} respectively), despite comparable chl-*a* (0.03 ± 0.01 mg m^{-3}) at the two stations.

A key feature of the temperature and salinity plot (Fig. 5.6) at this station was the low salinity surface water (due to the high annual rainfall of the region, up to 2000 mm y^{-1} ; Tchernia, 1980) (Figs. 5.2 and 5.6). Below the surface mixed layer there was a steep salinity gradient, with salinity increasing to 36.3; a value much closer to sub-surface NATL-E waters (e.g. Fig. 5.5a). Below ~ 35 m salinity rapidly decreased again, and this decrease was coincident with a sharp

decrease in temperature and dissolved O₂ concentrations, indicating the incursion of water from below. As in the rest of the province, the chl-a maximum was positioned just below the base of the thermo- and haloclines at ~ 60 m in low-O₂ water (~ 160 μM), but nitrate- and phosphate-replete waters (19.4 μM and 1.2 μM respectively). At this depth, the N/P ratio was 16.5 and close to the Redfield stoichiometry. Analysis of primary production rates in this region suggests that light is the limiting factor, rather than N or P (Poulton *et al.*, 2006), due to remineralisation of organic N and P in the tropical upwelling regions of the Atlantic (Mahaffey *et al.*, 2003).

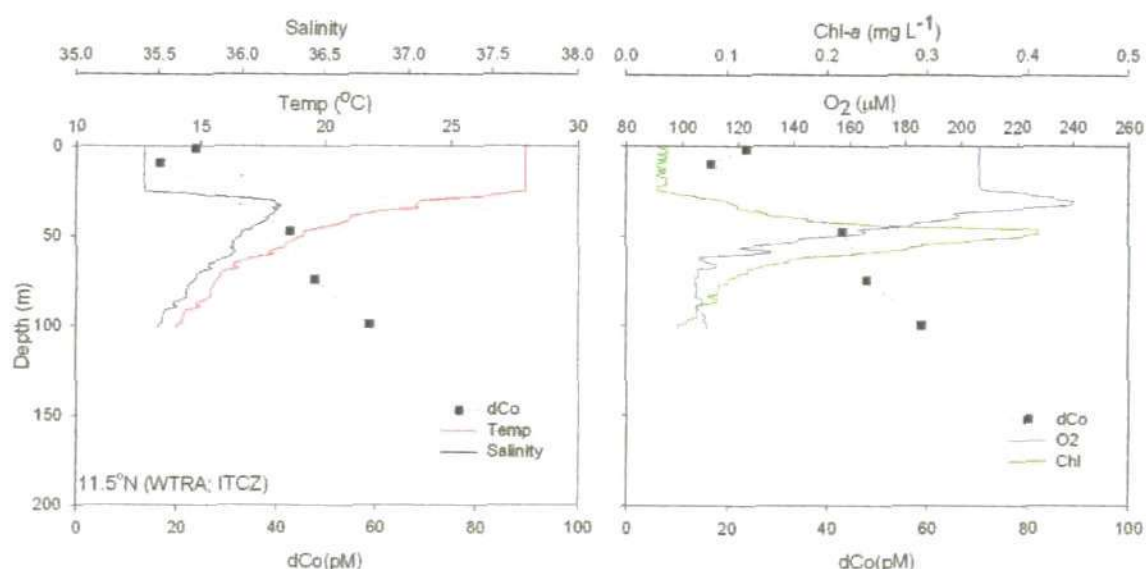


Figure 5. 6. Dissolved Co, salinity and temperature (left), and dCo, chl-a and O₂ (right) in the ITCZ (11.5°N, 32.5°W) during AMT-19 (sampled on 03/11/09).

There are very few rainwater data sets that report Co concentrations (Church *et al.*, in prep; Helmers and Screms, 1995), and this lack of field data hampers estimates of the contribution of wet deposition to the total depositional flux of aerosol Co. This contribution is an important consideration given the relatively

low pH in rainwater, and strong pH dependency of metal solubility, means that wet deposition may be as, or more important, in delivering certain trace metals to surface waters (Baker *et al.*, 2007; Helmers and Schrems, 1995; Jickells, 1999). Recent work has shown that wet deposition is indeed an important flux, at least in regions of high rainfall, such as the ITCZ. In the Bermuda region, where annual rainfall is similarly high ($\sim 1400 \text{ mm y}^{-1}$), wet deposition accounts for $\sim 85\%$ of the annual atmospheric deposition flux of Co (Church *et al.*, in prep.; Shelley *et al.*, submitted). This is in marked contrast to the atmospheric Fe flux, where only $\sim 30\%$ is delivered via wet deposition (Sholkovitz *et al.*, 2009). Due to the infrequency of rain events while at sea, underway sampling of rainwater is always done on an *ad hoc* basis. Therefore, studies in the high-rainfall ITCZ represent an opportunity to investigate the importance of wet deposition as a source of Co to surface waters. To date however, the few studies that have sampled the ITCZ have produced contrasting findings with both elevated (Bowie *et al.*, 2002a; Helmers and Schrems, 1995) and lower (Pohl *et al.*, 2010; Saito and Moffett, 2002) concentrations of dCo reported.

At the ITCZ station, the relationship of dCo with salinity was weakly positive ($r^2 = 0.4$, $n = 5$), which does not point to wet deposition as an important source of Co. However, given that rainfall in the ITCZ is concentrated between June and August (Duce *et al.* 1991), the contrasting results reported for dCo in this region (this study; Bowie *et al.*, 2002a (TdCo); Helmers and Schrems, 1995; Pohl *et al.*, 2010; Saito and Moffett, 2002) may reflect the timing of sample collection. The cruises that sampled the ITCZ in northern winter (this study; Pohl *et al.*, 2010; Saito and Moffett, 2002;) found lower or similar dCo concentrations

compared to adjacent waters, whereas those that sampled in the autumn (*i.e.* close to the maximum period of rainfall) and immediately after a rain event (Bowie *et al.*, 2002a) or sampled rainwater directly (Helmert and Schrems, 1995) found higher dCo concentrations in this region. This suggests that the timing of sample collection is critical. In winter and spring biological removal exceeds vertical diffusive-advective supply, whereas in summer and autumn wet deposition is an important additional source of Co to surface waters of the ITCZ. Better resolution of dCo distributions and continued rainwater sampling efforts in this region would help to resolve seasonal cycles in Co supply.

While lateral advection of continental Co from eastern boundaries is an important source of dCo in the Atlantic (Noble *et al.*, submitted), in the equatorial region (WRTA) surface concentrations of dCo also have a strong vertical advective component (*i.e.* upwelling) which determines water column distributions (Pohl *et al.*, 2010). The relatively low surface dCo (24 ± 1 pM) reported in the ITCZ during AMT-19 may not be a dilution effect, rather it may reflect variable rates of evaporation, the relative dominance of advective vertical supply or wet deposition, and differences in the intensity of biological drawdown at the different stations due to patchy algal distributions.

SATL – The higher dCo concentrations of the SATL parallel the higher concentrations of phosphorus observed in the South Atlantic gyre compared with the North (Mather *et al.*, 2008), but contrasts with the lower dFe of the SATL (< 0.2 nM compared with > 0.3 nM at similar latitudes in the NATL-E, Ussher *et al.*, in prep.; Wyatt *et al.*, in prep.). Given these low dFe

concentrations and that the South Atlantic receives an order of magnitude less dust annually than the North (Jickells *et al.*, 2005), the twofold higher concentrations of dCo observed in the southern gyre (SATL) are unlikely to result from dust deposition. As precipitation is also low (and evaporation high) in the gyres (the highest salinities in the Atlantic Ocean were observed in the two subtropical gyres; Fig. 5.2), it is unlikely that wet deposition is the dominant input either. Removal in the mixed layer was more intense than in the NATL-E, reducing dCo to less than 50% of surface concentrations (Figs. 5.4 and 5.5d). In comparison, removal in the northern gyre (NATL-E) resulted in little variability in dCo concentrations within the mixed layer (e.g. Figs. 5.4 and 5.5b, 20 ± 3 pM) despite comparable chl-a in the two provinces (0.03 and 0.04 mg chl-a m⁻³ in the NATL-E and SATL respectively). The difference in the intensity of drawdown likely reflects differences in phytoplankton community structure in the two provinces and/or differences in macro- and micronutrient availability combined with the absence of a significant flux of dCo to the NATL-E.

During AMT-19, high dCo concentrations were not confined to the O₂ deficient waters below the SCM, and extended further south than the extent of 150 µM O₂ horizon. The tongue of high dCo (71–80 pM) observed to the south of the upwelling region (WTRA) was not associated with low O₂ water, rather it coincided with the chl-a maximum (0.1–0.15 mg m⁻³ at 120–140 m depth) and notably the maximum of the numerically dominant genus *Prochlorococcus* (2.1×10^5 cells mL⁻¹). Given the high abundance of *Prochlorococcus* at this depth and their absolute cellular requirement for Co (Sunda and Huntsman, 1995a), which was found to inversely correlate with water column dCo in the Sargasso Sea (western NATL, Shelley *et al.*, submitted), this observation was

unexpected. To some extent transport along isopycnals (Fig. 5.4, top panel), via the South Equatorial Current (Fig. 5.1) (Noble *et al.*, submitted) provides a mechanism whereby high dCo WTRA water is laterally advected in a southerly direction, but there was only partial agreement between the position of the 'tongue' of high dCo and isopycnal horizons, suggesting that there are other processes interacting with lateral advective processes to account for the observed dCo distribution.

If microbially-mediated remineralisation is so efficient that particulate Co export is very low (Noble *et al.*, 2008), it is plausible that high dCo concentrations may be sustained concurrent with high algal abundance. Indeed, biological consumption of sinking POC results in release of trace metals, such as Co. Furthermore, there is strong evidence for the *in situ* biological production of Co-binding ligands (Saito *et al.*, 2002; 2005), and that the resulting complexes are highly stable Co(III) chelates, which stabilise Co in excess of its solubility in seawater and provide a stable, bioavailable form of Co to the prokaryotic phytoplankton that dominate the biomass in this province (Saito *et al.*, 2005). This, therefore, suggests that biological controls (*e.g.* internal recycling) combined with physical (advective vertical and lateral transport) processes may be more important than the chemical environment in mediating water column dCo distributions in the SATL.

SATL/SSTC boundary – At approximately 28° S the SATL is sub-divided into two cells separated by the subtropical countercurrent. To the south of this front (25–30° S) the Brazil Current (BC), a western boundary current which

transports water along the continental shelf, forms the southern extent of a recirculation cell (Mémery *et al.*, 2000 and references therein). The high surface dCo in this region (89 ± 4 pM at 28.8°S , 26.1°W) is attributed to offshore advection of continental Co. Slemons *et al.* (2010) demonstrated that the lower Equatorial Undercurrent was a significant source of dFe, mobilised in a highly active western boundary current region, to surface waters of the eastern equatorial Pacific. As the Atlantic coast of South America is also a western boundary region, it is plausible that a similar mechanism exists for an eastwards flux of continental Co. Indeed, Bown *et al.* (2011) report evidence of just such a mechanism in the Atlantic Ocean, noting high dCo in the eastward flowing jet of the Antarctic Circumpolar Current, north of the polar front, in waters that had previously interacted with the South American continental slope.

South of the subtropical front at $\sim 28^\circ\text{S}$, at the confluence of the Brazil and the Falkland (Malvinas) Currents, there is another dynamic frontal region with relatively high surface dCo (66 ± 1 pM; Fig. 5.5e). Falkland Current waters have been noted to be enriched in dCo relative to the more saline waters of the Brazil Current, (Bowie *et al.*, 2002a), likely due to a combination of the higher rates of production, and therefore biological uptake, in the Brazil Current and interaction with shelf sediments by the Falkland Current. Both currents flow along the continental shelf until they meet and are deflected offshore. Given that only $\sim 3\%$ of fluvial Co is estimated to be retained within river systems (Sholkovitz and Copland, 1981), it is plausible that the northward flowing Falkland current entrains and transports fluvial Co offshore, resulting in elevated surface concentrations in this region. Furthermore, a combination of the anticyclonic

circulation of the gyre and a strongly stratified water column suppresses upwelling of deep waters. Thus, lateral transport may be the dominant source of (micro-) nutrients to this region.

SSTC – Despite this province being described as dynamic by Longhurst (1998), the upper water column during *AMT-19* was well mixed, although there was structure to the dCo profile, with concentrations ranging from 35–57 pM. In this temperate province the highest chl-*a* concentrations ($> 0.3 \text{ mg m}^{-3}$) were much shallower ($< 50 \text{ m}$, extending all the way to the surface) than in the SATL ($> 100 \text{ m}$). With the exception of *Prochlorococcus* (less in the SSTC than SATL) and coccolithophores (similar abundance), which both have specific cellular Co requirements (Sunda and Huntsman, 1995a), all other quantified components of the phytoplankton assemblage (Cryptophyceae, *Synechococcus*, nano- and pico-eukaryotes) were present in significantly greater abundances (1–2 orders of magnitude) in this province than in the gyre (SATL) to the north (G. Tarran, pers. comm.). If, as proposed by Saito and Moffett (2002) and Bown *et al.* (2011), biological removal is the most significant dCo sink in the open ocean, then this shift in the phytoplankton assemblage could account for the shallower (10 m) dCo-minimum depth compared with stations further north, but if the algal assemblage is not dominated by species with high cellular Co demands then biological removal will be less important than in tropical and subtropical provinces.

5.3.4. Chemical speciation of cobalt

In order to determine the operationally-defined total dissolved Co (dCo, here defined as the fraction $< 0.2 \mu\text{m}$) in seawater samples, the Co bound to strong organic complexes ($K_S \geq 10^{15.7}$) must be liberated. This is achieved by UV-irradiating samples prior to determination of dCo, without incorporation of this step dissolved labile Co will be determined. While a number of laboratories have been aware of this requirement for some time (e.g. Donat and Bruland, 1988; Saito and Moffett, 2001; Vega and van den Berg, 1997), the recent SAFe/GEOTRACES intercalibration exercise has highlighted the discrepancy between dCo concentrations determined in samples that have been UV-irradiated, and those that have not (<http://es.ucsc.edu/~kbruland/Geotraces> SaFe/kwbGeotraces; Milne *et al.*, 2010; Shelley *et al.*, 2010).

Dissolved Co concentrations are presented in Figure 5.7 from UV-treated surface seawater ($< 10 \text{ m}$) samples from two separate cruises, *AMT-19* (this study) and *AMT-3* (Bowie *et al.* 2002a). These two cruises approximately covered the same gyre-centred, meridional transect. Data is presented as the average concentration of dissolved Co (+ 1s) in each province. The only difference in sample preparation was that dissolved Co was determined in unfiltered samples from *AMT-3* (samples from both cruises were acidified to $\sim \text{pH } 1.7$ with triple distilled HCl). As the samples from *AMT-3* were not filtered, the reported data includes Co that was loosely bound to any particulate matter in the samples, which would have been liberated following acidification to $\sim \text{pH } 1.7$. Thus, Bowie *et al.* (2002a) report the concentration of total dissolvable Co (TdCo) in samples from *AMT-3*. Although different analytical techniques were used for determination of dissolved Co (*AMT-19* = flow injection with

chemiluminescence detection; Shelley *et al.* 2010 and AMT-3 = adsorptive cathodic stripping voltammetry; Vega and van den Berg, 1997), the results can be compared because both techniques included a UV-irradiation step prior to determination of either dCo or TdCo.

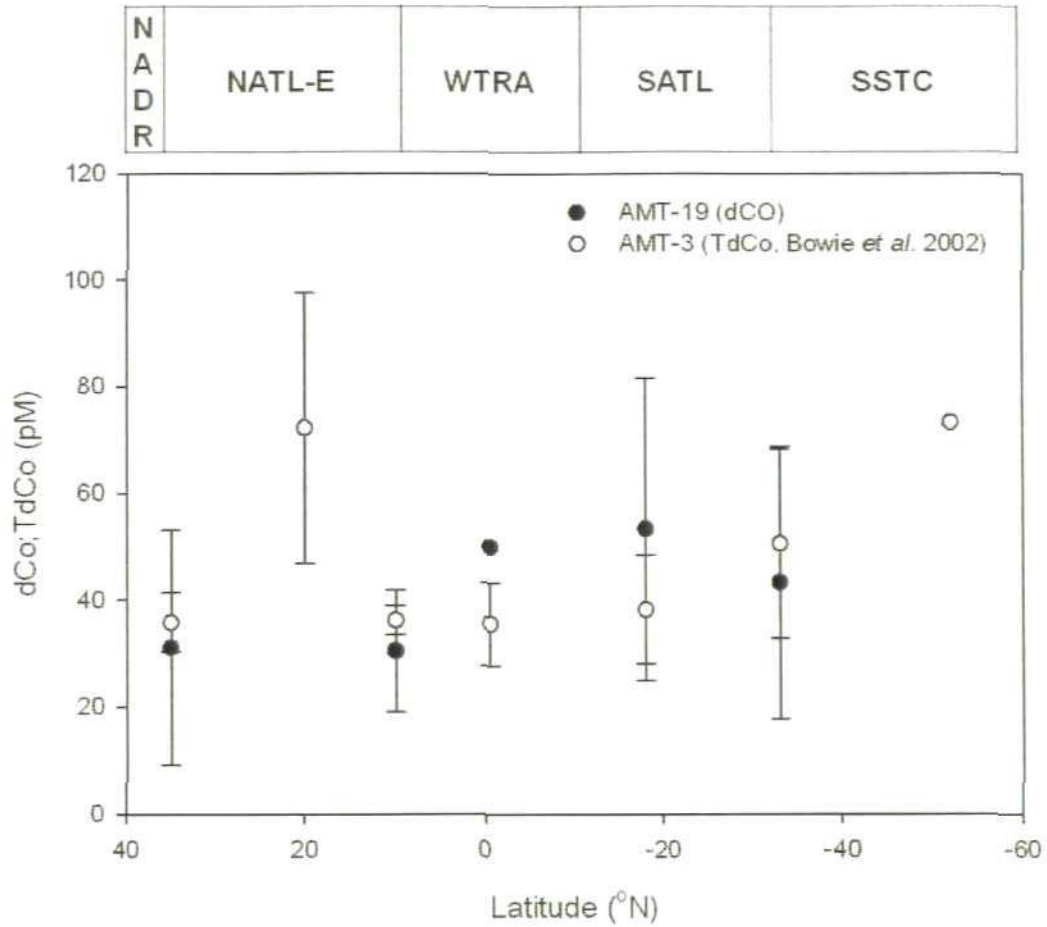


Figure 5. 7. Averaged concentrations of dCo (AMT-19, closed circles) and TdCo (AMT-3, open circles; Bowie *et al.*, 2002a) in surface waters (< 10 m) at similar latitudes in the Atlantic Ocean =, where the error bars represent 1s of the average concentration in each biogeochemical province.

The average concentration of dCo and TdCo in each biogeochemical province varied by < 15 pM between the two AMT cruises. The degree of consistency

observed between the average concentrations of dCo and TdCo in each province suggests that loosely-bound, particle-associated (labile) Co contributes little to sea-surface dissolved Co concentrations in the open Atlantic Ocean. Had appreciable amounts of labile particulate Co been present in samples from *AMT-3*, it would be reasonable to assume significantly higher concentrations of TdCo would have been observed as is the case for TdFe compared to dFe (Pohl *et al.*, 2010). The only other study that has directly compared dCo and TdCo concentrations was unable to UV-irradiate samples prior to analysis (Pohl *et al.*, 2010), although it was found that concentrations of TdCo were not consistently higher than dCo (with the exception of waters south of $\sim 12^{\circ}\text{S}$ in the Angola-Benguela frontal region and Benguela Current which were not sampled during *AMT-19* or *3*), which is consistent with the agreement between dCo and TdCo concentrations shown in Figure 5.7. The extremely low concentrations of dissolved Co compared to other bioactive trace metals, such as Fe, means that even relatively small inputs can have a large effect on water column concentrations. During *AMT-19* the highest concentrations of dCo were observed coincident with the highest density of particulate organic matter (POM) (*i.e.* the productive waters of the WRTA) suggests that sinking POM provides an important flux of labile Co, consistent with observations of Saito *et al.* (2004) and Noble *et al.* (2008)

5.3.5. Controls on dCo distribution in the Atlantic Ocean: a summary

5.3.5.1. Atmospheric inputs

Dust-laden air masses, having passed over the arid regions of NW Africa, emerge in the form of large-scale (atmospheric) cyclonic eddies which

propagate westwards across the tropical Atlantic Ocean above the trade wind moist layer (principally at a height of 1500–5000 m). As the air in the Saharan air layer traverses the Atlantic, particles are continuously deposited to the surface ocean (Carlson and Prospero, 1972). Thus, deposition of aerosol dust is a significant source of trace metals to the Atlantic Ocean. For Fe, aerosol dust deposition is thought to be the predominant source to oceanic surface waters (Duce and Tindale, 1991). However, no-one to date has been able to demonstrate a similar relationship between Co and dust supply. At present there is little evidence to suggest that atmospheric dry deposition is a significant source of Co to surface waters. However, as aerosol Co is significantly more soluble than aerosol Fe (Shelley *et al.*, submitted; Chapter 3), atmospheric supply may still play a critical role in controlling surface distributions of dCo.

5.3.5.2. Upwelling and advective transport

The equatorial upwelling supplies macro- and micronutrient (including dCo)-enriched water which sustained high algal biomass (up to 0.55 mg m⁻³ during AMT-19), which results in high levels of sinking detritus. It appears that the recycling of Co from sinking particles in the mixed layer is extremely efficient, quite possibly dominating input fluxes (Bown *et al.*, 2011; Noble *et al.*, 2008). Co (and Fe) is released from sinking particles during biological consumption, and is retained in solution due to the low concentrations of dissolved O₂ present and/or the *in situ* production of Co-binding ligands in this region. Both high dCo and dFe have previously been reported in the O₂-depleted waters of this region (Bowie *et al.* 2002a; Measures *et al.* 2008; Pohl *et al.* 2010). During AMT-19 this was also the case, with high dCo (> 60 pM, Fig. 4) and dFe (Wyatt *et al.*, in

prep.) concentrations broadly corresponding with the region of low O₂ water. The identification of a second shallower OMZ, just below the SCM, combined with previous observations of low concentrations of dissolved Mn (dMn) in the O₂-poor upwelling tropical Atlantic Ocean (Statham *et al.*, 1998) suggests that the high concentrations of dCo observed in this region result from release from sinking particles, rather than being supplied primarily by upwelling of waters that have been in contact with reducing sediments, although lateral advection is likely to represent an additional source of Co. If Mn precipitates preferentially, which is certainly plausible given that Co and Mn cycling is decoupled in oceanic waters (Saito and Moffett, 2002), this would account for the high dCo concentrations observed in low O₂ waters without concomitantly high dMn.

5.3.5.3. Biological processes affecting vertical dCo distributions

As Co is an essential nutritional requirement for many marine algae and bacteria (*e.g.* Morel *et al.*, 1994; Saito *et al.*, 2002; Sunda and Huntsman, 1995a; Timmermans *et al.*, 2001), biological uptake is an important removal mechanism in the euphotic zone (Bown *et al.*, 2011; Ellwood *et al.*, 2005; Ellwood and van den Berg, 2001; Noble *et al.*, 2008; Saito and Moffett, 2002; Saito *et al.*, 2004, 2005). Key prokaryotic phytoplankton genera, such as the *Prochlorococcus*, have an absolute cellular requirement for Co, being unable to substitute other trace metals (Cd, Zn) in essential metalloenzymes (Sunda and Huntsman, 1995a). Additionally, the majority of eukaryotic phytoplankton have a vitamin B₁₂ requirement (Droop, 1974, 2007); those that are unable to synthesize this Co-containing vitamin *de novo* must either extract it from their environment or have a metabolism that does not require this vitamin (Bertrand *et al.*, 2007).

Investigations into phytoplankton community structure during the *AMT* programme have revealed that throughout the surface mixed layer of the subtropical gyres *Prochlorococcus* dominates. *Synechococcus* (also a genus with an absolute requirement for Co; Sunda and Huntsman, 1995a) and picoeukaryotes only make significant contributions to picophytoplankton populations where the nitricline shallows (Tarran *et al.*, 2006). In addition to biologically-dominated removal processes, biological-mediated recycling in the mixed layer was an important source of dCo in the euphotic zone in this study.

Saito *et al.* (2005, 2008) have demonstrated Fe-Co co-limitation in tropical regions. During *AMT-19* the low dCo concentrations observed in the surface mixed layer of the NATL-E (21 ± 8 pM) could have conceivably (co-)limited growth for at least some key components of the assemblage (e.g. *Prochlorococcus*). For example, Saito and Moffett (2002) estimated that a population of 10^5 cells mL⁻¹ of *Prochlorococcus* would incorporate $0.3 \text{ pM L}^{-1} \text{ d}^{-1}$ of dCo into new cells, accounting for a significant proportion of the upper water column dCo inventory (20 ± 10 pM) in their study area (Sargasso Sea, western NATL). Given that *Prochlorococcus* abundance was of a similar magnitude, if not greater, during *AMT-19* (*Prochlorococcus* abundance during *AMT-19* was 10^5 – 10^6 cells mL⁻¹) and surface dCo was also similar, (co-)limitation by Co could have accounted for the relatively weak drawdown of dCo in the NATL-E compared to the SATL, which had concentrations of dCo approximately double that of the NATL-E (~ 20 and ~ 40 pM respectively), due to the lack of an obvious source of dCo to the remote NATL-E.

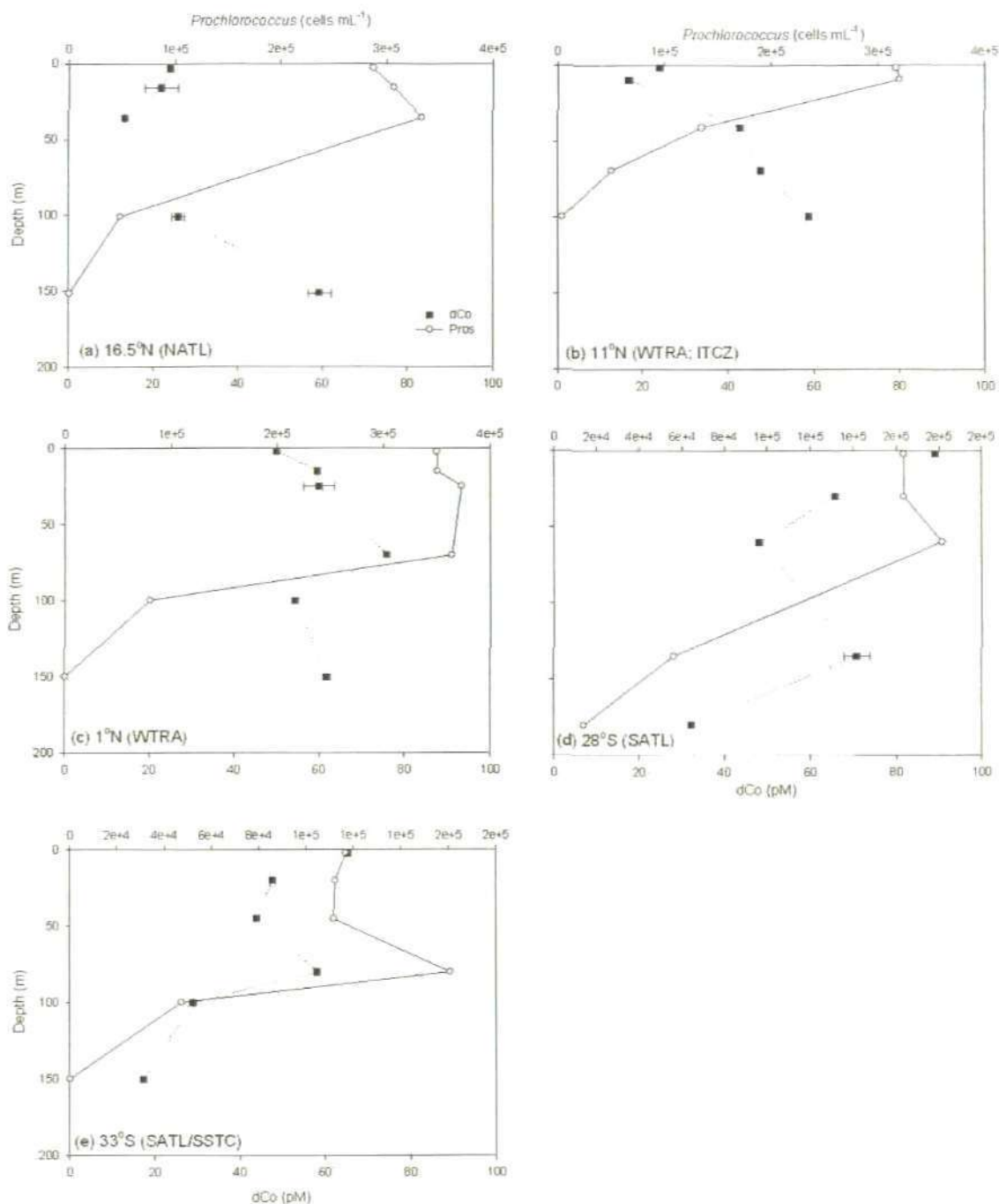


Figure 5. 8. Dissolved Co (pM, black squares) versus *Prochlorococcus* abundance (cells mL⁻¹, white circles) at (a) 16.5°N, NATL, (b) 11°N, WTRA, (c) 1° N, WTRA/ITCZ, (d) 28° S, SATL and (e) 33°S, SATL/SSTC. Note the lower abundance of *Prochlorococcus* in the southern hemisphere results in different scales for (d) and (e) compared to (a)-(c).

Dissolved Co depletion coincident with the *Prochlorococcus* maximum:

Drawdown of dCo in the gyres during AMT-19, and evidence for the dominance of biotic over abiotic removal mechanisms in the open ocean, points to the dominance of biological removal processes in the euphotic zone (Moffett and Ho, 1986). *Prochlorococcus*, a ubiquitous genus in tropical and sub-tropical oceans, dominates the biomass of the NATL-E and SATL (Poulton *et al.* 2006). It thrives in the oligotrophic conditions of the gyres, but has an absolute cellular requirement for Co that cannot be met through substitution with other trace metals (Sunda and Huntsman, 1995a). In euphotic waters of the gyres (NATL-E and SATL, Figs. 5.8a and 5.8d) and the ITCZ (Fig. 5.8b), *Prochlorococcus* abundance and dCo are inversely correlated (e.g. Fig. 5.8a correlation coefficient = -0.80; Fig. 5.8b correlation coefficient = -0.98). For example, in the ITCZ (Fig. 5.8b) the maximum abundance of *Prochlorococcus* (4.6×10^5 cells mL⁻¹ at 29 m) was located in nutrient-depleted surface waters (both nitrate and phosphate concentrations were below detection limits (< 0.01 μ M) shallower than 40 m), and was associated with the lowest dCo (17 ± 0.5 pM). The inverse relationship between *Prochlorococcus*, and dCo suggests that dCo availability has the potential to influence algal community structure, or vice versa, in these regions. While (co-)limitation has been demonstrated at the SCM of another upwelling regime (Saito *et al.* 2004), a question remains as to the potential for Co limitation in the ITCZ region of the equatorial upwelling, which has been shown to be light-limited (Poulton *et al.* 2006).

Dissolved Co repletion at the *Prochlorococcus* maximum: In other regions of the Atlantic Ocean maximum abundances of *Prochlorococcus* were observed

concurrent with maximum concentrations of dCo. In the equatorial upwelling (but not the ITCZ) continual supply of Co and macronutrient enriched waters from below sustains high algal biomass (e.g. Fig. 5.8c). High dCo and *Prochlorococcus* abundance was also observed in the SATL/SSTC frontal region (Fig. 5.8e). In this instance, continental Co appears to have been advected far offshore in the Falkland Current at concentrations high enough to support maximum abundances of 2×10^5 cells mL⁻¹.

Co-limitation in gyres? It seems unlikely that Co would be the only limiting nutrient in these oligotrophic regimes. In addition, the high cellular demand for Fe of diazotrophs (Kustka *et al.*, 2003), which favour the nutrient-poor waters of the oligotrophic gyres, suggests that other trace metals (in particular Fe) will become depleted faster than Co. However, at the low concentrations reported in the upper water column at some stations during this study, in particular stations in the NATL-E province where mixed layer (≤ 45 m) dCo was extremely low (19 ± 8 pM), it is plausible that *Prochlorococcus* may experience Fe-Co co-limitation. Such limitation may be more chronic in the south than the north due to the significantly lower inputs of aerosol dust deposited to the southern hemisphere (Jickells *et al.*, 2005), which results in considerably less dFe in the water column than at similar latitudes in the North Atlantic gyre.

5.4. Conclusions

In conclusion, this study has demonstrated that different processes dominate Co supply in the different biogeochemical provinces of the Atlantic Ocean. However, similar processes dominate at similar latitudes in both the North and

South Atlantic. In the temperate NADR and SSTC physical processes (advection of continental Co) dominate, whereas in the oligotrophic gyres, while there is evidence of a physical Co supply processes, biological removal and recycling are important controls on dCo distributions. Finally, in the equatorial upwelling (WTRA), no one control dominates; the chemical environment, especially dissolved O₂ concentration, combines with extremely efficient biologically-mediated recycling and a strong vertical (and lateral) advective flux to exert a profound influence on dCo distributions. In contrast to aerosol Fe supply, the atmospheric supply of Co is dominated (~ 85%) by the wet deposition flux, the relative importance of which appears to vary on a seasonal basis. This data highlights that atmospheric dry deposition does not have the same impact on upper water column distributions of dCo in the same way that it does for dFe and dAl. While the biogeochemical cycling of dCo and dFe is clearly linked, due to their respective bioactive roles, it is becoming clear that the biogeochemistry of Co in the open ocean is quite distinct from that of Fe. This is an important consideration for future biogeochemical models that incorporate these two trace metals.

Chapter 6

Conclusions and Future Work

6.1. Introduction

As approximately 50% of global photosynthesis occurs in marine environments (Falkowski, 1994; Field *et al.*, 1998), understanding the processes that mediate phytoplankton growth is fundamental to our knowledge of carbon cycling. The availability of dissolved inorganic carbon, major nutrients (N, P and Si), and trace elements (*e.g.* Co, Cu, Fe, Zn) are key factors in determining growth rates in marine phytoplankton (*e.g.* Morel and Price, 2003). While it is widely accepted that low Fe concentrations limit primary production in the major high nutrient, low chlorophyll (HNLC) regions and regulates phytoplankton growth in a number of other oceanic settings (*e.g.* Coale *et al.*, 1996; Boyd *et al.*, 2000 de Baar *et al.*, 2005; Boyd and Ellwood, 2010), there is increasing evidence to suggest that other trace elements such as Co, Cu and Zn also play an important role in regulating marine primary production (*e.g.* Morel and Price, 2003; Saito *et al.*, 2008).

Cobalt is an important micronutrient for marine phytoplankton as it forms the metal centre of the vitamin B₁₂ complex and is a co-factor in the enzyme, carbonic anhydrase, which is required for inorganic carbon acquisition (Provasoli and Carlucci, 1974; Lane and Morel, 2000). The nutritive role of Co is indicated by a correlation with phosphate in the upper water column across diverse oceanic regimes (Bown *et al.*, 2011; Noble *et al.*, 2008; Saito and Moffett, 2002; Saito *et al.*, 2010). The main focus of this study was the biogeochemical cycling of dCo in the Atlantic Ocean. Given that key prokaryotic phytoplankton genera (*e.g.* *Prochlorochoccus*, *Synechococcus*) have an absolute cellular requirement for Co (Sunda and Huntsman, 1995a), and that the vitamin B₁₂ requirements of eukaryotic phytoplankton must be met through uptake of this vitamin from seawater (Provasoli and Carlucci, 1974), it is

important to attain high quality data to characterise the distribution and behaviour of dCo across diverse oceanic regimes. The low concentrations of trace metals in the open Atlantic Ocean (e.g. dCo ~ 10–110 pM, Chapter 5; dFe ~ 0.3–1.5 nM, Chapter 4) requires the use of sensitive analytical techniques. In this study, a flow injection technique using chemiluminescence detection (FI-CL) was developed for the determination of picomolar concentrations of dissolved cobalt (dCo) in seawater (Shelley *et al.*, 2010). Seawater samples from three cruises to different regions of the Atlantic Ocean were analysed to examine the biogeochemical cycling of Co. *FeAST-6* was a small-scale study located in the Sargasso Sea in the western North Atlantic gyre, *INSPIRE* was also a small-scale study, this time located in the eastern North Atlantic gyre, whereas, *AMT-19* was a large-scale meridional transect from ~ 50°N - 50°S. In addition to the determination of dCo in the seawater samples, dFe and dCu was determined in samples from the *INSPIRE* cruise.

6.2. Development of analytical techniques for the determination of dissolved Co, Cu, Fe and Zn in seawater

The FI-CL method developed during this study for the determination of dCo in seawater (Shelley *et al.*, 2010) was found to be more sensitive than earlier FI-CL techniques (Sakamoto-Arnold and Johnson, 1987; Cannizzaro *et al.* 2000). A limit of detection of 4.5 pM was determined in laboratory experiments (Chapter 2), and excellent agreement with the SAFe and GEOTRACES consensus reference seawater samples was observed (SAFe D2 ($n = 9$) this study 40.9 ± 2.6 pM, consensus value 43 ± 3.2 pM ; GD ($n = 9$) this study 73 ± 3 pM, consensus value 68 ± 13 pM). The relative simplicity, low risk of contamination and portability make this method well suited for use in the

laboratory and for shipboard analyses. Both the dCo and dFe FI-CL techniques developed during this study are ideal methods for use at sea, thus enabling high-resolution, near real-time mapping of spatial and temporal trends in oceanic dCo and dFe distributions. The advantage of this FI-CL method over other techniques that can also be used to determine dCo and dFe whilst at sea, such as CSV, is that FI methods are generally less time-consuming.

Development of the dCo FI-CL technique conclusively demonstrated the absolute requirement for UV-irradiation in order to liberate organically complexed Co in acidified samples prior to determination of dCo using FI-CL (Shelley *et al.*, 2010). Previous FI-CL methods (and other analytical techniques) that have not included this step may only have determined dissolved labile Co (as defined by Noble *et al.*, 2008) rather than the operationally defined total dissolved cobalt (dCo). The use of the commercially available resin, Toyopearl AF-Chelate-650M, improved the reproducibility of the method and simplified the preparation of the analytical system. The introduction of a resin-conditioning step (acidified ammonium acetate rinse) also led to increased sensitivity.

Future work: The implementation of an automated sample selection valve would increase the sample throughput and further automate the system. The use of a commercially available column (*e.g.* Global FIA columns) may further improve the reliability and reproducibility of the separation/preconcentration step by minimising leakage and contamination. Such columns have successfully been used in other FI applications (*e.g.* Aguilas-Islas *et al.*, 2006; Lohan *et al.*, 2006), and would likely be suitable for application in this method. Due to the spread in

the dCo data submitted to the GEOTRACES Intercalibration Committee, more research needs to be performed to evaluate the intensity and duration of the UV pre-treatment required to release all the Co for the various analytical methods. Even with the slight caveat attached to the SAFe/GEOTRACES reference seawater samples for dCo, it is strongly recommended that future determination of dissolved Co, Cu, Fe and Zn (as well as other trace metals) in open ocean samples analyse SAFe and/or GEOTRACES seawater reference samples as a check for analytical accuracy and precision. The consensus values of the SAFe and GEOTRACES reference seawater samples are available at:

www.geotraces.org/Inter_calibration.html#standards_certifiedrefs and

<http://es.ucsc.edu/~kbruland/GeotracesSaFe/kwbGeotracesSaFe.html>.

In addition to dCo determination by FI-CL, dissolved Cu (dCu) was determined in seawater samples using an ICP-MS technique with offline preconcentration based on Milne *et al.* (2010). Recovery of dCu from the SAFe and GEOTRACES reference seawater samples showed good agreement with the consensus values from the SAFe/GEOTRACES intercalibration programmes. However, due to the poor recovery of dFe and dZn in the SAFe and GEOTRACES reference samples, the ICP-MS technique requires further optimisation (Chapter 2). When using a quadrupole ICP-MS as the detection system use of a collision cell is essential in order to minimise polyatomic interferences on Fe isotopes. As the use of collision cells reduces the instrumental sensitivity future work would need to investigate reducing the contribution of dCu from the blank. This might be possible by increasing the volume of Toyopearl resin in the clean-up column. For dZn, all future work

would need to be conducted with low-dZn seawater in order to achieve adequate sensitivity.

6.3. Biogeochemical cycling of dCo in the Sargasso Sea

Under a range of aerosol dust deposition conditions ($1-1040 \mu\text{g Fe m}^{-2} \text{d}^{-1}$; the annual range at Bermuda is $0.1-10\,000 \mu\text{g Fe m}^{-2} \text{d}^{-1}$, Sholkovitz *et al.*, 2009), the operational solubility of aerosol Co (8-100%) was found to be significantly higher than Fe (0.44-45%). The extremely labile association of Co with aerosol particles, results in atmospheric deposition being an important local source to the Sargasso Sea. In common with Fe, Co solubility varies as an inverse function of the Fe loading of the bulk aerosol. The covariation between dAl and dFe in surface waters indicates that dust was the predominant source of dFe to surface waters, with a general north-south increase in dust loading observed. In contrast, no relationship was observed between dCo and dust deposition in surface waters. Estimates of wet deposition of Co based on solubility data and elemental fluxes from the BATS region show the dominance of wet deposition over dry deposition, with ~85% of atmospheric Co being supplied via wet deposition, compared to just 30% for Fe. The results from this study demonstrate that the dry deposition and advective upwelling fluxes are equivalent ($47-1540 \text{ pmol m}^{-2} \text{d}^{-1}$ and $1.7-1430 \text{ pmol m}^{-2} \text{d}^{-1}$ respectively) and that wet deposition can dominate Co supply in this region.

A number of recent studies have recognised the importance of Co in influencing phytoplankton dynamics in the open ocean (*e.g.* Saito *et al.*, 2002; 2004; 2005; Bertrand *et al.*, 2007; Panzeca *et al.*, 2008; Saito and Goepfert, 2008). During this study, minimum concentrations of dCo (16-28 pM) occurred at 75 m, roughly coincident with maximum abundances of *Prochlorococcus* (mean = 3.1

$\times 10^6$ cells mL^{-1}). Euphotic zone minima of dFe (~ 100 m) were always deeper than the dCo minima, and were approximately coincident with the SCM and highest abundances of picoeukaryotes (570 cells mL^{-1} at ~ 100 - 150 m). A high cellular demand for dFe results in rapid removal of this element from surface waters, and an inverse relationship between dFe concentrations and eukaryotic phytoplankton. The inverse relationship between picoeukaryotic phytoplankton abundance and dFe distributions was evident throughout the euphotic zone in this study (at depths < 150 m); station K1 being the exception. Similarly, there was an inverse relationship between dCo concentrations and *Prochlorococcus*, suggesting that Co too may play a role in structuring the phytoplankton community in the Sargasso Sea.

Future work: In terms of the vertical distribution of dCo, atmospheric deposition and winter mixing both appear to supply Co to the euphotic zone of the Sargasso Sea. The extent to which one dominates over the other will be dependent on whether dCo binding-ligands are always saturated in the surface mixed layer and the influence this has on the residence time. Continued investigation of input pathways concurrent with measurements of Co speciation (organic/inorganic complexation) in this region will lead to improvements in our understanding of the biogeochemistry of dCo. The role of winter mixing could be examined by conducting seasonal studies and by comparison with vertical profiles in tropical regions which are less impacted by seasonal mixing.

6.4. The impact of trace metals (Co, Cu and Fe) additions on productivity and nitrogen fixation rates in the tropical Northeast Atlantic Ocean

Iron availability is proposed to limit N_2 fixation in the ocean (Berman-Frank *et al.*, 2001; Kustka *et al.*, 2003; Mills *et al.*, 2004). In this study, the stations with the highest dFe concentrations at T_0 (Stations A and B, 1.5 and 0.6 nM respectively) had the highest rates N_2 fixation (1.5 and 9.8 nM N L⁻¹ h⁻¹ respectively). Rates of N_2 fixation at Stations A, B and also C (1.47, 9.77 and 0.69 nM N L⁻¹ h⁻¹ respectively) were relatively high in comparison to those reported by Mills *et al.* (2004) (0.01–0.17 nM N L⁻¹ h⁻¹) at stations in the tropical North Atlantic where Fe and P were found to be co-limiting algal growth. As the concentration of dFe at Station A (1.5 nM) was higher than the range reported for surface waters this region (0.1–1.2 nM, Sarthou *et al.*, 2003; Rijkenberg *et al.*, 2008; Ussher *et al.*, 2010) and phosphate concentrations were very low (68 nM), the high rate of N_2 fixation reported for samples from Station A is thought to be a response to Fe contamination, most likely having occurred during the incubation or sample handling process. However, this response does affirm the link between N_2 fixation and dFe availability in this region. The rates of N_2 fixation at Stations B and C were comparable to those reported in Fe- and P-amended waters by Mills *et al.* (2004), which suggests that these stations were not Fe- (or P-) limited at the time of this study, perhaps due to their proximity to the Cape Verde Islands. Nitrogen fixation rates at T_0 at Station D-F (0.06–0.09 nM N L⁻¹ h⁻¹) were comparable to the rates reported in Mills *et al.* (2004) in non-amended waters. Although the highest rates of N_2 fixation occurred in bottles with the highest dFe concentrations, no correlation between N_2 fixation and dFe (or phosphate) was observed. In fact, the only parameter with which N_2 fixation correlated with was temperature, consistent with Langois *et al.* (2005). All

stations were N-limited during the *INSPIRE* cruise. The only increase in the rate of primary production in response to trace metal additions (Co, Cu, Fe and Zn) occurred when trace metal additions, of 0.5 nM Co, 2 nM Cu, 2 nM Fe or 1 nM Zn, were made simultaneously with inorganic N additions (nitrate and ammonium), which confirmed that primary production in this region is proximally N-limited. Heterotrophic bacterial production rates also provided no evidence for trace metal limitation.

Future work: The apparent lack of biological response to trace metal additions in the present study are consistent with the observation that phytoplankton growth in the North Atlantic gyre is proximally N-limited, and that alleviation of N-limitation shifts the system towards P-limitation (Mills *et al.*, 2004; Moore *et al.*, 2009). Further work to confirm N and P co-limitation of primary production in this region would need to undertake concomitant N, P and trace metal additions, over a longer incubation period (seven days is recommended) in order to determine the community response. Additionally, it is proposed that measurements of primary and heterotrophic bacterial production and N₂ fixation rates be determined in parallel incubations under the same experimental conditions. This would allow incubations to be terminated at the same time, while allowing the necessary manipulations required for the rate measurements (*e.g.* introduction of radio-labelled carbon) to be made without risk of contaminating the samples for trace metals.

6.5. Dissolved Co in surface waters during an Atlantic Meridional Transect

Dissolved Co concentrations ranging from 10–107 pM were determined in samples from the upper water column (< 200 m) between ~ 50°N and 50°S in the Atlantic Ocean. The highest concentrations of dCo (> 80 pM) were observed in vicinity of the equatorial upwelling, roughly coinciding with low-O₂ waters (< 150 μM O₂). This region was bounded by the subtropical gyres, which were characterised by much lower concentrations of dCo, the lowest (< 20 pM) being observed in the northern gyre (NATL-E). Concentrations of dCo in the southern gyre (SATL) were approximately double those of the NATL-E. No correlation was observed between mixed layer dCo and phosphate concentrations on the transect as a whole, but at individual stations some very strong correlations were observed (e.g. 1.3°N, 25.8°W, $r^2 = 0.91$, $n = 4$). This study showed that different processes dominate Co supply in the biogeochemical provinces, although the same processes appear to dominate at equivalent latitudes in both the northern and southern hemispheres. These processes are summarised in Table 6.1.

Table 6. 1. Dominant controls on dCo distributions in the upper water column of the Atlantic Ocean.

	Dominant control on dCo distributions in the upper water column
NADR	Lateral advective flux of continental Co
NATL-E	Lateral advective flux + biological (uptake & recycling)
WTRA	Vertical & lateral advective flux + biological (uptake & recycling) + chemical (redox)
SATL	Lateral advective flux + biological (uptake & recycling)
SSTC	Lateral advective flux of continental Co

In the temperate NADR and SSTC advection of continental Co in water masses is the dominant supply mechanism, whereas in the oligotrophic gyres, while there is evidence of physical processes supplying Co from continental shelf sediments, biological removal and recycling exert more of an influence on dCo distributions in the gyres than they do in the NADR and SSTC. The extremely low concentrations of dCo observed in the NATL-E (≤ 20 pM) are likely due to higher rates of biological uptake in response to the higher dFe concentrations in this province compared to the SATL (> 0.3 nM versus < 0.2 nM, Ussher *et al.*, in prep.; Wyatt *et al.*, in prep). In the equatorial upwelling region (WTRA), no one control dominates; the chemical environment, particularly dissolved O₂ concentration, combines with extremely efficient biologically-mediated recycling and a strong vertical advective flux to exert a profound influence on dCo distributions. In contrast to aerosol Fe supply, the atmospheric supply of Co is dominated ($\sim 85\%$) by the wet deposition flux (Church *et al.*, in prep.), the relative importance of which appears to vary on a seasonal basis, suggesting that wet deposition will be important seasonally and/or locally. Comparison with dCo concentrations determined in unfiltered seawater samples from an earlier gyre-centred AMT cruise (AMT-3) highlighted that there was no significant source of labile particulate Co between 50°N and 50°S, which has implications for Co availability to eukaryotic phytoplankton as they may be unable to access organically complexed-Co. Thus, providing another example of how Co availability could influence phytoplankton community dynamics.

Future work: This data highlights that atmospheric dry deposition does not have the same impact on upper water column distributions of dCo in the same way

that it does for dFe and dAl . Further work needs to be done to elucidate the different input (and removal) mechanisms that control dCo distributions in surface waters of the Atlantic Ocean. The *AMT* cruises are an ideal platform for such investigations, as they traverse diverse oceanographic regimes. In addition to meridional transects, cruises that run perpendicular to land masses may be particularly enlightening in establishing the role of continental margins in supplying dCo to remote regions. Monitoring of dCo in time-series data sets of rainwater samples from the Bermuda Tower has yielded some interesting, and unexpected, results in terms of the contribution of wet deposition to the total aerosol flux. Continued analysis will inform of seasonal patterns and other relationships.

Samples from the *AMT-19* cruise indicate that transport of continental Co in water masses is an important input to the biogeochemical provinces of the Atlantic Ocean between $50^{\circ}N$ and $50^{\circ}S$. Thus, water mass properties, in particular the dissolved O_2 concentration, play a crucial role in determining Co solubility and residence time in the upper water column, and merits further investigation. Despite the similarities with the biogeochemistry of Fe (e.g. redox and organic speciation), this study has highlighted that the biogeochemistry of Co in the open Atlantic Ocean is quite distinct from that of Fe. This is an important consideration for biogeochemical models that incorporate these two essential trace metals.

Appendix

Table i. Concentrations of (a) dCo, (b) dFe (data kindly provided by P.N. Sedwick) and (c) dAl (data kindly provided by P. Cabedo-Sanz) from the vertical cast stations (K1-K5) from *FeAST-6*, where shown $\pm 1s$.

(a) dCo (pM)

Depth (m)	K1	st dev	K2	st dev	K3	st dev	K4	st dev	K5	st dev
0	35.5	0.6	32.3	0.6	39.9	6.2	26.8	0.0	44.5	2.3
10	24.7	1.5	23.8	0.0	41.2	10.6	24.7	2.0	36.9	2.0
25	25.9	2.4	27.0	1.1	46.6	0.9	22.3	2.6	50.8	7.5
50	26.0	2.0	25.2	0.9	36.7	2.7	17.3	1.8	30.8	2.3
75	30.4	3.4	22.8	1.0	27.5	3.2	15.8	2.5	17.6	1.6
100	29.2	0.3	28.9	2.3	41.2	0.3	20.1	0.1	29.5	0.7
150	29.4	1.3	43.2	0.9	45.1	3.6	23.5	0.3	36.0	0.9
300	49.1	0.9	36.6	2.8	46.0	0.5	29.9	0.6	38.5	0.5
500	52.4	0.9	31.3	3.8	61.4	2.3	30.5	3.8	53.5	1.5
1000	70.1	3.0	50.9	1.1	63.3	2.3	50.9	3.2	64.6	2.8

(b) dFe (nM)

Depth (m)	K1	K2	K3	K4	K5
0	0.43	1.19	1.07	1.34	1.03
10	0.36	0.92	0.89	1.17	1.02
25	0.34	0.91	0.75	1.16	0.95
50	0.31	0.76	0.58	0.85	0.72
75	0.25	0.59	0.46	0.76	0.74
100	0.23	0.45	0.30	0.75	0.51
150	0.22	0.45	0.34	1.13	0.45
300	0.27	0.31	0.30	0.36	0.39
500	0.32	0.25	0.37	0.31	0.42
1000	0.59	0.56	0.60	0.66	0.60

(c) dAl (nM)

Depth (m)	K1	st dev	K2	st dev	K3	st dev	K4	st dev	K5	st dev
0	11.86	0.97	24.02	1.43	28.7	0.59	34.84	2.16	30.77	0.83
10	13.04	2.35	22.63	4.1	24.9	0.48	37.73	0.9	33.87	4.55
25	12.38	1.89	26.09	0.28	22.38	0.11	34.23	0.76	36.99	0.4
50	8.41	0.75	22.6	1.29	19.66	0.36	29.23	1.28	35.42	6.1 ?
75	18.01	2.18	22.26	1.21	18.04	1.57	33.2	0.89	32.67	0.17
100	13.56	3.1	19.89	2.95	16.51	0.68	28.95	2.08	25.76	5.93 ?
150	7.43	1.84	15.38	0.64	13.47	0.83	26.39	0.89	24.19	7.11 ?
300	9.22	8.45 ?	17.13	0.95	15.77	0	17.24	1.48	23.79	4.74
500	5.875	0.44	19.52	0.39	17.21	3.29	18.72	1.55	21.86	9.39 ?
1000	0.37	0.81	0.4	0.35	5.66	0	4.6	0.52	7.91	2.6

Table ii. Concentrations of dCo during AMT-19.

Station	Province	Date	Time	Lat (°N)	Long (°E)	Depth	Co (pM)	St dev (pM)
JC039006	NADR	10/16/2009	04:35	49.00	-16.67	5	16.9	1.3
JC039006		10/16/2009	04:35	49.00	-16.67	10	16.1	0.7
JC039006		10/16/2009	04:35	49.00	-16.67	20	15.1	3.2
JC039006		10/16/2009	04:35	49.00	-16.67	50	23.6	0.6
JC039006		10/16/2009	04:35	49.00	-16.67	75	38.6	0.8
JC039006		10/16/2009	04:35	49.00	-16.67	100	44.6	2.5
JC039008		10/17/2009	13:41	46.34	-18.80	5	76.9	1.5
JC039008		10/17/2009	13:41	46.34	-18.80	40	89.0	1.8
JC039008		10/17/2009	13:41	46.34	-18.80	60	49.0	1.0
JC039008		10/17/2009	13:41	46.34	-18.80	100	40.1	0.8
JC039008		10/17/2009	13:41	46.34	-18.80	250	41.8	1.6
JC039008		10/17/2009	13:41	46.34	-18.80	500	59.3	0.7
JC039011		10/19/2009	04:44	41.25	-22.60	2	28.5	0.6
JC039011		10/19/2009	04:44	41.25	-22.60	20	61.7	1.2
JC039011		10/19/2009	04:44	41.25	-22.60	40	86.1	1.7
JC039011		10/19/2009	04:44	41.25	-22.60	60	86.8	1.7
JC039011		10/19/2009	04:44	41.25	-22.60	100	66.6	2.1
JC039014	NATL-E	10/21/2009	13:07	37.10	-26.48	5	9.9	0.2
JC039014		10/21/2009	13:07	37.10	-26.48	60	21.2	0.2
JC039014		10/21/2009	13:07	37.10	-26.48	500	34.2	0.5
JC039015		10/22/2009	05:36	35.46	-28.65	2	11.3	0.8
JC039015		10/22/2009	05:36	35.46	-28.65	45	15.4	0.3
JC039015		10/22/2009	05:36	35.46	-28.65	75	25.4	0.5
JC039015		10/22/2009	05:36	35.46	-28.65	100	25.0	0.9
JC039017		10/23/2009	05:39	33.42	-31.26	2	32.2	1.8
JC039017		10/23/2009	05:39	33.42	-31.26	25	26.8	0.5
JC039017		10/23/2009	05:39	33.42	-31.26	35	11.3	0.2
JC039017		10/23/2009	05:39	33.42	-31.26	75	21.0	0.5
JC039017		10/23/2009	05:39	33.42	-31.26	85	23.7	0.5
JC039017		10/23/2009	05:39	33.42	-31.26	100	107.2	4.7
JC039019		10/24/2009	05:37	31.43	-33.73	2	46.4	0.9
JC039019		10/24/2009	05:37	31.43	-33.73	25	21.2	0.4
JC039019		10/24/2009	05:37	31.43	-33.73	40	19.0	2.7
JC039019		10/24/2009	05:37	31.43	-33.73	65	22.8	0.5
JC039019		10/24/2009	05:37	31.43	-33.73	85	29.7	0.6
JC039019		10/24/2009	05:37	31.43	-33.73	110	41.4	0.9
JC039021		10/25/2009	05:33	29.19	-35.99	2	20.8	0.4
JC039021		10/25/2009	05:33	29.19	-35.99	28	12.0	0.2
JC039021		10/25/2009	05:33	29.19	-35.99	40	15.8	2.2
JC039021		10/25/2009	05:33	29.19	-35.99	146	40.7	0.8
JC039023		10/26/2009	05:34	27.22	-37.88	2	22.8	0.5
JC039023		10/26/2009	05:34	27.22	-37.88	25	20.3	0.4
JC039023		10/26/2009	05:34	27.22	-37.88	40	16.2	0.9
JC039023		10/26/2009	05:34	27.22	-37.88	85	33.0	2.0
JC039023		10/26/2009	05:34	27.22	-37.88	110	35.3	0.7
JC039023		10/26/2009	05:34	27.22	-37.88	150	31.2	2.6
JC039025		10/27/2009	05:36	25.39	-39.60	40	10.9	0.2
JC039025		10/27/2009	05:36	25.39	-39.60	65	11.4	0.2
JC039027		10/28/2009	06:30	23.23	-40.72	25	15.8	0.3
JC039027		10/28/2009	06:30	23.23	-40.72	40	16.6	0.3
JC039027		10/28/2009	06:30	23.23	-40.72	65	27.2	0.5

JC039027		10/28/2009	06:30	23.23	-40.72	110	34.4	0.9
JC039027		10/28/2009	06:30	23.23	-40.72	150	36.0	0.7
JC039033		11/01/2009	06:41	16.57	-36.10	2	23.9	0.5
JC039033		11/01/2009	06:41	16.57	-36.10	20	21.8	3.8
JC039033		11/01/2009	06:41	16.57	-36.10	35	13.4	0.2
JC039033		11/01/2009	06:41	16.57	-36.10	60	25.9	1.5
JC039033		11/01/2009	06:41	16.57	-36.10	150	59.4	2.7
JC039037	WTRA	11/03/2009	05:39	11.47	-32.65	2	23.9	0.5
JC039037		11/03/2009	05:39	11.47	-32.65	10	16.7	0.5
JC039037		11/03/2009	05:39	11.47	-32.65	48	43.1	0.9
JC039037		11/03/2009	05:39	11.47	-32.65	75	47.8	1.0
JC039037		11/03/2009	05:39	11.47	-32.65	100	58.9	1.2
JC039043		11/06/2009	05:34	4.05	-27.69	2	43.6	0.9
JC039043		11/06/2009	05:34	4.05	-27.69	25	92.5	1.8
JC039043		11/06/2009	05:34	4.05	-27.69	35	65.4	1.3
JC039043		11/06/2009	05:34	4.05	-27.69	95	71.3	1.4
JC039043		11/06/2009	05:34	4.05	-27.69	125	72.4	0.3
JC039043		11/06/2009	05:34	4.05	-27.69	150	63.5	1.3
JC039045		11/07/2009	05:34	1.27	-25.85	2	49.9	1.0
JC039045		11/07/2009	05:34	1.27	-25.84	15	59.5	1.2
JC039045		11/07/2009	05:34	1.27	-25.84	25	60.0	3.6
JC039045		11/07/2009	05:34	1.27	-25.84	70	75.9	1.5
JC039045		11/07/2009	05:34	1.27	-25.84	100	54.2	1.1
JC039045		11/07/2009	05:34	1.27	-25.84	150	61.9	1.2
JC039051		11/11/2009	05:35	-7.37	-24.99	2	33.5	2.5
JC039051		11/11/2009	05:35	-7.37	-24.99	25	37.3	0.7
JC039051		11/11/2009	05:35	-7.37	-24.99	45	85.6	1.7
JC039051		11/11/2009	05:35	-7.37	-24.99	100	76.2	1.5
JC039051		11/11/2009	05:35	-7.37	-24.99	150	62.0	1.8
JC039059	SATL	11/15/2009	04:33	-19.50	-25.00	2	27.9	1.7
JC039059		11/15/2009	04:33	-19.50	-25.00	40	46.1	0.9
JC039059		11/15/2009	04:33	-19.50	-25.00	70	52.1	1.0
JC039059		11/15/2009	04:33	-19.50	-25.00	90	51.2	1.0
JC039059		11/15/2009	04:33	-19.50	-25.00	120	80.3	1.6
JC039059		11/15/2009	04:33	-19.50	-25.00	200	37.5	1.2
JC039063		11/17/2009	04:42	-26.10	-25.00	2	62.4	1.2
JC039063		11/17/2009	04:42	-26.10	-25.00	45	47.4	0.9
JC039065		11/18/2009	04:38	-28.79	-26.14	2	89.2	1.8
JC039065		11/18/2009	04:38	-28.79	-26.14	30	65.8	1.3
JC039065		11/18/2009	04:38	-28.79	-26.14	60	48.1	1.0
JC039065		11/18/2009	04:38	-28.79	-26.14	135	70.9	3.0
JC039065		11/18/2009	04:38	-28.79	-26.14	160	38.4	0.8
JC039065		11/18/2009	04:38	-28.79	-26.14	180	32.2	0.6
JC039069	SSTC	11/21/2009	05:42	-33.41	-34.26	2	65.6	1.3
JC039069		11/21/2009	05:42	-33.41	-34.26	20	47.8	0.6
JC039069		11/21/2009	05:42	-33.41	-34.26	45	43.9	0.9
JC039069		11/21/2009	05:42	-33.41	-34.26	80	58.3	1.2
JC039069		11/21/2009	05:42	-33.41	-34.26	100	29.0	0.2
JC039071		11/22/2009	05:19	-35.30	-37.11	2	17.3	0.3
JC039071		11/22/2009	05:19	-35.30	-37.11	15	15.5	0.3
JC039072		11/24/2009	05:36	-37.30	-40.19	2	48.7	1.0

JC039072	11/24/2009	05:36	-37.30	-40.19	10	34.6	0.7
JC039072	11/24/2009	05:36	-37.30	-40.19	20	57.1	1.1
JC039072	11/24/2009	05:36	-37.30	-40.19	32	38.7	0.8
JC039072	11/24/2009	05:36	-37.30	-40.19	80	36.3	0.7
JC039072	11/24/2009	05:36	-37.30	-40.19	150	50.4	1.0

References

- Achterberg, E.P., Holland, T.W., Bowie, A.R., Mantoura, R.F.C. & Worsfold, P.J. 2001. Determination of iron in seawater. *Analytica Chimica Acta*. **442**, 1-14.
- Aguilar-Islas, A.M., Resing, J.A. and Bruland, K.W. 2006. Catalytically enhanced spectrophotometric determination of manganese in seawater by flow injection analysis with a commercially available resin for on-line preconcentration. *Limnology and Oceanography: Methods*. **4**, 105-113.
- Aiken, J., Rees, N., Hooker, S., Holligan, P., Bale, A., Robins, D., Moore, G. Harris, R. and Pilgrim, D. 2000. The Atlantic Meridional Transect: overview and synthesis of data. *Progress in Oceanography*. **45**, 257-312.
- Arimoto, R., R. A. Duce, B. J. Ray, and U. Tomza., 2003. Dry deposition of trace elements to the western North Atlantic. *Global Biogeochemical Cycles*. **17**. Doi: 10.1029/2001GB001406.
- Arimoto, R., R. Duce, B. Ray, and C. Unni 1985. Atmospheric trace elements at Enewetak Atoll: 2. Transport to the ocean by wet and dry deposition. *Journal of Geophysical Research*. **9**, 2391-2408.
- Arimoto, R., R. A. Duce, B. J. Ray, W. G. Ellis Jr., J. D. Cullen, and J. T. Merrill. 1995. Trace elements in the atmosphere over the North Atlantic. *Journal of Geophysical Research*. **100**, 1199-1213. Doi: 10.1029/94JD02618.
- Baker, A.R. and Jickells, T.D. 2006. Mineral particle size as a control on aerosol iron solubility. *Geophysical Research Letters*. **33**. Doi: 10.1029/2006GL026557.
- Baker, A.R., Jickells, T.D., Witt M. and Linge, K.L. 2006. Trends in the solubility of iron, aluminium, manganese and phosphorus in aerosol collected over the Atlantic Ocean. *Marine Chemistry*. **98**, 43-58.
- Baker, A.R., Weston, K., Kelly, S. D., Voss, M., Streu, P., and Cape, J. N. 2007. Dry and wet deposition of nutrients from the tropical Atlantic atmosphere: Links to primary productivity and nitrogen fixation. *Deep Sea Research Part I: Oceanographic Research Papers*. **54**, 1704-1720.
- Barbeau, K., Moffett, J.W., Caron, D.A., Croot, P.L. and Erdner, D.L. 1996. Role of protozoan grazing in relieving iron limitation of phytoplankton. *Nature*. **380**, 61-64.

- Barbeau, K., Rue, E.L., Bruland, K.W. and Butler A. 2001. Photochemical cycling of iron in the surface ocean mediated by microbial iron(III)-binding ligands. *Nature*. **413**, 409-413.
- Behrenfeld, M.J., O'Malley, R.T., Siegel, D.A., McClain, C.R., Sarmiento, J.L., Feldman, G.C., Milligan, A.J., Falkowski, P.G., Letelier, R.M. and Boss, E.S. 2006. Climate-driven trends in contemporary ocean productivity. *Nature*. **444**, 752-755.
- Bennett, S.A, Achterberg, E.P., Connelly, D.P., Statham, P.J., Fones, G.R. and German, C.R. 2008. The distribution and stabilisation of dissolved Fe in deep-sea hydrothermal plumes. *Earth and Planetary Science Letters*. **270**, 157-167.
- Bergquist, B. A. and Boyle, E.A. 2006. Dissolved iron in the tropical and subtropical Atlantic Ocean, *Global Biogeochemical Cycles*. **20**. Doi: 10.1029/2005GB002505.
- Bergquist, B. A., Wu, J. and Boyle, E. A. 2007. Variability in oceanic dissolved iron is dominated by the colloidal fraction. *Geochimica et Cosmochimica Acta*. **71**, 2960-2974.
- Berman-Frank, I., Cullen, J.T., Shaked, Y., Sherrell, R.M., Falkowski, P.G. 2001. Iron Availability, Cellular Iron Quotas, and Nitrogen Fixation in *Trichodesmium*. *Limnology and Oceanography*. **46**, 1249-1260.
- Bertrand, E.M., Saito, M.A., Rose, J.M., Riesselman, C.R., Lohan, M.C., Nobel, A.E., Lee, P.E. and DiTullio, G.R. 2007. Vitamin B₁₂ and iron co-limitation of phytoplankton growth in the Ross Sea. *Limnology and Oceanography*. **52**, 1079-1093.
- Blain, S., Bonnet, S. and Guieu C. 2007. Dissolved iron distribution in the tropical and sub tropical South Eastern Pacific. *Biogeosciences Discussions*. **4**, 2845-2875.
- Bowen, E.J. 1964. Chemiluminescence from Dissolved Oxygen, *Nature*. **201**, 180-180.
- Bowie, A. R., Achterberg, E. P., Croot, P. L., de Baar, H. J. W., Laan, P., Moffett, J. W., Ussher, S. J., Worsfold, P. J. 2006. A community-wide intercomparison exercise for the determination of dissolved iron in seawater. *Marine Chemistry*. **98**, 81-99.
- Bowie, A.R., Achterberg, E.P., Mantoura, R.F.C., Worsfold, P.J. 1998. Determination of sub-nanomolar levels of iron in seawater using flow

- injection with chemiluminescence detection. *Analytica Chimica Acta*. **361**, 189-200.
- Bowie, A. R., Acterberg, E.P., Sedwick, P.N., Ussher, S. and Worsfold, P.J. 2002a. Real-time monitoring of picomolar concentrations of iron(II) in marine waters using automated flow injection-chemiluminescence instrumentation. *Environmental Science and Technology*. **36**, 4600-4607.
- Bowie, A.R. and Lohan, M.C. 2009. Determination of iron in seawater. In: Wurl, O. [ed.] *Practical guidelines for the analysis of seawater*. pp. 235-257. Boca Raton: CRC Press.
- Bowie, A. R., Whitworth, D. J., Achterberg, E. P., Mantoura, R. F. C. and Worsfold, P. J. 2002b. Biogeochemistry of Fe and other trace elements (Al, Co, Ni) in the upper Atlantic Ocean. *Deep Sea Research Part I: Oceanographic Research Papers*. **49**, 605-636.
- Bown, J., Boye, M., Baker, A., Duvieilbourg, E., Lacan, F., Le Moigne, F., Planchon, F., Speich, S. and Nelson, D.M. 2011. The biogeochemical cycle of dissolved cobalt in the Atlantic and the Southern Ocean south off the coast of South Africa. *Marine Chemistry*. Doi: 10.1016/j.marchem.2011.03.008.
- Boyd, P.W. and Ellwood, M. J. 2010. The biogeochemical cycle of iron in the ocean. *Nature Geoscience*. **3**, 675-682.
- Boyd, P.W., Jickells, T., Law, C.S., Blain, S., Boyle, E.A., Buesseler, K.O., Coale, K.H., Cullen, J.J., de Baar, H.J.W., Follows, M., Harvey, M., Lancelot, C., Levasseur, M., Owens, N.P.J., Pollard, R., Rivkin, R.B., Sarmiento, J., Schoemann, V., Smetacek, V., Takeda, S., Tsuda, A., Turner, S. and Watson, A.J. 2007. Mesoscale iron enrichment experiments 1993-2005: synthesis and future directions. *Science*. **315**, 612-617.
- Boyd, P.W., Watson, A.J., Law, C.S., Abraham, E.R., Trull, T., Murdoch, R., Bakker, D.C.E., Bowie, A.R., Buesseler, K.O., Chang, H., Charette, M., Croot, P., Downing, K., Frew, R., Gall, M., Hadfield, M., Hall, J., Harvey, M., Jameson, G., La Roche, J., Liddicoat, M., Ling, R., Maldonado, M.T., McKay, P.M., Nodder, S., Pickmere, S., Pridmore, R., Rintoul, S., Safi, K., Sutton, P., Strzepek, R., Tanneberger, K., Turner, S., Waite, A.,

- Zeldis, J. 2000. A mesoscale phytoplankton bloom in the polar Southern Ocean stimulated by iron fertilization. *Nature*. **407**, 695-702.
- Boyd, P.W., Law, C.S., Wong, C.S., Nojiri, Y., Tsuda, A., Levasseur, M., Takeda, S., Rivkin, R., Harrison, P.J., Strzepek, R., Gower, J., McKay, R.M., Abraham, E., Arychuk, M., Barwell-Clarke, J., Crawford, W., Hale, M., Harada, K., Johnson, K., Kiyosawa, H., Kudo, I., Marchetti, A., Miller, W., Needoba, J., Nishioka, J., Ogawa, H., Page, J., Robert, M., Saito, H., Sastri, A., Sherry, N., Soutar, T., Sutherland, N., Taira, Y., Whitney, F., Wong, S-K. E. and Yoshimura, T., 2004. The decline and fate of an iron-induced subarctic phytoplankton bloom. *Nature*. **428**, 549-553.
- Boyé, M., Aldrich, A., van den Berg, C. M. G., de Jong, J. T. M., Nirmaier, H., Veldhuis, M.J.W., Timmermans, K. R. and de Baar, H. J. W. 2006. The chemical speciation of iron in the north-east Atlantic Ocean. *Deep Sea Research Part I: Oceanographic Research Papers*. **53**, 667-683.
- Boyle, E. A., Bergquist, B.A., Kayser, R.A. and Mahowald, N. 2005. Iron, manganese, and lead at Hawaii Ocean Time-series station ALOHA: Temporal variability and an intermediate water hydrothermal plume. *Geochimica et Cosmochimica Acta*. **69**, 933-952.
- Boyle, E.A., Handy, B. and Van Geen, A. 1987. Cobalt determination in natural waters using cation-exchange liquid chromatography with luminol chemiluminescence detection. *Analytical Chemistry*. **59**, 1499-1503.
- Boyle, E.A., Husted, S.S. and Jones, S.P. 1981. On the distribution of copper, nickel and cadmium in surface waters of the North Atlantic and North Pacific Ocean. *Journal of Geophysical Research*. **86**, 8048-8066.
- Brand, L.E., Sunda, W.G. and Guillard, R.R.L. 1986. Reduction of marine phytoplankton reproduction rates by copper and cadmium. *Journal of Experimental Marine Biology and Ecology*. **96**, 225-250.
- Brown, M.T. and Bruland, K.W. 2008. An improved flow-injection analysis method for the determination of dissolved aluminium in seawater. *Limnology and Oceanography: Methods*. **6**, 87-95.
- Bruland, K. W. 1989. Complexation of zinc by natural organic ligands in the central North Pacific. *Limnology and Oceanography*. **34**, 269-285.
- Bruland, K.W., Orians, K.J. and Cowen, J.P., 1994. Reactive trace metals in the stratified central North Pacific. *Geochimica et Cosmochimica Acta*. **58**, 3171-3182.

- Bruland, K. W. and Lohan, M.C. 2003. Controls of trace metals in seawater. In *The Oceans and Marine Geochemistry. Treatise on Geochemistry vol.6.* (ed. H. Elderfield), pp 23-47. Oxford: Elsevier.
- Bruland, K. W., Rue, E. L., Smith, G. J., DiTullio, G. R. 2005. Iron, macronutrients and diatom blooms in the Peru upwelling regime: brown and blue waters of Peru. *Marine Chemistry*. **93**, 81-103.
- Bucciarelli, E., Blain, S., and Tréguer, P. 2001. Iron and manganese in the wake of the Kerguelen Islands (Southern Ocean). *Marine Chemistry*. **73**, 21-36.
- Buck, C.S., Landing, W.M., Resing, J.A. and Lebon, G.T. 2006, Aerosol iron and aluminum solubility in the northwest Pacific Ocean: Results from the 2002 IOC cruise, *Geochemistry Geophysics Geosystems*. **7**. Doi: 10.1029/2005GC000977.
- Buesseler, K.O., Doney, S.C., Karl, D.M., Boyd, P.W., Caldeira, K., Chai, F., Coale, K.H., de Baar, H.J.W., Falkowski, P.G., Johnson, K.S., Lampitt, R.S., Michaels, A.F., Naqvi, S.W.A., Smetacek, V., Takeda, S. and Watson, A.J. 2008. Ocean iron fertilization - moving forward in a sea of uncertainty. *Science*. **319**, 162.
- Campbell, L., Nolla, H.A. and Vaultot, D. 1994. The importance of *Prochlorococcus* to community structure in the central North Pacific Ocean. *Limnology and Oceanography*. **39**, 954-961.
- Cannizzaro, V., Bowie, A.R., Sax, A., Achterberg, E.P. and Worsfold, P.J. 2000. Determination of cobalt and iron in estuarine and coastal waters using flow injection with chemiluminescence detection. *Analyst*. **125**, 51-57.
- Carlson, T.N., and Prospero, J.M. 1972. The large-scale movement of Saharan air outbreaks over the North Equatorial Atlantic. *Journal of Applied Meteorology*. **11**, 283-297.
- Carritt, D.E. and Carpenter, J.H. 1966. Comparison and evaluation of currently employed modifications of the Winkler method for determining dissolved oxygen in seawater; a NASCO Report. *Journal of Marine Research*. **24**, 286-319.
- Cembella, A.D., Antia, N.J. and Harrison, P.J. 1982. The Utilization of Inorganic and Organic Phosphorous Compounds as Nutrients by Eukaryotic

- Microalgae: A Multidisciplinary Perspective: Part I, *Critical Reviews in Microbiology*. **10**, 317-391.
- Chase, Z., Paytan, A., Johnson, K.S., Street, J. and Chen, Y. 2006. Input and cycling of iron in the Gulf of Aquaba, Red Sea. *Global Biogeochemical Cycles*. **20**. Doi:10.1029/2005GB002646.
- Chen, L. and Duce, R.A. 1983. The sources of sulfate, vanadium and mineral matter in aerosol particles over Bermuda, *Atmospheric Environment*. **17**, 2055-2064.
- Chester, R., Nimmo, M. and Preston, M. R. 1999. The trace metal chemistry of atmospheric dry deposition samples collected at Cap Ferrat: a coastal site in the Western Mediterranean. *Marine Chemistry*. **68**, 15-30.
- Chisholm S.W., Falkowski P.G., & Cullen J.J. 2001. Dis-crediting Ocean Fertilization. *Science*. **294**, 309-310.
- Coale, K. H., and Bruland, K.W. 1988. Copper complexation in the northeast Pacific., *Limnology and Oceanography*. **33**, 1084-1101.
- Coale, K.H., Johnson, K.S., Fitzwater, S.E., Gordon, R.M., Tanner, S., Chavez, F.P., Ferioli, L., Sakamoto C., Rogers, P., Millero, F., Steinberg P., Nightingale, P., Cooper, D., Cochlan, W.P., Landry, M.R., Constantinou, J., Rollwagen, G., Trasvina, A., Kudela, R. 1996. A massive phytoplankton bloom induced by an ecosystem-scale iron fertilization experiment in the equatorial Pacific Ocean. *Nature*. **383**, 495-501.
- Croft, M.T., Lawrence, A.D., Raux-Deery, E., Warren, M.J. and Smith, A.G. 2005. Algae acquire vitamin B₁₂ through a symbiotic relationship with bacteria. *Nature*. **438**, 90-93.
- Cullen, J.T., Bergquist, B.A., and Moffett, J.W. 2006. Thermodynamic characterization of the partitioning of iron between soluble and colloidal species in the Atlantic Ocean. *Marine Chemistry*. **98**, 295-303.
- de Baar, H.J.W. and de Jong, J.T.M. 2001. Distributions, sources and sinks of iron in seawater., in *The Biogeochemistry of Iron in Seawater*. In: Turner, D. R. and Hunter, K.A. (eds) pp. 123-253, Chichester: John Wiley and Sons Ltd.
- de Baar, H. J. W., Timmermans, K. R., Laan, P., De Porto, H. H., Ober, S., Blom, J. J., Bakker, M. C., Schilling, J., Sarthou, G., Smit, M. G. and Klunder, M. 2008. Titan: A new facility for ultraclean sampling of trace

- elements and isotopes in the deep oceans in the international GEOTRACES program. *Marine Chemistry*. **111**, 4-21.
- de Baar, H.J.W. and La Roche, J. 2003. Trace Metals in the Oceans: evolution, biology and global change. In *Marine Science Frontiers for Europe*. (ed. G. Wefer, F. Lamy and F. Mantoura), pp 79-105. Berlin, Heidelberg, New York, Tokyo: Springer-Verlag.
- de Baar H.J.W., B.P.W., Coale K.H., Landry M.R., Tsuda A., Assmy P., Bakker D.C.E., Bozec Y., Barber R.T., Brzezinski M.A., Buesseler K.O., Boye M., Croot P.L., Gervais F., Gorbunov M.Y., Harrison P.J., Hiscock W.T., Laan P., Lancelot C., Law C.S., Levasseur M., Marchetti A., Millero F.J., Nishioka J., Nojiri Y., van Oijen T., Riebesell U., Rijkenberg M.J.A., Saito H., Takeda S., Timmermans K.R., Veldhuis M.J.W., Waite A.M. and Wong C.-S., 2005. Synthesis of Iron Fertilization Experiments: from the iron age in the age of enlightenment. *Journal of Geophysical Research*. **110**, DOI:10.1029/2004JC002601.
- de Jong, J. T. M., den Das, J., Bathmann, U., Stoll, M. H. C., Kattner, G., Nolting, R. F., and de Baar, H. J. W. 1998. Dissolved iron at subnanomolar levels in the Southern Ocean as determined by ship-board analysis. *Analytica Chimica Acta*. **377**, 113-124.
- de la Rocha, C.L. 2003. The Biological Pump. In *The Oceans and Marine Biogeochemistry, vol. 6 (Treatise on Geochemistry)*. (ed. H. Elderfield), pp. 83-111. Oxford: Elsevier.
- Desboeufs, K. V., Sofikitis, A., Losno, R., Colin, J. L. and Ausset, P. 2005. Dissolution and solubility of trace metals from natural and anthropogenic aerosol particulate matter. *Chemosphere*. **58**, 195-203.
- Dierssen, H., Balzer, W. and Landing, W.M. 2001. Simplified synthesis of an 8-hydroxyquinoline chelating resin and a study of trace metal profiles from Jellyfish Lake, Palau. *Marine Chemistry*. **73**, 173-192.
- Donat, J.R. and Bruland K.W. 1988. Direct determination of dissolved cobalt and nickel in seawater by differential pulse cathodic stripping voltammetry preceded by adsorptive collection of cyclohexane-1,2-dione dioxime complexes. *Analytical Chemistry*. **60**, 240-244.
- Draxler, R.R. and Rolph, G.D., 2010. HYSPLIT (HYbrid Single-Particle Lagrangian Integrated Trajectory) Model access via NOAA ARL READY

Website (<http://ready.arl.noaa.gov/HYSPLIT.php>), NOAA Air Resources Laboratory, Silver Spring, MD.

- Droop, M.R., 1974. The nutrient status of algal cells in continuous culture. *Journal of the Marine Biological Association of the United Kingdom*. **54**, 825-855.
- Droop, M.R., 2007. Vitamins, phytoplankton and bacteria: symbiosis or scavenging? *Journal of Plankton Research*. **29**, 107-113.
- Duce, R.A. 1986. The impact of atmospheric nitrogen, phosphorus and iron species on marine biological productivity, in: *The Role of Air-Sea Exchange in Geochemical Cycling*, edited by P. Buat-Menard, pp. 497-529, Reidel, Hingham.
- Duce, R.A. and Hoffman, G.L. 1976. Atmospheric vanadium transport to the ocean. *Atmospheric Environment*. **10**, 989-996.
- Duce, R. A., Liss, P. S., Merrill, J. T., Atlas, E. L., Buat-Menard, P., Hicks, B. B., Miller, J. M., Prospero, J. M., Arimoto, R., Church, T. M., Ellis, W., Galloway, J. N., Hansen, L., Jickells, T. D., Knap, A. H., Reinhardt, K. H., Schneider, B., Soudine, A., Tokos, J. J., Tsunogai, S., Wollast, R., and Zhou, M. 1991. The atmospheric input of trace species to the world ocean. *Global Biogeochemical Cycles*. **5**, 193-259.
- Duce, R. A. and Tindale, N.W. 1991. Atmospheric transport of iron and its deposition to the ocean. *Limnology and Oceanography*. **36**, 1715-1736.
- Dyhrman, S.T., and Palenik, B., 2003. Characterization of ectoenzyme activity and phosphate-regulated proteins in the coccolithophorid *Emiliania huxleyi*. *Journal of Plankton Research*. **25**, 1215-1225.
- Ellwood, M. J. 2008. Wintertime trace metal (Zn, Cu, Ni, Cd, Pb and Co) and nutrient distributions in the Subantarctic Zone between 40-52° S; 155-160° E. *Marine Chemistry*. **112**, 107-117.
- Elrod, V. A., Berelson, W.M., Coale, K.H., Johnson, K.S. 2004. The flux of iron from continental shelf sediments: a missing source for global budgets. *Geophysical Research Letters*. **31**. Doi: 10.1029/2004GL020216.
- Ellwood, M.J. and van den Berg, C.M. G. 2001. Determination of organic complexation of cobalt in seawater by cathodic stripping voltammetry. *Marine Chemistry*. **75**, 33-47.

- Ellwood, M.J., van den Berg, C. M. G., Boye, M., Veldhuis, M., de Jong, J. T. M., de Baar, H. J. W., Croot, P. L., and Kattner, G. 2005. Organic complexation of cobalt across the Antarctic Polar Front in the Southern Ocean. *Marine and Freshwater Research*. **56**, 1069-1075.
- Ellwood, M. J., Boyd, P.W. and Sutton, P. 2008. Winter-time dissolved iron and nutrient distributions in the Subantarctic Zone from 40-52 S:155-160 E. *Geophysical Research Letters*. **35**. DOI:10.1029/2008GL033699.
- Elrod, V.A., Johnson, K.S. and Coale, K.H. 1991. Determination of subnanomolar levels of iron(II) and total dissolved iron in seawater by flow injection analysis with chemiluminescence detection. *Analytical Chemistry*. **63**, 893-898.
- Emmerson M.C. and Huxham M. 2002. How can Marine Ecology Contribute to the Biodiversity-Ecosystem Functioning Debate? In *Biodiversity and Ecosystem Functioning: synthesis and perspectives*. (Ed. M. Loreau, S. Naeem and P. Inchausti), pp139-146. Oxford: Oxford University Press.
- Falkowski, P. G. 1994. The role of phytoplankton photosynthesis in global biogeochemical cycles. *Photosynthesis Research*. **39**, 235-258.
- Falkowski, P.G. and Raven, J.A. 1997. *Aquatic Photosynthesis*. Oxford: Blackwell Science.
- Falkowski, P.G., Scholes, R. J., Boyle, E., Canadell, J., Canfield D., Elser, J., Gruber, N., Hibbard, K., Högberg, P., Linder, S., Mackenzie, F. T., Moore III, B., Pedersen, T., Rosenthal, Y., Seitzinger, S., Smetacek, V. and Steffen, W. 2000. The global carbon cycle: a test of our knowledge of Earth as a system. *Science*. **290**, 291-296.
- Field, C.B., Behrenfeld, M.J., Randerson, J.T. and Falkowski, P.G. 1998. Primary production of the biosphere: Integrating terrestrial and oceanic components. *Science*. **281**, 237-240.
- Field, M.P., Cullen, J.T. and Sherrell, R.M. 1999. Direct determination of 10 trace metals in 50 mL samples of coastal seawater using desolvating micronebulization sector field ICP-MS. *Journal of Atomic Analytical Spectrometry*. **14**, 1425-1430.
- Fischer, A.C., Kroon, J. J., Verburg, T. G., Teunissen, T., and Wolterbeek, H. Th, 2007. On the relevance of iron adsorption to container materials in small-volume experiments on iron marine chemistry: ⁵⁵Fe-aided

- assessment of capacity, affinity and kinetics. *Marine Chemistry*. **107**, 533-546.
- Flegal, A.R., Sañudo-Wilhelmy, S.A.A. and Scelfo, G.M. 1995. Silver in the Eastern Atlantic Ocean. *Marine Chemistry*. **49**, 315-320.
- Gao, Y., Kaufman, Y.J., Tanre, D., Kolber, D. and Falkowski, P. 2001. Seasonal distributions of aeolian iron fluxes to the global ocean. *Geophysical Research Letters*. **28**, 29-32.
- German, C.R. and Van Damm, K.L. 2003. Hydrothermal Processes. In *The Oceans and Marine Geochemistry. Treatise on Geochemistry vol.6.* (ed. H. Elderfield), pp 181-222. Oxford: Elsevier.
- Gledhill, M. and van den Berg, C. M. G. 1994. Determination of complexation of iron(III) with natural organic complexing ligands in seawater using cathodic stripping voltammetry. *Marine Chemistry*. **47**, 41-54.
- Gledhill, M. and van den Berg, C. M. G. 1995. Measurement of the redox speciation of iron in seawater by catalytic cathodic stripping voltammetry. *Marine Chemistry*. **50**, 51-61.
- Goebel, N.L., Turk, K.A., Achilles, K.M., Paerl, R.W., Hewson, I. and Morrison, A.E., Montoya, J.P., Edwards, C.A., and Zehr, J.P. 2010. Abundance and distribution of major groups of diazotrophic cyanobacteria and their potential contribution to N₂ fixation in the tropical Atlantic Ocean. *Environmental Microbiology*. **12**, 3272–3289.
- Goericke, R. and Welschmeyer N.A. 1993. The marine prochlorophyte *Prochlorococcus* contributes significantly to phytoplankton biomass and primary production in the Sargasso Sea, *Deep Sea Research: Part I*. **40**, 2283-2294.
- Gong, N., Chen, C., Xie, L., Chen, H., Lin, X., and Zhang, R. 2005. Characterization of a thermostable alkaline phosphatase from a novel species *Thermus yunnanensis* sp. nov. and investigation of its cobalt activation at high temperature, *Biochimica Biophysica Acta*. **1750**, 103-111.
- Grashoff, K., Erhardt, M., and Kremling, K. 1983. *Methods in Seawater Analyses*. Weinheim: Verlag Chemie.
- Gruber, N. and Sarmiento, J.L. 1997. Global patterns of marine nitrogen fixation and denitrification. *Global Biogeochemical Cycles*. **11**, 235–266.

- Han, Q., Moore, J.K., Zender, C., Measures, C. and Hydes, D., 2008. Constraining oceanic dust deposition using surface ocean dissolved Al. *Global Biogeochemical Cycles*. **22**. Doi: 10.1029/2007gb002975.
- Helmers, E., and Schrems, O., 1995. Wet deposition of metals to the tropical North and the South Atlantic Ocean. *Atmospheric Environment*. **29**, 2475-2484.
- Ho, T.-Y.; Quigg, A., Finkel, Z. V., Milligan, A. J., Wyman, K., Falkowski, P.G. and Morel, F. M. M. 2003. The elemental composition of some phytoplankton. *Journal of Phycology*. **39**, 1145-1159.
- Howell, K.A., Achterberg, E.P., Braungardt, C.B., Tappin, A.D., Worsfold, P.J. and Turner D.R. 2003. Voltammetric *in situ* measurements of trace metals in coastal waters. *Trends in Analytical Chemistry*. **22**, 828-835.
- Huang, S. and Conte, M.H. 2009. Source/process apportionment of major and trace elements in sinking particles in the Sargasso sea, *Geochimica Cosmochimica Acta*. **73**, 65-90.
- Huang, S., Rahn, K. A., Arimoto, R., Graustein, W. C., and Turekian, K. K., 1999. Semiannual cycles of pollution at Bermuda, *Journal of Geophysical Research*. **104**. Doi:10.1029/1999JD900801.
- Hurst, M.P. and Bruland, K.W. 2008. The effects of the San Francisco Bay plume on trace metal and nutrient distributions in the Gulf of the Farallones. *Geochimica et Cosmochimica Acta*. **72**, 395-411.
- Hutchins, D. A., and Bruland, K.W. 1994. Grazer-mediated regeneration and assimilation of Fe, Zn and Mn from planktonic prey. *Marine Ecology Progress Series*. **110**, 259-269.
- Hutchins, D.A., Witter, A.E., Butler, A. and Luther, G.W., 1999. Competition among marine phytoplankton for different chelated iron species. *Nature*. **400**, 858-861.
- Jacobs, A. and Worwood, M. 1974. *Iron in Biogeochemistry and Medicine*. London:Academic.
- Jakuba, R.W., Moffett, J.W., and Dyhrman, S.T. 2008. Evidence for the linked biogeochemical cycling of zinc, cobalt, and phosphorus in the western North Atlantic Ocean, *Global Biogeochemical Cycles*. **22**. Doi: 10.1029/2007GB003119.

- Jickells, T. 1999. The inputs of dust derived elements to the Sargasso Sea; a synthesis. *Marine Chemistry*. **68**, 5-14.
- Jickells, T. D., An, Z.S., Andersen, K.K., Baker, A.R., Bergametti, G., Brooks, N., Cao, J.J., Boyd, P.W., Duce, R.A., Hunter, K.A., Kawahata, H., Kubilay, N., laRoche, J., Liss, P.J., Mahowald, N., Prospero, J.M., Ridgwell, A.J., Tegen, I. and Torres, R. 2005. Global iron connections between desert dust, ocean biogeochemistry and climate. *Science*, **308**, 67-71.
- Jickells, T. D. and Burton J. D. 1988. Cobalt, copper, manganese and nickel in the Sargasso Sea. *Marine Chemistry*. **23**, 131-144.
- Jickells, T., Church, T., Véron, A., Arimoto, R., 1994. Atmospheric inputs of manganese and aluminium to the Sargasso Sea and their relation to surface water concentrations., *Marine Chemistry*. **46**, 283-292.
- Johnson, K.S., Boyle, E., Bruland, K., Coale, K., Measures, C., Moffett, C.J., Aguilar-Islas, A., Barbeau, K., Bergquist, B., Bowie, A., Buck, K., Cai, Y., Chase, Z., Cullen, J., Doi, T., Elrod, V., Fitzwater, S., Gordon M., King, A., Laan, P., Laglera-Baquer, L., Landing, W., Lohan, M., Mendez, J., Milne, A., Obata, H., Ossiander, L., Plant, J., Sarthou, G., Sedwick, P., Smith, G.J., Sohts, B., Tanner, S., van den Berg, S. and Wu, J. 2007. Developing standards for dissolved iron in seawater. *Eos, Transactions, American Geophysical Union*. **88**, 131-132.
- Johnson, K. S., Gordon, R. M. and Coale, K. H. 1997. What controls dissolved iron concentrations in the world ocean? *Marine Chemistry*. **57**, 137-161.
- Johnson, K. W., Miller, LA., Sutherland, N. E. and Wong, C. S. 2005. Iron transport by mesoscale Haida eddies in the Gulf of Alaska, *Deep Sea Research Part II: Topical Studies in Oceanography*. **52**, 933-953.
- Johnson, K. S., Stout, P.M., Berelson, W.M. and Sakamoto-Arnold, C.M. 1988. Cobalt and copper distributions in the waters of the Santa Monica Basin, California. *Nature*. **332**, 527-530.
- Karl, D., Letelier, R., Tupas, L., Dore, J., Christian, J. and Hebel, D. 1997. The role of nitrogen fixation in biogeochemical cycling in the subtropical North Pacific Ocean. *Nature*. **388**, 533-538.

- Karl, D., Michaels, A., Bergman, B., Capone, D., Carpenter, E., and Letelier, R. Lipschultz, F., Paerl, H., Sigman, D. and Stal, L. 2002. Dinitrogen fixation in the world's oceans. *Biogeochemistry*. **57/58**, 47–98.
- Karstensen, J., Stramma, L. and Visbeck, M., 2008. Oxygen minimum zones in the eastern tropical Atlantic and Pacific Oceans. *Progress in Oceanography*. **77**, 331-350.
- Kearns, D.R. 1971. Physical and chemical properties of singlet molecular oxygen. *Chemical Reviews*. **71**, 395-427.
- King, A.L., Sañudo-Wilhelmy, S.A., Leblanc, K., Hutchins, D.A., and Fu, F. 2011. CO₂ and vitamin B₁₂ interactions determine bioactive trace metal requirements of a subarctic Pacific diatom. *ISME J*. Doi: 10.1038/ismej.2010.211.
- Kirchman, D. L. 1996. Microbial ferrous wheel. *Nature*. **383**, 303-304.
- Knauer, G.A., Martin, J.H. and Gordon, R.M. 1982. Cobalt in north-east Pacific waters. *Nature*. **297**, 49-51.
- Kondo, T., Tsinoremas, N.F., Golden, S.S., Johnson C.H., Kutsuna, S., and Ishiura, M. 1994. Circadian clock mutants of cyanobacteria. *Science*. **266**, 1233-1236.
- Kustka, A.B., Sañudo-Wilhelmy, S.A., Carpenter, E.J., Capone, D., Burns, J. and Sunda, W.G. 2003. Iron requirements for dinitrogen- and ammonium-supported growth in cultures of *Trichodesmium* (IMS 101): Comparison with nitrogen fixation rates and iron: carbon ratios of field populations. *Limnology and Oceanography*. **48**, 1869-1884.
- Landing, W.M. and Bruland, K.W. 1987. The contrasting biogeochemistry of iron and manganese in the Pacific Ocean. *Geochimica et Cosmochimica Acta*. **51**, 29-43.
- Landing, W.M., Haraldsson, C. and Paxeus N. 1986. Vinyl polymer agglomerate based transition metal cation chelating ion-exchange resin containing the 8-hydroxyquinoline functional group. *Analytical Chemistry*. **58**, 3031-3035.
- Lane, T.W., and Morel, F.M.M. 2000, Regulation of Carbonic Anhydrase expression by zinc, cobalt, and carbon dioxide in the marine diatom *Thalassiosira weissflogii*, *Plant Physiology*. **123**, 345-352.

- Langlois, R.J., Hummer, D. and LaRoche, J. 2008. Abundances and distributions of the dominant nifH phylotypes in the Northern Atlantic Ocean. *Applied Environmental Microbiology*. **74**, 1922–1931.
- Langlois, R.J., LaRoche, J. and Raab, P.A. 2005. Diazotrophic diversity and distribution in the tropical and subtropical Atlantic Ocean. *Applied Environmental Microbiology*. **71**, 7910–7919.
- Lannuzel, D., Remenyi, T., Lam, P., Townsend, A., Ibsanmi, E., Butler, E., Wagener, T., Schoemann, V. and Bowie, A.R. 2010. Distributions of dissolved and particulate iron in the sub-Antarctic and Polar Frontal Southern Ocean (Australian sector). *Deep Sea Research II*. (accepted 23 Dec. 2010).
- Letelier, R., Karl, D.M., Abbott, M.R., and Bridigare, R.R. 2004. Light driven seasonal patterns of chlorophyll and nitrate in the lower euphotic zone of the North Pacific Subtropical Gyre. *Limnology and Oceanography*. **49**, 508-519.
- Lin, J.-M. and Yamada, M. 2003. Microheterogenous systems of micelles and microemulsions as reaction media in chemiluminescent analysis. *Trends in Analytical Chemistry*. **22**, 99-106.
- Lohan, M. C., Aguilar-Islas, A.M. and Bruland, K.W. 2006. Direct determination of iron in acidified (pH 1.7) seawater samples by flow injection analysis with catalytic spectrophotometric detection: Application and intercomparison. *Limnology and Oceanography: Methods*. **4**, 164-171.
- Lohan, M.C., Aguilar-Islas, A.M., Franks R.P. and Bruland, K.W. 2005. Determination of iron and copper in seawater at pH 1.7 with a new commercially available chelating resin, NTA Superflow. *Analytica Chimica Acta*. **530**, 121-129.
- Longhurst, A. 1998. *Ecological Geography of the Sea*. Academic Press: San Diego.
- Mackey, D. J., O'Sullivan, J. E. and Watson, R. J. 2002. Iron in the western Pacific: a riverine or hydrothermal source for iron in the Equatorial Undercurrent? *Deep Sea Research Part I: Oceanographic Research Papers*. **49**, 877-893.
- Mackie, D.S., Boyd, P.W., Hunter, K., McTainsh, G.H., 2005. Simulating the cloud processing of iron in Australian dust: pH and dust concentration, *Geophysical Research Letters*. **32**. Doi: 10.1029/2004GL022122.

- Mackie, D.S., Peat, J.M., McTainsh, G.H., Boyd, P.W., Hunter, K.A., 2006. Soil abrasion and eolian dust production: implications for iron partitioning and solubility, *Geochemistry Geophysics Geosystems*. **7**. Doi, 10.1029/2006GC001404.
- Mahaffey, C., Michaels, A.F. and Capone, D.G. 2005. The conundrum of marine N₂ fixation. *American Journal of Science*. **305**, 546–595.
- Mahaffey, C., Williams, R.G., Wolff, G.A., Mahowald, N., Anderson, W., and Woodward, M. 2003. Biogeochemical signatures of nitrogen fixation in the eastern North Atlantic. *Geophysical Research Letters*. **30**. Doi: 10.1029/2002GL016542.
- Mahowald, N. M., Baker, A.R., Bergametti, G., Brooks, N., Duce, R.A., Jickells, T.D., Kubilay, N., Prospero, J.M. and Tegen, I. 2005. Atmospheric global dust cycle and iron inputs to the oceans. *Global Biogeochemical Cycles*, **19**. Doi: 10.1029/2004GB002402.
- Maldonado, M.T., Allen, A.E., Chong, J.S., Lin, K., Leus, D., Karpenko, N., and Harris, S.L., 2006. Copper-dependent iron transport in coastal and oceanic diatoms. *Limnology and Oceanography*. **51**, 1729-1743.
- Maldonado, M.T. and Price, N.M. 1999. Utilization of iron bound to strong organic ligands by plankton communities in the subarctic Pacific Ocean. *Deep Sea Research Part II: Topical Studies in Oceanography*. **46**, 2447-2473.
- Maldonado, M. T. and Price, N. M. 2001. Reduction and transport of organically bound iron by *Thalassiosira oceanica* (Bacillariophyceae). *Journal of Phycology*. **37**, 298-310.
- Mann, E.L., Ahlgren, N., Moffett, J.W. and Chisholm, S.W. 2002. Copper toxicity and cyanobacteria ecology in the Sargasso Sea. *Limnology and Oceanography*. **47**, 976–988.
- Mann, E.L., and Chisholm, S.W. 2000. Iron limits the cell division rate of *Prochlorococcus* in the eastern equatorial Pacific. *Limnology and Oceanography*. **45**, 1067–1076.
- Marañón, E., Behrenfeld, M.J., Gonzalez, N., Mourino, B., Zubkov, M.V., 2003. High variability of primary production in oligotrophic waters of the Atlantic Ocean: uncoupling from phytoplankton biomass and size structure. *Marine Ecology Progress Series*. **257**, 1-11.

- Martin, J.H. 1990. Glacial-interglacial CO₂ change: the iron hypothesis. *Paleoceanography*. **5**, 1-13.
- Martin, J. H., Fitzwater, S.E., Gordon, R.M., Hunter, C.N. and Tanner, S.J. 1993. Iron, primary production and carbon-nitrogen flux studies during the JGOFS North Atlantic Bloom Experiment. *Deep Sea Research. Part II, Topical Studies in Oceanography*. **40**, 115-134.
- Martin, J.H., Knauer, G.H., Karl, D.M. and Broenkow, W.W. 1989. VERTEX: carbon cycling in the northeast Pacific. *Deep Sea Research. Part A. Oceanographic research papers*. **34**, 267-285.
- Mather, R.L., Reynolds, S.E., Wolff, G.A., Williams, R.G., Torres-Valdes, S., Woodward, E.M.S., Landolfi, A., Pan, X., Sanders, R., and Achterberg, E.P., 2008. Phosphorus cycling in the North and South Atlantic Ocean subtropical gyres. *Nature Geoscience*. **1**, 439-443.
- McGillicuddy, D.J., Anderson, L.A., Bates, N.R., Bibby, T., Buesseler, K.O., Carlson, C.A., Davis, C.S., Ewart, C., Falkowski, P.G., Goldthwait, S.A., Hansell, D.A., Jenkins, W.J., Johnson, R., Kosnyrev, V.K., Ledwell, J.R., Li, Q.P., Siegel, D.A. and Steinberg, D.K., 2007. Eddy/wind interactions stimulate extraordinary mid-ocean plankton blooms. *Science*. **316**, 1021-1026.
- Measures, C.I. and Brown, M.T. 1996. Estimating dust input to the Atlantic Ocean using surface water Al concentrations, in: *The Impact of Desert Dust Across the Mediterranean*, edited by S. Guerzoni and R. Chester, pp. 301-311, Kluwer, Dordrecht.
- Measures, C. I., Landing, W.M., Brown, M.T. and Buck, C.S. 2008. High-resolution Al and Fe data from the Atlantic Ocean CLIVAR-CO₂ Repeat hydrography A16N transect: extensive linkages between dust and upper ocean geochemistry. *Global Biogeochemical Cycles*. **22**. Doi: 10.1029/2007GB003042.
- Measures, C.I. and Vink, S. 1999. Seasonal variations in the distribution of Fe and Al in the surface waters of the Arabian Sea, *Deep Sea Research. II*. **46**, 1597-1622.
- Measures, C.I. and Vink, S. 2000. On the use of dissolved aluminium in surface waters to estimate dust deposition to the ocean, *Global Biogeochemical Cycles*. **14**, 317-327.

- Measures, C.I., Yuan J. and Resing J.A. 1995. Determination of iron in seawater by flow injection analysis using in-line preconcentration and spectrophotometric detection. *Marine Chemistry*. **50**, 3-12.
- Mémery, L., Arhan, M., Alvarez-Salgado, X. A., Messias, M. J., Mercier, H., Castro, C. G., and Rios, A. F. 2000. The water masses along the western boundary of the south and equatorial Atlantic. *Progress in Oceanography*. **47**, 69-98.
- Merényi, G., Lind, J. and Eriksen, T.E. 1990. Luminol chemiluminescence: chemistry, excitation, emitter. *Journal of Bioluminescence and Chemiluminescence*. **5**, 53-56.
- Millero, F. and Pierrot, D. 2002. Speciation of metals in natural waters. In *Chemistry of Marine Waters and Sediments*. (ed. Gianguzza, A., Pelizzetti, E. and Sammartano, S.) pp 193-220. Berlin: Springer.
- Mills, M.M., Ridame, C., Davey, M., La Roche, J. & Geider, R.J. 2004. Iron and phosphorus co-limit nitrogen fixation in the eastern tropical North Atlantic. *Nature*. **429**, 292-294.
- Milne, A., Landing, W., Bizimis, M., and Morton, P. 2010. Determination of Mn, Fe, Co, Ni, Cu, Zn, Cd and Pb in seawater using high resolution magnetic sector inductively coupled mass spectrometry (HR-ICP-MS). *Analytica Chimica Acta*. **665**, 200-207.
- Moffett, J.W., Brand, L.E., Croot, P.L. and Barbeau, K.A. 1997. Cu speciation and cyanobacterial distribution in harbors subject to anthropogenic Cu inputs. *Limnology and Oceanography*. **42**, 789-799.
- Moffett, J.W. and Ho, J. 1996. Oxidation of cobalt and manganese in seawater via a commonly catalyzed pathway. *Geochimica et Cosmochimica Acta*. **60**, 3415-3424.
- Mohr, W., Grosskopf, T., Wallace, D.W., LaRoche, J. 2010. Methodological underestimation of oceanic nitrogen fixation rates. *PLoS One*. **5**, e12583.
- Montoya, J.P., Voss, M., Kahler, P. and Capone, D.G. 1996. A simple, high-precision, high-sensitivity tracer assay for N₂ fixation. *Applied Environmental Microbiology*. **62**, 986-993.
- Moody, J.L., S. J. Oltmans, H. Levy II, and J. T. Merrill., 1995. Transport climatology of tropospheric ozone: Bermuda, 1988-1991. *Journal of Geophysical Research*. **100**, 7179-7194. Doi:10.1029/94JD02830.

- Moore, J. K. and Braucher, O. 2008. Sedimentary and mineral dust sources of dissolved iron to the world ocean. *Biogeosciences*. **5**, 631-656.
- Moore, C.M., Mills, M.M., Milne, A., Langlois, R., Achterberg, E.P., Lochte, K., Geider, R.J., and La Roche, J., 2006. Iron limits primary productivity during spring bloom development in the central North Atlantic. *Global Change Biology*. **12**, 626-634.
- Moore, M.C., Mills, M.M., Achterberg, E.P., Geider, R.J., La Roche, J., Lucas, M.I., McDonagh, E.L., Pan, Xi., Poulton, A.J., Rijkenberg, M.J.A., Suggett, D.J., Ussher, S.J., and Woodward, E.M.S. 2009. Large-scale distribution of Atlantic nitrogen fixation controlled by iron availability. *Nature Geoscience*. **2**, 867-871.
- Morel, F.M.M., Kustka, A.B. and Shaked, Y. 2008. The role of unchelated Fe in the iron nutrition of phytoplankton. *Limnology and Oceanography*. **53**, 400-404.
- Morel F.M.M. and Price N.M. 2003. The Biogeochemical Cycles of Trace Metals in the Oceans. *Science*. **300**, 944-947.
- Morel, F.M.M., Reinfelder, J.R., Roberts, S.B., Chamberlain, C.P., Lee, J.G. and Yee, D. 1994. Zinc and carbon co-limitation of marine phytoplankton, *Nature*. **369**, 740-742.
- Ndung'u, K., Franks, R.P., Bruland, K.W. and Flegal, A.R. 2003. Organic complexation and total dissolved trace metal analysis in estuarine waters: comparison of solvent-extraction graphite furnace atomic absorption spectrometric and chelating resin flow injection inductively coupled plasma-mass spectrometric analysis. *Analytica Chimica Acta*. **481**, 127-138.
- Nielsdottir, M.C., Moore, C.M., Sanders, R., Hinz, D.J., and Achterberg, E.P., 2009. Iron limitation of the post bloom phytoplankton communities in the Iceland Basin. *Global Biogeochemical Cycles*, **23**.
DOI:10.1029/2008GB003410.
- Nishioka, J., Takeda, S., Wong, C. S. and Johnson, W. K. 2001. Size-fractionated iron concentrations in the northeast Pacific Ocean: distribution of soluble and small colloidal iron. *Marine Chemistry*. **74**, 157-179.

- Noble, A. E., Saito, M.A., Maiti, K. and Benitez-Nelson, C. 2008. Cobalt, manganese, and iron near the Hawaii Islands: a potential concentrating mechanism for cobalt within a cyclonic eddy and implications for the hybrid-type trace metals. *Deep Sea Research Part II: Topical Studies in Oceanography*. **55**, 1473-1490.
- Nürnberg, H.W. and Valenta, P. 1983. Voltammetry in chemical speciation of trace metals. In *Trace Metals in Sea Water*. (ed. C.S. Wong, E. Boyle, K.W. Bruland, J.D. Burton and E.D. Goldberg) pp 671-698. New York: Plenum Press.
- Obata, H., Karatani, H. and Nakayama, E. 1993. Automated determination of iron in seawater by chelating resin concentration and chemiluminescence detection. *Analytical Chemistry*. **65**, 1524-1528.
- Olson, R.J., Zettler, E.R., and DuRand, M.D. 1993. Phytoplankton analysis using flow cytometry, in *Handbook of methods in Aquatic Microbial Ecology*, edited by P. F. Kemp *et al.*, pp. 175-186, Lewis Publishers, Boca Raton, Florida.
- Orians, K.J., and Bruland, K.W. 1986. The biogeochemistry of aluminum in the Pacific Ocean, *Earth and Planetary Science Letters*. **78**, 397-410.
- Owens, N.J.P. and Rees, A.P. 1989. Determination of N-15 at submicrogram levels of nitrogen using automated continuous-flow isotope ratio mass-spectrometry. *Analyst*. **114**, 1655-1657.
- Panzeca, C., Beck, A.J., Leblanc, K., Taylor, G.T., Hutchins, D.A. and Sanudo-Wilhelmy, S.A. 2008. Potential cobalt limitation of vitamin B₁₂ synthesis in the North Atlantic Ocean. *Global Biogeochemical Cycles*, **22**. DOI: 10.1029/2007GB003124.
- Partensky, F., Hess, W.R. and Vaultot, D. 1999. *Prochlorococcus*, a marine photosynthetic prokaryote of global significance. *Microbiology and Molecular Biology Reviews*. **63**, 106-127.
- Pastor, M.V., Pelegrí, J.L., Hernández-Guerra, A., Font, J., Salat, J., and Emelianov, M., 2008. Water and nutrient fluxes off Northwest Africa. *Continental Shelf Research*. **28**, 915-936.
- Paytan, A., Mackey, K.R.M., Chen, Y., Lima, I.D., Doney, S.C., Mahowald, N., Labiosa, R., Post, A.F., 2009. Toxicity of atmospheric aerosols on marine phytoplankton. *Proceedings of the National Academy of Sciences*. **106**, 4601-4605.

- Peers, G. and Price, N.M. 2006. Copper-containing plastocyanin used for electron transport by an oceanic diatom. *Nature*. **441**, 341-344.
- Peers, G., Quesnel, S.-A. and Price, N.M. 2005. Copper requirements for iron acquisition and growth of coastal and oceanic diatoms. *Limnology and Oceanography*. **50**, 1149-1158.
- Pérez, V., Fernández, E., Marañón, E., Morán, X.A.G. and Zubkov, M.V. 2006. Vertical distribution of phytoplankton biomass, production and growth in the Atlantic subtropical gyres. *Deep Sea Research Part I: Oceanographic Research Papers*. **53**, 1616-1634.
- Pérez, V., Fernández, E., Marañón, E., Serret, P., Varela, R., Bode, A., Varela, M., Varela, M.M. Morán, X.A.G. Woodward, E.M.S., Kitidis, V., and García-Soto, C. 2005. Latitudinal distribution of microbial plankton abundance, production, and respiration in the Equatorial Atlantic in autumn 2000. *Deep Sea Research Part I: Oceanographic Research Papers*. **52**, 861-880.
- Petit, J. R., Jouzel, J., Raynaud, D., Barkov, N. I., Barnola, J.-M., Basile, I., Bender, M., Chappellaz, J., Davis, M., Delaygue, G., Delmotte, M., Kotlyakov, V. M., Legrand, M., Lipenkov, V. Y., Lorius, C., Pepin, L., Ritz, C., Saltzman, E. and Stievenard, M. 1999. Climate and atmospheric history of climate and atmospheric history the past 420,000 years from the Vostok ice core, Antarctica. *Nature*. **399**, 429-436.
- Plocke, D.J., Levinthal, C., and Vallee, B.L. 1962. Alkaline phosphatase of *Escherichia coli*: A zinc metalloenzyme. *Biochemistry*. **1**, 373-378.
- Pohl, C., Croot, P. L., Hennings, U., Daberkow, T., Budeus, G., and Rutgers van der Loeff, M. , 2010. Synoptic transects on the distribution of trace elements (Hg, Pb, Cd, Cu, Ni, Zn, Co, Mn, Fe, and Al) in surface waters of the Northern- and Southern East Atlantic. *Journal of Marine Systems*. **84**, 24-41.
- Pollard, R. T., Salter, I., Sanders, R.J., Lucas, M.I., Moore, M.C., Mills, R.A., Statham, P.J., Allen, J.T., Baker, A.R., Bakker, D.C.E., Charette, M.A., Fielding, S., Fones, G.R., French, M., Hickman, A.E., Holland, R.J., Hughes, J.A., Jickells, T.D., Lampitt, R.S., Morris, P.J., Nedelec, F.H., Nielsdottir, M., Planquette, H., Popova, E.E., Poulton, A., Read, J.F., Seeyave, S., Smith, T., Stinchcombe, M., Taylor, S., Thomalla, S.,

- Venables, H.J., Williamson, R. and Zubkov, M.V. 2009. Southern Ocean deep-water carbon export enhanced by natural iron fertilization. *Nature*. **457**, 577-580.
- Poulton, A.J., Holligan, P.M., Hickman, A., Kim, Y.-N., Adey, T.R., Stinchcombe, M.C., Holeton, C., Root, S., and Woodward, E.M.S., 2006a. Phytoplankton carbon fixation, chlorophyll-biomass and diagnostic pigments in the Atlantic Ocean. *Deep Sea Research Part II: Topical Studies in Oceanography*. **53**, 1593-1610.
- Prospero, J. M., and Carlson, T.N. 1972. Vertical and areal distribution of Saharan dust over the Equatorial North Atlantic Ocean., *Journal of Geophysical Research*. **77**. 5255-5265.
- Prospero, J. M., Ginoux, P., Torres, O., Nicholson, S.E. and Thomas, T.E. 2002. Environmental characterization of global sources of atmospheric dust identified with the Nimbus 7 Total Ozone Mapping Spectrometer (TOMS) absorbing aerosol product. *Reviews of Geophysics*. **40**. Doi: 10.1029/2000RG000095.
- Prospero, J. M., Glaccum, R.A. and Nees, R.T. 1981. Atmospheric transport of soil dust from Africa to South America. *Nature*. **289**, 570-572.
- Provasoli, L. and Carlucci, A.F. 1974. Vitamins and growth regulators. In: Stewart, W.D.P. and Abbott, M.R. (eds). *Algal Physiology and Biochemistry*. Malden, Mass.:Blackwell Science, pp 741-787.
- Raven, J.A., Brown, K., Mackay, M., Beardall, J., Giordano, M., Granum, E., Leegood, R.C., Kilminster, K. and Walker, D.I. 2005. Iron, nitrogen, phosphorus and zinc cycling and consequences for primary productivity in the oceans. In *Micro-organisms and Earth systems - advances in geomicrobiology. SGM symposium 65*. (ed. G.M. Gadd, K.T.Semple and H.M. Lappin-Scott) pp. 247-273. Cambridge: Cambridge University Press.
- Redfield, A.C. 1934. On the proportions of organic derivations in sea water and their relation to the composition of plankton. In: Daniel, R.J. (ed.) *James Johnstone Memorial Volume*. Liverpool: University Press of Liverpool.
- Rees, A.P., Law, C.S., and Woodward, E.M.S., 2006. High rates of nitrogen fixation during an in-situ phosphate release experiment in the Eastern Mediterranean Sea. *Geophysical Research Letters*. **33**. Doi: 10.1029/2006gl025791.

- Ren, J. L., Zhang, J., Luo, J.Q., Pei, X.K. and Jiang, Z.X. 2001. Improved fluorimetric determination of dissolved aluminium by micelle-enhanced lumogallion complex in natural waters, *Analyst*. **126**, 698-702.
- Resing, J.A. and Measures, C. I. 1994. Fluorometric determination of Al in seawater by flow injection analysis with in-line preconcentration, *Analytical Chemistry*. **66**, 4105-4111.
- Resing, J. A. and Mottl, M.J. 1992. Determination of manganese in seawater by flow injection analysis using online preconcentration and spectrophotometric detection. *Analytical Chemistry*. **64**, 2682-2687.
- Riebesell, U., Wolf-Gladrow, D.A. and Smetacek, V. 1993. Carbon dioxide limitation of marine phytoplankton growth rates. *Nature*. **361**, 249-251.
- Rijkenberg, M. J. A., Powell, C.F., Dall'Osto, M., Nielsdottir, M.C., Patey, M.D., Hill, P.G., Baker, A.R., Jickells, T.D., Harrison, R.M. and Achterberg, E.P. 2008. Changes in iron speciation following a Saharan dust event in the tropical North Atlantic Ocean. *Marine Chemistry*. **110**, 56-67.
- Robinson, C., Poulton, A.J., Holligan, P.M., Baker, A.R., Forster, G., Gist, N., Jickells, T.D., Malin, G., Upstill-Goddard, R., Williams, R.G., Woodward, E.M.S., Zubkov, M.V. 2006. The Atlantic Meridional Transect (AMT) Programme: A contextual view 1995-2005. *Deep Sea Research Part II: Topical Studies in Oceanography*. **53**, 1485-1515.
- Rolph, G.D., 2010. Real-time Environmental Applications and Display System (READY) Website (<http://ready.arl.noaa.gov>). NOAA Air Resources Laboratory, Silver Spring, MD.
- Rose, A.L. and Waite, T.D. 2001. Chemiluminescence of luminol in the presence of iron(II) and oxygen: oxidation mechanism and implications for its analytical use. *Analytical Chemistry*. **73**, 5909-5920.
- Rue, E.L. and Bruland, K.W. 1995. Complexation of iron (III) by natural organic ligands in the Central North Pacific as determined by a new competitive ligand equilibrium/ adsorptive cathodic stripping voltammetric method. *Marine Chemistry*. **50**, 117-138.
- Rue, E.L. and Bruland, K.W. 1997. The role of organic complexation on ambient iron chemistry in the equatorial Pacific Ocean and the response of a mesoscale iron addition experiment. *Limnology and Oceanography*. **42**, 901-910.

- Saager, P. M., de Baar, H. J. W., de Jong, J. T. M., Nolting, R. F. and Schijf, J. (1997.), Hydrography and local sources of dissolved trace metals Mn, Ni, Cu, and Cd in the northeast Atlantic Ocean., *Marine Chemistry*, **57**, 195-216.
- Saito, M.A., Bertrand, E.M., Dutkiewicz, S., Bulygin, V.V., Moran, D.M., Monteiro, F.M., Follows, M.J., Valois, F.W., and Waterbury, J.B. 2010. Iron conservation by reduction of metalloenzyme inventories in the marine diazotroph *Crocospaera watsonii*. *Proceedings of the National Academy of Sciences*. **108**, 2184-2189.
- Saito, M. A. and Goepfert, T. J. 2008. Zinc-cobalt colimitation of *Phaeocystis antarctica*. *Limnology and Oceanography*. **53**, 266-275.
- Saito, M.A., Goepfert, T.J. and Ritt, J.T. 2008. Some thoughts on the concept of colimitation: Three definitions and the importance of bioavailability. *Limnology and Oceanography*. **53**, 276-290.
- Saito, M. A. and Moffett, J.W. 2001. Complexation of cobalt by natural organic ligands in the Sargasso Sea as determined by a new high-sensitivity electrochemical cobalt speciation method suitable for open ocean work. *Marine Chemistry*. **75**, 49-68.
- Saito, M. A. and Moffett, J. W. 2002. Temporal and spatial variability of cobalt in the Atlantic Ocean. *Geochimica et Cosmochimica Acta*. **66**, 1943-1953.
- Saito, M. A., Moffett, J. W., Chisholm, S.W. and Waterbury, J.B. 2002. Cobalt limitation and uptake in *Prochlorococcus*. *Limnology and Oceanography*. **47**, 1629-1636.
- Saito, M. A., Moffett, J.W., and DiTullio, G.R. 2004. Cobalt and nickel in the Peru upwelling region: A major flux of labile cobalt utilized as a micronutrient. *Global Biogeochemical Cycles*. **18**.
doi:10.1029/2003GB002216.
- Saito, M. A., Rocap, G. and Moffett J.W. 2005. Production of cobalt binding ligands in a *Synechococcus* feature at the Costa Rica upwelling dome. *Limnology and Oceanography*. **50**, 279-290.
- Saito, M.A., Sigman, D.M. and Morel, F.M.M. 2003. The bioinorganic chemistry of the ancient ocean: the co-evolution of cyanobacterial metal requirements and biogeochemical cycles at the Archean-Proterozoic boundary? *Inorganica Chimica Acta*. **356**, 308-318.

- Sakamoto-Arnold, C.M. and Johnson, K.S. 1987. Determination of picomolar levels of cobalt in seawater by flow injection analysis with chemiluminescence detection. *Analytical Chemistry*. **59**, 1789-1794.
- Sañudo-Wilhelmy, S.A, Kustka, A.B., Gobler, C.J., Hutchins, D.A., Yang, M., Lwiza, K., Burns, J., Capone, D.G., Raven, J.A. and Carpenter, E.J. 2001. Phosphorus limitation of nitrogen fixation by *Trichodesmium* in the central Atlantic Ocean. *Nature*. **411**, 66–69.
- Sarthou, G., Baker, A.R., Blain, S., Achterberg, E.P., Boyé, M., Bowie, A.R., Croot, P., Laan, P., de Baar, H.J. W., Jickells, T.D. and Worsfold, P.J. 2003. Atmospheric iron deposition and sea-surface dissolved iron concentrations in the eastern Atlantic Ocean. *Deep Sea Research Part I: Oceanographic Research Papers*. **50**, 1339-1352.
- Sarthou, G. and Jeandel, C. 2001. Seasonal variations of iron concentrations in the Ligurian Sea and iron budget in the Western Mediterranean Sea. *Marine Chemistry*. **74**, 115-129.
- Sedwick, P.N., Bowie, A.R. and Trull, T.W. 2008. Dissolved iron in the Australian sector of the Southern Ocean (CLIVAR-SR3 section): meridional and seasonal trends, *Deep-Sea Research: Part I: Oceanographic Research Papers*. 911-925. **8**. Doi: 10.1016/j.dsr.2008.03.011.
- Sedwick, P. N., Church, T.M., Bowie, A.R., Marsay, C.M., Ussher, S.J., Achilles, K.M., Lethaby, P.J., Johnson, R.J., Sarin, M.M. and McGillicuddy, D.J. 2005. Iron in the Sargasso Sea (Bermuda Atlantic Time-series Study): Eolian imprint, spatiotemporal variability, and ecological implications. *Global Biogeochemical Cycles*. **19**. Doi: 10.1029/2004GB002445.
- Sedwick, P. N., Sholkovitz, E.R. and Church, T.M. 2007. Impact of anthropogenic combustion emissions on the fractional solubility of aerosol iron: evidence from the Sargasso Sea. *Geochemistry, Geophysics, Geosystems*. **8**. Doi: 10.1029/2007GC001586.
- Shelley, R.U., Sedwick, P.N., Bibby, T.S., Cabedo-Sanz, P., Church, T.M., Johnson, R.J., Macey, A.I., Marsay, C.M., Sholkovitz, E.R., Ussher, S.J., Worsfold, P.J., and Lohan, M.C. Controls on dissolved cobalt in surface waters of the Sargasso Sea. Submitted to *Global Biogeochemical Cycles*.

- Shelley, R. U., Zachhuber, B., Sedwick, P.J., Worsfold, P.J. and Lohan, M.C. 2010. Determination of total dissolved cobalt in UV-irradiated seawater using flow injection with chemiluminescence detection. *Limnology and Oceanography: Methods*. **8**, 352-362.
- Sherrell, R.M., and Boyle, E.A. 1992. The trace metal composition of suspended particles in the oceanic water column near Bermuda. *Earth and Planetary Science Letters*. **111**, 155 - 174.
- Sholkovitz, E.R. and Copland, D. 1981. The coagulation, solubility and adsorption properties of Fe, Mn, Cu, Ni, Cd, Co and humic acids in a river water. *Geochimica cosmochimica acta*. **45**, 181-189.
- Sholkovitz, E., R., Sedwick, P.N. and Church, T.M. 2009. Influence of anthropogenic combustion emissions on the deposition of soluble aerosol iron to the ocean: Empirical estimates for island sites in the North Atlantic. *Geochimica et Cosmochimica Acta*. **73**, 3981-4003.
- Siedler, G., Zangenberg, N., Onken, R., and Morlière, A. 1992. Seasonal Changes in the Tropical Atlantic Circulation: Observation and Simulation of the Guinea Dome. *Journal of Geophysical Research*. **97**, 703-715.
- Siegel, D.A., McGillicuddy, D.J., Fields, E.A. 1999. Mesoscale eddies, satellite altimetry, and new production in the Sargasso Sea. *Journal of Geophysical Research*. **104**, 13359-13379.
- Slawinska, D. and Slawinski, J. 1977. Chemiluminescent flow method for the determination of formaldehyde. *Analytical Chemistry*. **47**, 2101-2109.
- Slawinski, J. 1971. Chemiluminescence in the process of oxidative ring-opening of purpurogallinquinones. *Photochemistry and Photobiology*. **13**, 489-497.
- Slemons, L.O., Murray, J.W., Resing, J., Paul, B. and Dutrieux, P. 2010. Western Pacific coastal sources of iron, manganese, and aluminum to the Equatorial Undercurrent. *Global Biogeochemical Cycles*. **24**. Doi: 10.1029/2009gb003693.
- Smirnov, A., Holben, B.N., Kaufman, Y.J., Dubovik, O., Eck, T.F., Slutsker, I., Pietras, C., and Halthore, R.N. 2002. Optical Properties of Atmospheric Aerosol in Maritime Environments. *Journal of the Atmospheric Sciences*. **59**, 501-523.

- Smith, D.C and Azam, F. 1992. A simple, economical method for measuring bacterial protein synthesis rates in seawater using ^3H -leucine. *Marine Microbial Foodwebs*. **6**, 107-114.
- Smith, S.V., 1984. Phosphorus versus nitrogen limitation in the marine environment. *Limnology and Oceanography*, **29**, 1149-1160.
- Sohrin, Y., Urushihara, S., Nakatsuka, S., Kono, T., Higo, E., Minami, T., Norisuye, K. and Umetani, S. 2008. Multielement determination of GEOTRACES key trace metals in seawater by ICPMS after preconcentration using an ethylenediaminetriacetic acid chelating resin. *Analytical Chemistry*. **80**, 6267-6273.
- Spokes, L.J., Jickells, T.D. and Lim, B. 1994. Solubilisation of aerosol trace metals by cloud processing: A laboratory study. *Geochimica et Cosmochimica Acta*. **58**, 3281-3287.
- Spokes, L., Jickells, T. and Jarvis, K. 2001. Atmospheric inputs of trace metals to the northeast Atlantic Ocean: the importance of southeasterly flow. *Marine Chemistry*. **76**, 319-330.
- Satham, P. J., German, C. R. and Connelly, D. P. 2005. Iron (II) distribution and oxidation kinetics in hydrothermal plumes at the Kairei and Edmond vent sites, Indian Ocean. *Earth and Planetary Science Letters*. **236**, 588-596.
- Satham, P. J., Yeats, P.A. and Landing, W.M. 1998. Manganese in the eastern Atlantic Ocean: processes influencing deep and surface water distributions. *Marine Chemistry*. **61**, 55-68.
- Stieg, S. and Nieman, T.A. 1977. Determination of trace concentrations of cobalt(II) and other metals by the chemiluminescent oxidation of gallic acid. *Analytical Chemistry*. **49**, 1322-1325.
- Steinberg, D.K., Carlson, C. A., Bates, N. R., Johnson, R.J., Michaels, A. F., and Knap, A.H. 2001. Overview of the US JGOFS Bermuda Atlantic Time-series Study (BATS): a decade-scale look at ocean biology and biogeochemistry. *Deep Sea Research Part II: Topical Studies in Oceanography*. **48**, 1405-1447.
- Stramma, L., Huttel, S., Schafstall, J. 2005. Water masses and currents in the upper tropical northeast Atlantic off northwest Africa. *Journal of Geophysical Research*, 110(C12006). Doi: 10.1029/2005JC002939.

- Stramma, L. and Schott, F. 1999. The mean flow of the tropical Atlantic Ocean. *Deep Sea Research Part II: Topical Studies in Oceanography*. **46**, 279-303.
- Strzepek, R. F., Maldonado, M.T., Higgins, J.L., Hall, J., Safi, K., Wilhelm, S.W. and Boyd, P.W. 2005. Spinning the "Ferrous Wheel": the importance of the microbial community in an iron budget during the FeCycle experiment. *Global Biogeochemical Cycles*. **19**. Doi: 10.1029/2005GB002490.
- Sunda, W.G. and Huntsman, S.A. 1995a. Cobalt and zinc inter-replacement in marine phytoplankton: biological and geochemical implications. *Limnology and Oceanography*. **40**, 1404-1417.
- Sunda, W.G., and Huntsman, S.A. 1995b. Iron uptake and growth limitation in oceanic and coastal phytoplankton. *Marine Chemistry*. **50**, 189-206.
- Sundby, B., Anderson, L.G., Hall, P.O. J., Iverfeldt, Å. And Rutgers van der Loeff, M..M. and Westerlund, S.F. G. 1986. The effect of oxygen on release and uptake of cobalt, manganese, iron and phosphate at the sediment-water interface. *Geochimica et Cosmochimica Acta*. **50**, 1281-1288.
- Sultan, B., and Janicot, S. 2000. Abrupt shift of the ITCZ over West Africa and intra-seasonal variability. *Geophysical Research Letters*. **27**, 3353-3356.
- Tagliabue, A., Bopp, L., Dutay, J.-C., Bowie, A.R., Chever, F., Jean-Baptiste, P., Bucciarelli, E., Lannuzel, D., Remenyi, T., Sarthou, G., Aumaont, O., Gehlen, M. and Jeandel, C. 2010. Hydrothermal contribution to the oceanic iron inventory, *Nature Geoscience*. **3**, 252-256.
- Tarran, G.A., Heywood, J.L. and Zubkov, M.V. 2006. Latitudinal changes in the standing stocks of nano- and picoeukaryotic phytoplankton in the Atlantic Ocean. *Deep Sea Research Part II: Topical Studies in Oceanography*. **53**, 1516-1529.
- Tchernia, P. 1980. *Descriptive Regional Oceanography*. New York: Pergamon.
- Tebo, B., Nealson, K., Emerson, S. and Jacobs, L. 1984. Microbial mediation of Mn(II) and Co(II) precipitation at the O₂/H₂O₂ interfaces in two anoxic fjords. *Limnology and Oceanography*. **29**, 1247-1258.

- Thuróczy, C.-E., Boyé, M., and Losno, R., 2010. Dissolution of cobalt and zinc from natural and anthropogenic dusts in seawater. *Biogeosciences*. **7**, 1927-1936. Doi: 10.5194/bg-7-1927-2010.
- Tian, Z., Olliver, P., Veron, A., and Church T.M., 2008. Atmospheric Fe deposition modes at Bermuda and the adjacent Sargasso Sea, *Geochemistry, Geophysics, Geosystems*. **9**. Doi: 10.1029/2007GC001868.
- Timmermans, K.R., Snoek, J., Gerringa, L.J.A., Zondervan, I., de Baar, H.J.W. 2001. Not all eukaryotic algae can replace zinc with cobalt: *Chaetoceros calcitrans* (Bacillariophyceae) versus *Emiliana huxleyi* (Prymnesiophyceae). *Limnology and Oceanography*. **46**, 699-703.
- Toggweiler, J. R., Dixon, K. and Broecker W. S. 1991. The Peru Upwelling and the Ventilation of the South Pacific Thermocline. *Journal of Geophysical Research*. **96**, 20467-20497. Doi: 10.1029/91JC02063.
- Toner, B. M., Fakra, S.C., Manganini, S.J., Santelli, C.M., Marcus, M.A., Moffett, J.W., Rouxel, O., German, C.R. and Edwards, K.J. 2009. Preservation of iron(II) by carbon-rich matrices in a hydrothermal plume. *Nature Geoscience*. **2**, 197-201.
- Tortell, P.D., Maldonado, M.T., Granger, J. and Price, N.M. 1999. Marine bacteria and biogeochemical cycling of iron in the oceans. *FEMS Microbiology Ecology*. **29**, 1-11.
- Tosoh Bioscience. 2008. <http://separations.us.tosohbioscience.com/Products/ProcessMedia/ByMode/AFC/ToyopearlAF-Chelate-650.htm>
- Turner, A., and Millward, G.E. 2002. Suspended particles: their role in estuarine biogeochemical cycles. *Estuarine, Coastal and Shelf Science*. **55**, 857-883.
- Turk, K.A., Rees, A.P., Zehr, J.P., Pereira, N., Swift, P., Shelley, R. Lohan, M., Woodward, E.M.S. and Gilbert, J. 2011. Nitrogen fixation and nitrogenase (nifH) expression in tropical waters of the eastern North Atlantic. *ISME Journal*. Doi: 10.1038/ismej.2010.205.
- Tyrrell, T. 1999. The relative influences of nitrogen and phosphorus on oceanic primary production. *Nature*, **400**, 525-531.

- Ussher, S.J., Achterberg, E.P., Sarthou, G., Laan, P., de Baar, H.J.W. and Worsfold, P.J. 2010. Distribution of size fractionated dissolved iron in the Canary Basin. *Marine Environmental Research*. **70**, 46-55.
- Ussher, S. J., Yaqoob, M., Achterberg, E. P., Nabi, A., and Worsfold, P. J. 2005. Effect of model ligands on iron redox speciation in natural waters using flow injection with luminol chemiluminescence detection, *Analytical Chemistry*. **77**, 1971-1978.
- van den Berg, C.M.G. 1995. Evidence for organic complexation of iron in seawater. *Marine Chemistry*. **50**, 139-157.
- Vega, M. and van den Berg, C.M.J. 1997. Determination of cobalt in seawater by catalytic adsorptive cathodic stripping voltammetry. *Analytical Chemistry*. **69**, 874-881.
- Véron, A.J. and T.M. Church (1997), Use of stable lead isotopes and trace metals to characterize air mass sources into the eastern North Atlantic, *Journal of Geophysical Research*. **102**. Doi:10.1029/97JD01527.
- Vink, S. and Measures, C. I. 2001. The role of dust deposition in determining surface water distributions of Al and Fe in the South West Atlantic. *Deep Sea Research Part II: Topical Studies in Oceanography*. **48**, 2787-2809.
- Vraspir, J.M. and Butler, A., 2009. Chemistry of marine ligands and siderophores. *Annual Review of Marine Science* 2009. **1**, 43-63.
- Wallace, D.W.R., and Bange, H.W. 2004. Introduction to special section: Results of the Meteor 55: Tropical SOLAS Expedition. *Geophysical Research Letters*. **31**. Doi: 10.1029/2004gl021014.
- Warnken, K. W., Tang, D., Gill, G.A. and Santschi, P.H. 2000. Performance optimization of a commercially available iminodiacetate resin for the determination of Mn, Ni, Cu, Cd and Pb by on-line preconcentration inductively coupled plasma-mass spectrometry. *Analytica Chimica Acta*. **423**, 265-276.
- Welschmeyer, N.A. 1994. Fluorometric analysis of chlorophyll a in the presence of chlorophyll b and pheopigments. *Limnology and Oceanography*. **39**, 1985-1992.
- Wilhelm, S.W. and Trick, C.G. 1995. Effects of vitamin B-12 concentration on chemostat cultured synechococcus strain PCC-7002. *Canadian Journal of Microbiology*. **41**, 145-151.

- Willie, S. N., Iida, Y., and McLaren, J.W. 1998. Determination of Cu, Ni, Zn, Mn, Co, Pb, Cd and V in seawater using flow injection ICP-MS. *Atomic Spectroscopy*. **19**, 67-72.
- Willie, S. N., Lam, J.W.H., Yang, L. and Tao, G. 2001. On-line removal of Ca, Na and Mg from iminodiacetate resin for the determination of trace elements in seawater and fish otoliths by flow injection ICP-MS. *Analytica Chimica Acta*. **447**, 143-152.
- Witter, A. E., Lewis, B.L. and Luther III, G.W. 2000. Iron speciation in the Arabian Sea. *Deep Sea Research Part II: Topical Studies in Oceanography*. **47**, 1517-1539.
- Woodward, E.M.S., Rees, A.P., and Stephens, J.A. 1999. The influence of the south-west monsoon upon the nutrient biogeochemistry of the Arabian Sea. *Deep Sea Research Part II: Topical Studies in Oceanography*. **46**, 571-591.
- Wong, G. T. F., Pai, S.-C., Chung, S.-W. 1995. Cobalt in the West Philippine Sea, *Oceanologica Acta*. **18**, 631-638.
- Wu, J. and Boyle, E. 2002. Iron in the Sargasso Sea: Implications for the processes controlling dissolved Fe distribution in the ocean, *Global Biogeochemical Cycles*. **16**. Doi:10.1029/2001GB001453.
- Wu, J., Sunda, W., Boyle, E. and Karl, D.M. 2000. Phosphate depletion in the western North Atlantic Ocean. *Science*. **289**, 759-762.
- Xu W, Sandford, R.C., Worsfold, P.J., Carlton, A. and Hanrahan, G. 2005. Flow Injection Techniques in Aquatic Environmental Analysis: recent applications and technological advances. *Critical Reviews in Analytical Chemistry*. **35**, 237-246.
- Zeebe, R.E. and Archer, D., 2005. Feasibility of ocean fertilization and its impact on future atmospheric CO₂ levels. *Geophysical Research Letters*. **32**, DOI: 10.1029/2005GL022449.
- Zehr, J.P., Jenkins, B.D., Short, S.M. and Steward, G.F. 2003. Nitrogenase gene diversity and microbial community structure: a cross-system comparison. *Environmental Microbiology*. **5**, 539-554.
- Zehr, J.P. and Paerl, H.W. 2008. Molecular ecological aspects of nitrogen fixation in the marine environment. In: Kirchman, D.L. (ed). *Microbial*

Ecology of the Oceans. 2nd ed. Durham, NC: Wiley-Liss Inc., pp 481–525.

- Zubkov, M.V. and Burkill, P.H. 2006. Syringe pumped high speed flow cytometry of oceanic phytoplankton. *Cytometry Part A*. **69A**, 1010-1019.
- Zubkov, M.V., Sleigh, M.A., Burkill, P.H., and Leakey, R.J.G. 2000. Bacterial growth and grazing loss in contrasting areas of North and South Atlantic. *Journal of Plankton Research*. **22**, 685-711.

Determination of total dissolved cobalt in UV-irradiated seawater using flow injection with chemiluminescence detection

Rachel U. Shelley^{1,2*}, Bernhard Zachhuber³, Peter N. Sedwick⁴, Paul J. Worsfold^{1,2}, Maeve C. Lohan^{1,2}

¹Marine Institute, University of Plymouth, UK

²School of Geography, Earth and Environmental Sciences, University of Plymouth, UK

³Institute of Analytical Chemistry, Vienna University of Technology, Austria

⁴Ocean, Earth and Atmospheric Sciences, Old Dominion University, Norfolk, Virginia, USA

Abstract

A sensitive flow-injection method with chemiluminescence detection (FI-CL) for the determination of dissolved cobalt in open ocean samples, suitable for shipboard use has been developed. To date, FI methods for dissolved cobalt have been used only in coastal and estuarine waters. Therefore, significant modifications to existing methods were required, including (1) the use of a commercially available iminodiacetate (IDA) resin (Toyopearl AF-chelate 650M) in place of resin immobilized 8-hydroxyquinoline for online preconcentration and matrix removal, (2) the introduction of acidified ammonium acetate (pH 4) as a column-conditioning step before sample loading and rinse steps, and most importantly, (3) UV irradiation of acidified seawater samples to determine total dissolved cobalt, rather than an operationally defined fraction. This method had a detection limit of 4.5 pM (3 σ of the blank). The accuracy of the method was evaluated by determining total dissolved cobalt in acidified North Pacific deep seawater (1000 m) samples from the Sampling and Analysis of Iron (SAFe) program and NASS-5. The method yields a mean (\pm SD) value of 40.9 ± 2.6 pM ($n = 9$), which is in excellent agreement with the SAFe consensus value of 43 ± 4 pM, and 208 ± 30 pM for NASS-5 (certified value 187 ± 51 pM). This study demonstrates that UV irradiation is an essential step for the determination of total dissolved cobalt in seawater by FI-CL. The method was applied to vertical profiles from the Sargasso Sea, indicating that total dissolved cobalt is influenced by both biological and physical processes.

Cobalt is an essential micronutrient for phytoplankton growth in the oceans. It is the central metal cofactor in the vitamin B₁₂ (cobalamin) complex. In addition, cobalt is a metal cofactor in the enzyme carbonic anhydrase (CA), which is required for inorganic carbon acquisition by marine phytoplankton (Lane and Morel 2000). Whereas certain groups of phytoplankton (e.g., the centric diatoms) are able to substitute zinc for cobalt or cadmium as the metal cofactor in CA, others (particularly *Prochlorococcus* and *Synechococcus* spp.), hav-

ing an absolute requirement for cobalt, cannot (Sunda and Huntsman, 1995; Saito et al. 2002). Given that *Prochlorococcus* may be the most abundant autotroph in the ocean (Partensky et al. 1999) and responsible for a significant proportion of global photosynthesis (Goericke and Welschmeyer 1993; Campbell et al. 1994), there is a need to understand the factors that control the growth and distribution of this organism.

A combination of extremely low concentrations in the open ocean (~4–120 pM, e.g., Knauer et al. 1982; Martin et al. 1989; Saito et al. 2004) and the complexity of the seawater matrix (which contains the major seawater ions at concentrations 10⁹ greater than dissolved cobalt) makes the determination of dissolved cobalt in ocean waters a formidable challenge. Determination of dissolved cobalt therefore requires a preanalysis step that entails both the separation of the analyte from the bulk seawater matrix and preconcentration of the analyte to increase the effective sensitivity of the analytical method. These steps have been achieved in a variety of ways: (1) chelation/solvent extraction (Bruland et al. 1979; Martin and Gordon 1988), (2) voltammetric techniques (Saito and Moffett 2001), and (3) use of chelating ion-exchange resins

*Corresponding author: E-mail: *rachel.shelley@plymouth.ac.uk

Acknowledgments

The authors thank Geoffrey Smith for providing the SAFe samples used in the method development and Simon Ussher and Christopher Marsay for assistance collecting samples during the FeAST-6 cruise. The authors also thank Mak Saito and an anonymous reviewer for their invaluable comments on an earlier version of this manuscript. This work was funded by a University of Plymouth, Marine Institute PhD scholarship to R. U. Shelley and US National Science Foundation grant OCE-0550594 to P. N. Sedwick.

DOI 10.4319/lom.2010.8.352

(Sakamoto-Arnold and Johnson 1987; Cannizzaro et al. 2000; Sohrin et al. 2008; Milne et al. 2010). In recent years, the increased use of inductively coupled plasma mass spectrometry (ICP-MS) and flow injection (FI) techniques for trace metal analysis has resulted in widespread use of chelating ion exchange resins for separation and preconcentration.

Traditionally, the preconcentration resin of choice for the FI analysis of trace metals has contained 8-hydroxyquinoline (8-HQ) as the chelating group. Resin-immobilized 8-HQ is attractive, as it has a strong affinity for binding a number of trace metals of interest in seawater (Landing et al. 1986). Because resin-immobilized 8-HQ is not commercially available, however, it needs to be synthesized (Landing et al. 1986; Dierssen et al. 2001), which produces resins of varying quality. Commercially available chelating resins are arguably preferable since the quality of the resins is reproducible, and such resins have been successfully used in FI systems (e.g., Aguilar-Islas et al. 2006; Lohan et al. 2006) and combined with ICP-MS detection (Lohan et al. 2005; Sohrin et al. 2008; Milne et al. 2010). Commercially available resins that have been used for the analysis of trace metals in seawater include an NTA-type chelating resin for Fe and Cu (Lohan et al. 2005), an EDTA-type resin for Al, Cd, Co, Cu, Fe, Mn, Ni, Pb, and Zn (Sohrin et al. 2008), and Toyopearl AF-Chelate 650M resin, which contains tridentate iminodiacetate functional groups, for Al, Cd, Co, Cu, Mn, Ni, Pb, and Zn (Warnken et al. 2000; Ndung'u et al. 2003; Aguilar-Islas et al. 2006; Brown and Bruland 2008; Milne et al. 2010).

Flow injection systems are particularly well suited to oceanographic analyses, since they are portable and robust, contain relatively simple and inexpensive components, and offer analytical determinations over a dynamic range of as much as three orders of magnitude (e.g., Xu et al. 2005). Modern FI systems are capable of high sensitivity, although the limits of detection vary with the method of detection and the analyte. Flow injection systems can also be coupled with towed, trace metal-clean sampling devices, enabling the near-real-time determination of trace metals in surface ocean waters (e.g., Bowie et al. 2002; Bruland et al. 2005). In addition, FI methods are ideal for kinetic catalytic methods that use the analyte of interest as a reaction catalyst, resulting in highly sensitive analytical techniques (Resing and Mottl 1992; Measures et al. 1995; Aguilar-Islas et al. 2006). Previously developed FI methods for the determination of dissolved cobalt in coastal and estuarine waters have used the Trautz-Schorigen reaction (TSR), which involves the oxidation of either gallic acid (3,4,5-trihydroxybenzoic acid; Sakamoto-Arnold and Johnson, 1987) or pyrogallol (Cannizzaro et al. 2000) with hydrogen peroxide in the presence of cobalt as a catalyst to produce chemiluminescence emission in the visible region.

The aim of the work described in this article was to develop an FI method that can determine total dissolved cobalt in open-ocean waters and to highlight the need to UV-irradiate seawater samples before determination of dissolved cobalt.

The recent launch of the international GEOTRACES program, which aims to determine trace metal concentrations in diverse oceanic regions, requires accurate methods that are highly sensitive. The focus of the study described here was the analysis of dissolved cobalt in open-ocean seawater, for which no FI method has been developed to date. This method was then applied to water column samples collected from the oligotrophic Sargasso Sea in June 2008.

Materials and procedures

Apparatus—A schematic diagram of the flow-injection manifold used is shown in Fig. 1; it consists of an eight-channel peristaltic pump (Minipuls 3, Gilson); two micro-electronically actuated six-port, two-position injection valves (VICI, Valco Instruments); a photomultiplier tube (PMT, Hamamatsu H 6240-01) containing a quartz glass spiral flow cell (internal volume 130 μ L; Baumbach and Co.); and a thermostatic water bath (Grant). The peristaltic pump tubing used was two-stop accurate™ PVC (Elkay). All other manifold tubing was 0.8 mm i.d. PFA Teflon (Cole-Parmer). The FI manifold had one mixing coil (1.85 m) and one reaction coil (5 m). The reaction coil was constructed by French-knitting 5 m of 0.8 mm i.d. PFA Teflon tubing using a four-pronged knitting spool. Two acrylic columns (internal volume 70 μ L), with porous HDPE frits (BioVion F, 0.75 mm thick), were incorporated in-line, one on the sample-buffer line to remove trace-metal impurities from the buffer solution, and a second for the preconcentration of cobalt and removal of the cations from the seawater sample matrix. Both columns were filled with Toyopearl AF-Chelate-650M resin (Tosohaas) (hereafter referred to as "IDA-Toyopearl"). The direction of flow through the cleanup column was one-way, so it was necessary to reverse the column at the end of each day to prevent the resin from becoming compacted. This was not required for the sample preconcentration column, which was loaded and eluted in opposing flow directions. The T-piece before the 1.85-m mixing coil, the mixing coil itself, and the 5-m reaction coil were maintained at 60°C by placing them inside a thermostatic water bath (Grant). The data acquisition module (Ruthern Instruments) and valve control software (LabVIEW v. 7.1) were operated using a laptop computer (Dell). To minimize contamination, all sample handling was carried out in a Class-100 clean bench. The FI system was flushed daily and after any configuration changes (such as pump tube or reagent replacement) with 1 M HCl solution.

Reagents—Unless otherwise stated, all chemicals were obtained from Fisher Scientific, and used as received. All solutions were prepared inside a Class-100 clean bench using ultra-high-purity (UHP) water (≥ 18.2 M Ω cm, Elgastat Maxima). The eluent, 0.1 M hydrochloric acid (HCl), was prepared by diluting 8.8 mL of 10 M ultrapure subboiling distilled HCl (SpA, Romil) to 1 L in UHP water. The 0.05 M ammonium acetate column rinse and conditioning solution was prepared by dissolving 3.8 g of ammonium acetate crys-

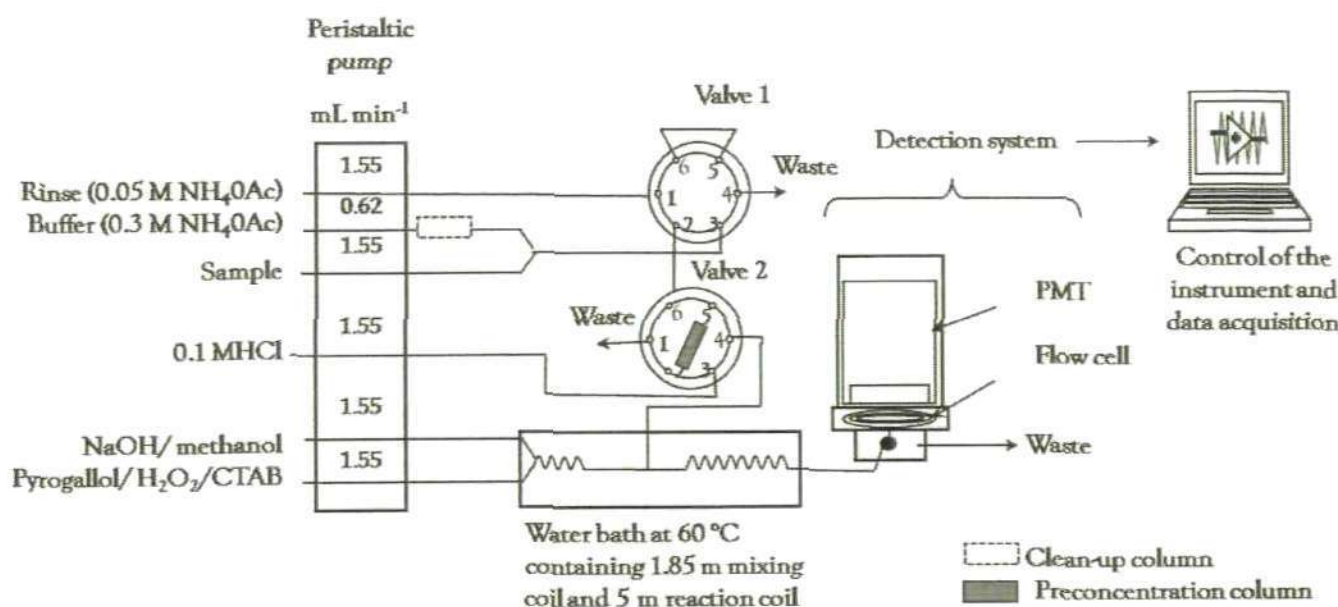


Fig. 1. FI-CL manifold configuration for the determination of total dissolved cobalt in seawater.

tals in 1 L UHP water and adjusting to pH 4 with 3.8 mL of 10 M ultrapure HCl (SpA, Romil). The 0.3-M ammonium acetate sample buffer solution was also prepared in UHP water from ammonium acetate crystals (23.11 g L⁻¹), and the acidified seawater samples were buffered online to between pH 5.2 and 5.5 by mixing with this solution. Because the detection limit of FI methods is often limited by the blank value rather than the sensitivity of the instrumental technique (Bowie and Lohan 2009), the potential contribution to the blank from the sample buffer solution was minimized by using a cleanup column (identical to the preconcentration column) on the sample buffer line. The 0.17-M sodium hydroxide (NaOH) reaction buffer solution was prepared by dissolving sodium hydroxide (NaOH) pellets (6.7 g L⁻¹) in 1 L solution (20% vol/vol methanol [HPLC grade], 80% vol/vol UHP water). The 50 mM pyrogallol reagent was prepared by sonicating 6.30 g pyrogallol and 9.12 g acetyltrimethylammonium bromide (CTAB) in UHP water; when the pyrogallol and CTAB were fully dissolved, 58.4 mL of 35% hydrogen peroxide (H₂O₂) was added, and the solution was diluted to 1 L with UHP water. As the pyrogallol solution is reportedly stable for only 48 hours (Cannizzaro 2001), this reagent was prepared daily as required.

Sample collection and pretreatment—Surface seawater (0–1 m depth) was collected using a trace metal-clean pole sampler: two 1-L widemouth low-density polyethylene (LDPE, Nalgene) bottles were secured in a Plexiglas frame at the end of a bamboo pole, which was extended from the ship's stern for sample collection while backing slowly into the wind. Water column samples were collected in modified 5-L Teflon-lined external closure Niskin-X samplers (General Oceanics) sus-

pended from a Kevlar line using a stainless-steel end weight and solid PVC messengers (Sedwick et al. 2005). Samples were immediately filtered at sea inside a shipboard Class-100 clean container laboratory, through a 0.4- μ m pore-size Supor Acropak filter capsule (Pall) that was prerinsed with 5 L UHP water followed by several hundred milliliters of sample. Filtered samples were acidified to 0.024 M with ultrapure HCl (SpA, Romil) before analysis.

Procedure—The peristaltic pump (Minipuls 3, Gilson) was set at 5.50 rpm to attain the flow rates shown in Fig. 1. After stabilization of the baseline (typically 30–45 min), with valve 1 and valve 2 in position B, acidified ammonium acetate was passed through the preconcentration column for 40 s. Valve 1 was then switched to position A, and a buffered sample was loaded onto the preconcentration column for 300 s. Valve 1 was then switched to position B, and the preconcentration column was rinsed for 40 s with the acidified ammonium acetate solution. After this rinse step, valve 2 was switched to position A for 90 s, and the eluent (0.1 M HCl) was passed over the chelating resin in the opposite direction to that of the loading phase, thus eluting the cobalt from the preconcentrating resin into the reagent stream that was then carried to the PMT detector. In total, one complete analytical cycle took 7.8 min. During the load and rinse phases, the eluting acid bypassed the column and mixed with the other reagents to produce the baseline signal.

Standardization—The analytical system was calibrated daily by simple linear regression of standard curves. Stock standard solutions were prepared in acidified UHP water by serial dilution of a 17-mM cobalt atomic absorption standard solution (Spectrosol). Working standards (additions of 12.5–75 pM) were

prepared in acidified low-trace-metal seawater (Atlantic Ocean surface seawater collected from 28°51'S, 4°41'W; total dissolved cobalt 13.7 ± 2.7 pM). Standards were run at the beginning and end of each program of analysis in triplicate, and concentrations were calculated from peak heights. Standard curves were linear ($r^2 > 0.99$) up to concentrations of 2 nM.

Assessment

In this section, an assessment of the commercially available chelating resin, Toyopearl AF-chelate 650M, in the preconcentration step of the FI-CL method for the determination of total dissolved cobalt in seawater is presented. The accuracy of the method was assessed using SAFE seawater reference samples, and the method was applied to the determination of total dissolved cobalt in water-column profiles from the Sargasso Sea. The key analytical parameters are shown in Table 1. Of particular interest is the improvement in detection limit of this FI-CL method compared with a previously published FI method (the average detection limit of this new method was 4.5 pM, c.f. ~ 8 pM for the method of Sakamoto-Arnold and Johnson 1987), and the wide dynamic range of this method (more than three orders of magnitude, ~ 4.5 –2000 pM).

Online chelating resins—The commercially available IDA-Toyopearl chelating resin was compared with resin-immobilized 8-HQ, which has been used in previous FI-CL methods for cobalt determination (Sakamoto-Arnold and Johnson 1987; Cannizzaro et al. 2000). Figure 2 shows the FI elution profiles for resin-immobilized 8-HQ and IDA-Toyopearl resin. The same analytical conditions were used for both resins to allow a direct comparison. The use of IDA-Toyopearl provided consistently higher sensitivity and sharper elution profiles, e.g., for a 50-pM Co standard addition to seawater (Figure 2), use of IDA-Toyopearl gave a peak height of 1.28 mV, compared with 0.59 mV for resin-immobilized 8-HQ.

A comparison of the characteristics of the two resins is presented in Table 2. One of the advantages of IDA-Toyopearl is its greater binding capacity compared with resin-immobilized 8-HQ (25 – 45 $\mu\text{Eq mL}^{-1}$ versus 10 $\mu\text{Eq mL}^{-1}$, respectively). The breakthrough capacity (defined as the concentration of cobalt sorbed to the resin before 5% of the total concentration of the analyte in the eluant was detected) of the two resins (profiles not shown) was determined using inductively coupled plasma optical emission spectroscopy detection (ICP-OES, Varian 725-ES). An acidified 10- μM cobalt solution (pH 1.7) was buffered

to pH 5.2 and loaded onto a column containing a preconcentration resin (either IDA-Toyopearl or 8-HQ). Cobalt in the column eluent was continuously monitored by ICP-OES at an emission wavelength of 238.9 nm. The IDA-Toyopearl resin retained 25.3 nM Co before the 5% breakthrough limit was exceeded, compared with 13.4 nM Co for the resin-immobilized 8-HQ. Therefore, IDA-Toyopearl was selected as the preferred chelating resin for this method.

Reaction conditions—

Column-loading pH: Using ICP-MS as a detection system, Willie et al. (1998; 2001) demonstrated that Toyopearl AF-Chelate-650M quantitatively preconcentrated cobalt from seawater over the pH range 5.0–6.0. In the present study, the optimum pH range for the quantitative preconcentration of cobalt from seawater samples was found to be 5.2–5.5. Seawater samples were buffered online with 0.3 M ammonium acetate solution. Ammonium acetate buffers effectively within the pH range 3.8–5.8 ($pK_a \approx 4.8$) and is therefore suitable for this FI-CL method. A critical component of cobalt determination is characterization of the blank: even very low-level contamination (≤ 10 pM) of reagents can obscure the accuracy of a data set. Because the buffer is loaded on the column for the same period as the sample, any cobalt in the buffer solution could constitute a significant contribution to the blank (Willie et al. 1998). Therefore, a cleanup column, packed with IDA-Toyopearl resin, was placed in the sample buffer line before the sample preconcentration column, to remove any cobalt that might be present in the buffer solution.

Column-conditioning and rinse step: Previous FI-CL methods using resin-immobilized 8-HQ for cobalt determination (Sakamoto-Arnold and Johnson 1987; Cannizzaro et al. 2000) used UHP water as a column rinse solution and did not use a column-conditioning step. On the other hand, FI methods that have used IDA-Toyopearl as the chelating resin have included a column-conditioning step using a buffer with a pH similar to that of the in-line buffered seawater sample to ensure an optimum pH in the resin column before sample preconcentration (Aguilar-Islas et al. 2006; Brown and Bruland 2008). The column-conditioning step removes any residual acid that remains from the previous sample elution step and ensures that the resin is no longer in the protonated form, which might otherwise reduce retention of the analyte and thereby lessen the sensitivity of the method. Willie et al. (2001) demonstrated that a 0.1-M ammonium acetate rinse

Table 1. Key analytical parameters.

Parameter	This study	Literature values
Detection limit (seawater), pM	4.5	~ 8 (Sakamoto-Arnold and Johnson 1987)
Detection limit (UHP water), pM	3.8	5 (Cannizzaro et al. 2000)
Linear range, pM	3.8–2000	5–850 pM (Cannizzaro et al. 2000)
Blanks, pM	4.2 ± 1.5	
RSD ($n = 9$)	$\leq 4\%$	

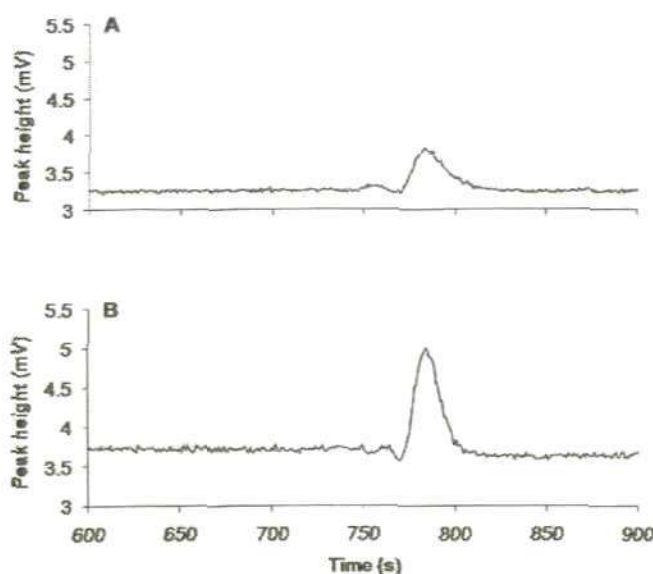


Fig. 2. Effect of two different chelating resins, resin-immobilized 8-hydroxyquinoline (A) and Toyopearl AF-Chelate 650M (B), on sensitivity and elution profile for a 50-pM standard in seawater using the same analytical conditions for both resins.

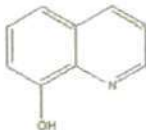
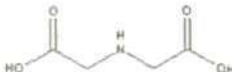
solution, buffered in the range of pH 3–5, was sufficient to eliminate seawater matrix components while still retaining the analyte on the IDA-Toyopearl chelating resin. Investigations during this study found that a further reduction in strength of this ammonium acetate rinse solution to 0.05 M did not result in reduced sensitivity, so the lower concentration was used. Thus the column-conditioning and rinse steps were incorporated in the analytical cycle to remove sea salt and excess acid from the preconcentration column before the sample loading and elution steps.

Eluting acid concentration: A range of ionic strengths of eluting acid are reported in the literature for FI systems using chelating resins for the preconcentration of dissolved cobalt from seawater. For example, Cannizzaro et al. (2000) used 0.05 M HCl to elute cobalt from an 8-HQ chelating resin. In this study, it was essential to maintain an optimum reaction pH of 10.35 ± 0.2 . A reaction pH outside this range resulted in changes to the baseline signal and significantly reduced sensitivity; e.g., at pH 10.6 the signal for a 25 pM cobalt addition was reduced by ~44%. To determine a suitable eluent strength while maintaining this reaction pH, eluents of 0.05, 0.1, and 0.5 M HCl were investigated, with standard additions of 25–75 pM cobalt in seawater. Increasing the acid concentration from 0.05 M (Cannizzaro et al. 2000) to 0.1 M HCl resulted in the rapid elution of cobalt from the IDA-Toyopearl resin and produced sharp sample peaks with CL detection, although there was no further improvement in peak shape between 0.1 and 0.5 M HCl. The increase in the eluting acid concentration (from 0.05 to 0.1 M HCl) required that the concentration of the NaOH solution be increased from 0.15 to 0.17 M to achieve the optimum reaction pH of 10.35.

Matrix effects and interferences: An investigation of the potential suppression of the cobalt CL signal by the major seawater cations was conducted by directly injecting solutions containing 9.9 nM cobalt in UHP water spiked with the chloride salts of Na, K, Ca, and Mg for 300 s (i.e., without a preconcentration step). These cobalt solutions were spiked with NaCl (10.7 g L⁻¹ Na), KCl (0.387 g L⁻¹ K), CaCl₂ (0.413 g L⁻¹ Ca), or MgCl₂ (1.29 g L⁻¹ Mg). A control solution contained cobalt and no added salts. Between injections, a solution of 0.05 M HCl (SpA, Romil) was injected for 120 s to rinse the previously injected solution.

With respect to the CL signal of the control cobalt solution, the alkaline earths produced the strongest reduction in chemiluminescence (51% and 55% reduction in signal for calcium

Table 2. Comparison of 8-HQ and IDA-Toyopearl resin characteristics.

	8-HQ ^a	Toyopearl AF-Chelate-650 M ^b
Bead	HW-75F	HW-65
Chelating group	8-hydroxyquinoline (8-HQ)	Iminodiacetic acid (IDA)
Chelating group structure		
Capacity	10 µEq mL ⁻¹	25–45 µEq mL ⁻¹
Particle size	32–63 µm	65 µm
Pore size	>1000 Å	1000 Å
Exclusion limit	50 MDa	5 MDa

^aLanding et al. (1986).

^bTosoh Bioscience (2008).

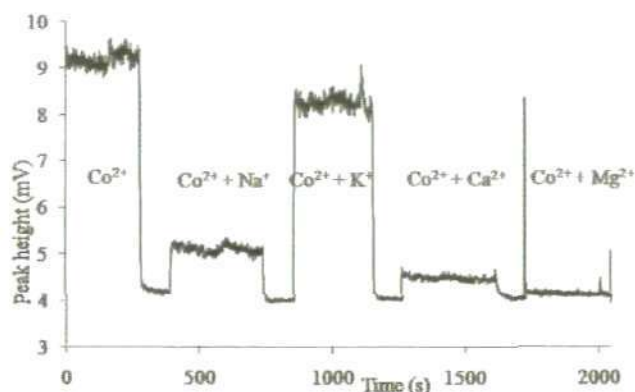


Fig. 3. Effect of the major seawater cations on the chemiluminescence signal (0.5 M Na⁺, 0.01 M K⁺, 0.01 M Ca²⁺, and 0.05 M Mg²⁺).

and magnesium, respectively; Fig. 3). This significant reduction in chemiluminescence, combined with a 44% signal reduction in the presence of sodium ions, illustrates the need for a matrix elimination step to remove the major seawater cations before the CL reaction and detection of the analyte.

For the analysis described here, the online preconcentration column must ideally have low affinity for the major ions in seawater, while quantitatively retaining the analyte on the resin. Elimination of the seawater ions can be achieved by rinsing the column with a dilute ammonium acetate solution before eluting the analyte with HCl. Even with the inclusion of this rinse step, however, some residual seawater matrix ions could still reduce the sensitivity of the method. Comparing standard additions of cobalt to seawater versus UHP water (12.5–75 pM), a 35% reduction in sensitivity was observed for standards prepared in seawater (data not shown). Consistent with this finding is the lower detection limit for standards prepared in UHP water compared with those prepared in seawater (Table 1). Therefore the sensitivity of this technique was monitored via calibration with standard additions (12.5–75 pM) before commencing analysis.

The potential for interference by the metal ions Ag⁺, Fe³⁺, Cu²⁺, Pb²⁺, Mn²⁺, and Cd²⁺ in the determination of Co²⁺ in seawater of the pyrogallol reaction was investigated by Cannizzaro et al. (2000). Of the ions tested, only Ag⁺ was found to cause a detectable interference, although it was concluded that this species was unlikely to interfere with cobalt analysis given the typical Ag concentrations in open ocean seawater (≤ 0.7 pM, Flegal et al. 1995).

Reaction temperature: Chemiluminescence reactions are sensitive to temperature, with the rate of reaction typically doubled for every 10°C increase in temperature. Cannizzaro et al. (2000) used a reaction temperature of 80°C; however, optimization experiments during this study showed that a reaction temperature of 60°C provided good sensitivity. The advantages of working at this lower temperature are twofold.

First, by working below the boiling point of methanol (64.7°C), the formation of bubbles in the NaOH/methanol reagent stream is avoided. Second, the use of this lower reaction temperature reduces evaporation losses from the thermostatic bath, thus avoiding the need to refill it (and potentially alter the reaction temperature) during the analysis.

Sample treatment for determination of total dissolved cobalt—

UV-irradiation: Similar to several other bioessential trace metals in seawater, a large fraction (>90%) of dissolved cobalt is complexed by uncharacterized organic ligands (Ellwood and van den Berg 2001). When using other analytical techniques, such as cathodic stripping voltammetry (CSV) and cation-exchange liquid chromatography with luminol chemiluminescence detection (LC-CL) as the analytical method, it is well established that it is necessary to break down these ligands to achieve full recovery of total dissolved cobalt (CSV, Donat and Bruland 1988, Vega and Van den Berg 1997, Saito and Moffett 2001, and Noble et al. 2008; LC-CL, Boyle et al. 1987). Because the degree of retention of organically bound cobalt by chelating resins is unknown, investigations were conducted to establish whether it was necessary to UV-irradiate seawater samples before determination of total dissolved cobalt by FI-CL. Previously acidified samples collected from 1000-m depth in the North Pacific subtropical gyre (30°N, 140°W) as part of the Sampling and Analysis of Iron (SAFE) program (Johnson et al. 2007) were analyzed to allow comparison between samples with and without UV pretreatment. Acidified SAFE samples were UV-irradiated in acid-washed quartz vials for 3 h using a 400-W medium-pressure Hg lamp (Photochemical Reactors). After UV irradiation, samples were decanted into acid-clean LDPE bottles and left for 48 h before analytical determination, to eliminate UV-generated free radicals that might otherwise interfere with the CL reaction. The concentration of total dissolved cobalt determined in UV-irradiated SAFE seawater samples was 40.9 ± 2.6 pM ($n = 9$), which was almost double the concentration measured in nonirradiated samples (25.4 ± 1.2 pM, $n = 8$). The results of this experiment demonstrate conclusively that UV irradiation is essential for the determination of total dissolved cobalt in acidified seawater by FI-CL.

There is evidence for the presence of strong, cobalt-binding organic ligands in seawater that have a stability constant (K_s) of 10^{16-360} (Saito and Moffett 2001; Saito et al. 2005) compared with the reported K_s value of $10^{12.08}$ for strong Fe(III)-binding ligands in seawater (Rue and Bruland 1997). However, in contrast to organic iron complexes, which appear to fully dissociate when seawater samples are acidified to pH 1.7 (Lohan et al. 2005), the results of this and earlier UV-irradiation experiments using other analytical techniques (e.g., Donat and Bruland 1988; Vega and van den Berg 1997; Noble et al. 2008; Milne et al. 2010) indicate that organic cobalt complexes do not completely dissociate at pH 1.7.

Although IDA-based resins such as Toyopearl AF-Chelate 650M are able to selectively complex free metal ions and other metal species that are thermodynamically and kinetically

labile, they may be unable to extract metals bound to strong organic ligands. Where it is necessary to increase pH to ≥ 5 before the preconcentration step, such as is the case for FI-CL analysis of acidified samples, some of the metal analyte may become recomplexed to form thermodynamically or kinetically inert complexes (in terms of chelation by the resin) with organic ligands present in the sample, and thus pass through the column without being retained on the resin. Unless the dissolved organic material (DOM) that contains these ligands is destroyed (e.g., by UV irradiation), such organic complexation may result in trace metal analytes not being fully retained by the preconcentrating resin (Ndung'u et al. 2003), and hence the determination of only the labile (rather than total) dissolved concentrations of trace metals such as cobalt. The recent GEOTRACES intercalibration exercise and program launch serves as a timely reminder that it is essential to UV-irradiate samples before determination of dissolved cobalt.

Addition of a reducing agent: The pyrogallol-FI-CL method described here determines dissolved cobalt by reducing the thermodynamically and kinetically labile cobalt fraction to Co(II). The SAFE samples were collected and acidified to pH 1.7 in 2004. Lohan et al. (2005) reported that the longer a sample was acidified, the greater the percentage of iron that exists as Fe(II). Noting the similarity between the redox speciation of iron and cobalt in seawater (both are present in the +2 and +3 oxidation states under typical seawater conditions), cobalt may similarly tend toward Co(II) in acidified seawater. However, to verify that the reduction of Co(III) to Co(II) was complete in this method, an experiment was conducted to investigate the effect of incorporating a strong reducing agent in the reaction scheme. A buffered 0.04-M solution of sodium sulfite (NaSO_3) was prepared by dissolving 0.202 g of NaSO_3 in 30 mL UHP water plus 10 mL of 0.4 M ammonium acetate buffer, to ensure no changes in the sample pH that could affect the sensitivity of the CL reaction. Before use, this solution was passed through two columns in series containing IDA-Toyopearl resin, to remove trace metal impurities; the first 10 mL of the purified NaSO_3 solution was discarded, and the next 30 mL was collected and left for at least 24 h to stabilize before the acidified SAFE seawater was spiked with 25 μL per 10 mL sample. Samples were then left at least 8 h, to allow time for the reduction of Co(III) to Co(II), before dissolved cobalt was determined by FI-CL. The samples used in this experiment were not UV-irradiated. Using a *t*-test, no significant difference ($P = 0.06$) was observed between samples with and without NaSO_3 addition (25.4 ± 1.2 and 30.5 ± 1.7 pM, respectively; $n = 8$), suggesting that the method effectively determines all dissolved cobalt in previously acidified seawater samples.

Saito et al. (2005) described natural cobalt-binding ligand complexes with stability constants greater than $10^{16.8}$ (c.f. $10^{11.48}$ – $10^{13.08}$ for iron-binding ligands in seawater; Rue and Bruland 1995) and reported that addition of excess Ni(II) ions did not liberate organically complexed cobalt. On this basis, it

was argued that organically bound cobalt was present as Co(III) complexes—a further parallel with iron biogeochemistry, since dissolved iron is thought to exist mainly as organically complexed Fe(III) in seawater (e.g., Rue and Bruland 1995). Acidification of samples may dissociate these organic complexes, releasing Co(III), which is then reduced to Co(II) over time, thus explaining the apparent lack of effect of the added reducing agent (see above). If this were the case, however, one would predict no increase in total dissolved cobalt determined after UV irradiation of acidified samples, which is inconsistent with the results presented here. This then implies that it may not be the redox chemistry of cobalt that is preventing complete recovery of total dissolved cobalt from acidified seawater samples on the IDA-Toyopearl resin, but rather that the acidified samples contain organic ligands that complex dissolved cobalt upon readjustment of the sample pH (Ndung'u et al. 2003; Saito et al. 2005).

The addition of a reducing agent resulting in no difference in cobalt concentrations has been previously reported by Vega and van den Berg (1997). However, their results contrast with results of a similar study by Donat and Bruland (1988), using sodium borohydride (NaBH_4) as the reducing agent, who found that it was still necessary to add a reducing agent even after samples had been UV-irradiated, to fully recover total dissolved cobalt. Vega and van den Berg (1997) argue that the reason for this contrast may result from the less extensive UV-irradiation step used by Donat and Bruland (1988). As no difference in cobalt concentration was observed between samples with and without addition of a reducing agent, it is suggested that the samples in this study contained Co(II).

Without UV irradiation, the dissolved cobalt concentration in the SAFE D2 reference samples was 38% lower. A similarly reduced concentration was observed by Donat and Bruland (1988) in their non-UV-irradiated samples, using CSV. However, the key differences between this study and Donat and Bruland's (1988) was the addition of reducing agent to samples after UV irradiation. It is therefore important to investigate the amount of time necessary to UV-irradiate open-ocean samples before analysis using SAFE or GEOTRACES reference samples. In addition, further insights might be gained by investigating the redox state of complexed cobalt during the analytical process.

Analytical figures of merit—

Blanks and detection limits: For this FI-CL method, the major contribution to the blank was from the addition of the ammonium acetate sample buffer. Although Cannizzaro et al. (2000) found no detectable signal from the added ammonium acetate buffer, this was not the case in the present work. The extremely low concentrations of cobalt in the open-ocean samples analyzed in this study required a fivefold increase in loading time compared with those used for estuarine samples (300 versus 60 s, respectively). Because the sample buffer and sample are loaded simultaneously, any cobalt present in the buffer potentially contributes to the analytical signal. There-

fore, a cleanup column (containing IDA-Toyopearl resin) was added to the sample buffer line to reduce the amount of cobalt loaded onto the preconcentration column. In common with other flow injection techniques, the manifold blank was determined by running an analytical cycle without the sample (e.g., loading the sample buffer only onto the preconcentration column) (Bowie and Lohan 2009), resulting in a concentration of 4.2 ± 1.5 pM ($n = 21$). The detection limit was calculated as the cobalt concentration corresponding to three times the SD of the blank, resulting in a detection limit of 4.5 pM ($n = 21$) in seawater.

Accuracy and precision: The accuracy of previous methods determining dissolved cobalt in seawater has been assessed using the North Atlantic Surface Seawater (NASS; National Research Council of Canada) certified reference material (CRM). In this study, a concentration of 208 ± 30 pM for total dissolved cobalt was determined in UV-irradiated NASS-5, which is within the certified range (187 ± 51 pM). This result is within error, and is consistent with the results of Vega and van den Berg's (1997) determination of total dissolved cobalt in UV-irradiated NASS-2. Like NASS-2, NASS-5 has a large standard deviation, and has a mean concentration that is up to 20 times greater than typical open-ocean surface concentrations of dissolved cobalt. Therefore, the combination of a large uncertainty and high cobalt concentration combined with the lack of a certified concentration of cobalt after UV irradiation renders this CRM unsuitable with respect to the determination of dissolved cobalt in open-ocean surface waters. Consequently, an alternative low-level cobalt reference sample was analyzed to assess the accuracy and precision of this FI-CL technique. The concentration of total dissolved cobalt was determined in acidified seawater samples (D2) collected from 1000-m depth in the North Pacific as part of the SAFE program (Johnson et al. 2007). Sample collection details were described by Johnson et al. (2007). The cobalt concentrations for the SAFE D2 reference samples after UV irradiation (40.9 ± 2.6 pM; $n = 9$) are in excellent agreement with results obtained for the same sample by other analytical techniques that also used a UV-pretreatment step (43 ± 3.2 pM, <http://es.ucsc.edu/~kbruland/GeotracesSaFe/kwbGeotracesSaFe.html>). The analytical precision of the method was determined from repeat analyses of the SAFE D2 reference sample, yielding an uncertainty of $\pm 4\%$ expressed as relative SD of the mean ($n = 9$). Samples that were not UV-irradiated were also in excellent agreement with the consensus values for non-UV-treated SAFE D2 samples (this study, 25.4 ± 1.2 pM, $n = 8$; SAFE D2 non-UV, 26.9 ± 4.7 pM).

From the data already submitted to the GEOTRACES/SAFE intercalibration Web site (<http://es.ucsc.edu/~kbruland/GeotracesSaFe/kwbGeotracesSaFe.html>) it has become apparent that a UV-irradiation step is necessary to determine total dissolved cobalt in the SAFE reference samples. At present, however, there is too much spread in the cobalt values for the SAFE reference samples, and further work needs to be conducted to investigate optimal UV-irradiation parameters (Bruland, pers. comm.). As

additional laboratories continue to submit data for SAFE and GEOTRACES reference samples, using UV pretreatment, confidence in the consensus values will increase.

Application to water column samples from the Sargasso Sea: This method was used to determine dissolved cobalt in samples from the FeAST-6 cruise in the Sargasso Sea, during which water column samples were collected in the region southeast of Bermuda. As an example, the vertical concentration profile of dissolved cobalt from the analysis of samples collected on June 6, 2008 from $31^{\circ}29'N$, $62^{\circ}45'W$, close to the Bermuda Atlantic Time Series (BATS) station, is shown in Fig. 4. The data shows a nutrientlike profile, but unlike a typical nutrientlike element, this profile exhibits surface enrichment (see Fig. 4). In contrast to Saito and Moffett (2001), who reported modest surface depletion (19 pM at 15 m), this study observed enrichment at a similar depth (40.2 pM at 10 m), followed by rapid depletion to a minimum of 25.3 ± 2.2 pM between 25 and 50 m, consistent with concentrations reported at the equivalent depths by Saito and Moffett (2001). The cobalt concentrations increased below 200 m, associated with remineralization below the base of the permanent pycnocline, to the maximum depth in this study (1000 m), where 70.1 ± 3.0 pM was determined, compared with 68.6 pM at the equivalent depth (1200 m) reported in Saito and Moffett (2001). The cobalt concentration at 300 m depth was higher in this study compared to Saito and Moffett (2001) (49.1 ± 0.9 pM, c.f. 33.7 pM), indicative of a shallower permanent pycnocline, possibly associated with the passing of a cyclonic eddy. The FeAST-6 cruise took place during a season of high eolian dust deposition, the effect of which was evident by the degree of enrichment of aluminum in surface waters (data not shown). In apparent contrast to conclusions drawn from analysis of time-series data of total dissolved cobalt from the MITESS mooring near the BATS station (Saito and Moffett 2002), these findings indicate that there may be a correlation

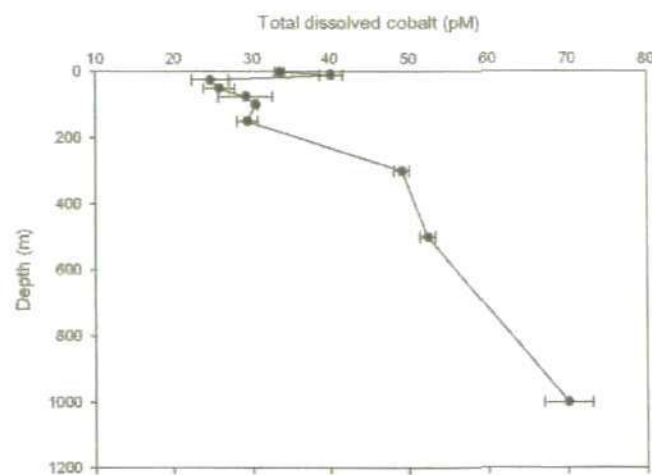


Fig. 4. Vertical concentration profile of total dissolved cobalt (dCo) in the subtropical North Atlantic Ocean ($31^{\circ} 29'N$, $62^{\circ} 45'W$) with error bars of ± 1 SD.

between eolian dust deposition events and surface concentrations, raising questions about the nature of the primary control of this micronutrient in the Sargasso Sea. However, the data reported by Saito and Moffett (2002) is from the MITESS sampler, which is moored at ≤ 40 m, below the seasonal pycnocline, and may therefore mask any atmospheric inputs that would be isolated in the shallow mixed layer, thus obscuring any potential relationship.

Discussion

The UV-irradiation experiment represents an important analytical development in the analysis of dissolved cobalt in seawater by FI-CL, in that it demonstrates the absolute requirement for UV irradiation to liberate organically complexed cobalt in acidified samples before FI-CL determination of dissolved cobalt. Previous FI-CL methods (and other analytical techniques) that did not include this step may have measured only dissolved labile cobalt (as defined in Noble et al. 2008). The use of the commercially available resin Toyopearl AF-Chelate 650M improves the reproducibility of the method and simplifies the preparation of the analytical system, as there is no need to synthesize the chelating resin. The introduction of a resin-conditioning step (acidified ammonium acetate rinse) also led to increased sensitivity. In addition to highlighting the need to UV-irradiate seawater samples and the advantages of using a column-conditioning step, this method also demonstrates the importance of effective sample buffering, both for the pH at which the sample is loaded onto the chelating resin column (pH 5.2–5.5), and the reaction pH of the combined reagent stream as it enters the detector (pH 10.35 ± 0.2). In this method, incorrect buffering results in a significant reduction of sensitivity.

The FI-CL method presented here is selective, has a low detection limit (4.5 pM), and is portable, making it an ideal method for determining total dissolved cobalt in open ocean regimes. The suitability of this method for shipboard use enables the mapping of total dissolved cobalt distributions while at sea, which make this technique an attractive analytical tool for examining high-resolution spatial and temporal trends in the oceanic distribution of cobalt. Although CSV can be used to determine total dissolved cobalt, FI methods are generally less time-consuming. Given that cobalt is an essential micronutrient for carbon acquisition for certain key groups of phytoplankton (e.g., *Prochlorococcus*, *Synechococcus*), it is important to attain high-quality data to further our understanding of the biogeochemical cycling of this element in marine waters.

Comments and further recommendations

The relative simplicity and low risk of contamination make this method well suited for use in the laboratory and for shipboard analyses. The implementation of an automated sample selection valve could further reduce the risk of contamination associated with transferring the sample line from one sample

to the next. In this study, the preconcentration columns were fabricated according to Cannizzaro et al. (2000). Commercially available columns potentially improve the reliability and reproducibility of the separation/preconcentration step by minimizing leakage and contamination. Such columns have successfully been used in other FI applications (e.g., Aguilar-Islas et al. 2006; Lohan et al. 2006), and would likely be suitable for application in this method.

Owing to the absence of a suitably low-concentration certified reference material for cobalt, it is recommended that SAFE and GEOTRACES seawater reference samples be used for quality assurance when analyzing open-ocean samples. The consensus values of the SAFE reference seawater materials are now available at: <http://es.ucsc.edu/~kbruland/GeotracesSafe/kwbGeotracesSafe.html> and www.geotraces.org/Intercalibration.html#standards_certifiedrefs. The GEOTRACES values are soon to be published on the same two Web sites. However, a cautionary note must be added at this point with regard to the cobalt numbers. A UV-irradiation step is necessary to determine total dissolved cobalt in the SAFE reference samples. However, at present there is still too much variation in the values, even after UV irradiation, to make a definitive conclusion. Consequently more research needs to be performed to evaluate the intensity and duration of the UV pretreatment required to release all the cobalt for the various analytical methods. Therefore, although there is a slight caveat attached to the accuracy of the cobalt values, the use of these low-metal, open-ocean reference materials is strongly advocated as they will likely benefit scientists determining dissolved cobalt and other trace elements in much the same way as they have done for the determination of total dissolved iron in seawater.

References

- Aguilar-Islas, A. M., J. A. Resing, and K. W. Bruland. 2006. Catalytically enhanced spectrophotometric determination of manganese in seawater by flow injection analysis with a commercially available resin for on-line preconcentration. *Limnol. Oceanogr. Methods* 4:105-113.
- Bowie, A. R., E. P. Acterberg, P. N. Sedwick, S. Ussher, and P. J. Worsfold. 2002. Real-time monitoring of picomolar concentrations of iron(II) in marine waters using automated flow injection-chemiluminescence instrumentation. *Env. Sci. Tech.* 36:4600-4607 [doi:10.1021/es020045v].
- , and M. C. Lohan. 2009. Determination of iron in seawater. p. 235-257. *In* O. Wurl [ed.] *Practical guidelines for the analysis of seawater*. CRC Press.
- Brown, M. T., and K. W. Bruland. 2008. An improved flow-injection analysis method for the determination of dissolved aluminum in seawater. *Limnol. Oceanogr. Methods* 6:87-95.
- Boyle, E. A., B. Handy, and A. Van Geen. 1987. Cobalt determination in natural waters using cation-exchange liquid chromatography with luminol chemiluminescence detection. *Anal. Chem.* 59:1499-1503 [doi:10.1021/ac00138a005].

- Bruland, K. W., R. P. Franks, G. A. Knauer, and J. H. Martin. 1979. Sampling and analytical methods for the determination of copper, cadmium, zinc and nickel in seawater. *Anal. Chim. Acta.* 105:233-245 [doi:10.1016/S0003-2670(01)83754-5].
- , E. L. Rue, G. J. Smith, and G. R. DiTullio. 2005. Iron, macronutrients and diatom blooms in the Peru upwelling regime: brown and blue waters of Peru. *Mar. Chem.* 93:81-103 [doi:10.1016/j.marchem.2004.06.011].
- Campbell, L., Nolla, H. A., and Vulot, D. 1994. The importance of *Prochlorococcus* to community structure in the central North Pacific Ocean. *Limnol. Oceanogr.* 39:954-961 [doi:10.4319/lo.1994.39.4.0954].
- Cannizzaro, V. 2001. Determination of Co and Mn in marine waters using flow injection with chemiluminescence detection. PhD thesis, University of Plymouth.
- , A. R. Bowie, A. Sax, E. P. Achterberg, and P. J. Worsfold. 2000. Determination of cobalt and iron in estuarine and coastal waters using flow injection with chemiluminescence detection. *Analyst* 125:51-57 [doi:10.1039/a907651d].
- Dierssen, H., W. Balzer, and W. M. Landing. 2001. Simplified synthesis of an 8-hydroxyquinoline chelating resin and a study of trace metal profiles from Jellyfish Lake, Palau. *Mar. Chem.* 73:173-192 [doi:10.1016/S0304-4203(00)00107-9].
- Donat, J. R., and K. W. Bruland. 1988. Direct determination of dissolved cobalt and nickel in seawater by differential pulse cathodic stripping voltammetry preceded by adsorptive collection of cyclohexane-1,2-dione dioxime complexes. *Anal. Chem.* 60:240-244 [doi:10.1021/ac00154a011].
- Ellwood, M. J., and C. M. G. Van den Berg. 2001. Determination of organic complexation of cobalt in seawater by cathodic stripping voltammetry. *Mar. Chem.* 75:33-47 [doi:10.1016/S0304-4203(01)00024-X].
- Flegel, A. R., S. A. A. Sañudo-Wilhelmy, and G. M. Scelfo. 1995. Silver in the Eastern Atlantic Ocean. *Mar. Chem.* 49:315-320 [doi:10.1016/0304-4203(95)00021-I].
- Goericke, R. A., and N. A. Welschmeyer. 1993. The marine prochlorophyte *Prochlorococcus* contributes significantly to phytoplankton biomass and primary production in the Sargasso Sea. *Deep Sea Res. Part I.* 40:2283-2294 [doi:10.1016/0967-0637(93)90104-B].
- Knauer, G. A., J. H. Martin, and R. M. Gordon. 1982. Cobalt in north-east Pacific waters. *Nature.* 297:49-51 [doi:10.1038/297049a0].
- Johnson, K. S., and others. 2007. Developing standards for dissolved iron in seawater. *EOS Trans. Am. Geophys. Union.* 88:131-132 [doi:10.1029/2007EO110003].
- Landing, W. M., C. Haraldsson, and N. Paxeus. 1986. Vinyl polymer agglomerate based transition metal cation chelating ion-exchange resin containing the 8-hydroxyquinoline functional group. *Anal. Chem.* 58:3031-3035 [doi:10.1021/ac00127a029].
- Lane, T. W., and F. M. M. Morel. 2000. A biological function for cadmium in marine diatoms. *Proc. Nat. Acad. Sci. U. S. A.* 97:4627-4631 [doi:10.1073/pnas.090091397].
- Lohan, M. C., A. M. Aguilar-Islas, R. P. Franks, and K. W. Bruland. 2005. Determination of iron and copper in seawater at pH 1.7 with a new commercially available chelating resin, NTA Superflow. *Anal. Chim. Acta* 530:121-129 [doi:10.1016/j.aca.2004.09.005].
- , ———, and K. W. Bruland. 2006. Direct determination of iron in acidified (pH 1.7) seawater samples by flow injection analysis with catalytic spectrophotometric detection: Application and intercomparison. *Limnol. Oceanogr. Methods* 4:164-171.
- Martin, J. H., and R. M. Gordon. 1988. Northeast Pacific iron distributions in relation to phytoplankton productivity. *Deep-Sea Res.* 35:177-196 [doi:10.1016/0198-0149(88)90035-0].
- , G. H. Knauer, D. M. Karl, and W. W. Broenkow. 1989. VERTEX: carbon cycling in the northeast Pacific. *Deep Sea Res. I.* 34:267-285.
- Measures, C. I., J. Yuan, and J. A. Resing. 1995. Determination of iron in seawater by flow injection analysis using in-line preconcentration and spectrophotometric detection. *Mar. Chem.* 50:3-12 [doi:10.1016/0304-4203(95)00022-J].
- Milne, A., W. Landing, M. Bizimis, and P. Morton. 2010. Determination of Mn, Fe, Co, Ni, Cu, Zn, Cd and Pb in seawater using high resolution magnetic sector inductively coupled mass spectrometry (HR-ICP-MS). *Anal. Chim. Acta* 665:200-7 [doi:10.1016/j.aca.2010.03.027].
- Ndung'u, K., R. P. Franks, K. W. Bruland, and A. R. Flegel. 2003. Organic complexation and total dissolved trace metal analysis in estuarine waters: Comparison of solvent-extraction graphite furnace atomic absorption spectrometric and chelating resin flow injection inductively coupled plasma-mass spectrometric analysis. *Anal. Chim. Acta* 481:127-138 [doi:10.1016/S0003-2670(03)00063-1].
- Noble, A. E., M. A. Saito, K. Maiti, and C. Benitez-Nelson. 2008. Cobalt, manganese, and iron near the Hawaiian Islands: A potential concentrating mechanism for cobalt within a cyclonic eddy and implications for the hybrid-type trace metals. *Deep Sea Res. II.* 55:1473-1490 [doi:10.1016/j.dsr2.2008.02.010].
- Partensky, F., W. R. Hess, and D. Vulot. 1999. *Prochlorococcus*, a marine photosynthetic prokaryote of global significance. *Microbiol. Mol. Biol. Rev.* 63:106-127.
- Resing, J. A., and M. J. Mottl. 1992. Determination of manganese in seawater by flow injection analysis using online preconcentration and spectrophotometric detection. *Anal. Chem.* 64:2682-2687 [doi:10.1021/ac00046a006].
- Rue, E. L., and K. W. Bruland. 1995. Complexation of iron (III) by natural organic ligands in the Central North Pacific as determined by a new competitive ligand equilibrium/adsorptive cathodic stripping voltammetric method. *Mar. Chem.* 50:117-138 [doi:10.1016/0304-4203(95)00031-L].
- , and ———. 1997. The role of organic complexation on

- ambient iron chemistry in the equatorial Pacific Ocean and the response of a mesoscale iron addition experiment. *Limnol. Oceanogr.* 42:901-910 [doi:10.4319/lo.1997.42.5.0901].
- Saito, M. A., and J. W. Moffett. 2001. Complexation of cobalt by natural organic ligands in the Sargasso Sea as determined by a new high-sensitivity electrochemical cobalt speciation method suitable for open ocean work. *Mar. Chem.* 75:49-68 [doi:10.1016/S0304-4203(01)00025-1].
- , and ———. 2002. Temporal and spatial variability of cobalt in the Atlantic Ocean. *Geochim. Cosmochim. Acta* 66:1943-1953 [doi:10.1016/S0016-7037(02)00829-3].
- , ———, S. W. Chisholm, and J. B. Waterbury. 2002. Cobalt limitation and uptake in *Prochlorococcus*. *Limnol. Oceanogr.* 47:1629-1636 [doi:10.4319/lo.2002.47.6.1629].
- , ———, and G. R. DiTullio. 2004. Cobalt and nickel in the Peru upwelling region: A major flux of labile cobalt utilized as a micronutrient. *Glob. Biogeo. Cycles* 18 [doi:10.1029/2003GB002216].
- , G. Rocap, and J. W. Moffett. 2005. Production of cobalt binding ligands in a *Synechococcus* feature at the Costa Rica upwelling dome. *Limnol. Oceanogr.* 50:279-290 [doi:10.4319/lo.2005.50.1.0279].
- Sakamoto-Arnold, C. M., and K. S. Johnson. 1987. Determination of picomolar levels of cobalt in seawater by flow injection analysis with chemiluminescence detection. *Anal. Chem.* 59:1789-1794 [doi:10.1021/ac00141a011].
- Sedwick, P. N., and others. 2005. Iron in the Sargasso Sea (Bermuda Atlantic Time-series Study): Eolian imprint, spatiotemporal variability, and ecological implications. *Glob. Biogeo. Cycles* 19 [doi:10.1029/2004GB002445].
- Sohrin, Y., and others. 2008. Multielement determination of GEOTRACES key trace metals in seawater by ICPMS after preconcentration using an ethylenediaminetriacetic acid chelating resin. *Anal. Chem.* 80:6267-6273 [doi:10.1021/ac800500f].
- Sunda, W. G., and S. A. Huntsman. 1995. Cobalt and zinc inter-replacement in marine phytoplankton: Biological and geochemical implications. *Limnol. Oceanogr.* 40:1404-1417 [doi:10.4319/lo.1995.40.8.1404].
- Tosoh Bioscience. 2008. <<http://separations.us.tosohbioscience.com/Products/ProcessMedia/ByMode/AFC/ToyoppearlAF-Chelate-650.htm>>. Accessed July 5, 2010.
- Warnken, K. W., D. Tang, G. A. Gill, and P. H. Santschi. 2000. Performance optimization of a commercially available iminodiacetate resin for the determination of Mn, Ni, Cu, Cd and Pb by on-line preconcentration inductively coupled plasma-mass spectrometry. *Anal. Chim. Acta.* 423:265-276 [doi:10.1016/S0003-2670(00)01137-5].
- Willie, S. N., Y. Iida, and J. W. McLaren. 1998. Determination of Cu, Ni, Zn, Mn, Co, Pb, Cd and V in seawater using flow injection ICP-MS. *At. Spectrosc.* 19:67-72.
- , J. W. H. Lam, L. Yang, and G. Tao. 2001. On-line removal of Ca, Na and Mg from iminodiacetate resin for the determination of trace elements in seawater and fish otoliths by flow injection ICP-MS. *Anal. Chim. Acta* 447:143-152 [doi:10.1016/S0003-2670(01)01301-0].
- Vega, M., and C. M. J. Van den Berg. 1997. Determination of cobalt in seawater by catalytic adsorptive cathodic stripping voltammetry. *Anal. Chem.* 69:874-881 [doi:10.1021/ac960214s].
- Xu W, R. C. Sandford, P. J. Worsfold, A. Carlton, and G. Hanrahan. 2005. Flow injection techniques in aquatic environmental analysis: Recent applications and technological advances. *Crit. Rev. Anal. Chem.* 35:237-246 [doi:10.1080/10408340500323362].

Submitted 8 September 2009

Revised 29 April 2010

Accepted 19 June 2010

ORIGINAL ARTICLE

Nitrogen fixation and nitrogenase (*nifH*) expression in tropical waters of the eastern North Atlantic

Kendra A Turk¹, Andrew P Rees², Jonathan P Zehr¹, Nicole Pereira^{1,2}, Paul Swift³, Rachel Shelley⁴, Maeve Lohan⁴, E Malcolm S Woodward² and Jack Gilbert^{2,5,6}

¹Department of Ocean Sciences, University of California Santa Cruz, Santa Cruz, CA, USA; ²Plymouth Marine Laboratory, Prospect Place, The Hoe, Plymouth, UK; ³NERC Centre for Ecology and Hydrology, CEH Oxford, Oxford, UK; ⁴University of Plymouth, Drake Circus, Plymouth, UK; ⁵Argonne National Laboratory, Institute of Genomic and Systems Biology and Department of Biosciences, Argonne, IL, USA and ⁶Department of Ecology and Evolution, University of Chicago, Chicago, IL, USA

Expression of *nifH* in 28 surface water samples collected during fall 2007 from six stations in the vicinity of the Cape Verde Islands (north-east Atlantic) was examined using reverse transcription-polymerase chain reaction (RT-PCR)-based clone libraries and quantitative RT-PCR (RT-qPCR) analysis of seven diazotrophic phylotypes. Biological nitrogen fixation (BNF) rates and nutrient concentrations were determined for these stations, which were selected based on a range in surface chlorophyll concentrations to target a gradient of primary productivity. BNF rates greater than $6 \text{ nmol N l}^{-1} \text{ h}^{-1}$ were measured at two of the near-shore stations where high concentrations of Fe and PO_4^{3-} were also measured. Six hundred and five *nifH* transcripts were amplified by RT-PCR, of which 76% are described by six operational taxonomic units, including *Trichodesmium* and the uncultivated UCYN-A, and four non-cyanobacterial diazotrophs that clustered with uncultivated *Proteobacteria*. Although all five cyanobacterial phylotypes quantified in RT-qPCR assays were detected at different stations in this study, UCYN-A contributed most significantly to the pool of *nifH* transcripts in both coastal and oligotrophic waters. A comparison of results from RT-PCR clone libraries and RT-qPCR indicated that a γ -proteobacterial phylotype was preferentially amplified in clone libraries, which underscores the need to use caution interpreting clone-library-based *nifH* studies, especially when considering the importance of uncultivated proteobacterial diazotrophs.

The ISME Journal advance online publication, 13 January 2011; doi:10.1038/ismej.2010.205

Subject Category: microbial ecology and functional diversity of natural habitats

Keywords: nitrogen fixation; *nifH*; nitrogenase; molecular; Cape Verde; Atlantic

Introduction

Nitrogen is often a limiting nutrient in terrestrial and aquatic ecosystems, including the open ocean (Vitousek and Howarth, 1991). Biological nitrogen fixation (BNF), the reduction of atmospheric N_2 to biologically available ammonium, is an important source of N for oligotrophic oceans (Gruber and Sarmiento, 1997; Karl *et al.*, 1997; Mahaffey *et al.*, 2005). BNF is performed by a limited, but diverse, group of microorganisms known as diazotrophs (Zehr *et al.*, 2003b; Zehr and Paerl, 2008). For many years, BNF in the oceans was believed to be due to *Trichodesmium*, a filamentous, aggregate-forming, non-heterocystous cyanobacterium, and *Richelia*, the heterocystous symbiont of diatoms (LaRoche

and Breitbarth, 2005; Mahaffey *et al.*, 2005), until the discovery of unicellular diazotrophic Cyanobacteria (Zehr *et al.*, 2001; Montoya *et al.*, 2004). These microorganisms were discovered by polymerase chain reaction (PCR) amplification of the *nifH* gene, which encodes the iron protein of nitrogenase, the enzyme that catalyzes N_2 fixation, as they are small, low in abundance and unidentifiable as diazotrophs using microscopy or 16S *rRNA* gene sequences. Non-cyanobacterial N_2 -fixing microorganisms have also been detected with PCR (Zehr *et al.*, 2001; Bird *et al.*, 2005), but their significance in marine BNF is not well understood. Relatively little is known about the distribution of diazotrophs (Falcón *et al.*, 2002; Langlois *et al.*, 2005, 2008; Foster *et al.*, 2007, 2009b; Hewson *et al.*, 2007; Church *et al.*, 2008; Moisander *et al.*, 2010), or the factors that control their distribution and activity (Berman-Frank *et al.*, 2007; Moisander *et al.*, 2010).

The nitrogenase proteins require iron (reviewed by Kustka *et al.* (2002)), and the availability of both phosphorus and iron are factors that may be important in limiting or co-limiting BNF

Correspondence: KA Turk, Department of Ocean Sciences, University of California Santa Cruz, 1156 High Street, Santa Cruz, CA 95064, USA.

E-mail: kturk@ucsc.edu

Received 26 August 2010; revised 18 November 2010; accepted 18 November 2010

(Sanudo-Wilhelmy *et al.*, 2001; Karl *et al.*, 2002; Mills *et al.*, 2004) in some areas of the world's oceans. It is clear that no one factor controls marine BNF rates and that nitrogenase activity is determined by a combination of variables that differ depending on the geographic region and diazotroph community composition (Mahaffey *et al.*, 2005). This study focused on BNF rates and *nifH* expression near the Cape Verde Islands, in the eastern North Atlantic, and was performed as part of the UK SOLAS-funded INSPIRE cruise (D325). This is a unique study area as nutrient concentrations are generally depleted, but can be influenced by local upwelling effects associated with the islands. This region is also strongly influenced by Saharan dust deposition (Chiapello *et al.*, 1995), which supplies both iron and phosphorus to surface waters (Mills *et al.*, 2004; LaRoche and Breitbarth, 2005). Previous studies in the North Atlantic and the equatorial North Atlantic have documented the presence of diverse N_2 -fixing Cyanobacteria and bacteria (Langlois *et al.*, 2005, 2008; Goebel *et al.*, 2010). This study focused on describing the diversity of *nifH*-containing organisms actively transcribing *nifH* via reverse transcription (RT)-PCR, quantifying the number of *nifH* transcripts from seven major cyanobacterial and non-cyanobacterial diazotrophs using quantitative RT-PCR (RT-qPCR), and measuring BNF rates along with physical and chemical parameters in this region. It is hypothesized that BNF rates will correlate both to Fe concentrations and to the magnitude of *nifH* expression of some or all the diazotrophs assayed using qPCR.

Experimental procedures

Sample collection

Surface seawater samples were collected in a trace metal clean laboratory with a 'towed torpedo fish' system using a Teflon diaphragm pump (Almatec A-15, Kamp-Lintfort, Germany) from six oceanographic stations during November–December 2007 (Table 1). The site selection was guided by processed surface ocean color satellite images supplied daily by the UK Natural Environment Research Council Earth Observation Data Acquisition and Analysis Service (<http://www.neodaas.ac.uk/>) at Plymouth Marine Laboratory. Six sites were chosen to give a gradient of conditions from near-shore coastal waters off Cape Verde Islands (Stations B and C), immediately offshore waters (Stations A and D) and open, oligotrophic waters (Stations E and F). At Stations C–F, a six-point time series was collected over a 20-h period to assess diel variability of *nifH* expression. This diel cycle was sampled under a Lagrangian framework (following the same parcel of seawater) using a free-floating drifter buoy, which was deployed at a depth of 15 m. For each sample, 10 l of seawater was filtered using a peristaltic pump through a 0.22- μ m Sterivex filter (Millipore,

Billerica, MA, USA), which was stored at -80°C until nucleic acid extraction. Filtration time did not exceed 30 min.

N_2 fixation rates

Surface seawater samples, obtained using the Royal Research Ship Discovery's seawater pump, were distributed into triplicate 1-l polycarbonate bottles and 2 ml of $^{15}\text{N-N}_2$ was added. Bottles were transferred to on-deck incubators, maintained at sea surface temperature, and incubated without light-attenuating filters for 6 h. Six-hour incubations were chosen to provide a gross BNF rate throughout a diel cycle and correspond with samples collected for molecular analysis. Experiments were terminated by filtration onto 25-mm GF/F filters (Millipore), which were dried at 50°C for 12 h and stored over silica gel desiccant until return to Plymouth Marine Laboratory. Particulate nitrogen and ^{15}N atom% were measured using continuous-flow stable isotope mass spectrometry (PDZ-Europa 20-20 and GSL; Owens and Rees, 1989), with rates and ^{15}N enrichment determined according to Montoya *et al.* (1996). Background ^{15}N content of particulate material was determined from unamended 1-l aliquots of seawater filtered immediately upon collection.

Dissolved iron analysis

Samples for dissolved iron were collected using the 'towed torpedo fish' approach described above. Seawater was filtered through acid-cleaned 0.2- μ m polycarbonate track-etched membrane filters (Nucleopore; Millipore) held in a PTFE Teflon filter holder. Filtrate was collected in 125-ml acid-cleaned low-density polyethylene bottles and acidified to pH 1.7 using UHP HCl (SpA; Romil, UK). All operations were carried out in clean room conditions under a class 100 laminar-flow hood.

Total dissolved iron was determined using flow injection with chemiluminescence detection (FI-CL) as described by de Jong *et al.* (1998), with modifications described in de Baar *et al.* (2008). Stock standard solutions were prepared in acidified UHP water from an iron atomic absorption standard solution (Spectrosol, UK). Working standards (0.125–1.5 nM) were prepared in acidified low trace metal seawater and used in daily calibrations. The analytical detection limit was 0.08 nM ($n = 8$).

Nutrient and chlorophyll *a* analysis

Samples collected for the analysis of NO_2^- , NO_3^- and PO_4^{3-} were analyzed within 2 h of collection. PO_4^{3-} was determined according to Kirkwood (1989), and NO_2^- and NO_3^- were measured with a segmented flow colorimetric auto-analyzer according to Brewer and Riley (1965) for nitrate and Grasshoff *et al.* (1999) for nitrite. The detection limit was 20 nM for all three nutrients and the precision was better than

Table 1 Environmental conditions and *nifH* RT-qPCR results at Cape Verde sampling stations

Sample	Station	Lat. (°N)	Long. (°W)	Date (dd.mm.yy)	Time (hh:mm)	Temp (°C)	Salinity (Psu)	BNF rate (nmolN ⁻¹ h ⁻¹)	Nitrate+ nitrite (µM)	PO ₄ ³⁻ (µM)	Iron (nM)	Chl a (µg l ⁻¹)	<i>nifH</i> transcripts per l						
													UCYN-A	UCYN-B	Tricho.	RR	HR	γ-prot	α-prot
1	A	17.72	-22.74	17.11.07	4:09	24.9	36.8	6.3	<0.02	0.05	1.51	0.1	1.3E+05	DNQ	UD	8.8E+02	UD	UD	UD
2	B	16.89	-24.83	22.11.07	4:34	25.3	36.7	6.0	0.05	0.09	0.58	0.33	1.0E+04	UD	4.9E+03	UD	UD	UD	UD
3	B	16.89	-24.83	22.11.07	13:53	25.2	36.8	6.0	0.06	0.10		0.38	1.4E+03	UD	UD	DNQ	DNQ	DNQ	UD
4*	B	16.89	-24.83	22.11.07	13:53	25.2	36.8	6.0	4.12	0.33			1.9E+03	DNQ	5.2E+02	UD	2.2E+03	UD	UD
5	C	16.01	-23.66	28.11.07	6:50	24.9	36.8	0.5	0.12	0.06	0.32	0.19	UD	UD	6.3E+02	DNQ	8.6E+02	UD	UD
6	C	16.02	-23.73	28.11.07	6:45	24.7	36.5	0.1	0.06	0.06		0.22	UD	UD	9.0E+02	DNQ	1.1E+03	UD	UD
7	C	16.02	-23.74	28.11.07	10:15	24.7	36.5	0.3	0.06	0.06	0.32		UD	UD	2.5E+03	DNQ	1.0E+03	UD	UD
8	C	16.03	-23.76	28.11.07	14:10	24.7	36.4	0.4	0.053	0.04			UD	UD	UD	UD	ND	UD	UD
9	C	16.04	-23.78	28.11.07	18:15	24.7	36.5	0.5	0.053	0.04			UD	UD	DNQ	UD	ND	UD	UD
10	C	16.03	-23.78	28.11.07	23:35	24.7	36.5	0.2	0.053	0.04			UD	UD	UD	UD	ND	UD	UD
11	C	16.02	-23.77	28.11.07	2:00	24.6	36.5	0.2	0.05	0.04			UD	UD	UD	DNQ	UD	UD	UD
12	D	17.72	-22.95	02.12.07	6:15	23.9	36.8	0.1	<0.02	0.08	0.3	0.12	4.1E+04	UD	UD	DNQ	ND	DNQ	UD
13	D	17.78	-22.96	02.12.07	10:10	23.9	36.8	0.3	<0.02	0.12			7.3E+04	1.5E+03	DNQ	DNQ	UD	DNQ	UD
14	D	17.79	-22.97	02.12.07	14:15	24	36.8	0.2	<0.02	0.12			1.6E+04	UD	UD	ND	ND	DNQ	UD
15	D	17.80	-23.00	02.12.07	18:15	24	36.8	0.3	<0.02	0.12			DNQ	UD	UD	DNQ	UD	UD	UD
16	D	17.81	-23.05	02.12.07	23:05	24	36.9	0.2	<0.02	0.12			4.5E+03	UD	UD	DNQ	UD	UD	UD
17	D	17.81	-23.09	03.12.07	2:30	23.9	36.9	0.1	<0.02	0.14			DNQ	UD	UD	1.0E+03	UD	UD	UD
18	E	20.65	-24.96	07.12.07	5:30	23.9	36.9	0.1	<0.02	0.06	0.35	0.08	7.6E+04	UD	DNQ	UD	UD	DNQ	UD
19	E	20.85	-25.01	07.12.07	6:25	23.9	37.0	0.1	<0.02	0.05			4.5E+04	UD	9.5E+02	DNQ	UD	8.1E+03	UD
21	E	20.94	-25.04	07.12.07	14:00	23.9	36.9	0.3	<0.02	0.05			2.4E+04	UD	DNQ	UD	UD	DNQ	UD
22	E	20.98	-25.05	07.12.07	18:25	23.9	36.9	0.1	<0.02	0.05			3.4E+03	DNQ	UD	UD	UD	8.7E+03	UD
23	E	21.04	-25.05	07.12.07	22:55	23.8	36.9	ND	<0.02	0.05			4.4E+04	UD	UD	DNQ	UD	DNQ	UD
24	E	21.08	-25.05	08.12.07	1:55	23.8	36.9	ND	<0.02	0.05			1.2E+05	UD	UD	UD	UD	UD	UD
25	F	26.05	-23.99	12.12.07	6:15	23.3	37.4	bdl	<0.02	<0.02	0.54	0.06	DNQ	UD	DNQ	DNQ	ND	DNQ	UD
26	F	26.05	-23.98	12.12.07	10:15	22.7	37.3	0.1	<0.02	<0.02			DNQ	UD	1.2E+03	1.6E+03	DNQ	DNQ	UD
27	F	26.07	-23.99	12.12.07	14:15	22.9	37.3	0.1	<0.02	<0.02			UD	DNQ	DNQ	DNQ	DNQ	DNQ	UD
28	F	26.09	-24.01	12.12.07	18:20	22.7	37.3	0.1	<0.02	<0.02			DNQ	1.4E+03	DNQ	DNQ	1.5E+03	6.8E+03	UD
29	F	26.08	-24.00	12.12.07	23:10	22.6	37.3	0.1	<0.02	<0.02			DNQ	UD	UD	9.5E+02	DNQ	UD	UD
30	F	26.10	-23.99	13.12.07	2:30	22.6	37.3	bdl	<0.02	<0.02			6.8E+02	UD	DNQ	3.2E+03	DNQ	DNQ	UD

Abbreviations: α-prot, α-24809A06; bdl, below detection limit; BNF, biological nitrogen fixation; DNQ, detected not quantified; γ-prot, γ-24774A11; HR, *Richelia* in *Hemiaulus*; ND, no data; RR, *Richelia* in *Rhizosolenia*; RT-qPCR, quantitative reverse transcription-polymerase chain reaction; UD, undetected. Sites are divided into Stations A–F, grouped by similar latitude and longitudes. Diel sampling occurred at Stations C–F. All samples were taken within the mix layer, thus considered to be surface or near-surface samples, with the exception of B4 (marked with an asterisk), which was sampled at 50 m.

± 10 nM. Chlorophyll *a* was determined on acetone extractions using a Turner fluorometer (Turner Designs, Sunnyvale, CA, USA) according to Welschmeyer (1994).

RNA extraction and cDNA generation

The phenol/chloroform Sterivex extraction method of Neufeld *et al.* (2007) was used to extract total nucleic acids. After extraction, RNA was isolated and DNA was removed using the RNA-Easy mini prep kit (Qiagen, Germantown, MD, USA) and Turbo-DNA free kit (Ambion, Austin, TX, USA) following the manufacturer's guidelines. RNA purity and integrity was checked using an RNA6000 chip on an Agilent Bioanalyser. cDNA was synthesized for RT-PCR by RT of purified RNA using the SuperScript III First Strand Synthesis System for RT-qPCR (Invitrogen, Carlsbad, CA, USA) following the manufacturer's guidelines, using 10 ng purified RNA extract and 0.5 μ M of *nifH3* reverse primer (Zani *et al.*, 2000). Negative controls (no-RTs) were generated for each sample.

For RT-qPCR analysis, cDNA was generated directly from the total nucleic acid extract using the protocol described above, after DNA removal using amplification grade DNaseI (Invitrogen), according to the manufacturer's guidelines. Negative controls were processed for a subset of samples to confirm complete degradation of DNA. An additional modification in cDNA generation for RT-qPCR was the use of equimolar quantities (0.25 μ M) of *nifH2* (Zehr and McReynolds, 1989) and *nifH3* primers.

RT-PCR

The first round of *nifH* amplification proceeded as follows: 1 μ l of cDNA was added to a 24 μ l PCR reaction containing 4 mM MgCl₂, 1X GoTaq buffer, 0.2 mM dNTPs, 2 pmol primers (*nifH3* and *nifH4*) (Zani *et al.*, 2000) and 1.25 U of Taq (Promega, Madison, WI, USA). The reaction was performed with 35 cycles of 95 °C (1 min), 55 °C (1 min) and 72 °C (1 min). The second amplification used 1 μ l of the first-round PCR product, the primers *nifH1* and *nifH2* (Zehr and McReynolds, 1989) and reaction conditions identical to the first round. PCR products were twice gel purified with a Wizard SV Gel Clean-Up System kit (Promega). The purified PCR products were cloned using the pGem-T Easy vector kit (Promega) following the manufacturer's guidelines. Random inserts were sequenced from the 28 samples using M13 primers (ABI BigDye 3.1 used at one-eighth reaction). This sequence data has been submitted to GenBank under accession numbers HQ611353–HQ611956.

RT-qPCR

Expression of *nifH* from five different cyanobacterial and two proteobacterial phylotypes was quantified

using TaqMan RT-qPCR assays (Table 2). All qPCR reactions were set up as described in Moisander *et al.* (2010) using undiluted cDNA, and only 1 μ l template in *Richelia* in *Rhizosolenia* (RR) and *Richelia* in *Hemaulus* (HR) assays. In 96-well reaction plates, each RT and no-RT reaction were run in duplicate, along with a minimum of two no-template controls and a standard curve (10^0 – 10^7 *nifH* copies per reaction) generated with linearized recombinant plasmids with the appropriate target (Table 2).

Amplifications were carried out using the Applied Biosystems 7500 Real time PCR system and the 7500 System SDS software using the thermocycling method described in Moisander *et al.* (2010). RTs and no-RTs were tested for inhibition as described in Goebel *et al.* (2010). No inhibition was observed in any of the 28 samples.

The limit of detection and limit of quantification have been determined to be 1 and 8 *nifH* copies per reaction, respectively (data not shown), and are reported as *nifH* transcripts per l in Table 2. Samples that amplified but fell below the limit of quantification were designated 'detected not quantified (DNQ)'. The efficiency (*E*) of amplifications was determined using the formula $E = 10^{-1/m} - 1$, where *m* is the slope from the regression described above (Table 2).

Linear regressions were used to determine whether correlations could be made between *nifH* expression, BNF rates and environmental parameters (Supplementary Table 1). If necessary, data were first transformed to meet conditions of normality and homoscedasticity.

Bioinformatic and phylogenetic analysis

Nucleic acid sequences were quality checked, trimmed and imported into a publically available *nifH* database (Zehr *et al.*, 2003b) with >150 000 sequences from GenBank (<http://www.es.ucsc.edu/~wwwzehr/research/database/>) in the software program ARB (Ludwig *et al.*, 2004). Translated amino acid sequences were aligned using a Hidden Markov Model from PFAM (Finn *et al.*, 2010). Nucleotide sequences were re-aligned according to the aligned amino-acid sequences, and operational taxonomic units (OTUs) were defined using 91% similarity cutoff in DOTUR v1.53 (Schloss and Handelsman, 2005). Nearest neighbors for OTUs were determined using the parsimony quick add function in ARB. A neighbor-joining tree of partial *nifH* sequences was constructed in ARB and branch lengths were computed using the Jukes–Cantor correction. Bootstrapping (1000 replicates) was performed in MEGA 4.0.

Results and discussion

Nitrogen fixation rates and environmental variables

There was a gradient of surface water temperatures between stations nearest to the Cape Verde Islands

Table 2 qPCR primers and probes used in this study

Phylo-type target	Forward primer (5'–3')	Probe (5'–3')	Reverse primer (5'–3')	GenBank accession no. of standard	Efficiency (E)	LOD (nIH transcripts per l)	LOQ (nIH transcripts per l)
UCYN-A (Church <i>et al.</i> , 2005a)	AGCTATAACAAGGTTTATAGCGTTGA	TCTGGTGGTCTGAGCGTTGA	ACCAGGACGACGACATCGA	AF059642	104 ± 3%	72	576
UCYN-B (Moisan-der <i>et al.</i> , 2010)	CCTAATGCTCGAAGGCTTGA	CAATGTGTAGAAATCTGGTGGTCTGAGCC	CAGCAGGACGACACCAACT	DQ481411	96 ± 3%	72	576
<i>Trichodesmium</i> (Church <i>et al.</i> , 2005a)	GACGAAGTATTGAAGCGAGTTTC	CATTAAGTGTCTCAATCTGGTGGTCTGAGCC	CGGCGACGGCAACCTA	DQ404414	98 ± 3%	72	576
<i>Richelia</i> associated with <i>R. clevis</i> (RR) (Church <i>et al.</i> , 2005b)	CGGTTTCGGTGGTGTAGGTT	TEGGTGGTCTGAGCGTTGT	AATAGCAGGACGGCGGCAAC	DQ225757	97 ± 2%	144	1150
<i>Richelia</i> associated with <i>H. bowkii</i> (HR) (Foster <i>et al.</i> , 2007)	TECTTACCGCTCATGTACGTT	TCTGGTGGTCTGAGCGTTGT	AATGGCGGACGACGCAAC	DQ225753	101 ± 1%	144	1150
γ -Proteobacteria (γ -24774A11) (Moisan-der <i>et al.</i> , 2010) ^a	CGGTAGAGGAGTCTGAGGTTGAA	AAGTGCTTAAAGTTGGCTTTGGCGACA	CACCTGACTCCAGCCACTTG	EU059413	98 ± 6%	72	576
α -Proteobacteria (α -24809A06) ^a (Moisan-der <i>et al.</i> , 2010) ^b	TCTCATCTCTCAACTCCAAAGCA	ACCCTGCTGACCTGGGCG	TCTTAAACCGAACCATTTC	EU052488	104 ± 1%	72	576

Abbreviations: LOD, limit of detection; LOQ, limit of quantitation; qPCR, quantitative polymerase chain reaction; RT, reverse transcription.
^aThe oligonucleotide sequences for the reverse primer has an error in the original reference. LOD and LOQs are determined by considering dilutions made during the RT reactions, volume of extract used in RT-qPCR reactions, nucleic acid extraction volumes and volume of seawater filtered.

and at lower latitudes (B/C) and stations farthest from the islands at higher latitudes (E/F) from 25.3 °C at Station B to 22.6 °C at Station F. Sea surface temperatures positively correlated with a gradient of chloroform *a* concentrations (Table 1, Supplementary Table 1). Temperature–salinity plots (Supplementary Figure 1) show that the same water masses were sampled during diel samplings at Stations C–F using the drogue, with the exception of sample C5. NO₃⁻ concentrations were generally low, but ranged from below detection to over 0.12 μM at Station C. Dissolved iron concentrations were within the range reported in previous studies in this region (Sarhou *et al.*, 2003; Rijkenberg *et al.*, 2008), with the exception of Station A (1.5 nM). Five-day air mass back trajectories, calculated by the HYPSPPLIT transport and dispersion model (NOAA Air Resources Laboratory), showed the presence of dust over Station A, which was responsible for the high concentration of Fe. Fe and PO₄³⁻ concentrations were replete relative to NO₃⁻; thus, N:P ratios were low (<1.9), indicating potential N-limiting conditions consistent with Mills *et al.* (2004).

Stations A and B had the highest BNF rates measured during this study, at 6.3 and 6.0 nmolNl⁻¹h⁻¹, respectively. Although rates of similar magnitude have been reported in the Eastern Mediterranean (5.3 nmolNl⁻¹h⁻¹) (Rees *et al.*, 2006), BNF rates at Stations A and B are relatively high in comparison to rates from the North Pacific (a region where Fe and P may also be limiting or co-limiting), which are generally less than 1.9 nmolNl⁻¹h⁻¹ (Montoya *et al.*, 2004; Zehr *et al.*, 2007; Fong *et al.*, 2008; Grabowski *et al.*, 2008). Stations C–F had rates <1 nmolNl⁻¹h⁻¹, which are comparable to rates reported in Fe- and P-amended waters 800 km south of Station C by Mills *et al.* (2004) and the temperate coastal waters of the English Channel (Rees *et al.*, 2009).

The highest BNF rates measured in this study coincided with the highest measured dissolved Fe concentrations (1.51 and 0.58 nM) (Table 1). Although both Fe and PO₄³⁻ have been hypothesized to limit or co-limit N₂ fixation in this region (Sanudo-Wilhelmy *et al.*, 2001; Karl *et al.*, 2002; Mills *et al.*, 2004), linear regressions indicate that BNF had positive correlations to Fe ($r^2 = 0.63$, $P = 0.05$, $n = 6$) and temperature ($r^2 = 0.37$, $P = 0.001$, $n = 25$), but not to PO₄³⁻ (Supplementary Table 1). None of the other environmental parameters measured could be correlated to BNF rates. These data confirm that dissolved Fe concentrations are an important factor in N₂ fixation in this region.

It is important to note that a recent study by Mohr *et al.* (2010) has shown that the ¹⁵N-tracer method developed by Montoya *et al.* (1996) used here and widely throughout the scientific community may underestimate N₂ fixation rates. Mohr *et al.* (2010) determined that bubble injections of ¹⁵N₂ gas are slow to equilibrate using traditional shipboard incubation techniques, which has a significant

impact on calculations used in determining BNF rates. As such, the timing of $^{15}\text{N}_2$ injections relative to peak nitrogenase activity in diel studies can have a variable impact on measured BNF rates. It is unclear as to what extent our current understanding of global BNF rates will be altered as the community adopts the modified technique developed by Mohr *et al.* (2010) to address this underestimation.

nifH gene diversity (RT-PCR)

A total of 605 *nifH* transcript sequences were amplified from the 28 samples. Using cluster designations as in Zehr *et al.* (2003b), there were 567 Cluster I (93.7%), three Cluster II (0.5%) and 35 Cluster III (5.8%) *nifH* sequences. Forty-nine *nifH* OTUs were designated using a 91% nucleotide sequence similarity cutoff. The top six most highly recovered OTUs, which accounted for 76% of all transcripts, were Cluster I sequences; four were of proteobacterial origin, and two were of cyanobacterial origin (Figure 1, Supplementary Table 2).

The most highly recovered OTU, CV1, accounted for 30.4% of all transcript sequences, and was amplified from all stations. CV1 clustered with uncultivated γ -proteobacterial sequences that have been widely reported in DNA-based studies (PCR and qPCR) from regions in the North Pacific (Church *et al.*, 2005b; Fong *et al.*, 2008), South Pacific (Moisander *et al.*, 2010), Arabian Sea (Bird *et al.*, 2005), South China Sea (Moisander *et al.*, 2007), Equatorial Atlantic (Foster *et al.*, 2009b), tropical Atlantic (Langlois *et al.*, 2008) and in the Mediterranean Sea (Man-Aharonovich *et al.*, 2007). It has also been reported actively expressing *nifH* in numerous studies (Bird *et al.*, 2005; Church *et al.*, 2005b; Man-Aharonovich *et al.*, 2007). The γ -proteobacteria in all of these studies, as well as CV1, were targeted with the qPCR assay designed by Moisander *et al.* (2008) for γ -24774A11.

The second most highly recovered OTU, CV2 (15.5%), amplified from Stations C–F, also clustered with uncultivated γ -proteobacterial sequences, and has a high sequence similarity to environmental sequences from the English Channel (EF407529, EF407533 and EF407537) and the Amazon River Plume (DQ481447–DQ481449).

The third and fourth most highly recovered OTUs, CV3 and CV4, clustered with Cyanobacteria, and together accounted for 20% of the transcripts. CV3 (13%) clusters with *Trichodesmium*, and has >99% nucleotide sequence similarity to environmental sequences from the tropical Atlantic (AY896353; Langlois *et al.*, 2005) and the South China Sea (EU052348; Moisander *et al.*, 2008). This phylotype was amplified from all stations, except offshore Station D. CV4 (7%) clustered with UCYN-A, which has been previously reported in this region of the ocean (Langlois *et al.*, 2005, 2008; Goebel *et al.*, 2010). CV4 was amplified from offshore and oligotrophic stations A, D, E and F and has 99.7%

nucleotide sequence similarity to sequences reported in the North Pacific (e.g., EU159536; Fong *et al.*, 2008) and Gulf of Aqaba (DQ825729; Foster *et al.*, 2009a).

CV5 (5.1%) is most closely related (90% nucleotide similarity) to a *nifH* sequence from an uncultivated α -proteobacteria (AF389713) associated with a marsh cordgrass, *Spartina alterniflora* (Lovell *et al.*, 2001). This phylotype is closely related (88% nucleotide similarity) to α -24809A06, which Moisander *et al.* (2008) used in the design of a qPCR assay, but has too many mismatches in the primer/probe region to be amplified. CV6 (4.8%) is related to a γ -proteobacteria (82% nucleotide sequence similarity) described in DNA-derived *nifH* clone libraries in an anti-cyclonic eddy near Station ALOHA (Fong *et al.*, 2008).

Transcripts originating from other diazotrophic Cyanobacteria were amplified, but were not among the most highly recovered phylotypes. One UCYN-B *nifH* transcript (CV34) was amplified from F25, and three *nifH* transcripts (CV21) were amplified from D17 and F25 that formed a bootstrap-supported cluster with *Richelia* sequences (Figure 1). The UCYN-B sequence had no mismatches in the region of the qPCR primers and probe used in this study, and thus represented a phylotype that would be amplified in RT-qPCR assays. However, the *Richelia*-like sequences had multiple mismatches to the RR and HR qPCR primers and probes, hence are not representative of the phylotypes amplified in the RT-qPCR assays.

Of the remaining 43 OTUs recovered, none account for more than 2% of the total transcripts and it is difficult to assess their relative importance to BNF. Diazotrophs are typically found in low abundance in marine systems, and a nested PCR protocol (>55 amplification cycles) is required to amplify the *nifH* gene. Clone libraries generated using these amplicons may contain heterotrophic *nifH* sequences amplified from organisms or nucleic acids present in PCR reagents (Kulakov *et al.*, 2002; Zehr *et al.*, 2003a; Goto *et al.*, 2005; Farnelid *et al.*, 2009), high-purity water systems (Matsuda *et al.*, 1996) or sampling equipment. It is insufficient to run negative controls, as amplification of contaminant *nifH* is sporadic and difficult to reproduce. Furthermore, it is difficult to determine from *nifH* sequences alone whether a heterotrophic sequence came from the environment or contamination, and sometimes the contaminant sequences amplify more efficiently in the presence of target DNA (Zehr *et al.*, 2003b).

A representative subset of sequences identified as contaminants have been included in Figure 1. Although most of these are Cluster I sequences, a Cluster III sequence has been reported (AB198377; Goto *et al.*, 2005). CV9 has 99% nucleotide similarity to a known PCR contaminant, AB198391 (Goto *et al.*, 2005), and is presumed to be a contaminant. Other sequences may be contaminants based on



Figure 1 Neighbor-joining tree of partial *nifH* cyanobacterial sequences obtained from Cape Verde transcripts. Branch lengths were computed using the Jukes-Cantor correction in the ARB software. Bootstrapping was performed in MEGA 4.0, and bootstraps greater than 70% (1000 replicates) are shown next to the branches. Cape Verde transcripts are marked according to the key to emphasize the number of sequences represented by each OTU. All *Trichodesmium*, UCYN-A, UCYN-B and γ -24774A11 transcript sequences are targeted by the qPCR assays used in this study. Sequences that are related, but not identical, to phylotypes that are targeted with qPCR assays are marked with a white arrow. Sequences that are suspected contaminants are underlined, and those that have been determined to be contaminants in *nifH*-based PCR studies are marked with an asterisk.

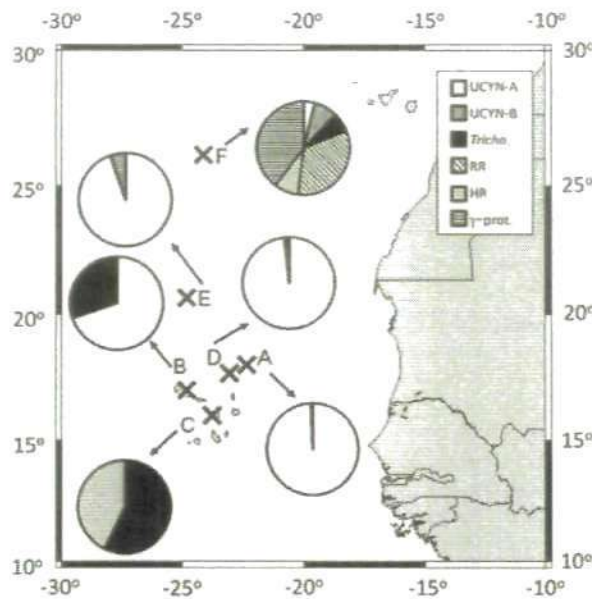


Figure 2 Relative contribution of individual diazotrophs to overall *nifH* transcript pools quantified in surface waters at each station as determined by RT-qPCR. Results from sample B4 were not included, as it was taken below the mix layer. The α -24809A06 phylotype was not detected in any sample. Map produced using http://www.aquarius.geomar.de/omc/make_map.html.

their sequence similarity to known or suspected contaminants, for example, CV37. As definitively identifying contaminants in *nifH* clone libraries is nearly impossible, this study focuses on highly recovered OTUs and those for which qPCR assays have been designed.

Quantitative *nifH* gene expression (RT-qPCR)

The *nifH* expression of five Cyanobacteria, *Trichodesmium*, UCYN-A and UCYN-B, two symbiotic strains of *Richelia intracellularis* (referred to as RR and HR when associated with diatom *Rhizosolenia* and *Hemiaulus hauckii*, respectively), as well as two proteobacteria, γ -24774A11 and α -24809A06, was quantified for each sample (Table 1, Figure 2). UCYN-A was responsible for the highest *nifH* expression measured, 1.3×10^5 *nifH* transcripts per l, in the offshore waters at Station A (Table 1). UCYN-A *nifH* expression also dominated the quantified *nifH* transcripts at Stations B, D and E (Figure 2). UCYN-A *nifH* transcripts were not detected at Station C, in which the lowest salinities were measured (near-shore coastal), and were low in abundance at Station F (open ocean oligotrophic) (Table 1). This high UCYN-A *nifH* expression contrasts with *nifH* expression dominated by *Trichodesmium* in the eastern equatorial Atlantic (approximately 3000 km southeast), despite the presence of UCYN-A (Foster et al., 2009b). However, Goebel et al. (2010) reported high abundances of UCYN-A near the Cape Verde Islands, and based on modelled

BNF rates, concluded UCYN-A may be responsible for a majority of the BNF in this region. Although no overall correlation was supported between UCYN-A *nifH* expression and BNF rates ($r^2 = 0.12$, $P = 0.09$, $n = 25$) across these six stations (Supplementary Table 1), these findings suggest that UCYN-A may contribute to the high BNF rate measured at Station A. As indicated by the linear regression results, however, high UCYN-A *nifH* transcript abundance does not always correlate to high BNF, exemplified by Station E (Table 1).

Trichodesmium was the dominant *nifH*-expressing phylotype at only one station, the near-shore coastal Station C. *Trichodesmium nifH* transcripts also accounted for ~25% of the quantified *nifH* transcripts at the other near-shore coastal site, Station B. These were the only two stations where $\text{NO}_3 + \text{NO}_2$ was detected. *Trichodesmium nifH* expression did not have any significant correlations to BNF rates or other environmental parameters measured (Supplementary Table 1).

RR and HR had the highest *nifH* expression at Stations F and C, respectively (Table 1, Figure 2). Station F constitutes an open ocean, oligotrophic environment where sea surface temperatures ranged between 22.6°C and 23.3°C, while station C is coastal, relatively nutrient replete and slightly warmer (24.6–24.9°C) (Table 1). RR *nifH* copies per l were found to be inversely correlated with temperature ($r^2 = 0.18$, $P = 0.03$, $n = 27$), which is consistent with observations in the eastern equatorial Atlantic by Foster et al. (2009b), in which highest RR *nifH* transcription was detected at stations with lower sea surface temperatures.

Although there were no *nifH* transcripts detected in any sample for α -24809A06, γ -24774A11 was detected at four stations and quantified at Stations E and F (Table 1), and found to be positively correlated to salinity ($r^2 = 0.18$, $P = 0.03$, $n = 27$) and RR *nifH* copies per l ($r^2 = 0.62$, $P = 0.04$, $n = 7$) and negatively correlated to temperature ($r^2 = 0.23$, $P = 0.01$, $n = 27$). At Station F, the northernmost station with the lowest temperature and the highest salinity, γ -24774A11 *nifH* transcripts accounted for 40% of the quantified transcripts (Figure 2). This was the only station where a proteobacteria dominated *nifH* expression, which is surprising considering that all of the cyanobacterial phylotypes were also detected. Although BNF rates were low at this station, these findings indicate that γ -24774A11 may contribute to N_2 fixation in oligotrophic waters.

Diel cycling of *nifH* gene expression (RT-qPCR)

At Stations C–F, samples were taken every 4 h over a 20-h cycle, and can be used to examine diel *nifH* gene expression patterns of *nifH* phylotypes. Interpretations of temporal patterns assume that consistent populations of diazotrophs were sampled, but it must also be considered that patterns could be due, in part, to variability in biomass between samples.

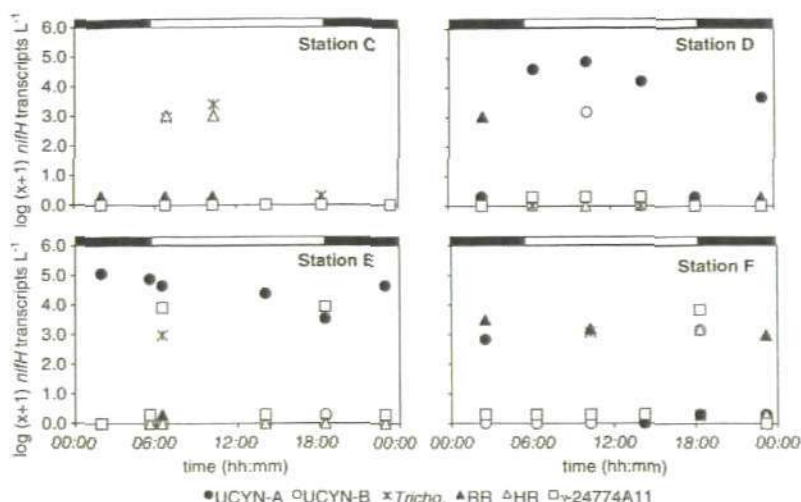


Figure 3 Diel expression of cyanobacterial and proteobacterial *nifH* gene expression determined using RT-qPCR at Stations C–F. Sample C5 has been omitted from these plots owing to discrepancies in T/S. Bars at the top of each graph indicate night time (black) and daytime (white). If *nifH* transcripts per l were measured as DNQs, they were conservatively estimated to be 1 *nifH* transcript per l. Tricho.—*Trichodesmium*; RR—*Richelia* associated with *Rhizosolenia*; HR—*Richelia* associated with *Hemiaulus*.

UCYN-A exhibited different diel patterns of *nifH* expression at Stations D and E (Figure 3). At Station D, highest *nifH* expression was detected during daylight at 1010 hours (7.3×10^4 *nifH* transcripts per l). In contrast, at Station E, the highest *nifH* expression (1.2×10^5 *nifH* transcripts per l) was measured at 0155 hours and was considerably lower during the daytime (Figure 3). It is now known that UCYN-A has a photofermentative metabolism, as sequencing of the complete genome revealed it lacks photosystem II as well as all known carbon fixation pathways (Zehr *et al.*, 2008; Tripp *et al.*, 2010). Therefore, oxidative stress is not a factor directly impacting the temporal patterns of N_2 fixation in UCYN-A.

The other unicellular diazotrophs, UCYN-B and γ -24774A11, had similar diel expression patterns at Station F, in which *nifH* transcription peaked in early evening at 1820 hours (Figure 3). At Station D, UCYN-B *nifH* expression peaked during the daytime, which is inconsistent with previous reports of UCYN-B temporally separating N_2 fixation from oxygenic photosynthesis to protect nitrogenase from oxidative damage (Bergman *et al.*, 1997). At Station E, *nifH* expression in γ -24774A11 appeared to have two peaks of similar magnitude in the early morning (0625 hours) and early evening (1825 hours). Consistent with findings from Church *et al.* (2005b), it appears that *nifH* expression in γ -24774A11 is not directly impacted by light intensity.

Diel expression of *nifH* in *Trichodesmium* was consistent with that observed in culture (Wyman *et al.*, 1996; Chen *et al.*, 1998) and *in situ* (Church *et al.*, 2005b), with highest *nifH* transcript copies quantified in the early (Stations E) or mid-morning (Stations C and F). HR and RR showed slightly different diel patterns, with RR showing highest

nifH expression at 0230 hours at Stations D and F, and HR in the early to mid-morning at Station C.

Comparison between *nifH* expression via RT-PCR and RT-qPCR

Results of RT-qPCR indicate that Cyanobacteria are responsible for the majority of *nifH* transcription at the time of sampling around the Cape Verde Islands. It must be noted, however, that diazotrophic phylotypes not specifically targeted by these qPCR assays may contribute to the pool of *nifH* transcripts, and possibly BNF rates. However, the RT-qPCR results contrast with those from RT-PCR clone libraries, which are dominated by non-cyanobacterial sequences.

Out of the seven phylotypes targeted by RT-qPCR assays, four were amplified in the RT-PCR libraries and had 0 or very few (<2) mismatches in the regions of the primers and probes. These were UCYN-A (CV4), UCYN-B (CV34), *Trichodesmium* (CV3) and γ -24774A11 (CV1). Three of these phylotypes are among those most highly amplified in the clone libraries.

To compare the two methods, the number of *nifH* transcripts amplified via RT-PCR from these four phylotypes were normalized to a subset of the total number of sequences recovered at each station (omitting all phylotypes but CV1, CV3, CV4 and CV34). Likewise, the number of *nifH* transcripts per l for these four phylotypes from the RT-qPCR study were summed and used to normalize each individual phylotype. A comparison of normalized distributions of these four phylotypes from RT-PCR libraries and RT-qPCR results at each station indicate that γ -24774A11 was preferentially amplified at all stations (Figure 4). This is most clearly

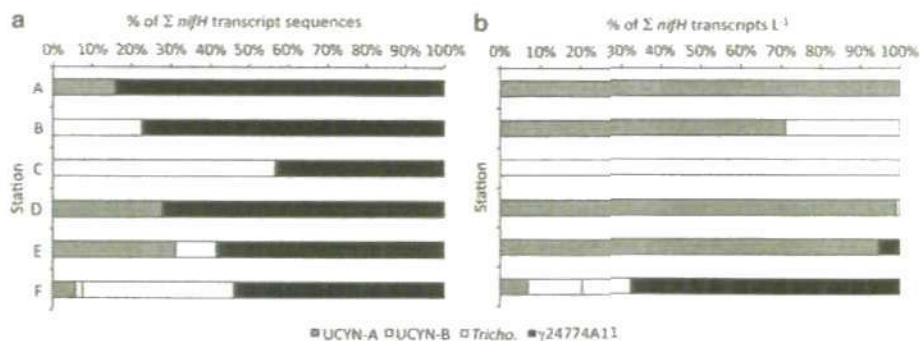


Figure 4 Comparison of results from RT-PCR and RT-qPCR for UCYN-A, UCYN-B, *Trichodesmium* and γ -24774A11 at each station. (a) Frequency of each phylotype occurring in the RT-PCR clone libraries normalized to the sum of frequencies for all four phylotypes. (b) Percent contribution of individual phylotypes to the total *nifH* transcripts per l detected via RT-qPCR at all stations.

shown at Station D, in which no γ -24774A11 *nifH* transcripts were quantified via RT-qPCR, but CV1 accounted for 34/54 transcript sequences.

There were minor differences in the cDNA generation for the RT-PCR and RT-qPCR portions of this study (described above). It is unclear as to what effect, if any, this may have on the results. Whether the preferential amplification of γ -24774A11 in the RT-PCR libraries resulted from minor protocol differences, or the nature of PCR amplification, these findings underscore the importance of coupling PCR-based analysis with more quantitative molecular approaches.

Conclusions

This study documented high rates of BNF at several stations, which are comparable with BNF rates reported in the Eastern Mediterranean and oligotrophic Pacific. As in previous studies, the rate of BNF was positively correlated with dissolved Fe concentration, providing evidence for a more substantial link between BNF and Saharan dust deposition.

Although this study draws attention to the limitations of RT-PCR-based studies, two phylotypes for which no qPCR assays exist, CV2 and CV5, were highly amplified and may be ecologically relevant diazotrophs in this region of the ocean.

UCYN-A had the highest *nifH* expression among the targeted phylotypes and dominated at the station with the highest BNF rate, which indicates they may be important contributors to BNF in this region. The most oligotrophic site had the lowest BNF rate, but was also the only station in which transcripts from all cyanobacterial phylotypes and γ -24774A11 were quantified. Although this study did not reveal a significant correlation between any one diazotroph and measured BNF rates, it is the first study that documents *nifH* expression in waters near the Cape Verde Islands and makes a significant contribution to understanding diazotrophic community composition in the tropical eastern North Atlantic.

Conflict of interest

The authors declare no conflict of interest.

Acknowledgements

We thank Dr. Gill Malin and the officers and crew of the Royal Research Ship Discovery during Cruise D325. This work was supported by Natural Environment Research Council through the UK SOLAS research programme and contributes to Theme 2 of the Plymouth Marine Laboratory Oceans2025 core programme. Natural Environment Research Council provided additional funding under Grant NE/C507902/1. Molecular work was supported by a Gordon and Betty Moore Foundation Marine Investigator Grant.

References

- Bergman B, Gallon JR, Rai AN, Stal LJ. (1997). N_2 fixation by non-heterocystous cyanobacteria. *FEMS Microbiol Rev* **19**: 139–185.
- Berman-Frank I, Quigg A, Finkel ZV, Irwin AJ, Haramaty L. (2007). Nitrogen-fixation strategies and Fe requirements in cyanobacteria. *Limnol Oceanogr* **52**: 2260–2269.
- Bird C, Martinez Martinez J, O'Donnell AG, Wyman M. (2005). Spatial distribution and transcriptional activity of an uncultured clade of planktonic diazotrophic γ -proteobacteria in the Arabian Sea. *Appl Environ Microbiol* **71**: 2079–2085.
- Brewer PG, Riley JP. (1965). The automatic determination of nitrate in sea water. *Deep-Sea Res* **12**: 765–772.
- Chen Y-B, Dominic B, Mellon MT, Zehr JP. (1998). Circadian rhythm of nitrogenase gene expression in the diazotrophic filamentous nonheterocystous cyanobacterium *Trichodesmium* sp. strain IMS 101. *J Bacteriol* **180**: 3598–3605.
- Chiappello I, Bergametti G, Gomes L, Chatenet B, Dulac F, Pimenta J et al. (1995). An additional low layer transport of Sahelian and Saharan dust over the North-Eastern Tropical Atlantic. *Geophys Res Lett* **22**: 3191–3194.
- Church MJ, Bjorkman KM, Karl DM, Saito MA, Zehr JP. (2008). Regional distributions of nitrogen-fixing bacteria in the Pacific Ocean. *Limnol Oceanogr* **53**: 63–77.

- Church MJ, Jenkins BD, Karl DM, Zehr JP. (2005a). Vertical distributions of nitrogen-fixing phylotypes at Stn ALOHA in the oligotrophic North Pacific Ocean. *Aquat Microb Ecol* **38**: 3–14.
- Church MJ, Short CM, Jenkins BD, Karl DM, Zehr JP. (2005b). Temporal patterns of nitrogenase gene (*nifH*) expression in the oligotrophic North Pacific Ocean. *Appl Environ Microbiol* **71**: 5362–5370.
- de Baar HJW, Timmermans KR, Laan P, de Porto HH, Ober S, Blom JJ et al. (2008). Titan: A new facility for ultraclean sampling of trace elements and isotopes in the deep oceans in the international Geotraces program. *Mar Chem* **111**: 4–21.
- de Jong JTM, den Das J, Bathmann U, Stoll MHC, Kattner G, Nolting RF et al. (1998). Dissolved iron at subnanomolar levels in the Southern Ocean as determined by ship-board analysis. *Anal Chim Acta* **377**: 113–124.
- Falcón LI, Cipriano F, Chistoserdov AY, Carpenter EJ. (2002). Diversity of diazotrophic unicellular cyanobacteria in the tropical North Atlantic Ocean. *Appl Environ Microbiol* **68**: 5760–5764.
- Farnelid H, Oberg T, Riemann L. (2009). Identity and dynamics of putative N-2-fixing picoplankton in the Baltic Sea proper suggest complex patterns of regulation. *Environ Microbiol Rep* **1**: 145–154.
- Finn RD, Mistry J, Tate J, Coggill P, Heger A, Pollington JE et al. (2010). The Pfam protein families database. *Nucl Acids Res* **38**: D211–D222.
- Fong AA, Karl D, Lukas R, Letelier RM, Zehr JP, Church MJ. (2008). Nitrogen fixation in an anticyclonic eddy in the oligotrophic North Pacific Ocean. *ISME J* **2**: 663–676.
- Foster RA, Paytan A, Zehr JP. (2009a). Seasonality of N₂ fixation and *nifH* diversity in the Gulf of Aqaba (Red Sea). *Limnol Oceanogr* **54**: 219–233.
- Foster RA, Subramaniam A, Mahaffey C, Carpenter EJ, Capone DG, Zehr JP. (2007). Influence of the Amazon River plume on distributions of free-living and symbiotic cyanobacteria in the western tropical North Atlantic Ocean. *Limnol Oceanogr* **52**: 517–532.
- Foster RA, Subramaniam A, Zehr JP. (2009b). Distribution and activity of diazotrophs in the Eastern Equatorial Atlantic. *Environ Microbiol* **11**: 741–750.
- Goebel NL, Turk KA, Achilles KM, Paerl RW, Hewson I, Morrison AE et al. (2010). Abundance and distribution of major groups of diazotrophic cyanobacteria and their potential contribution to N₂ fixation in the tropical Atlantic Ocean. *Environ Microbiol* **12**: 3272–3289.
- Goto M, Ando S, Hachisuka Y, Yoneyama T. (2005). Contamination of diverse *nifH* and *nifH*-like DNA into commercial PCR primers. *FEMS Microbiol Lett* **246**: 33–38.
- Grabowski MNW, Church MJ, Karl DM. (2008). Nitrogen fixation rates and controls at Stn ALOHA. *Aquat Microb Ecol* **52**: 175–183.
- Grasshoff K, Kremling K, Ehrhardt M (eds) (1999). *Methods of Seawater Analysis*. Wiley-VCH: Weinheim, pp 600.
- Gruber N, Sarmiento JL. (1997). Global patterns of marine nitrogen fixation and denitrification. *Global Biogeochem Cy* **11**: 235–266.
- Hewson I, Moisaner PH, Morrison AE, Zehr JP. (2007). Diazotrophic bacterioplankton in a coral reef lagoon: phylogeny, diel nitrogenase expression and response to phosphate enrichment. *ISME J* **1**: 78–91.
- Karl D, Letelier R, Tupas L, Dore J, Christian J, Hebel D. (1997). The role of nitrogen fixation in biogeochemical cycling in the subtropical North Pacific Ocean. *Nature* **388**: 533–538.
- Karl D, Michaels A, Bergman B, Capone D, Carpenter E, Letelier R et al. (2002). Dinitrogen fixation in the world's oceans. *Biogeochem* **57/58**: 47–98.
- Kirkwood DS. (1989). Simultaneous determination of selected nutrients in sea water. *ICES CM 1989/C*: 29.
- Kulakov LA, McAlister MB, Ogden KL, Larkin MJ, O'Hanlon JF. (2002). Analysis of bacteria contaminating ultrapure water in industrial systems. *Appl Environ Microbiol* **68**: 1548–1555.
- Kustka A, Carpenter EJ, Sanudo-Wilhelmy SA. (2002). Iron and marine nitrogen fixation: progress and future directions. *Res Microbiol* **153**: 255–262.
- Langlois RJ, Hummer D, LaRoche J. (2008). Abundances and distributions of the dominant *nifH* phylotypes in the Northern Atlantic Ocean. *Appl Environ Microbiol* **74**: 1922–1931.
- Langlois RJ, LaRoche J, Raab PA. (2005). Diazotrophic diversity and distribution in the tropical and subtropical Atlantic Ocean. *Appl Environ Microbiol* **71**: 7910–7919.
- LaRoche J, Breitbarth E. (2005). Importance of the diazotrophs as a source of new nitrogen in the ocean. *J Sea Res* **53**: 67–91.
- Lovell CR, Friez MJ, Longshore JW, Bagwell CE. (2001). Recovery and phylogenetic analysis of *nifH* sequences from diazotrophic bacteria associated with dead aboveground biomass of *Spartina alterniflora*. *Appl Environ Microbiol* **67**: 5308–5314.
- Ludwig W, Strunk O, Westram R, Richter L, Meier H, Yadhukumar et al. (2004). ARB: a software environment for sequence data. *Nucleic Acids Res* **32**: 1363–1371.
- Mahaffey C, Michaels AF, Capone DG. (2005). The conundrum of marine N₂ fixation. *Am J Sci* **305**: 546–595.
- Man-Aharonovich D, Kress N, Bar Zeev E, Berman-Frank I, Beja O. (2007). Molecular ecology of *nifH* genes and transcripts in the eastern Mediterranean Sea. *Environ Microbiol* **9**: 2354–2363.
- Matsuda N, Agui W, Tougo T, Sakai H, Ogino K, Abe M. (1996). Gram-negative bacteria viable in ultrapure water: identification of bacteria isolated from ultrapure water and effect of temperature on their behavior. *Colloids Surfaces B* **5**: 279–289.
- Mills MM, Ridame C, Davey M, La Roche J, Geider RJ. (2004). Iron and phosphorus co-limit nitrogen fixation in the eastern tropical North Atlantic. *Nature* **429**: 292–294.
- Mohr W, Grosskopf T, Wallace DW, LaRoche J. (2010). Methodological underestimation of oceanic nitrogen fixation rates. *PLoS One* **5**: e12583.
- Moisaner PH, Beinart RA, Hewson I, White AE, Johnson KS, Carlson CA et al. (2010). Unicellular cyanobacterial distributions broaden the oceanic N₂ fixation domain. *Science* **327**: 1512–1514.
- Moisaner PH, Beinart RA, Voss M, Zehr JP. (2008). Diversity and abundance of diazotrophic microorganisms in the South China Sea during intermonsoon. *ISME J* **2**: 954–967.
- Moisaner PH, Morrison AE, Ward BB, Jenkins BD, Zehr JP. (2007). Spatial-temporal variability in diazotroph assemblages in Chesapeake Bay using an oligonucleotide *nifH* microarray. *Environ Microbiol* **9**: 1823–1835.
- Montoya JP, Holl CM, Zehr JP, Hansen A, Villareal TA, Capone DG. (2004). High rates of N₂ fixation by

- unicellular diazotrophs in the oligotrophic Pacific Ocean. *Nature* **430**: 1027–1031.
- Montoya JP, Voss M, Kahler P, Capone DG. (1996). A simple, high-precision, high-sensitivity tracer assay for N_2 fixation. *Appl Environ Microbiol* **62**: 986–993.
- Neufeld JD, Schafer H, Cox MJ, Boden R, McDonald IR, Murrell JC. (2007). Stable-isotope probing implicates *Methylophaga* spp and novel gammaproteobacteria in marine methanol and methylamine metabolism. *ISME J* **1**: 480–491.
- Owens NJP, Rees AP. (1989). Determination of nitrogen-15 at sub-microgram levels of nitrogen using automated continuous-flow isotope ratio mass spectrometry. *Analyst* **114**: 1655–1657.
- Rees AP, Gilbert JA, Kelly-Gerreyn BA. (2009). Nitrogen fixation in the western English Channel (NE Atlantic Ocean). *Mar Ecol-Prog Ser* **374**: 7–12.
- Rees AP, Law CS, Woodward EMS. (2006). High rates of nitrogen fixation during an *in-situ* phosphate release experiment in the Eastern Mediterranean Sea. *Geophys Res Lett* **33**: L10607.
- Rijkenberg MJA, Powell CF, Dall'Osto M, Nielsdottir MC, Patey MD, Hill PG et al. (2008). Changes in iron speciation following a Saharan dust event in the tropical North Atlantic Ocean. *Mar Chem* **110**: 56–67.
- Sanudo-Wilhelmy SA, Kustka AB, Gobler CJ, Hutchins DA, Yang M, Lwiza K et al. (2001). Phosphorus limitation of nitrogen fixation by *Trichodesmium* in the central Atlantic Ocean. *Nature* **411**: 66–69.
- Sarthou G, Baker AR, Blain S, Achterberg EP, Boye M, Bowie AR et al. (2003). Atmospheric iron deposition and sea-surface dissolved iron concentrations in the eastern Atlantic Ocean. *Deep Sea Res* **50**: 1339–1352.
- Schloss PD, Handelsman J. (2005). Introducing DOTUR, a computer program for defining operational taxonomic units and estimating species richness. *Appl Environ Microbiol* **71**: 1501–1506.
- Tripp HJ, Bench SR, Turk KA, Foster RA, Desany BA, Niazi F et al. (2010). Metabolic streamlining in an open ocean nitrogen-fixing cyanobacterium. *Nature* **464**: 90–94.
- Vitousek PM, Howarth RW. (1991). Nitrogen limitation on land and in the sea: How can it occur? *Biogeochem* **13**: 87–115.
- Welschmeyer NA. (1994). Fluorometric analysis of chlorophyll a in the presence of chlorophyll b and phaeopigments. *Limnol Oceanogr* **39**: 1985–1992.
- Wyman M, Zehr JP, Capone DG. (1996). Temporal variability in nitrogenase gene expression in natural population of the marine cyanobacterium *Trichodesmium thiebautii*. *Appl Environ Microbiol* **62**: 1073–1075.
- Zani S, Mellon MT, Collier JL, Zehr JP. (2000). Expression of *nifH* genes in natural microbial assemblages in Lake George, NY detected with RT-PCR. *Appl Environ Microbiol* **66**: 3119–3124.
- Zehr JP, Bench SR, Carter BJ, Hewson I, Niazi F, Shi T et al. (2008). Globally distributed uncultivated oceanic N_2 -fixing cyanobacteria lack oxygenic Photosystem II. *Science* **322**: 1110–1112.
- Zehr JP, Crumbliss LL, Church MJ, Omoregie EO, Jenkins BD. (2003a). Nitrogenase genes in PCR and RT-PCR reagents: implications for studies of diversity of functional genes. *Biotechniques* **35**: 996–1005.
- Zehr JP, Jenkins BD, Short SM, Steward GF. (2003b). Nitrogenase gene diversity and microbial community structure: a cross-system comparison. *Environ Microbiol* **5**: 539–554.
- Zehr JP, McReynolds LA. (1989). Use of degenerate oligonucleotides for amplification of the *nifH* gene from the marine cyanobacterium *Trichodesmium thiebautii*. *Appl Environ Microbiol* **55**: 2522–2526.
- Zehr JP, Montoya JP, Jenkins BD, Hewson I, Mondragon E, Short CM et al. (2007). Experiments linking nitrogenase gene expression to nitrogen fixation in the North Pacific subtropical gyre. *Limnol Oceanogr* **52**: 169–183.
- Zehr JP, Paerl HW. (2008). Molecular ecological aspects of nitrogen fixation in the marine environment. In: Kirchman DL (ed). *Microbial Ecology of the Oceans* 2nd edn. Wiley-Liss Inc.: Durham, NC, pp 481–525.
- Zehr JP, Waterbury JB, Turner PJ, Montoya JP, Omoregie E, Steward GF et al. (2001). Unicellular cyanobacteria fix N_2 in the subtropical North Pacific Ocean. *Nature* **412**: 635–638.

Supplementary Information accompanies the paper on The ISME Journal website (<http://www.nature.com/ismej>)